(12) INTERNATIONAL APPLICATION PUBLISHED UNDER THE PATENT COOPERATION TREATY (PCT)

(19) World Intellectual Property Organization
International Bureau

(43) International Publication Date
15 June 2023 (15.06.2023)

WIPO | PCT

(10) International Publication Number
WO 2023/104904 A2

(51) International Patent Classification:
A61K 39/12 (2006.01) *C07K 16/10* (2006.01)
A61K 39/215 (2006.01) *G01N 33/569* (2006.01)
A61P 31/14 (2006.01) *C12N 15/50* (2006.01)
C07K 14/165 (2006.01)

(21) International Application Number:
PCT/EP2022/084833

(22) International Filing Date:
07 December 2022 (07.12.2022)

(25) Filing Language: English

(26) Publication Language: English

(30) Priority Data:
FR2113141 08 December 2021 (08.12.2021) FR

(71) Applicant: **GENCLIS** [FR/FR]; 15 rue du Bois de la Champelle, 54500 Vandoeuvre-lès-Nancy (FR).

(72) Inventors: **BIHAIN, Bernard**; 23 rue St Michel, 54000 NANCY (FR). **ROITEL, Olivier**; 13 rue du Général de Castelnau, 54110 COURBESSEAUX (FR). **THOUVENOT, Benoît**; 109 bis Chemin de Courberail, 54230 CHALIGNY (FR).

(74) Agent: **CABINET BEAU DE LOMENIE**; 158 Rue de l'Université, 75340 PARIS CEDEX 07 (FR).

(81) Designated States *(unless otherwise indicated, for every kind of national protection available)*: AE, AG, AL, AM, AO, AT, AU, AZ, BA, BB, BG, BH, BN, BR, BW, BY, BZ, CA, CH, CL, CN, CO, CR, CU, CV, CZ, DE, DJ, DK, DM, DO, DZ, EC, EE, EG, ES, FI, GB, GD, GE, GH, GM, GT, HN, HR, HU, ID, IL, IN, IQ, IR, IS, IT, JM, JO, JP, KE, KG, KH, KN, KP, KR, KW, KZ, LA, LC, LK, LR, LS, LU, LY, MA, MD, MG, MK, MN, MW, MX, MY, MZ, NA, NG, NI, NO, NZ, OM, PA, PE, PG, PH, PL, PT, QA, RO, RS, RU, RW, SA, SC, SD, SE, SG, SK, SL, ST, SV, SY, TH, TJ, TM, TN, TR, TT, TZ, UA, UG, US, UZ, VC, VN, WS, ZA, ZM, ZW.

(84) Designated States *(unless otherwise indicated, for every kind of regional protection available)*: ARIPO (BW, CV, GH, GM, KE, LR, LS, MW, MZ, NA, RW, SD, SL, ST, SZ, TZ, UG, ZM, ZW), Eurasian (AM, AZ, BY, KG, KZ, RU, TJ, TM), European (AL, AT, BE, BG, CH, CY, CZ, DE, DK, EE, ES, FI, FR, GB, GR, HR, HU, IE, IS, IT, LT, LU, LV, MC, ME, MK, MT, NL, NO, PL, PT, RO, RS, SE, SI, SK, SM, TR), OAPI (BF, BJ, CF, CG, CI, CM, GA, GN, GQ, GW, KM, ML, MR, NE, SN, TD, TG).

Published:
— *without international search report and to be republished upon receipt of that report (Rule 48.2(g))*
— *with sequence listing part of description (Rule 5.2(a))*

(54) Title: THE SARS-COV-2 AND VARIANTS USE TWO INDEPENDENT CELL RECEPTORS TO REPLICATE

(57) Abstract: The present disclosure relates to a compositions and methods for prevention and/or treatment of COVID-19 disease caused by the SARS-CoV-2. The Angiotensin-Converting Enzyme 2 (ACE2) that delivers viral RNA into the cytoplasm was heretofore the sole known SARS- CoV-2 receptor. Disclosed herein is the identification of another SARS-CoV-2 receptor. Namely, the Lipolysis Stimulated Receptor (LSR). LSR provides an endocytic route as effective for the replication of SARS-CoV-2 as ACE2. LSR and ACE2 contributions to viral replication are coordinated by free fatty acids (FFA). Unsaturated FFA irreversibly suppress SARS-CoV-2 capacity to bind ACE2. At the same time, both saturated and unsaturated FFA activate LSR. Activated LSR endocytoses ACE2 competent and incompetent SARS-CoV-2 yielding immediate or delayed production of ACE2 competent progeny. Disclosed herein are compositions and methods directed toward both ACE2 and LSR mediated routes of viral entry and replication, which reduce the severity and transmission of SARS-CoV-2.

WO 2023/104904 A2

THE SARS-COV-2 AND VARIANTS USE TWO INDEPENDENT CELL RECEPTORS TO REPLICATE

REFERENCE TO RELATED APPLICATIONS

[0001] This application claims the benefit of priority to French Patent Application No. 21 13141, filed December 8, 2021, the contents of which are hereby incorporated by reference in their entirety and for all purposes.

TECHNICAL FIELD

[0002] The disclosure relates generally to SARS-CoV-2 spike protein and its interaction with cellular entry receptors. Until now, the angiotensin-converting enzyme (ACE2) was thought to be the sole receptor by which SARS-CoV-2 is able to gain entry to the cell interior and replicate. However, disclosed herein is the discovery of another receptor for SARS-CoV-2 cellular entry, the Lipolysis Stimulated Receptor (LSR). Regions of the spike protein that interact with LSR are characterized, and LSR binding domains (LBDs) are mapped relative to the wild type (Wuhan strain) spike protein. The disclosure further relates to compositions and methods that utilize the LBDs to provide immunogenic compositions, characterize the receptor-binding preference of SARS-CoV-2 variants, and to treat and/or prevent COVID-19, including long COVID syndrome (long COVID-19 syndrome).

BACKGROUND

[0003] SARS-CoV-2 is the causative agent of COVID-19. Manifestations of COVID-19 can include a wide variety of symptoms that include but are not limited to Severe Acute Respiratory Syndrome (SARS), multiple organ failures, and death. As of October 2021, SARS-CoV-2 has infected more than 237 million people worldwide and has led to more than 4.8 million deaths globally, and uncounted numbers of long COVID-19 syndrome, which can be disabling. Thus, the COVID-19 pandemic threatens public health worldwide.

[0004] Although vaccines effectively reduce COVID-19 severity, and significantly reduce elderly mortality, secondary infections do occur, and vaccinated individuals who are infected with SARS-CoV-2 are still capable of transmitting the virus to others. As a result, the pandemic shows few signs of regression.

[0005] Therefore, what is needed in the art are new vaccine compositions, therapeutic agents and methods, which are highly effective against current strains of SARS-CoV-2 and which can quickly be adapted to address emerging SARS-CoV-2 variants of concern.

[0006] Fortunately, as will be apparent from the detailed description that follows, the present disclosure provides for these and other needs.

SUMMARY

[0007] Disclosed herein, is the discovery and characterization of a cellular receptor for binding of the SARS-CoV-2 spike protein, in addition to ACE2, which permits cellular entry and replication of SARS-CoV-2. The spike domains responsible for binding are also disclosed and characterized. Compositions and methods that utilize this new discovery are also provided.

[0008] Accordingly, in one aspect, the disclosure provides an immunogenic composition for inhibiting SARS-CoV-2 replication. The composition comprises: at least one nucleic acid encoding at least one immunogen that comprises a lipolysis-stimulated receptor binding domain (LBD) of a SARS-CoV-2 spike protein, wherein the at least one nucleic acid encoding the immunogen is operably linked to an expression control sequence and wherein the LBD is selected from LBD1 and LBD2. In one or more embodiments, the LBD is LBD1. In one or more embodiments, the nucleic acid that encodes the LBD1 encodes a polypeptide that comprises an amino acid sequence having at least 90% sequence identity to amino acid 25 to amino acid 85 of SEQ ID NO: 1. In one or more embodiments, the sequence identity is 91%, 92%, 93%, 94%, 95%, 96%, 97%, 98%, 99%, or 100%. In one or more embodiments, the LBD is LBD2. In one or more embodiments, the nucleic acid that encodes the LBD2 encodes a polypeptide that comprises an amino acid sequence having at least 90% sequence identity to amino acid 607 to amino acid 691 of SEQ ID NO: 1. In one or more embodiments, the sequence identity is 91%, 92%, 93%, 94%, 95%, 96%, 97%, 98%, 99%, or 100%. In one or more embodiments, the at least one nucleic acid that encodes the at least one immunogen, encodes a polypeptide that comprises LBD1 and LBD2.

[0009] In one or more embodiments, the immunogenic composition further comprises a nucleic acid that encodes at least one immunogen that comprises an ACE2 binding domain (ABD) operably linked to an expression control sequence. In one or more

embodiments, the LBD1, LBD2, and ABD are encoded by the same nucleic acid. In one or more embodiments, the nucleic acid encoding the LBD1, LBD2, and ABD encodes a polypeptide that comprises an amino acid sequence having at least 90% sequence identity to amino acid 25 to amino acid 691 of SEQ ID NO: 1. In one or more embodiments, the sequence identity is 91%, 92%, 93%, 94%, 95%, 96%, 97%, 98%, 99%, or 100%. In one or more embodiments, the LBD1, LBD2, and ABD are encoded by different nucleic acids.

[0010] In one or more embodiments, the one or more immunogens are coupled to one or more Transcription Infidelity (TI) segments. In one or more embodiments, the immunogenic composition further comprises at least one adjuvant.

[0011] In another aspect, the disclosure provides a method for immunizing a subject against COVID-19 disease resulting from a SARS-CoV-2 infection, the method comprising: inoculating a subject with the immunogenic composition of one or more embodiments herein. In one or more embodiments, the method reduces the severity of COVID-19 disease. In one or more embodiments, the method reduces transmission of SARS-CoV-2.

[0012] In another aspect, the disclosure provides a method of making an antibody or antigen binding fragment that specifically binds to at least one LBD of a SARS-CoV-2 spike protein, the method comprising: immunizing a mammal with a polypeptide that comprises an LBD peptide, wherein the LBD peptide selected from the group consisting of LBD1 and LBD2. In one or more embodiments, the polypeptide comprises LBD1 and LBD2. In one or more embodiments, the LBD1 comprises an amino acid sequence having at least 90% sequence identity to amino acid 25 to amino acid 85 of SEQ ID NO: 1. In one or more embodiments, the sequence identity is 91%, 92%, 93%, 94%, 95%, 96%, 97%, 98%, 99%, or 100%. In one or more embodiments, the LBD2 comprises an amino acid sequence having at least 90% sequence identity to amino acid 607 to amino acid 691 of SEQ ID NO: 1. In one or more embodiments, the sequence identity is 91%, 92%, 93%, 94%, 95%, 96%, 97%, 98%, 99%, or 100%. In one or more embodiments, the polypeptide comprises an amino acid sequence having at least 90% sequence identity to amino acid 25 to amino acid 691 of SEQ ID NO: 1. In one or more embodiments, the sequence identity is 91%, 92%, 93%, 94%, 95%, 96%, 97%, 98%, 99%, or 100%. In one or more embodiments, the polypeptide further comprises an ACE2 binding domain (ABD). In one

or more embodiments, the polypeptide is coupled to one or more Transcription Infidelity (TI) segments.

[0013] In one or more embodiments, the method further comprises recovering antiserum from the immunized mammal and purifying polyclonal antibodies that specifically bind to at least one LBD of a SARS-CoV-2 spike protein.

[0014] In one or more embodiments, the method further comprises recovering B-lymphocytes from the immunized mammal; fusing the recovered B-lymphocytes with a myeloma cell to produce a hybridoma cell; and selecting individual hybridoma cells that produce monoclonal antibodies that specifically bind to at least one LBD of a SARS-CoV-2 spike protein.

[0015] In another aspect, the disclosure provides a nucleic acid encoding the antibody or antigen-binding fragment made by the method of making an antibody or antigen binding fragment that specifically binds to at least one LBD of a SARS-CoV-2 spike protein.

[0016] In another aspect, the disclosure provides a pharmaceutical composition comprising the antibody or antigen binding fragment which is a product of the method of making an antibody or antigen binding fragment that specifically binds to at least one LBD of a SARS-CoV-2 spike protein.

[0017] In one or more embodiments, the pharmaceutical composition further comprises a second therapeutic agent. In one or more embodiments, the second therapeutic agent is a second antibody, or an antigen-binding fragment thereof, that binds a SARS-CoV-2 spike protein.

[0018] In another aspect, the disclosure provides a method for treating or preventing COVID-19. The method comprises administering a pharmaceutically effective amount of an antibody or antigen binding fragment, or the pharmaceutical composition of one or more embodiments herein to a subject in need thereof. In one or more embodiments, the method results in one or more of: an acceleration in intestinal clearance of SARS-CoV-2; a reduction of transmission of SARS-CoV-2; an alleviation of one or more symptoms of long COVID-19 syndrome, or a combination thereof in the subject.

[0019] In another aspect, the disclosure provides a method for assaying SARS-CoV-2 cellular entry *in vitro*. The method comprises: (1) pre-incubating a first subpopulation of

SARS-CoV-2 pseudovirus (PV) with a long-chain unsaturated free fatty acid (uFFA), thereby providing ACE2 incompetent PV, and either pre-incubating a second subpopulation of SARS-CoV-2 PV with a long-chain saturated free fatty acid (sFFA) or not pre-incubating SARS-CoV-2 PV, thereby providing ACE2 competent PV; (2) incubating the ACE2 incompetent and ACE2 competent PV with host cells, to provide a first and a second host cell culture; wherein the first host cell culture comprises ACE2 incompetent SARS-CoV-2, and the second host cell culture comprises ACE2 competent SARS-CoV-2; wherein the host cells comprising the first cell culture and the second host cell culture express an ACE2 receptor and a lipolysis stimulated receptor (LSR); (3) transiently exposing the host cell cultures to a long-chain unsaturated fatty acid, or a long-chain saturated fatty acid; and (4) observing the PV in the host cell cultures over time, to determine timing of PV entry into the host cells; wherein timing of the PV entry is early or late; and wherein early entry indicates entry via ACE2 receptor, and late entry indicates entry via LSR. In one or more embodiments, the transient exposure of the host cell cultures to a long-chain free fatty acid (FFA) is carried out 3 times without adding new PV. In one or more embodiments, the SARS-CoV-2 PV comprises: (a) a nucleic acid that encodes a green fluorescent protein (GFP) operably linked to an expression control sequence, wherein the GFP is expressed upon entry into a host cell; and (b) a nucleic acid that encodes a SARS-CoV-2 spike protein, wherein the spike protein comprises one or more of an LBD1, LBD2, or ABD. In one or more embodiments, observing the PV over time comprises observing the level of fluorescence in the host cell cultures over time, wherein the level of fluorescence increases with the number of PV that are able to enter the host cells; and wherein early fluorescence indicates entry via ACE2 receptor, and late fluorescence indicates entry via LSR. In one or more embodiments, the method further comprises: selecting PV that show late fluorescence indicative of entry via LSR, thereby providing LSR specific pseudoviruses. In one or more embodiments, the method is used to evaluate the effectiveness of a test antibody directed against LBD1, LBD2, ABD or combinations thereof, for neutralizing entry via LSR, wherein the method comprises incubating the test antibody with the PV and host cells in step (2); and observing the effect on late fluorescence as compared late fluorescence in the absence of the antibody.

[0020] In another aspect, the disclosure provides a method for assaying coronavirus cellular entry or replication *in vitro*. The method comprises: (1) pre-incubating a first subpopulation of live coronavirus with a long-chain unsaturated free fatty acid (uFFA),

thereby providing a population of ACE2 incompetent virus; and either pre-incubating a second subpopulation of live coronavirus with a long-chain saturated free fatty acid (sFFA) or not pre-incubating the second subpopulation of live coronavirus with any FFA, thereby providing ACE2 competent virus; (2) incubating an initial titer of the ACE2 incompetent and ACE2 competent virus with host cells, to provide a first and a second host cell culture; wherein the first host cell culture comprises the ACE2 incompetent virus, and the second host cell culture comprises the ACE2 competent virus; and wherein the host cells comprising the first cell culture and the second host cell culture express an ACE2 receptor and a lipolysis stimulated receptor (LSR); (3) transiently exposing the first and second host cell cultures to a long-chain free fatty acid (FFA), and (4) observing timing of viral production, wherein viral production is measured by the number of virus produced as compared to the initial titer of the ACE2 incompetent or ACE2 competent virus, and wherein an increase in the number of virus is indicative of viral entry and replication; wherein timing of the viral production is early or late; and wherein early timing of the viral production indicates entry via ACE2 receptor, and late timing of the viral production indicates entry via LSR.

[0021] In one or more embodiments, the live coronavirus comprises a nucleic acid that encodes a coronavirus spike protein, and the spike protein comprises one or more of an LBD1, LBD2, or ABD. In one or more embodiments, the transient exposure of the first and second host cell cultures to a long-chain free fatty acid (FFA) is carried out 3 times without adding new virus. In one or more embodiments, the coronavirus is selected from the group consisting of SARS-CoV-2, SARS-CoV, MERS-CoV, OC43, a bovine coronavirus, a feline coronavirus, and a porcine coronavirus. In one or more embodiments, the coronavirus is SARS-CoV-2. In one or more embodiments, the long-chain uFFA is selected from oleate and linoleate. In one or more embodiments, the long-chain uFFA is oleate. In one or more embodiments, transient exposure to a long-chain free fatty acid (FFA) comprises transient exposure to a long-chain free fatty acid selected from the group consisting of a long-chain unsaturated fatty acid, and a long-chain saturated fatty acid. In one or more embodiments, transient exposure to a long-chain FFA comprises transient exposure to a long-chain saturated fatty acid. In one or more embodiments, the long-chain saturated fatty acid is selected from palmitate, stearate, octanoate, and heptanoate. In one or more embodiments, the long-chain saturated fatty acid is palmitate.

[0022] In one or more embodiments, the method is used to screen mutant libraries for ACE2 and/or LSR incompetent viral variants. In one or more embodiments, the live coronavirus is SARS-CoV-2. In one or more embodiments, the ACE2 and/or LSR incompetent viral variants are sequenced, and the resulting sequences are used to create viruses that are immunogenic, but non-replicative.

[0023] In one or more embodiments, the method further comprises in step (2), adding a putative inhibitor of entry via either or both LSR and ACE2, to screen for inhibitors that block cell entry and replication by LSR, ACE2, or LSR and ACE2. In one or more embodiments, the putative inhibitor is a small molecule inhibitor. In one or more embodiments, the putative inhibitor is an antibody. In one or more embodiments, the antibody is directed against one or more of LBD1, LBD2, or ABD. In one or more embodiments, the putative inhibitor is a lactoferrin derivative. In one or more embodiments, the method further comprises selecting a lactoferrin derivative having improved ACE2 and LSR neutralizing activity. In one or more embodiments, the disclosure provides for the use of an inhibitor of one or more embodiments described herein, to treat a subject experiencing severe COVID-19.

[0024] In one or more embodiments, the method for assaying coronavirus cellular entry or replication *in vitro* further comprises adding an inhibitor of cellular entry via either LSR or ACE2, to the initial titer of the ACE2 incompetent and ACE2 competent virus, to determine the receptor for cellular entry or replication of a coronavirus. In one or more embodiments, the inhibitor of cellular entry is a known inhibitor. In one or more embodiments, the coronavirus is a coronavirus variant. In one or more embodiments, the inhibitor of cellular entry is a recombinant LBD1 or LBD2. In one or more embodiments, the recombinant LBD1 or LBD2 blocks late entry, and the receptor for cellular entry is LSR. In one or more embodiments, the inhibitor of cellular entry is a recombinant ABD. In one or more embodiments, the recombinant ABD blocks early entry and the receptor for cellular entry is ACE2. In one or more embodiments, the inhibitor of cellular entry is a recombinant trimeric spike polypeptide. In one or more embodiments, the recombinant trimeric spike polypeptide comprises one or more mutations relative to a wild type trimeric spike polypeptide. In one or more embodiments, the method is used to characterize coronavirus variants. In one or more embodiments, the coronavirus is SARS-CoV-2. In one or more embodiments, the SARS-CoV-2 is a SARS-CoV-2 variant selected from the

group consisting of an alpha (α), beta (β), gamma (γ), delta (δ), epsilon (ε), or omicron (ο) variant. In one or more embodiments, the SARS-CoV-2 is a SARS-CoV-2 variant having a gain of function mutation. In one or more embodiments, the gain of function mutation is substitution mutation D80A of SEQ ID NO: 1, and the receptor for cellular entry is LSR. In one or more embodiments, the SARS-CoV-2 is a SARS-CoV-2 variant has a loss of function mutation. In one or more embodiments, the loss of function mutation is H655Y of SEQ ID NO: 1 and the receptor for cellular entry is ACE2. In one or more embodiments, the loss of function mutation is selected from substitution mutations L452R and T478K of SEQ ID NO: 1 and the receptor for cellular entry is LSR.

[0025] In another aspect, the disclosure provides a method for evaluating the neutralizing capacity of antibodies directed against SARS-CoV-2, the method comprising: removing free fatty acids from the serum prior to testing and evaluating the level of immune protection against COVID-19 disease. In one or more embodiments, the antibodies and serum are patient antibodies and patient serum.

[0026] In one or more embodiments, the method is used to evaluate the effectiveness of a vaccine. In one or more embodiments, the evaluating includes evaluating multiple measurements, such as multiple measurements that are taken over time. In one or more embodiments, the neutralizing capacity after removal of free fatty acids is compared to the neutralizing capacity before removal of free fatty acids. In one or more embodiments, a difference is observed in the neutralizing capacity after removal of free fatty acids compared to the neutralizing capacity before removal of free fatty acids, wherein the neutralizing capacity after removal of free fatty acids is greater than the neutralizing capacity before removal of free fatty acids. The difference observed in the neutralizing capacity after removal of free fatty acids compared to the neutralizing capacity before removal of free fatty acids may be a large difference, according to one or more embodiments described herein.

[0027] In one or more embodiments, the method further comprises administering to the patient an inhibitor of lipolysis-stimulated receptor (LSR). In one or more embodiments, the LSR inhibitor is an LSR specific antibody or a siRNA molecule that targets LSR.

[0028] In another aspect, the disclosure provides a siRNA molecule that targets a lipolysis stimulated receptor (LSR).

[0029] In another aspect, the disclosure provides a pharmaceutical composition comprising the one or more siRNA molecules and a pharmaceutically acceptable carrier. In one or more embodiments, the siRNA molecule targets LSRβ. In one or more embodiments, the pharmaceutical composition comprises at least two different siRNA molecules that target the LSR, wherein a first siRNA targets LSRα and a second siRNA targets LSRβ. In one or more embodiments, the pharmaceutical composition further comprises at least one other therapeutic agent. In one or more embodiments, the at least one therapeutic other agent is selected from suramin and lactoferrin.

[0030] In another aspect, the disclosure provides a method of treating a subject suffering from a SARS-CoV-2 infection, the method comprising: administering to the subject a pharmaceutically effective amount of the pharmaceutical composition comprising the one or more siRNA molecules, and a pharmaceutically acceptable carrier. In one or more embodiments, treating the subject with the effective amount of the pharmaceutical composition results in one or more of: an acceleration in intestinal clearance of SARS-CoV-2, a reduction of transmission of SARS CoV-2, an alleviation of one or more symptoms of long COVID-19 syndrome, or a combination thereof.

[0031] In another aspect, the disclosure provides a method of treating a subject suffering from a SARS-CoV-2 infection. The method comprises, reducing or temporarily suppressing the physiological supply of free fatty acids to the subject. In one or more embodiments, reducing or temporarily suppressing the physiological supply of free fatty acids to the subject comprises administering to the subject a composition suitable for treatment of diabetes or hyperlipidemia. In one or more embodiments, the composition is suitable for treatment of diabetes. In one or more embodiments, the composition comprises metformin. In one or more embodiments, the method the composition is suitable for treatment of hyperlipidemia. In one or more embodiments, the composition comprises acipimox. In one or more embodiments, the method further comprises administering a therapeutic agent to treat the SARS-CoV-2 infection. In one or more embodiments, the therapeutic agent the therapeutic agent is selected from remdesivir, ritonavir, nirmatrelvir, tocilizumab, sotrovimab, propofol-lipuro 1%, bamlanivimab, etesevimab, casirivimab, imdevimab, adalimumab, baricitinib, COVID-19 convalescent plasma, regiocit replacement, freesenius kabi propoven, and combinations thereof.

[0032] In another aspect, the disclosure provides a polypeptide that includes a lipolysis-stimulated receptor binding domain (LBD) of a SARS-CoV-2 spike protein. In one or more embodiments, the LBD is LBD1. In one or more embodiments, the polypeptide includes an amino acid sequence having at least 90% sequence identity to amino acid 25 to amino acid 85 of SEQ ID NO: 1. In one or more embodiments, the LBD is LBD2. In one or more embodiments, the polypeptide includes an amino acid sequence having at least 90% sequence identity to amino acid 607 to amino acid 691 of SEQ ID NO: 1. In one or more embodiments, the polypeptide includes LBD1 and LBD2. In one or more embodiments, the polypeptide includes an ACE2 binding domain (ABD). In one or more embodiments, the polypeptide includes an amino acid sequence having at least 90% sequence identity to amino acid 25 to amino acid 691 of SEQ ID NO: 1. In one or more embodiments, the polypeptide is coupled to one or more Transcription Infidelity (TI) segment. In one or more embodiments, the coupling of the TI segment is terminal (coupled at a terminus). In one or more embodiments the polypeptide is A, an antigen part, and the TI segment is P, having the structure A-P, P-A, or A1-P-A2, where A1 and A2 are two parts of A.

[0033] In another aspect, the disclosure relates to a method for immunizing a subject against COVID-19 disease resulting from a SARS-CoV-2 infection, the method comprising: administering to a subject with one or more embodiments of the polypeptide disclosed herein. In one or more embodiments, the method reduces the severity of COVID-19 disease. In one or more embodiments, the method reduces transmission of SARS-CoV-2.

[0034] In another aspect, the disclosure relates to a composition for inhibiting SARS-CoV-2 replication that includes one or more embodiments of the polypeptide disclosed herein. In one or more embodiments, the composition includes at least one adjuvant.

[0035] In another aspect, the disclosure relates to a method for immunizing a subject against COVID-19 disease resulting from a SARS-CoV-2 infection, the method including administering to a subject with one or more embodiments of the immunogenic composition disclosed herein. In one or more embodiments, the method reduces the severity of COVID-19 disease. In one or more embodiments, the method reduces transmission of SARS-CoV-2.

[0036] Other features, objects, and advantages will be apparent from the disclosure that follows.

BRIEF DESCRIPTION OF THE FIGURES

[0037] **FIG. 1A:** SARS-CoV-2 copy numbers in media and cell layer of BGM cells infected with SARS-CoV-2 was measured using quantitative reverse transcription PCR (RTqPCR) to quantify the production of viral RNA copies in the media and the cell layers. At day 4 post infection (DPI 4), 10^9 to 10^{10} viral RNA copies were produced in BGM cells, the copy number was equivalent in the media and cell layers.

[0038] **FIG. 1B:** Protein content of infected BGM cells of FIG. 1A. No detectable changes in the cell layer protein content were found.

[0039] **FIG. 1C:** SARS-CoV-2 copy numbers in media and cell layer of BGM infected with SARS-CoV-2 (Wild Strain, 10^8 viruses per well) in the presence of Casirivimab (30 µg/ml), Imdevimab (30 µg/ml) or the combination of both (Casirivimab: 15 µg/ml; and Imdevimab: 15 µg/ml).

[0040] **FIG. 1D:** Increasing concentrations of OA were added along with wild-type (WT) SARS-CoV-2 to BGM cells during the infection phase. After 150 min, the infective media was removed and replaced by culture media without any OA supplementation. The viral production measured at DPI 4 decreased by 87 % and 99 % with 0.5 mM and 1 mM OA.

[0041] **FIG. 1E:** SARS-CoV-2 pre-incubated with oleate/oleic acid (1 mM) followed by removal of unbound free fatty acids (FFA) before infection of BGM cells, shows a 99% reduction in their replicative capacity.

[0042] **FIG. 1F:** Illustrates the effect of unsaturated fatty acids (oleic acid, linoleic acid) and saturated fatty acids (palmitic acid, stearic acid) on cell entry. Pseudoparticles (pseudoviruses) were pre-incubated with 1 mM oleic acid (OA) or linoleic acid (LA) or with palmitic acid (PA) or Stearic Acid (SA). Unbound fatty acids were removed by size exclusion chromatography, and the recovered pseudoparticles were incubated with 80% confluent BGMK cells. After 24 h incubation, the cells were washed, and fluorescence intensity measured. Pseudoparticles pre-treated with OA or LA exhibited decreased cell fluorescence by comparison to pseudoparticles that were not pre-treated with any fatty

acids. In contrast, the same pseudoparticle pretreatment with the saturated fatty acids, palmitic acid (PA) or Stearic Acid (SA) did not inhibit PV entry.

[0043] **FIG. 1G:** Fluorescence intensity after 24 and 48 h of culture of BGM exposed to pseudoviruses pre-incubated or not with oleate (1 mM).

[0044] **FIG. 1H:** Fluorescence intensity of BGM cells incubated with pseudoviruses that were pretreated prior to infection with no FFA followed by no FFA, with oleate followed by oleate, with oleate followed by palmitate, and twice with palmitate. After each incubation unbound FFA were removed. Palmitate after oleate did not reverse the inhibitory effects of oleate.

[0045] **FIG. 1I:** Illustrates the effect of different fatty acids on cell entry. Pseudoparticles were pre-incubated with 1 mM of the indicated FFA, separated from unbound free fatty acids (FFA) by size exclusion chromatography, and then incubated with 80% confluent BGMK cells. After 24 hours (h) incubation, the cells were washed, and fluorescence intensity measured.

[0046] **FIG. 1J:** Pseudoviruses were first incubated with either no FFA (top), oleate (1 mM) (bottom left), or palmitate (1 mM) (bottom right). Pseudoviruses were then separated from the media by size exclusion chromatography, and each of the three fractions were again incubated without any FFA, with oleate or with palmitate (1 mM). Pseudoviruses were again separated from unbound FFA. The separated pseudoviruses were added to BGMK cells to initiate infection. Cell fluorescence was measured after 24 h of incubation.

[0047] **FIG. 1K:** Fluorescence intensity of BGM cells incubated with pseudoviruses that were pretreated prior to infection with no FFA (na FA) followed by no FFA (no FA), with palmitate followed by oleate, with oleate followed by palmitate, and twice with palmitate. After each incubation unbound FFA were removed. Pseudoparticles failed to enter BGM cells when pre-incubated with OA then with PA or vice-versa, followed by the removal of unbound fatty acids. Notably, oleate added after palmitate fully inhibited PV binding to ACE2. Two pre-incubations with palmitate had no inhibitory effect on PV entry.

[0048] **FIG. 1L:** Shows recombinant monomeric glycosylated wild type SARS-CoV-2 S protein on western blot.

[0049] **FIG. 1M:** Effect of increasing concentrations of the indicated FFA (oleate, palmitate, stearate, linoleate, octanoate, heptanoate) on monomeric recombinant SARS-CoV-2 spike protein (100 μg/mL) capacity to compete HRP labeled ABD for binding to wells coated with recombinant human ACE2. The data show the difference in Optical Density (OD) generated by HRP-ABD bound to the ACE2 without and with competing S protein.

[0050] **FIG. 1N:** Optical density (OD) generated by HRP-ABD added to human ACE2 coated wells in the absence or presence of oleate (1 mM).

[0051] **FIG. 1O:** Optical density (OD) generated by HRP-ABD bound to human ACE2 coated wells pre-incubated with or without oleate (1 mM).

[0052] **FIG. 1P:** A competitive assay to assess the effect of fatty acids (FA) on the S protein interaction with the human ACE2 was carried out utilizing the three recombinant proteins: the trimeric wild type (WT)-Spike, Horse Radish Peroxidase (HRP) labeled RBD, and human ACE2 coated wells on a plate. Oleic acid and linoleic acid, but not palmitic acid or stearic acid suppressed the S protein capacity to compete the binding of HRP-RBD to the ACE2.

[0053] **FIG. 1Q:** Optical density (OD) generated by HRP-RBD added to human ACE2 coated wells in the absence or presence of oleate (1 mM). Oleic acid did not inhibit the direct binding of HRP-RBD to the ACE2.

[0054] **FIG. 1R:** Structure of the SARS-CoV-2 spike protein FFA binding pocket filled with linoleate.

[0055] **FIG. 1S:** Structure of the SARS-CoV-2 spike protein FFA binding pocket filled with oleate.

[0056] **FIG. 1T:** The effect of oleate on the replication of live viruses (wild type, Wuhan strain). Replicative SARS-CoV-2 (Wuhan strain 10^8 copies per well) were applied to BGMK cells for 2 h 30 min without or with the indicated concentration of oleate. The cells were washed and incubated with fresh media for 96 hours. The media was removed, and the cell layer washed and recovered with trypsin. The amount of viral RNA in the media and cell layers was measured by quantitative PCR (qPCR).

[0057] **FIG. 1U:** Replicative SARS-CoV-2 was pre-incubated without FFA or with 1 mM oleate or with 0.4 mM palmitate. Viruses were re-isolated by size exclusion chromatography and added to BGMK (10^8 copies per well) for 2 h 30 min. The infective media were removed, and the cells were incubated for 96 hours. Pre-incubation of the virus with oleate (1 mM) reduced viral replication by more than 99.9 %, but pre-incubation with palmitate (0.4 mM) did not change the amount of viral RNA released in the media or detected in the cell layers.

[0058] **FIG. 1V:** SARS-CoV-2 virus was pre-incubated 150 min at room temperature in the absence or presence of 1 mM of the FA: OA or PA. Unbound FA was removed using a desalting column, and the virus from the eluate was added to BGM cells (10^8 particles/well). After a 150 min infection period, cells were washed, and total viral mRNA in media and cell layers was measured on DPI4.

[0059] **FIG. 1W:** Using the same FA protocol as described for FIG. 1V, total viral RNA levels are shown on DPI4 after infection of BGM cells (10^4 particles/well) with wild type (WT), Delta, and Omicron strains pre-incubated with 1 mM OA.

[0060] **FIG. 1X:** SARS-CoV-2 was pre-incubated 10 min at room temperature with the indicated concentrations of OA, and then added to BGM cells (10^8 particles/well). After 150 min incubation at 37°C, the virus-containing media was removed and replaced with fresh media. At day post infection 4 (DPI4), viral RNA levels were determined in media and in cells as described in Materials and Methods. Results are shown as % viral production.

[0061] **FIG. 1Y:** BGM cells were incubated for 24h with pseudoparticles pretreated without (No FA) or with 1 mM OA, linoleic acid (LA), PA, or stearic acid (SA) followed by removal of unbound FA. Cell fluorescence intensity was measured after removing the media containing pseudoparticles, followed by cell washing.

[0062] **FIG. 1Z:** BGM cells were infected with increasing titers of SARS-CoV-2 in the presence of Casirivimab and Imdevimab (C&I) (15+15 µg/mL). The viral copy number was measured at DPI4.

[0063] **FIG. 2A:** A single oleate incubation at the same time as the virus, reduced viral production by >99.9 % in both the media and the cell layers as compared to virus not

exposed to oleate at the time of infection. Two short incubations with oleate every 24 h without adding new viruses did not consistently alter viral production. However, after three oleate cycles, the number of viral particles released in the media increased by 6.8 x 10^2 and that in the cell layers by 2.5 x 10^3 fold. After 3 cycles with oleate (1 mM) without new viruses, the increase viral production as detected in the media and cell layers was statistically significant.

[0064] **FIG. 2B:** SARS-CoV-2 copy numbers in media and cell layer in BGM infected for 150 min with SARS-CoV-2 (10^8 per well) in the absence or in the presence of palmitate (0.4 mM).

[0065] **FIG. 2C:** Pre-incubating the virus with oleate reduced viral replication. However, pre-incubating the virus with 0.4 mM palmitate, did not affect viral replication.

[0066] **FIG. 2D:** SARS-CoV-2 copy numbers in media and cell layer in BGM infected for 150 min with SARS-CoV-2 (10^8 per well) in the absence of FFA or in the presence of oleate (1 mM on Day 1) and oleate (Day 1), followed by palmitate (0.4 mM) on day 2 without adding new viruses, or palmitate (0.4 mM) day 2 and 3 post-infection without adding new viruses.

[0067] **FIG. 2E:** SARS-CoV-2 copy numbers in media and cell layer in BGM infected for 150 min with the indicated viral load in the absence of FFA (solid line), or in the presence of 1 mM oleate on Day 1 followed by palmitate on Day 2 and Day 3 (dotted line).

[0068] **FIG. 2F:** Viral RNA released in the media using the O+2P protocol corresponded to authentic SARS-CoV-2 replicating through the ACE2.

[0069] **FIG. 2G:** The effect of different FFA on the replication of ACE2 incompetent SARS-CoV-2. BGMK cells were infected with SARS-CoV-2 in presence or absence of oleate as above (Wuhan strain 10^8 copies per well, for 2 h 30 min). After this, cells incubated with oleate received either no further incubation with any free fatty acids or two transient incubations with the indicated FFA (2 h 30 min), 24 h apart followed by replacement with media without FFA. Viral production was measured 96 h post initial infection. Viral production was significantly increased after two rounds of exposure to 0.4 mM palmitate or stearate.

[0070] **FIG. 2H:** SARS-CoV-2 copy numbers in media and cell layer after infection with 10^7 SARS-CoV-2 per well in the absence of FFA (Gray) or using the O+2P protocol (shaded) in the indicated simian (BGMK), human (Caco2), and mouse cells (4T1). All measures were in triplicate, and the error bars show standard deviation (SD).

[0071] **FIG. 2I:** Inhibition of SARS-CoV-2 replication by oleate (1 mM) added with the SARS-CoV-2 (Wild type, 10^8 viruses per well) infecting human Caco-2.

[0072] **FIG. 2J:** BGM cells were infected with SARS-CoV-2 virus (10^8 particles/well) and incubated in the absence or presence of 1 mM OA (day (D)0). After 150 min incubation, cells were washed and placed in fresh media. On D1, the FA indicated was added to cells and then removed after 150 min by replacing with fresh media; the same FA treatment was repeated on D2, followed by measurement of viral RNA production on DPI4. FA used for D1+D2 treatments were 1 mM OA. Statistical significance is indicated as $^{**}p < 0.01$.

[0073] **FIG. 2K:** BGM cells were infected with SARS-CoV-2 virus (10^8 particles/well) and incubated in the absence or presence of 1 mM OA (day (D)0). After 150 min incubation, cells were washed and placed in fresh media. On D1, the FA indicated was added to cells and then removed after 150 min by replacing with fresh media; the same FA treatment was repeated on D2, followed by measurement of viral RNA production on DPI4. FA used for D1+D2 treatments were 0.4 mM PA. Statistical significance is indicated as $^{***}p < 0.001$.

[0074] **FIG. 2L:** BGM cells were infected with SARS-CoV-2 virus (10^8 particles/well) and incubated in the absence or presence of 1 mM OA (day (D)0). After 150 min incubation, cells were washed and placed in fresh media. On D1, the FA indicated was added to cells and then removed after 150 min by replacing with fresh media; the same FA treatment was repeated on D2, followed by measurement of viral RNA production on DPI4. Fatty acid(s) (FA) used for D1+D2 treatments were 0.4 mM LA and 0.4 mM SA. Statistical significance is indicated as $^{***}p < 0.001$.

[0075] **FIG. 3A:** Western blot showing the presence of ACE2 and LSR in protein extracts of BGM cells, Caco2 cells, and 4TI cells using anti-ACE2 and anti-LSR IgG. Anti-GAPDH specific IgG served as a control.

[0076] **FIG. 3B:** Effect of scrambled and LSR specific siRNA on the expression of, ACE2, LSR, and GAPDH in BGM.

[0077] **FIG. 3C:** LSR specific siRNA inhibition of wild-type SARS-CoV-2 production in BGM cells treated with LSR specific siRNA. LSR specific siRNA inhibited SARS-CoV-2 production by 75% as compared to production by cells treated with scrambled siRNA.

[0078] **FIG. 3D:** Western blots of lysate from BGM and Caco2 cells were examined in order to confirm that the reduction in viral production in BGM cells seen with LSR specific siRNA was due to a reduction of LSR expression and not a reduction in CD36 expression (the other plasma membrane proteins shown to specifically bind or interact with fatty acids). As shown, western blots of lysate from BGM and Caco2 cells revealed proteins reactive with specific anti-LSR antibodies, but no protein reactive with anti-CD36 antibodies. Human adipose tissue protein extracts (Human FAT) were used as positive control for anti-CD36 blots. As expected, BGM and Caco2 cells expressed the ACE2.

[0079] **FIG. 3E:** Forty-eight hours after LSR silencing using LSR specific siRNA, BGM cells were infected with the Delta variant at a multiplicity of infection equal to 1 (MOI=1) using the O+2P protocol. After 96 hours of culture, viral RNA copy number was about 1.6×10^8 in cells transfected with control siRNA, and about 5×10^3 in cells transfected with LSR specific siRNA.

[0080] **FIG. 3F:** The effect of LSR silencing on BGM cells infected in the presence or absence of palmitic acid (PA) (a FFA). To verify that the LSR enabled the replication of wild-type SARS-CoV-2, the effect of LSR silencing on BGM cells infected in the presence of palmitic acid (top right) or absence of palmitic acid (bottom right) was tested, compared to control in the presence of palmitic acid (top left) or absence of palmitic acid (bottom left). Infection with PA was cytopathic in BGM cells transfected with control siRNA, but not in those transfected with LSR specific siRNA. In the absence of PA, BGM cell infection caused plaque formation, but no destruction of the cell layer, irrespective of control or LSR specific siRNA.

[0081] **FIG. 3G:** Expression of LSR and ACE-2 mRNA expressed as Transcripts Per Million (TPM) in human nasal epithelium.

[0082] **FIG. 3H:** Expression of LSR and ACE-2 mRNA expressed as Transcripts Per Million (TPM) in human tongue.

[0083] **FIG. 3I:** After 30 min pre-incubation at room temperature of the SARS-CoV-2 with RBD-specific monoclonal antibodies Casirivimab and Imdevimab (C&I) (15+15 µg/ml) or irrelevant antibody Adalimumab (Ada or A) with SARS-CoV-2, 1 mM OA was added, and the entire mixture (10^7 particles per well) was transferred to BGM cell monolayers. Representative images obtained using phase contrast microscopy are shown of cells after 24h incubation at 37°C with the different conditions indicated.

[0084] **FIG. 3J:** Cells were incubated 24 h in the absence or presence (1E5 or 1E7) of virus mixed with C, I, or C& I in the absence of fatty acid as described for FIG. 3I. Box plots show the well protein content after washing.

[0085] **FIG. 3K:** Cells were incubated 24 h in the absence or presence (1E5 or 1E7) of virus mixed with C, I, or C& I in the presence of 1 mM OA as described for FIG. 3I. Box plots show the well protein content after washing.

[0086] **FIG. 3L:** Cell protein content (box plots) after 24 h following infection (150 min) without or with virus (10^7 particles/well) mixed with 0.4 mM OA or PA either alone, or with C&I or Ada as described for FIG. 3I.

[0087] **FIG. 3M:** Representative immunoblots performed to detect LSR, ACE2, and CD36 in BGM, Caco-2, and 4T1 cells. GAPDH was used as an internal control. Human adipocyte lysates were used as a positive control for CD36 AB.

[0088] **FIG. 3N:** A mixture of virus with Ada or C&I and 0.4 mM OA prepared as described for FIG. 3I were added to cells (150 min) at D3 post transfection with control or LSR siRNA. Cell layer protein levels were measured after 24 h incubation.

[0089] **FIG. 3O:** On D3 after treatment with control or LSR siRNA, BGM cells were infected with SARS-CoV-2 virus (10^4 particles/well) and incubated 150 min with virus and 1 mM OA. Cells were washed, and then exposed to 1 mM OA for 150 min on D1 and D2 as described in FIG. 2J. Viral production was measured at DPI4. Statistical significance is indicated as $*p < 0.05$, $**p < 0.01$, $***p < 0.001$.

[0090] **FIG. 3P:** Representative images of BGM cell layers 24 hours following no infection (top left panel), infection with SARS-CoV-2 (10^7 gec (genome equivalent copies), top right panel), with incubations with OA 1 mM without the virus (bottom left panel) or with OA 1 mM with C&I (15+15 µg/mL) (bottom right panel).

[0091] **FIG. 3Q:** BGM cells transfected with LSR or control si-RNA were infected with the SARS-CoV-2 (2.10^6 gec) on day three post-transfection. The infective media was removed after 150 minutes, and the SARS-CoV-2 copy numbers were measured at DPI4.

[0092] **FIG. 4A:** Shows a map of the SARS-CoV-2 spike annotated for its currently known functional domains. In addition, the amino acids (AA) indicative of the FFA pocket, the ACE2 binding domain and motif, the N terminal domain with the putative sites of ACE2 independent SARS-CoV-2 vulnerability and of infectivity enhancing antibodies, those targeted by Casirivimab and Imdevimab, the TMPRSS2 cleavage site and the two C terminal segments contributing to the fusion of the viral envelop with the cell membrane are indicated. In addition, the predicted AA involved in the interactions with S Protein and the LSR are also shown. The protein segments included in recombinant LBD1 and LBD2 are also shown.

[0093] **FIG. 4B:** Viral production in BGM with and without recombinant monomeric spike or nucleocapsid protein added to the infective media without FFA (gray) or using the O+2P (shaded) protocol.

[0094] **FIG. 4C:** Shows a three-dimensional model of the SARS-CoV-2 spike structure in closed and open conformation annotated for the ABD and the two segments constitutive of the LBD.

[0095] **FIG. 4D:** Representative 12% SDS-PAGE gels showing purified bands of LSR binding domains LBD1, LBD2, and LBDx revealed by Coomassie blue staining. The putative recombinant LSR binding domains (rLBD1 or LBD1 and rLBD2 or LBD2) (and rLBDx or LBDx) were produced and purified from *E. coli*.

[0096] **FIG. 4E:** Viral production of wild-type (Wuhan) strain in BGM infected without FFA (gray) or the O+2P protocol (black) in absence or presence rLBD1 (100 µg/ml) or rLBD2 (100 µg/mL). In cells infected according to the O+2P protocol, competition using either rLBD1 or rLBD2 lowered viral replication from 10^9 to

background levels. All measurements were in triplicate, and error bars indicate standard deviation (SD).

[0097] **FIG. 4F:** Similar competition experiments as shown in Fig. 4E were carried out infecting cells with the Delta variant. Delta variant was used to infect BGM cells without FFA (Gray) or using the O+2P protocol in absence or presence rLBD1 (100 µg/ml) or rLBD2 (100 µg/mL). In cells infected according to the O+2P protocol, competition using either rLBD1 or rLBD2 lowered viral replication the Delta variant by 6 logs.

[0098] **FIG. 4G:** Representative images of cell monolayers 24 h after 150 min infection with the SARS-CoV-2 (10^7 gec) mixed with C&I, 0.4 mM OA, and without LBDx (top) or with 100 µg/mL LBDx (bottom).

[0099] **FIG. 4H:** Protein content in wells incubated under the same conditions with the indicated LBDx concentration (no LBDx, 1 µg/mL, 10 µg/mL, or 100 µg/mL).

[00100] **FIG. 4I:** SARS-CoV-2 copy number at DPI4 in cells infected with 10^4 gec using the O+2P protocol and in the presence of increasing concentrations of LBDx maintained throughout the incubation period. Results are presented as % of maximal value; LBDx concentrations are shown on a log scale.

[00101] **FIG. 4J:** WT, Delta, and Omicron SARS-CoV-2 viral production at DPI4 following infection (10^4 gec) of BGM cells using the O+2P protocol as in FIG. 4I and the absence or presence of 100 µg/mL LBDx. Statistical significance is indicated as **$p<0.01$, ***$p<0.001$.

[00102] **FIG. 5A:** SARS-CoV-2 copy numbers in media of BGM infected with SARS-CoV-2 Delta variants isolated from three different patients and incubated without FFA (grey) or with the O+2P protocol (black).

[00103] **FIG. 5B:** SARS-CoV-2 copy numbers in media and cell layer in BGM infected with the indicated wild type SARS-CoV-2 and Delta variant each at two different infective dose (10^4 and 10^8 per well respectively) after incubation in the absence of FFA (grey) or using the O+2P protocol (black).

[00104] **FIG. 5C:** Shows SARS-CoV-2 copy numbers in media and cell layer of BGM infected with the indicated SARS-CoV-2 variant at two different infective doses (10^4 and

10^8 per well respectively) after incubation in the absence of FFA (grey) or using the O+2P protocol (black).

[00105] FIG. 5D: Shows the production of wild-type virus (Wuhan strain) and three variants of concern (VOC) when the infection was initiated at MOI=1 using either the ACE2 protocol, i.e., the No-FA-protocol, or the O+2P protocol. Strikingly, both the Beta and Delta variants replicated far less efficiently through the ACE2 than through the FA-activated receptor.

[00106] FIG. 5E: Shows the production of wild-type virus (Wuhan strain) produced in the media and in the cell layer for wild-type SARS-CoV-2 and three variants of concern (VOC) when the infection was initiated at MOI=1 using the ACE2 protocol, i.e. the No-FA-protocol, or the O+2P protocol. As in FIG. 5D, both the Beta and Delta variants (MOI=1) replicated far less efficiently through the ACE2 than through the FA-activated receptor.

[00107] FIG. 5F: Shows the production of wild-type virus (Wuhan strain) produced in the media and in the cell layer for wild-type SARS-CoV-2 and three variants of concern (VOC) when the infection was initiated at MOI=10,000 using the ACE2 protocol, i.e., the No-FA-protocol, or the O+2P protocol. Even starting with a much higher multiplicity of infection, it is clear that both the Beta and Delta variants replicated far less efficiently through the ACE2 than through the FA-activated receptor.

[00108] FIG. 5G: To further confirm that the ACE2- mediated replication of the Delta variant was less efficient than that of the WT SARS-CoV-2, HEK293T cells that did or did not overexpress the human ACE2 were used. In the absence of any FA supplementation, ACE2 overexpression increased by three logs the WT SARS-CoV-2 RNA copy numbers but did not change the Delta variant copy numbers. Accordingly, the data show that the FA-activated receptor is more efficient than the ACE2 for replicating the Delta variant.

[00109] FIG. 5H: BGM cells were infected 150 min with SARS-CoV-2 Delta or Omicron (10^7 gec) mixed with C&I and in the absence or presence of 0.4 mM OA or PA as described in FIG. 3L. After 24 h incubation, cell monolayer was washed and protein content was determined.

[00110] **FIG. 5I:** Parallel experiments were performed with SARS-CoV-2 Delta mixed with C&I, OA, or PA in the absence and presence of 100 µg/mL LBDx.

[00111] **FIG. 5J:** Representative images of cell monolayers 24 h after 150 min infection with the SARS-CoV-2(10^8 gec) without (top) with PA (0.4 mM) (middle) and with PA and LBDx (100 µg/mL, bottom).

[00112] **FIG. 5K:** BGM cells were infected with the WT SARS-CoV-2 (10^4 gec) in the absence of or presence of 1 mM OA for 150 min before replacing with fresh media. PA (0.4 mM) was added on DPI1, DPI 1 and 2, DPI 1, 2, and 3 for 150 min with media changes between incubations. The number of viral copies in the media 24 h after the last media replacement was measured.

[00113] **FIG. 5L:** Cells were infected 150 min with SARS-CoV-2 (10^4 gec) and treated with the No-FA or O+2P protocol and the indicated concentrations of nirmatrelvir.

[00114] **FIG. 5M:** Cells were infected 150 min with SARS-CoV-2 (10^4 gec) and treated with the No-FA or O+2P protocol and the indicated concentrations of ritonavir.

[00115] **FIG. 5N:** Cells were infected with SARS-CoV-2 WT mixed with C&I, 0.4 mM OA or PA (as in FIG. 5H), and in the absence of or presence of 100 µM nirmatrelvir or ritonavir. Protein levels in the wells were determined after 24 h incubation and cell washing.

[00116] **FIG. 5O:** Representative images of cell monolayers 24 h after infection (150 min) with the SARS-CoV-2 (10^7 gec) with PA (0.4 mM) (top row), the same with 10^8 gec and PA 0.4 mM (middle row) and with 10^8 gec, PA (0.4 mM PA) and LBDx (100 µg/mL) (bottom row). From columns left to right, WT, Delta, and Omicron SARS-CoV-2.

[00117] **FIG. 5P:** LSR and ACE2 expression in the indicated tissues determined from public databases as described in Materials and Methods and shown as TPM (transcripts per million).

[00118] **FIG. 6:** Presents a schematic representation of the ACE-2 and LSR contribution to wild type and Delta variant replication.

[00119] **FIG. 7** Shows the expression of LSR, ACE-2, and TMPRSS2 mRNA expressed as Transcripts Per Million (TPM) in VeroE6 cells and Calu3 cells. LSR expression vastly exceeds that of the ACE2 in these cell lines.

[00120] **FIG. 8A:** BGM cells were infected with the WT SARS-CoV-2 (10^4 gec) in the absence of presence of 1 mM OA for 150 min before replacing with fresh media. PA (0.4 mM) was added on DPI1 1, DPI 1, 2, and DPI 1,2,3 for 150 min with media changes between incubations. The number of viral copies in the media 24 h after the last media replacement was measured.

[00121] **FIG. 8B:** Representative images of cell monolayers 24 h after 150 min infection with the SARS-CoV2 (10^8 gec) without (top) with PA (0.4 mM) (middle) and with PA and LBDx (100 µg/mL, bottom).

[00122] **FIG. 8C:** BGM cells were infected 150 min with the indicated titers of SARS-CoV-2 in the absence or presence of 0.4 mM OA or PA. After 24 h incubation, cell monolayers were washed and protein content determined.

[00123] **FIG. 8D:** Cell protein content after BGM cells were infected 150 min with 10^8 gec of SARS-CoV-2 in the absence or presence of 0.4 mM PA without and with LBDx (50 µg/ml).

[00124] **FIG. 8E:** BGM cell were transfected with LSR or scrambled siRNA three days prior to infection. Cell protein content after BGM cells were infected 150 min with 10^8 gec of SARS-CoV-2 in the absence or presence of 0.4 mM PA without and with LBDx (50 µg/ml). Statistical significance is indicated as $^{**}p < 0.01$, $^{***}p < 0.001$.

[00125] **FIG. 8F:** Cell protein content after BGM cells were infected 150 min with 10^8 gec of Delta or Omicron variant in the absence or presence of 0.4 mM PA without and with LBDx (50 µg/ml). Statistical significance is indicated as $^{**}p < 0.01$, $^{***}p < 0.001$.

[00126] **FIG. 8G:** Cell protein content after BGM cells were infected 150 min with 10^8 gec of SARS-CoV-2 in the absence or presence of 0.4 mM PA without and with the indicated monoclonal antibodies (30 µg/ml).

[00127] **FIG. 8H:** Cells were infected 150 min with SARS-CoV-2 (10^4 gec) and treated with the No-FA or O+2P protocol and the indicated concentrations of nirmatrelvir top panel or ritonavir bottom panel. The viral RNA copy number was measured at DPI4.

[00128] **FIG. 8I:** Cell protein content after BGM cells were infected 150 min with 10^8 gec of SARS-CoV-2 in the absence or presence of 0.4 mM PA without and with nirmatrelvir or ritonavir (100 µM). Cell protein were measured in six independently treated wells.

[00129] **FIG. 9:** BGM cells were supplemented for 150 min without or with 5 µg/ml of virus free full length recombinant spike protein in absence or presence of OA (0.4mM) or PA (0.4 mM) without or with recombinant LBDx (100 µg/ml). The cell protein contents were determined after washing and each boxes show the results of 6 determination. Statistical significance is indicated as $^{**}p < 0.01$, $^{***}p < 0.001$.

DETAILED DESCRIPTION OF THE EMBODIMENTS

[00130] **Definitions**

[00131] Unless otherwise defined, all terms of art, notations and other scientific terminology used herein are intended to have the meanings commonly understood by those of skill in the art to which this disclosure pertains. In some cases, terms with commonly understood meanings are defined herein for clarity and/or for ready reference, and the inclusion of such definitions herein should not necessarily be construed to represent a difference over what is generally understood in the art. The techniques and procedures described or referenced herein are generally well understood and commonly employed using conventional methodologies by those skilled in the art, such as, for example, the widely utilized molecular cloning methodologies described in Sambrook *et al.*, *Molecular Cloning: A Laboratory Manual* 2nd ed. (1989) Cold Spring Harbor Laboratory Press, Cold Spring Harbor, NY. As appropriate, procedures involving the use of commercially available kits and reagents are generally carried out in accordance with manufacturer-defined protocols and conditions unless otherwise noted.

[00132] As used herein, the singular forms "a," "an," and "the," include the plural referents unless the context clearly indicates otherwise.

[00133] The term "about," as used herein, indicates and encompasses an indicated value and a range above and below that value. In one or more embodiments, the term "about" indicates the designated value ± 10%, ± 5%, or ± 1%. In one or more embodiments, the term "about" indicates the designated value ± one standard deviation of that value.

[00134] The term "combinations thereof," as used herein, includes every possible combination of elements to which the term refers to.

[00135] The term "coronavirus," as used herein, refers to enveloped viruses of the *Coronaviridae* family, comprising a large single-strand, positive-sense RNA genome (ranging from 26 to 32 kilobases in length) with 5'-cap and 3'- poly-A tail (see *e.g.*, Chen, Y., *et al.* (2020) J. of Med. Virol. 92:418-423). The term "coronavirus," includes members of the genera *alphacoronavirus*, *betacoronavirus*, *gammacoronavirus*, and *deltacoronavirus*. In one or more embodiments, a coronavirus is a *betacoronavirus*, selected from the group consisting of SARS-CoV-2, SARS-CoV, MERS-CoV, OC43, a bovine coronavirus, a feline coronavirus, and a porcine coronavirus. The term "live coronavirus," as used herein, refers a replication competent coronavirus.

[00136] The term "SARS-CoV-2," as used herein, refers to severe acute respiratory syndrome coronavirus 2. SARS-CoV-2 is a coronavirus of the genus *betacoronavirus*. The genome of the "wild-type" (Wuhan) strain is 29,903 bases in length and encodes 9860 amino acids (Wu, F., *et al.* Nature 579 (7798), 265-269 (2020); GenBank No. MN908947). SARS-CoV-2 is the causative agent of COVID-19 disease.

[00137] SARS-CoV-2 is highly infectious and has infected millions of people worldwide, thus producing the COVID-19 pandemic. SARS-CoV-2 infection can cause a variety of symptoms, which can range from about non-existent to severe. COVID-19 symptoms include, but are not limited to: fever or chills; cough; shortness of breath or difficulty breathing; fatigue; muscle or body aches; headache; new loss of taste or smell; sore throat; congestion or runny nose; nausea or vomiting; diarrhea; etc. Severe disease symptoms include, but are not limited to: severe inflammation and damage to endothelial cells in the heart, kidneys, liver, and intestines; trouble breathing; persistent pain or pressure in the chest; new confusion; inability to wake or stay awake; pale, gray, or blue-colored skin, lips, or nail beds, depending on skin tone, and death.

[00138] The term "SARS-CoV-2 spike protein," or "SARS-CoV-2 S protein," or "S protein," as used herein, refers to a protein having at least about 80% amino acid sequence identity, at least about 85%, 90%, 91%, 92%, 93%, 94%, 95%, 96%, 97%, 98%, 99%, or 100% identity to GenBank accession QHD43416.1 (SEQ ID NO: 1, *see also* UniProtKB - P0DTC2). Functional S protein assembles into trimers, which are able to interact with the receptors to gain entry into a cell to initiate infection. Thus, a "trimeric spike polypeptide" as used herein, refers to functionally assembled trimeric spike protein or fragment thereof, *e.g.*, an LBD, RBD, ABD, etc.

[00139] The term "immunogen," as used herein, refers to an antigen, which may be a peptide or protein, polysaccharide, or any other substance that is capable of stimulating an immune response, for example, by stimulating the production of antibodies. Not every antigen can evoke an immune response. Those antigens that are capable of inducing an immune response are said to be immunogenic and are referred to herein as immunogens. As will be discussed in detail below, the immunogenicity of an antigen can be enhanced by coupling the antigen with one or more Transcription Infidelity (TI) segments.

[00140] Thus, an "immunogenic composition," as used herein, refers to a composition comprising an immunogen, or a nucleic acid encoding an immunogen, that, when administered to a subject elicits an immune response in the subject.

[00141] The term "operably-linked," as used herein, refers to a functional linkage between two elements, regardless of orientation or distance between the two elements, such that the function of one element is controlled or affected by the other element. For example, operable linkage with reference to a promoter and heterologous coding sequence means that the transcription of the heterologous coding sequence is under the control of, or driven by, the promoter. In another example, operable linkage with reference to an enhancer and promoter means that the enhancer increases the level of transcription driven by a promoter.

[00142] A "heterologous coding sequence," as used herein, refers to nucleic acid sequence present in a polynucleotide, vector, or host cell that encodes a peptide or polypeptide, or a polynucleotide that itself has a function or activity, such as an antisense or inhibitory oligonucleotide, including antisense DNA and RNA (*e.g.*, miRNA, siRNA,

and shRNA), where the heterologous coding sequence is not naturally found in the polynucleotide, vector, or host cell, i.e. is non-native.

[00143] The term "expression control sequence," as used herein, refers to a sequence capable of effecting the expression of a nucleic acid molecule in a suitable host or under suitable *in vitro* conditions.

[00144] As will be discussed in detail below, the term "Transcription Infidelity (TI)," as used herein, refers to a mechanism that increases RNA and protein diversity. "Transcription Infidelity segments," or "TI segments," as used herein refers to short amino acid segments added to an antigen of interest which function to increase the immunogenicity of the antigen, thereby eliciting production of specific, high affinity antibodies to any selected antigen of interest, *e.g.*, SARS-CoV-2 spike protein or a fragment thereof, *e.g.*, LDB1, LBD, 2ABD, etc. Transcription Infidelity is known in the art. *See e.g.,* WO2008/009751; WO2017/158202; Atkins (2016) Nucleic Acids Res. 44(15): 707-778; Thouvenot, *et al.* (2020) The Journal of Clinical Investigation 130(10): 5477-5492.

[00145] The term "cellular entry," as used herein, refers broadly to the ability of SARS-CoV-2, or other coronavirus, to enter host cells. "Cellular entry" is typically initiated with binding of the SARS-CoV-2 spike protein to cell surface receptor(s). Bound SARS-CoV-2 subsequently enters endosomes, and eventually fuses viral and lysosomal membranes. Coronavirus entry into host cells is an important determinant of viral infectivity and pathogenesis.

[00146] The phrase "neutralizing entry," as used herein, refers to blocking or inhibiting cellular entry.

[00147] The term "inhibitor of entry," or "inhibitors that block cell entry," or "inhibitor of cellular entry," as used herein, refers to any substance or condition that prevents binding of a coronavirus, *e.g.*, a SARS-CoV-2, to its cellular entry receptor(s), thereby preventing the coronavirus from gaining entry to the interior of the cell where it would be able to replicate. In one or more embodiments, an "inhibitor of cellular entry" is a chemical substance such as, *e.g.*, lactoferrin, which inhibits cellular entry of the wild-type SARS-CoV-2 by both ACE2 and LSR. In one or more embodiments, an "inhibitor of cellular entry," is an antibody directed against the cellular entry receptor. In one or more

embodiments, an "inhibitor of cellular entry," is a siRNA directed against the cellular entry receptor. In one or more embodiments, an "inhibitor of cellular entry," is an antibody directed against an LBD or against an LBD and an ABD. The LSR is an endocytic receptor (see e.g., Bihain et al. (1992) Biochemistry 31(19):4628-36) while the ACE2 is a fusion receptor. In one or more embodiments endosome inhibitors e.g., chloroquine, are effective against SARS-CoV-2 that rely heavily on LSR for cellular entry, e.g., Delta and Omicron.

[00148] The term "ACE2 binding domain," or "ABD," as used herein, refers to a subdomain of the SARS-CoV-2 spike protein receptor-binding domain (RBD) that interacts with the ACE2 receptor. The ABD spans amino acid residues Y449 to Y505 of SEQ ID NO: 1.

[00149] The terms "FA," "FFA," "fatty acid," or "free fatty acid" as used herein, refer generally to both saturated and unsaturated fatty acids such as those disclosed herein e.g., palmitic acid, oleic acid, linoleic acid, stearic acid, heptanoic acid, octanoic acid, etc. The term "uFFA" may be used herein, to refer generally to an unsaturated fatty acid. Similarly, the term "sFFA" may be used herein, to refer generally to a saturated fatty acid.

[00150] The terms "palmitic acid," "palmitate," or "PA" are used interchangeably herein, to refer to hexadecanoic acid, a saturated straight-chain, sixteen-carbon fatty acid.

[00151] The terms "oleic acid," "oleate," or "OA" are used interchangeably herein, to refer to cis-9-octadecenoic acid, an eighteen-carbon monounsaturated omega-9 fatty acid.

[00152] The terms "linoleic acid," "linoleate," or "LA" are used interchangeably herein, to refer to (9Z,12Z)-octadeca-9,12-dienoate, an eighteen-carbon polyunsaturated omega 6 fatty acid.

[00153] The terms "stearic acid," "stearate," or "SA" are used interchangeably herein, to refer to octadecanoic acid, a straight-chain, eighteen carbon, saturated fatty acid.

[00154] The term "octanoate" as used herein, refers to an eight-carbon straight chain fatty acid.

[00155] The term "heptanoate" as used herein, refers to a seven-carbon straight chain fatty acid.

[00156] The term "ACE2 incompetent," as used herein, refers to a coronavirus, *e.g.*, a SARS-CoV-2, that has been exposed to a long-chain unsaturated fatty acid, *e.g.,* oleate or linoleate, such that they have lost their ability to bind their cognate receptor, ACE2. Accordingly, "ACE2 incompetent" coronavirus cannot use ACE2 for cellular entry and subsequent replication and therefore, uses one or more other receptors if the coronavirus is to gain cellular entry and replicate.

[00157] The term "ACE2 competent," as used herein, refers to coronavirus, *e.g.*, SARS-CoV-2, that are able to bind ACE2 to gain entry into the cell where subsequently they can replicate. In one or more embodiments, an "ACE2 competent" coronavirus, *e.g.*, SARS-CoV-2, has not been exposed to any FFA of any kind. In one or more embodiments, an "ACE2 competent" coronavirus has been exposed to a short, medium, or long-chain saturated fatty acid (sFFA).

[00158] The term "lipolysis stimulated receptor," or "LSR," as used herein, refers to a lipoprotein receptor primarily expressed in the liver. LSR undergoes conformational changes and is activated upon binding of free fatty acids. (*See e.g.,* OMIM 616582; GenBank BC047376; UniProtKB-Q86X29; Mann, et al. (1995) Biochemistry 34(33):10421-10431; Bihain, *et al.* (1999) J. Biol. Chem. 274(19):12951-13728; Yen, *et al.* (1999) J. Biol. Chem. 274: 13390-13398; Yen, et al., (2008) J. Biol. Chem. 283(37):25650-25659).

[00159] The term "LSR incompetent," as used herein, refers to a coronavirus, *e.g.*, SARS-CoV-2, that are not able to bind their activated cognate receptor, the lipolysis stimulated receptor (LSR). "LSR incompetent" coronavirus refers to properties of the virus and not the receptor. Thus, "LSR incompetent" SARS-CoV-2 may arise as a result of mutation at particular amino acid residues in LBD1 or LBD2, or as a result of mutations or modification at any amino acid position that interacts with an LSR, or which disrupts the fatty acid binding pocket.

[00160] The term "LSR competent," as used herein, refers to a coronavirus, *e.g.*, SARS-CoV-2, that are able to bind an activated LSR to gain entry into the cell where subsequently the SARS-CoV-2 can replicate. In one or more embodiments, an "LSR competent" SARS-CoV-2 has been exposed to a long-chain unsaturated fatty acid. In one

or more embodiments, the unsaturated fatty acid has a carbon-chain length of 18. In one or more embodiments, the unsaturated fatty acid is selected from oleate and linoleate.

[00161] The term "lipolysis-stimulated receptor binding domain," or "LBD," as used herein, refers to a subdomain of the SARS-CoV-2 spike protein that interacts with the Lipolysis Stimulated receptor (LSR). The spike protein comprises two LBD domains: LBD1 which spans amino acid residues P25 to P85 of SEQ ID NO: 1; and LBD2 which spans amino acid residues Q607 to S691 of SEQ ID NO: 1. In addition to LBD1 and LBD2, in one or more embodiments, the SARS-CoV-2 spike protein also interacts with the LSR at any one or more of amino acids R214, R237, Y269, K529, and/or N532.

[00162] The term "ACE2 protocol," as used herein, refers to SARS-CoV-2 that are either not pretreated with any free fatty acid, or which are pre-treated with palmitate prior to the initiation of infection of susceptible cells, wherein the treatment, or lack thereof, produces a SARS-CoV-2 that is capable of binding ACE2 to gain cell entry and replicate.

[00163] The term "O/P protocol," "oleate/palmitate protocol," or "O+2P protocol," or "O+2P" as used herein, refers to SARS-CoV-2 that are either pre-treated by exposure to oleate or which are exposed to oleate at the time of infection, to render the SARS-CoV-2 "ACE2 incompetent." Cells infected/incubated with "ACE2 incompetent" SARS-CoV-2 are then subsequently contacted with palmitate. Typically, cells are contacted with palmitate twice with an intervening incubation period between contacts as disclosed herein. As disclosed herein, an "O/P protocol" activates LSR allowing cellular entry by the SARS-CoV-2.

[00164] The term "ACE2 neutralizing activity," as used herein, refers to the ability of a substance, *e.g.*, an antibody, a chemical, an unsaturated free fatty acid, etc., to block cellular entry of SARS-CoV-2 via ACE2.

[00165] The term "LSR neutralizing activity," as used herein, refers to the ability of a substance, *e.g.*, lactoferrin, suramin, an antibody, etc., to block cellular entry/endocytosis of SARS-CoV-2 via LSR.

[00166] The term "immunizing," as used herein, refers to administering to a subject an immunogenic composition in order to induce an immune reaction in the subject. Administering may include contacting a subject with an immunogenic composition.

[00167] The term "severity of COVID-19 disease," as used herein, refers to the presentation of a range of clinical manifestations, from no symptoms to critical illness, wherein no symptoms is classified as mild disease and critical illness is severe disease. The presentation of symptoms along this spectrum is a manifestation of the severity of COVID-19 disease.

[00168] The term "long COVID-19 syndrome," or "post COVID-19 condition," as used herein, refers to the persistence of one or more symptoms of COVID-19 for weeks, months, or years after a subject or patient has, by measures other than the manifest symptoms, *e.g.*, negative PCR test, fought off the SARS-CoV-2 infection (*see e.g.*, Nalbandian et al., (2021) Nat. med. 27:601-615). According to the World health organization (WHO) "post COVID-19 condition" occurs in individuals with a history of probable or confirmed SARS CoV-2 infection, usually 3 months from the onset of COVID-19 with symptoms and that last for at least 2 months and cannot be explained by an alternative diagnosis. Common symptoms include fatigue, shortness of breath, cognitive dysfunction and also others and generally have an impact on everyday functioning. Symptoms may be new onset following initial recovery from an acute COVID-19 episode or persist from the initial illness. Symptoms may also fluctuate or relapse over time (*see* WHO/2019-nCoV/Post_COVID-19_condition/Clinical_case_definition/2021.1).

[00169] The term "transmission of SARS-CoV-2," as used herein, refers to the person-to-person transfer of SARS-CoV-2. Person-to-person respiratory transfer of SARS-CoV-2 is the primary means of transmission. Secondary transmission routes may include physical contact with surfaces contaminated by respiratory secretions followed by touching eyes, nose, or mouth. The risk of transmission from an individual with SARS-CoV-2 infection varies by the type and duration of exposure, use of preventive measures, and individual factors such as the amount of virus in respiratory secretions.

[00170] Thus, the phrase "reduction of transmission," as used herein, refers to reduced probability that a subject who is infected with SARS-CoV-2 will successfully transfer SARS-CoV-2 to another person. Typically, a reduction of transmission is brought about by a treatment or intervention, *e.g.*, by vaccination, by treatment with monoclonal antibodies. Therefore, the phrase "reduction of transmission" is a relative term wherein reduction is measured in a treated individual and compared to untreated individuals, or to a treated individual at an initial time point compared to a subsequent time point.

[00171] The term "pseudovirus," or "pseudoparticle," (or plural form) as used herein, refers to a chimeric virus, having a core set of genes for viral packaging which are derived from one virus, and one or more genes that express surface proteins, which are derived from another virus. "Pseudoviruses" may also comprise one or more genes expressing a reporter such a green fluorescent protein. For example, an HIV-1 packaging system incorporating luciferase reporter can be co-transfected into cells e.g., HEK293T cells, together with a plasmid that expresses S protein and/or variants thereof. Once inside the cell, the HIV packaging proteins are expressed as is the S protein. Packaging proteins package the DNA, including DNA comprising any reporter genes, into viral particles that express the S protein on the surface. The surface expressed S protein mediates viral entry in a fashion similar to that of the wild type virus. Pseudoviruses are known in the art *see e.g.*, Chen, M., *et al.* (2021) Int. J. Biol. Sci. Vol. 17: 1574-1580; Yang, et al. (2020) Biosaf Health. 2(4): 226–231. In one or more embodiments, the reporter is an RNA encoded reporter. RNA reporters are typically used for endocytic receptors such as the LSR. Please also include the use single- cycle replicon. See attached paper

[00172] The term "therapeutic agent," as used herein, refers to a drug, protein, peptide, gene, compound or other pharmaceutically active ingredient.

[00173] The term "pharmaceutically effective amount," or "therapeutically effective amount," or "effective amount," as used herein, refers to the amount of a composition that will elicit a biological or medical response of a tissue, system, or subject that is being sought by a researcher, veterinarian, medical doctor, or other clinician. Thus, a "pharmaceutically effective amount" is effective to treat a disease or disorder. The term "therapeutically effective amount," includes that amount of a composition that, when administered, is sufficient to prevent development of, or alleviate at least to some extent, one or more of the signs or symptoms of the disorder or disease (*e.g.*, COVID-19) being treated. In one or more embodiments, an "effective amount," is sufficient to reduce transmission of a disease-causing organism, *e.g.*, SARS-CoV-2. In one or more embodiments, a pharmaceutically effective amount or effective amount refers to an amount of an antibody or composition, *e.g.*, an immunogenic composition, that when administered to a subject is effective to prevent or ameliorate a disease or the progression of the disease, or reduce transmission of a disease-causing organism, *e.g.*, SARS-CoV-2. The

therapeutically effective amount will vary depending on the composition, the disease and its severity and the age, weight, etc., of the subject being treated.

[00174] The term "immunoglobulin," as used herein, refers to a class of structurally related proteins generally comprising two pairs of polypeptide chains: one pair of light (L) chains and one pair of heavy (H) chains. In an "intact immunoglobulin," all four of these chains are interconnected by disulfide bonds. The structure of immunoglobulins is well characterized. *See, e.g.,* Paul, *Fundamental Immunology* 7th ed., Ch. 5 (2013) Lippincott Williams & Wilkins, Philadelphia, PA. Briefly, each heavy chain typically comprises a heavy chain variable region (V_H) and a heavy chain constant region (C_H). The heavy chain constant region typically comprises three domains, abbreviated C_{H1}, C_{H2}, and C_{H3}. Each light chain typically comprises a light chain variable region (V_L) and a light chain constant region. The light chain constant region typically comprises one domain, abbreviated C_L.

[00175] The term "antibody," as used herein, refers to a type of immunoglobulin molecule and is used herein in its broadest sense. An antibody specifically includes intact antibodies (*e.g.*, intact immunoglobulins), and antibody fragments. Antibodies comprise at least one antigen-binding domain. One example of an antigen-binding domain is an antigen-binding domain formed by a V_H -V_L dimer.

[00176] The V_H and V_L regions may be further subdivided into regions of hypervariability ("hypervariable regions (HVRs);" also called "complementarity determining regions" (CDRs)) interspersed with regions that are more conserved. The more conserved regions are called framework regions (FRs). Each V_H and V_L generally comprises three CDRs and four FRs, arranged in the following order (from N-terminus to C-terminus): FR1 - CDR1 - FR2 - CDR2 - FR3 - CDR3 - FR4. The CDRs are involved in antigen binding, and influence antigen specificity and binding affinity of the antibody. See Kabat *et al.*, *Sequences of Proteins of Immunological Interest* 5th ed. (1991) Public Health Service, National Institutes of Health, Bethesda, MD, incorporated by reference in its entirety.

[00177] The light chain from any vertebrate species can be assigned to one of two types, called kappa and lambda, based on the sequence of the constant domain.

[00178] The heavy chain from any vertebrate species can be assigned to one of five different classes (or isotypes): IgA, IgD, IgE, IgG, and IgM. These classes are also

designated α, δ, ε, γ, and μ, respectively. The IgG and IgA classes are further divided into subclasses based on differences in sequence and function. Humans express the following subclasses: IgG1, IgG2, IgG3, IgG4, IgA1, and IgA2.

[00179] The amino acid sequence boundaries of a CDR can be determined by one of skill in the art using any of a number of known numbering schemes, including those described by Kabat *et al.*, *supra* ("Kabat" numbering scheme); Al-Lazikani *et al.*, 1997, *J. Mol. Biol.*, 273:927-948 ("Chothia" numbering scheme); MacCallum *et al.*, 1996, *J. Mol. Biol.* 262:732-745 ("Contact" numbering scheme); Lefranc *et al.*, *Dev. Comp. Immunol.*, 2003, 27:55-77 ("IMGT" numbering scheme); and Honegge and Plückthun, *J. Mol. Biol.*, 2001, 309:657-70 ("AHo" numbering scheme), each of which is incorporated by reference in its entirety.

[00180] CDRs may be assigned, for example, using antibody numbering software, such as Abnum, available at www.bioinf.org.uk/abs/abnum/, and described in Abhinandan and Martin, *Immunology*, 2008, 45:3832-3839, incorporated by reference in its entirety.

[00181] The term "antigen-binding fragment," or "antibody fragment," as used herein, refers to a portion of an intact antibody, such as the antigen binding or variable region of an intact antibody. Antibody fragments include, for example, Fv fragments, Fab fragments, F (ab')$_2$ fragments, Fab' fragments, scFv (sFv) fragments, and scFv-Fc fragments.

[00182] "Fv" fragments comprise a non-covalently linked dimer of one heavy chain variable domain and one light chain variable domain.

[00183] "Fab" fragments comprise, in addition to the heavy and light chain variable domains, the constant domain of the light chain and the first constant domain (C_{H1}) of the heavy chain. Fab fragments may be generated, for example, by recombinant methods or by papain digestion of a full-length antibody.

[00184] "F(ab')$_2$" fragments contain two Fab' fragments joined, near the hinge region, by disulfide bonds. F(ab')$_2$ fragments may be generated, for example, by recombinant methods or by pepsin digestion of an intact antibody. The F(ab') fragments can be dissociated, for example, by treatment with ß-mercaptoethanol.

[00185] "Single-chain Fv" or "sFv" or "scFv" antibody fragments comprise a V_H domain and a V_L domain in a single polypeptide chain. The V_H and V_L are generally linked

by a peptide linker. *See* Plückthun A. (1994) Antibodies from *Escherichia coli*. In Rosenberg M. & Moore G.P. (Eds.), *The Pharmacology of Monoclonal Antibodies* vol. 113 (pp. 269-315). Springer-Verlag, New York, incorporated by reference in its entirety.

[00186] "scFv-Fc" fragments comprise an scFv attached to an Fc domain. For example, an Fc domain may be attached to the C-terminus of the scFv. The Fc domain may follow the V_H or V_L, depending on the orientation of the variable domains in the scFv (i.e., V_H-V_L or V_L-V_H). Any suitable Fc domain known in the art or described herein may be used. In some cases, the Fc domain comprises an IgG1 Fc domain.

[00187] The term "monoclonal antibody," as used herein, refers to an antibody from a population of substantially homogeneous antibodies. A population of substantially homogeneous antibodies comprises antibodies that are substantially similar and that bind the same epitope(s), except for variants that may normally arise during production of the monoclonal antibody. Such variants are generally present in only minor amounts. A monoclonal antibody is typically obtained by a process that includes the selection of a single antibody from a plurality of antibodies. For example, the selection process can be the selection of a clone from a plurality of clones, such as a pool of hybridoma clones, phage clones, yeast clones, bacterial clones, or other recombinant DNA clones. The selected antibody can be further altered, for example, to improve affinity for the target ("affinity maturation"), to humanize the antibody, to improve its production in cell culture, and/or to reduce its immunogenicity in a subject.

[00188] The term "polyclonal antibody," as used herein, refers to antibody that is actually a collection of antibodies, created as an immune response in an animal by immunization with an antigen, that bind multiple epitopes of that antigen. Polyclonal antibodies are inexpensive and relatively quick to produce (+/- 3 months), show a high overall antibody affinity against the antigen due to the recognition of multiple epitopes, and thus have a high sensitivity for detecting low-quantity proteins.

[00189] The term "chimeric antibody," as used herein, refers to an antibody in which a portion of the heavy and/or light chain is derived from a particular source or species, while the remainder of the heavy and/or light chain is derived from a different source or species.

[00190] "Humanized" forms of non-human antibodies are chimeric antibodies that contain minimal sequence derived from the non-human antibody. A humanized antibody is

generally a human immunoglobulin (recipient antibody) in which residues from one or more CDRs are replaced by residues from one or more CDRs of a non-human antibody (donor antibody). The donor antibody can be any suitable non-human antibody, such as a mouse, rat, rabbit, chicken, or non-human primate antibody having a desired specificity, affinity, or biological effect. In some instances, selected framework region residues of the recipient antibody are replaced by the corresponding framework region residues from the donor antibody. Humanized antibodies may also comprise residues that are not found in either the recipient antibody or the donor antibody. Such modifications may be made to further refine antibody function. For further details, *see e.g.,* Jones *et al*., *Nature*, 1986, 321:522-525; Riechmann *et al*., *Nature*, 1988, 332:323-329; and Presta, *Curr. Op. Struct. Biol.*, 1992, 2:593-596.

[00191] A "human antibody" is one which possesses an amino acid sequence corresponding to that of an antibody produced by a human or a human cell or derived from a non-human source that utilizes a human antibody repertoire or human antibody-encoding sequences (*e.g.*, obtained from human sources or designed *de novo*). Human antibodies specifically exclude humanized antibodies.

[00192] The term "isolated," as used herein, refers to a substance that has been separated and/or recovered from its natural environment. For example, a naturally occurring polynucleotide or polypeptide present in a living animal is not isolated, but the same polynucleotide or polypeptide, separated from some or all of the co-existing materials in the natural system, is isolated. Such polynucleotide could be part of a vector and/or such polynucleotide or polypeptide could be part of a composition (*e.g.*, a cell lysate), and still be isolated in that such vector or composition is not part of the natural environment for the nucleic acid or polypeptide.

[00193] Thus, an "isolated antibody," as used herein, refers to an antibody that is one that has been separated and/or recovered from at least one component of its natural environment *e.g.*, enzymes, hormones, and other proteinaceous or nonproteinaceous materials. In one or more embodiments, an isolated antibody is purified to a degree sufficient to obtain at least 15 residues of N-terminal or internal amino acid sequence, for example by use of a spinning cup sequenator. In one or more embodiments, an isolated antibody is purified to homogeneity by gel electrophoresis (*e.g.*, SDS-PAGE) under reducing or nonreducing conditions, with detection by Coomassie blue or silver stain. An

isolated antibody includes an antibody *in situ* within recombinant cells, since at least one component of the antibody's natural environment is not present. In some aspects, an isolated antibody is prepared by at least one purification step.

[00194] In one or more embodiments, an isolated antibody is purified to at least 80%, 85%, 90%, 95%, or 99% by weight. In one or more embodiments, an isolated antibody is purified to at least 80%, 85%, 90%, 95%, or 99% by volume. In one or more embodiments, an isolated antibody is provided as a solution comprising at least 85%, 90%, 95%, 98%, 99% to 100% by weight. In one or more embodiments, an isolated antibody is provided as a solution comprising at least 85%, 90%, 95%, 98%, 99% to 100% by volume.

[00195] An "affinity matured" antibody is one with one or more alterations in one or more CDRs or FRs that result in an improvement in the affinity of the antibody for its antigen, compared to a parent antibody which does not possess the alteration(s). In one or more embodiments, an affinity-matured antibody has nanomolar or picomolar affinity for the target antigen. Affinity matured antibodies may be produced using a variety of methods known in the art. For example, Marks *et al.* (*Bio/ Technology*, 1992, 10:779-783, incorporated by reference in its entirety) describes affinity maturation by V_H and V_L domain shuffling. Random mutagenesis of CDR and/or framework residues is described by, for example, Barbas *et al.*, *Proc. Nat. Acad. Sci. U.S.A.*, 1994, 91:3809-3813; Schier *et al.*, *Gene*, 1995, 169:147-155; Yelton *et al.*, *J. Immunol.*, 1995, 155:1994-2004; Jackson *et al.*, *J. Immunol.*, 1995, 154:3310-33199; and Hawkins *et al*, *J. Mol. Biol.*, 1992, 226:889-896, each of which is incorporated by reference in its entirety.

[00196] The term "epitope," as used herein, refers to a portion of an antigen capable of specific binding to an antibody. Epitopes frequently consist of surface-accessible amino acid residues and/or sugar side chains and may have specific three-dimensional structural characteristics, as well as specific charge characteristics. Conformational and non-conformational epitopes are distinguished in that the binding to the former but not the latter is lost in the presence of denaturing solvents. An epitope may comprise amino acid residues that are directly involved in the binding, and other amino acid residues, which are not directly involved in the binding. The epitope to which an antibody binds can be determined using known techniques for epitope determination such as, for example, testing for antibody binding to variants of a lipolysis stimulated receptor-binding domain (LBD) of a SARS-CoV-2 spike protein with different point-mutations.

[00197] "Affinity" refers to the strength of the sum total of non-covalent interactions between a single binding site of a molecule (*e.g.*, a receptor or antibody) and its binding partner (*e.g.*, ligand or antigen). Unless indicated otherwise, as used herein, "binding affinity" refers to intrinsic binding affinity, which reflects a 1:1 interaction between members of a binding pair (*e.g.*, receptor and ligand). The affinity of a molecule X for its partner Y can be represented by the dissociation constant (K_D). Affinity can be measured by common methods known in the art, for example, using surface plasmon resonance (SPR) technology, such as a Biacore® instrument. In one or more embodiments, the affinity is determined at 25°C.

[00198] With regard to the binding of receptor to a target molecule (ligand), the terms "specific," "specific binding," "specifically binds to," "specific for," "selectively binds," or "selective for," as used herein, refers to a particular receptor or ligand that exhibits binding that is measurably different from a non-specific or non-selective interaction. Specific binding can be measured, for example, by determining binding of a molecule compared to binding of a control molecule. Specific binding can also be determined by competition with a control molecule that competes with the ligand for binding to the receptor. In that case, specific binding is indicated if the binding of the ligand to the receptor is competitively inhibited by the control molecule.

[00199] The term "k_d" (sec^{-1}), as used herein, refers to the dissociation rate constant of a particular receptor-ligand interaction. This value is also referred to as the k_{off} value.

[00200] The term "k_a" ($M^{-1} \times sec^{-1}$), as used herein, refers to the association rate constant of a particular receptor-ligand interaction. This value is also referred to as the k_{on} value.

[00201] The term "K_D" (M), as used herein, refers to the dissociation equilibrium constant of a particular receptor-ligand interaction. $K_D = k_d/k_a$.

[00202] The term "K_A" (M^{-1}), as used herein, refers to the association equilibrium constant of a particular receptor-ligand interaction. $K_A = k_a/k_d$.

[00203] The terms "identical," or "percent identity," in the context of two or more polypeptide or nucleic acid molecule sequences, means two or more sequences or subsequences that are the same or have a specified percentage of amino acid residues or nucleotides that are the same over a specified region (*e.g.*, 60%, 65%, 70%, 75%, 80%,

85%, 90%, 91%, 92%, 93%, 94%, 95%, 96%, 97%, 98%, 99%, or 100% identity), when compared and aligned for maximum correspondence over a comparison window, or designated region, as measured using methods known in the art, such as a sequence comparison algorithm, by manual alignment, or by visual inspection. Alignment for purposes of determining percent amino acid sequence identity can be achieved in various ways that are within the skill in the art, for instance, using publicly available computer software such as BLAST (Altschul *et al*. Nucleic Acids Res. 2007, 25, 3389-3402), BLAST-2, ALIGN, MEGALIGN (DNASTAR), CLUSTALW, CLUSTAL OMEGA, or MUSCLE software. Those skilled in the art can determine appropriate parameters for aligning sequences, including any algorithms needed to achieve maximal alignment over the full length of the sequences being compared. Within the context of this disclosure, it is understood that where sequence analysis software is used for analysis, the results of the analysis are based on the "default values" of the program referenced. "Default values" mean any set of values or parameters which originally load with the software when first initialized.

[00204] A “conservative substitution,” or a “conservative amino acid substitution,” as used herein, refers to the substitution of an amino acid with a chemically or functionally similar amino acid. Conservative substitution tables providing similar amino acids are well known in the art. Polypeptide sequences having such substitutions are known as “conservatively modified variants.” Such conservatively modified variants are in addition to and do not exclude polymorphic variants, interspecies homologs, and alleles. By way of example, the groups of amino acids provided in Tables 1-3 are, in one or more embodiments, considered conservative substitutions for one another.

[00205] **Table 1.** Selected groups of amino acids that are considered conservative substitutions for one another, in one or more embodiments.

Acidic Residues	D and E
Basic Residues	K, R, and H
Hydrophilic Uncharged Residues	S, T, N, and Q
Aliphatic Uncharged Residues	G, A, V, L, and I
Non-polar Uncharged Residues	C, M, and P
Aromatic Residues	F, Y, and W
Alcohol Group-Containing Residues	S and T
Aliphatic Residues	I, L, V, and M
Cycloalkenyl-associated Residues	F, H, W, and Y
Hydrophobic Residues	A, C, F, G, H, I, L, M, R, T, V, W, and Y

Negatively Charged Residues	D and E
Polar Residues	C, D, E, H, K, N, Q, R, S, and T
Positively Charged Residues	H, K, and R
Small Residues	A, C, D, G, N, P, S, T, and V
Very Small Residues	A, G, and S
Residues Involved in Turn Formation	A, C, D, E, G, H, K, N, Q, R, S, P, and T
Flexible Residues	Q, T, K, S, G, P, D, E, and R

[00206] **Table 2.** Additional selected groups of amino acids that are considered conservative substitutions for one another, in one or more embodiments.

Group 1	A, S, and T
Group 2	D and E
Group 3	N and Q
Group 4	R and K
Group 5	I, L, and M
Group 6	F, Y, and W

[00207] **Table 3.** Further selected groups of amino acids that are considered conservative substitutions for one another, in one or more embodiments.

Group A	A and G
Group B	D and E
Group C	N and Q
Group D	R, K, and H
Group E	I, L, M, V
Group F	F, Y, and W
Group G	S and T
Group H	C and M

[00208] Additional conservative substitutions may be found, for example, in Creighton, *Proteins: Structures and Molecular Properties* 2nd ed. (1993) W. H. Freeman & Co., New York, NY. A polypeptide or protein generated by making one or more conservative substitutions of amino acid residues in a parent polypeptide or protein is referred to as a "conservatively modified variant."

[00209] The term "amino acid," as used herein, refers to the twenty common naturally occurring amino acids**.** Naturally occurring amino acids include alanine (Ala; A), arginine (Arg; R), asparagine (Asn; N), aspartic acid (Asp; D), cysteine (Cys; C); glutamic acid (Glu; E), glutamine (Gln; Q), Glycine (Gly; G); histidine (His; H), isoleucine (Ile; I), leucine (Leu; L), lysine (Lys; K), methionine (Met; M), phenylalanine (Phe; F), proline (Pro; P), serine (Ser; S), threonine (Thr; T), tryptophan (Trp; W), tyrosine (Tyr; Y), and valine (Val; V).

[00210] Naturally encoded amino acids are the proteinogenic amino acids known to those of skill in the art. They include the 20 common amino acids (alanine, arginine, asparagine, aspartic acid, cysteine, glutamine, glutamic acid, glycine, histidine, isoleucine, leucine, lysine, methionine, phenylalanine, proline, serine, threonine, tryptophan, tyrosine, and valine) and the less common pyrrolysine and selenocysteine. Naturally encoded amino acids include post-translational variants of the 22 naturally occurring amino acids such as prenylated amino acids, isoprenylated amino acids, myrisoylated amino acids, palmitoylated amino acids, N-linked glycosylated amino acids, O-linked glycosylated amino acids, phosphorylated amino acids and acylated amino acids.

[00211] "Treating" or "treatment" of any disease or disorder *e.g.*, COVID-19, refers, in one or more embodiments, to ameliorating the disease or disorder that exists in a subject. In one or more embodiments, "treating," or "treatment," includes ameliorating at least one physical parameter, which may be indiscernible by the subject. In one or more embodiments, "treating," or "treatment," includes modulating the disease or disorder, either physically (*e.g.*, stabilization of a discernible symptom) or physiologically (*e.g.*, stabilization of a physical parameter) or both. In one or more embodiments, "treating," or "treatment," includes delaying or preventing the onset of the disease or disorder.

[00212] The term "subject," as used herein, refers to a mammalian subject. Exemplary subjects include, but are not limited to humans, monkeys, dogs, cats, mice, rats, cows, pigs, horses, camels, avians, goats, and sheep. In one or more embodiments, the subject is a human. In one or more embodiments, the subject has a disease that can be treated or diagnosed with an antibody provided herein.

[00213] I. Introduction

[00214] SARS-CoV-2 is a highly infectious coronavirus that threatens global public health. SARS-CoV-2 is the causative agent of COVID-19, and thus, is the cause of an ongoing worldwide pandemic. According to the World Health Organization (WHO) as of October 2021, SARS-CoV-2 has infected more than 237 million people worldwide, has led to more than 4.8 million deaths globally, and to uncounted numbers of long COVID-19 syndrome, which can be disabling.

[00215] The Angiotensin-Converting Enzyme 2 (ACE2) that delivers SARS-CoV-2 RNA into the cytoplasm was heretofore the sole known SARS-CoV-2 receptor. However,

as disclosed herein, another SARS-CoV-2 receptor, the Lipolysis Stimulated Receptor (LSR), has now been discovered to provide a second endocytic route equally effective for the replication of the SARS-CoV-2. Like ACE2, the LSR interacts with SARS-CoV-2 through the SARS-CoV-2 spike (S) protein. Accordingly, S protein comprises at least two binding domains for interaction with LSR.

[00216] Consistent with the finding that LSR functions as lipoprotein receptor only when activated by FFA (*see e.g.*, Mann, et al. (1995); Bihain, *et al.* (1999); Yen, *et al.* (1999); Yen, et al., (2008) *supra*) the LSR interacts with SARS-CoV-2 spike only when activated by free fatty acids (FFA). Thus, the coordinated use by SARS-CoV-2 of the ACE2 and LSR receptors for cellular entry and replication is coordinated by fatty acids. Both saturated and unsaturated FFA enable LSR mediated viral uptake, but as is demonstrated in Example 2, only saturated FFA cause immediate viral replication. Furthermore, as demonstrated herein, unsaturated FFA irreversibly suppress the ability of S protein to bind ACE2, thus inhibiting replication by the ACE2 mediated pathway (*see* Example 1, below).

[00217] The LSR, activated by FFA, endocytoses both ACE2 competent and ACE2 incompetent SARS-CoV-2, yielding immediate or delayed production of ACE2 competent progeny. Without being bound by theory it is believed that the LSR may deliver SARS-CoV-2 into a replicative or a latent compartment and does not immediately deliver its cargo to the compartment where viral RNA is transferred to the cytoplasm (*see* Example 4, below).

[00218] The discovery of a second entry receptor, regulated by fatty acids, that delivers the virus into a replicative or a latent compartment sheds new light on the mechanisms of viral spreading and the diversity of the clinical outcomes of this infection. For example, the discovery of a replicative or a latent compartment might help explain the observation that the virus is detected in the intestine of 7 out of 14 convalescent asymptomatic patients four months after moderate COVID-19.

[00219] Furthermore, FFA concentrations needed to suppress SARS-CoV-2 binding to ACE2 or to activate the LSR *in vitro* are below those found in the intestine at endothelial sites of lipolysis or even in the plasma of patients with severe disease. In these patients, intestinal concentrations of FFA ranged between 0.5 mM and 5 mM. These concentrations

are likely to suppress ACE2 mediated viral replication and activate the LSR. Accordingly, the LSR may become the dominant receptor for cell entry in late stage disease.

[00220] Excessive dietary fat is the common factor associated with the four main comorbidities increasing COVID-19 severity i.e., obesity, diabetes, hypertension, and cardiovascular diseases. The increased viral replication induced by palmitate (see Example 2, below) provides an explanation for the observation that the excessive consumption of saturated fat contributes to all four comorbidities. Very high FFA concentrations are found in patients with severe COVID-19 (*see* Example 8, below). As noted above, in patients with severe COVID-19, the FFA concentrations are such that it is unlikely that the SARS-CoV-2 can bind to the ACE2. The loss of such critical function is compensated by an alternative route of viral entry, otherwise lipid infusions would cure COVID-19. Therefore, without being bound by theory, it is believed that the ACE2 provides a first line of entry, and that the virus relies on the LSR when confronted with conditions, such as high FFA concentrations, that suppress the ACE2 binding.

[00221] Although current vaccines effectively reduce COVID-19 severity, and significantly reduce elderly mortality, secondary infections do occur, and vaccinated individuals who are infected with SARS-CoV-2 are still capable of transmitting the virus to others. As a result, the pandemic shows few signs of regression. Accordingly, it is likely that to cure COVID-19, and suppress viral transmission, both the ACE2 and LSR routes of viral entry must be neutralized.

[00222] II. SARS-CoV-2 and other coronaviruses

[00223] Coronaviruses (CoVs) are enveloped viruses of the *Coronaviridae* family, comprising a large single-strand, positive-sense RNA genome (ranging from 26 to 32 kilobases in length) with 5'-cap and 3'-poly-A tail. A member of the *Coronaviridae* family, the *betacoronavirus* SARS-CoV-2, has a genome that is about 29,903 bases in length and encodes 9860 amino acids (Wuhan strain; Wu, F., *et al.* Nature 2020, *supra*). SARS-CoV-2 is the causative agent of COVID-19, and as such is a major threat to public health.

[00224] A number of SARS-CoV-2 are known in the art *see e.g.,* Aleem et al. (2022). *Emerging Variants of SARS-CoV-2 And Novel Therapeutics Against Coronavirus (COVID-19).* 2022 Feb 6. In: StatPearls [Internet]. Treasure Island (FL): StatPearls Publishing; 2022

Jan–. PMID: 34033342. Some variants are of concern (variants of concern or VOC) because they are prone to causing more severe disease, are more contagious, or both, or because they pose other risks to the human population. Exemplary variants of concern include but are not limited to the Alpha variant (see e.g., GenBank: MZ344997.1; Washington N.L., et al (2021) *Genomic epidemiology identifies emergence and rapid transmission of SARS-CoV-2 B.1.1.7 in the United States*. MedRxiv. 2021 doi: 10.1101/2021.02.06.21251159. 2021.02.06.21251159), the Beta variant (*see e.g.*, GenBank: MW598419.1), the Gamma variant (*see e.g.*, GenBank: MZ169911.1), Delta variant (*see e.g.*, GenBank: MZ359841.1); the Omicron variant BA.1 (*see e.g.*, GenBank: OL672836.1) and Omicron BA.2 (*see e.g.*, GenBank: OM296922.1).

[00225] The host receptors for SARS-CoV-2 cell entry include the angiotensin-converting enzyme 2 (ACE2), and as disclosed herein, Lipolysis Stimulated Receptor, LSR. SARS-CoV-2 binds to its cognate receptors through the discrete receptor-binding domains of its spike protein.

[00226] **A. 1. Spike protein**

[00227] The SARS-CoV-2 S gene encodes a 1273 amino acid protein which assembles into trimers on the virion surface. Trimeric spike proteins create the characteristic crown-like appearance or corona. A large number of glycosylated S proteins cover the surface of SARS-CoV-2 and bind to host cell receptors that mediate viral cell entry.

[00228] The amino acid sequence of the wild-type (Wuhan strain) S protein is provided below as SEQ ID NO: 1.

MFVFLVLLPL VSSQCVNLTT RTQLPPAYTN SFTRGVYYPD KVFRSSVLHS
TQDLFLPFFS NVTWFHAIHV SGTNGTKRFD NPVLPFNDGV YFASTEKSNI
IRGWIFGTTL DSKTQSLLIV NNATNVVIKV CEFQFCNDPF LGVYYHKNNK
SWMESEFRVY SSANNCTFEY VSQPFLMDLE GKQGNFKNLR EFVFKNIDGY
FKIYSKHTPI NLVRDLPQGF SALEPLVDLP IGINITRFQT LLALHRSYLT
PGDSSSGWTA GAAAYYVGYL QPRTFLLKYN ENGTITDAVD CALDPLSETK
CTLKSFTVEK GIYQTSNFRV QPTESIVRFP NITNLCPFGE VFNATRFASV
YAWNRKRISN CVADYSVLYN SASFSTFKCY GVSPTKLNDL CFTNVYADSF
VIRGDEVRQI APGQTGKIAD YNYKLPDDFT GCVIAWNSNN LDSKVGGNYN
YLYRLFRKSN LKPFERDIST EIYQAGSTPC NGVEGFNCYF PLQSYGFQPT

NGVGYQPYRV VVLSFELLHA PATVCGPKKS TNLVKNKCVN FNFNGLTGTG
VLTESNKKFL PFQQFGRDIA DTTDAVRDPQ TLEILDITPC SFGGVSVITP
GTNTSNQVAV LYQDVNCTEV PVAIHADQLT PTWRVYSTGS NVFQTRAGCL
IGAEHVNNSY ECDIPIGAGI CASYQTQTNS PRRARSVASQ SIIAYTMSLG
AENSVAYSNN SIAIPTNFTI SVTTEILPVS MTKTSVDCTM YICGDSTECS
NLLLQYGSFC TQLNRALTGI AVEQDKNTQE VFAQVKQIYK TPPIKDFGGF
NFSQILPDPS KPSKRSFIED LLFNKVTLAD AGFIKQYGDC LGDIAARDLI
CAQKFNGLTV LPPLLTDEMI AQYTSALLAG TITSGWTFGA GAALQIPFAM
QMAYRFNGIG VTQNVLYENQ KLIANQFNSA IGKIQDSLSS TASALGKLQD
VVNQNAQALN TLVKQLSSNF GAISSVLNDI LSRLDKVEAE VQIDRLITGR
LQSLQTYVTQ QLIRAAEIRA SANLAATKMS ECVLGQSKRV DFCGKGYHLM
SFPQSAPHGV VFLHVTYVPA QEKNFTTAPA ICHDGKAHFP REGVFVSNGT
HWFVTQRNFY EPQIITTDNT FVSGNCDVVI GIVNNTVYDP LQPELDSFKE
ELDKYFKNHT SPDVDLGDIS GINASVVNIQ KEIDRLNEVA KNLNESLIDL
QELGKYEQYI KWPWYIWLGF IAGLIAIVMV TIMLCCMTSC CSCLKGCCSC
GSCCKFDEDD SEPVLKGVKL HYT

[00229] FIG. 4A provides a map of the SARS-CoV-2 spike annotated for its currently known functional domains. As shown in FIG. 4A, the RBD, or receptor binding domain, spans a region comprising amino acids R319 to S541. The RBD is regarded as the region primarily responsible for S protein binding to ACE2. Within the RBD is a sub-domain which interacts specifically with ACE2, and which is referred to herein as the ACE2 binding domain (ABD). The ABD spans a region comprising amino acids Y449 to Y505. Until now, it was believed that S protein binding to ACE2 was the sole pathway to cellular entry and subsequent replication for SARS-CoV-2. Consequently, S protein, and particularly RBD, have been viewed as primary antigen candidates for the development of vaccines and therapeutic antibodies (*see e.g.,* Arashkia, A., *et al.* Rev Med Virol. 2020;e2183).

[00230] However, the present inventors have now discovered that the Lipolysis Stimulated Receptor (LSR) provides another cellular entry receptor for SARS-CoV-2. The S protein regions that interact with the LSR are referred to herein as Lipolysis Stimulated Receptor binding domains (LBD). As shown in FIG. 4A, there are two such binding domains. The first, LBD1, spans a region comprising amino acids P25 to P85. Within this region, there are eight amino acids in the S protein that directly contact the LSR: amino

acids P25, Y28, N30, F32, F59, N61, N74, and P85. The second LBD, LBD2, spans a region comprising amino acids Q607 to S691. Within this region, there are sixteen amino acids in the S protein that directly contact the LSR: amino acids Q607, H625, D627, S637, G639, S640, N641, G652, E654, H655, R682, R685, S686, A688, Q690, and S691. An additional five amino acid residues outside of the main LBD1 and LBD2, also interact with the LSR: R214, R237, Y269, K529, and N532.

[00231] Thus, the viral spike mediates the binding of SARS-CoV-2 to both LSR and ACE2. As shown in FIG. 4C, the three ACE2 binding domains form the apex of the spike. The LSR binding domains (LBDs) are also in the upper part of the spike but on the flanks of the ACE2 binding domains. The close proximity of three ACE2 binding domains enables their cooperation. In contrast, the LSR binding domains are distant from one another. This may explain the higher affinity of the wild type (Wuhan) strain for the ACE2 than for the LSR. This organization of the receptor binding domains may result in specific antibodies effectively suppressing the binding to one while leaving the other unaffected in spite of steric hindrance.

[00232] Mutations carried by the SARS-CoV-2 variants, alpha (α), beta (β), gamma (γ), delta (δ), epsilon (ε), and omicron (ο) are known in the art (see e.g., SARS-CoV-2 Variant Classifications and Definitions webpage of the U.S. Centers for Disease Control; Cosar et al. Cytokine Growth Factor Rev. 2021 Jul 2 doi: 10.1016/j.cytogfr.2021.06.001 [Epub ahead of print]; and *supra*). Spike proteins of different variants have been sequenced *see e.g.,* Alpha (GenBank: QWE88920.1), Beta (GenBank: QRN78347.1), Gamma (GenBank: QVE55289.1), Delta (GenBank: QWK65230.1), epsilon (GenBank: MW453103.1), Omicron BA.1 (GenBank: UFO69279.1), and Omicron BA.2 (GenBank: UJE45220.1). As is discussed in further detail in the Example section herein below, the mutations carried by a given variant may define and explain the receptor used by that variant for cellular entry.

[00233] Furthermore, as disclosed herein, the choice of receptor used by SARS-CoV-2 for cellular entry is influenced and coordinated by free fatty acids (FFA). In particular, as demonstrated in Example 1, long-chain unsaturated FFA suppress SARS-CoV-2 spike binding to ACE2 and thus, block viral replication by this pathway. Furthermore, as demonstrated in Example 2, FFA also activate LSR, thereby permitting cellular entry and replication of SARS-CoV-2 by this pathway. Thus, FFA play a central role in determining and coordinating the cellular entry and replication by SARS-CoV-2. In this context, it is

interesting that the S protein comprises a FFA binding pocket that binds unsaturated FFA. R408 and Q409 anchor the acidic head group of the unsaturated fatty acid and phenyalanines at amino acid positions 338, 342, 374, 377 and 392 comprise the binding pocket that forms within the trimeric spike (*see e.g.*, Toelzer, C., *et al.* (2020) Science 370(6517):725-730).

[00234] III. Preparation of Immunogenic Compositions

[00235] Immunogenic compositions can be prepared using any method known in the art. Typically, preparation of immunogenic compositions employs techniques familiar to those having ordinary skill in the art of molecular biology, biochemistry, and immunology. Basic texts disclosing the general terms in molecular biology and genetics include, *e.g.*, Lackie, *Dictionary of Cell and Molecular Biology*, Elsevier (5th ed. 2013). Basic texts disclosing methods in recombinant genetics and molecular biology include, *e.g.*, Sambrook *et al*, *Molecular Cloning— A Laboratory Manual*, Cold Spring Harbor Press 4th Edition (Cold Spring Harbor, N.Y. 2012) and *Current Protocols in Molecular Biology* Volumes 1-3, John Wiley & Sons, Inc. (1994-1998) and Supplements 1-115 (1987-2016). Basic texts disclosing the general methods and terms in biochemistry include, *e.g.*, Lehninger *Principles of Biochemistry* sixth edition, David L. Nelson and Michael M. Cox eds. W.H. Freeman (2012). Basic texts disclosing the general methods and terms immunology include *Janeway's Immunobiology* (Ninth Edition) by Kenneth M. Murphy and Casey Weaver (2017) Garland Science; *Fundamental Immunology* (Seventh Edition) by William E. Paul (2013) Lippincott, Williams and Wilkins.

[00236] Immunogenic compositions can be of any form or composition so long as they are capable of stimulating an immune response when administered to a subject. In one or more embodiments, the immunogenic composition is a vaccine. In one or more embodiments, the vaccine is an mRNA vaccine.

[00237] In one or more embodiments, an immunogenic composition comprises an immunogenic protein or peptide. In one or more embodiments, the immunogenicity of an immunogenic protein or peptide is enhanced by coupling the immunogenic protein or peptide to one or more transcription Infidelity (TI) segments (discussed below).

[00238] In one or more embodiments, immunogenic compositions comprise at least one nucleic acid that encodes at least one immunogen. In one or more embodiments,

immunogenic compositions comprise at least one nucleic acid that encodes at least one immunogen coupled to one or more Transcription Infidelity (TI) segments. In one or more embodiments, the nucleic acid that encodes an immunogen encodes at least one lipolysis-stimulated receptor binding domain (LBD) of a SARS-CoV-2 spike protein. Other forms of immunogenic compositions useful for the compositions and methods disclosed herein are apparent to those skilled in the art.

[00239] A. Transcription Infidelity

[00240] In one or more embodiments, the disclosure provides compositions and methods that increase the immune response against the S protein of SARS-CoV-2 in a subject. The method comprises administering to the subject at least one chimeric immunogen comprising the S protein, or a fragment thereof, *e.g.*, an LBD1, LBD2, ABD, etc., coupled to one or more TI segments.

[00241] RNA sequences occasionally differ from their canonical DNA templates (see e.g., Li, et al., (2011) *supra*; Ju, et al. (2011) Nat. Genet. 43(8): 745-752). These RNA-DNA divergences (RDD) occur during, or immediately after, transcription and are collectively referred to as transcription infidelity (TI) or RNA editing. TI results from RNA Pol II errors, causing base substitutions within and across base families. RNAs carrying TI events are often translated (*see e.g.,* Li M, *et al.* Science. 2011;333(6038):53-58)

[00242] Transcription infidelity (TI) is a mechanism that increases RNA and protein diversity. TI has been observed in normal prokaryotic and eukaryotic cells, and is increased in cancer cells (Ju *et al.*, (2011) Nat Genet, 2011; 43(8): 745-752; Li M., *et al.* (2011) Science 333(6038):53-58; Wons *et al.*, (2015) Nucleic Acids Research (2015); 43:3950 3963; Brulliard M., *et al.*, (2007) Proc Natl Acad Sci, 104: 7522-7527). Most TI events are base substitutions. However, TI also causes single base gaps, and the resulting frameshifted RNA translates into proteins with a carboxyterminal segment that generally becomes cationic. The resulting TI proteins afford specific immunological properties (Thouvenot *et al.,* (2020) The J. Clin. Invest. 130(10): 5477-5492).

[00243] Disclosed herein are TI segments that have immunological properties and which can confer on molecules (*e.g.*, proteins) of interest, the capacity to induce the production of antibodies without the need of any adjuvant. Furthermore, the isotype of

these antibodies as well as their affinity can be determined by the amino acid (AA) composition of the TI segment.

[00244] The methods disclosed herein, may be used to elicit production of antibodies of the desired isotype and with the desired affinity directed against any protein, *e.g.*, SARS-CoV-2 LBD1, LBD2, ABD, with or without any post-translational modification, *e.g.*, glycosylation.

[00245] A. 1. Chimeric Immunogens

[00246] As disclosed in Example 6, immunization of mice with a chimera generated by coupling a TI segment to an antigen of interest, *e.g.*, a SARS-CoV-2 5ES antigen, leads to a potent humoral response.

[00247] Coupling of the TI segment to an antigen may be covalent or non-covalent. Preferably, coupling is covalent. Coupling may be performed directly between the TI segment and the target antigen, *e.g.*, though a direct chemical bonding between the two or more entities, or indirectly through a linker group.

[00248] Chimeric antigen-TI segment can be prepared by any method known in the art. In one or more embodiments, the antigen is coupled through a peptide bond, formed by expression of a recombinant gene encoding the antigen and a TI segment. In one or more embodiments, the antigen is coupled through a peptide bond by chemical reaction.

[00249] Coupling may be performed with any suitable residue at any suitable position(s) on the segment and antigen. Coupling can be at one or more N-terminal and/or C-terminal ends of the TI segment and/or the antigen, as well as at any internal reactive group of the TI segment and the antigen. For example, at reactive groups carried by internal amino acid side chains or any posttranslational modification/decoration. For example, coupling can be carried out at any site of the segment or antigen where functional groups such as -OH, -SH, $-CO_2H$, $-NH_2$, $-SO_3H$ or $-PO_2H$ are naturally present or have been introduced. Methods for covalent chemical coupling of proteins are known in the art *see, e.g.,* Chandrudu *et al.*, (2013) Molecules 18(4):4373-4388.

[00250] Covalent chemical coupling, may utilize coupling agents selected from bi- or multifunctional agents comprising alkyl, aryl or segment groups by esters, aldehydes or alkyl or aryl acids, anhydride, sulfhydryl or carboxyl groups, groups derived from

cyanogen bromide or chloride, carbonyldiimidazole, succinimide esters, sulphonic halides, etc.

[00251] In one or more embodiments, the chimeric immunogen comprises one antigen, *e.g.*, a polypeptide having an amino acid sequence comprising amino acid 25 to amino acid 691 of SEQ ID NO: 1 which encodes LBD1, ABD, and LBD2, or a fragment thereof, *e.g.*, a polypeptide comprising amino acid 25 to amino acid 85 of SEQ ID NO: 1, which encodes LBD1, coupled to one TI segment. In one or more embodiments, the chimeric immunogen has the structure A-P or P-A. The polypeptide is A, the antigen part of the molecule, and the TI segment is P. In one or more embodiments, coupling is terminal. The TI segment can also be inserted inside the antigen (sequence) such that the chimeric immunogen has the structure A1-P-A2, where A1 and A2 are the two parts of the antigen A and the TI segment is P.

[00252] In one or more embodiments, the chimeric immunogen comprises one antigen, or a fragment thereof, coupled to two or more TI segments. In one or more embodiments, the two or more TI segments are the same or different. In one or more embodiments, the TI segments are conjugated at different positions on the antigen, or on the same position. Accordingly, in one or more embodiments, the chimeric immunogen has the structure Pn-A-Pn, or A-P-Pn, where A is the antigen part of the molecule, P is a TI segment, and n is the number of TI segments and is an integer from 1 to 5.

[00253] The chimeric immunogen may be prepared by any method known in the art, such as by recombinant techniques, chemically, enzymatically, or through a combination of these techniques. *See e.g.,* Sambrook, *supra*. The chimeric immunogen may also be generated *in situ* by gene modification by methods known in the art, such as editing (WO2008/009751, WO2017/158202, Thouvenot, 2020, *supra*). The chimeric immunogen may be purified, concentrated, placed in solution, and/or lyophilized, and/or frozen.

[00254] In one or more embodiments, the chimeric immunogen is further combined with one or more pharmaceutically acceptable carriers or excipients, thus forming a pharmaceutical or veterinary composition. Thus, disclosure provides compositions comprising at least one chimeric immunogen and one or more pharmaceutically or veterinary acceptable carriers or excipients, sprays, or aerosols.

[00255] In one or more embodiments, the composition is an immunogenic composition for the treatment or prevention of COVID-19. In one or more embodiments, the composition is a vaccine. In one or more embodiments, the vaccine is provided to a subject in several sequential administrations of a same or different chimeric immunogen(s) e.g., utilizing techniques of TI-assisted sequential immunization (TIASI). In one or more embodiments, compositions comprising a chimeric immunogen are administered at least three times.

[00256] In one or more embodiments, the composition is an immunogenic composition for stimulating an immune response for the production of antibodies. In one or more embodiments, the antibodies are monoclonal antibodies, wherein the antibodies directed against a chimeric SARS-CoV-2 antigen that comprises one or more of LBD1, LBD2, or ABD coupled to a TI segment.

[00257] TI segments as disclosed herein, include any TI amino acid (AA) sequence resulting from Transcription Infidelity (TI) in any protein. They may be selected from any TI segment of any mammalian proteins generated through TI. Alternatively, methods of isolating such mammalian proteins, or for artificially conceiving such TI segments, have been disclosed by applicants, *e.g.*, in WO2008/009751, which is incorporated by reference herein. From such methods, TI segments can be identified, isolated, and/or artificially synthesized. Examples of TI segments useful for coupling to a SARS-CoV-2 antigen, *e.g.*, LBD1, LBD2, ABD, etc., are disclosed in Table 4.

[00258] **Table 4.** TI segments coupled to canonical proteins to generate chimeric antigens

TI segment designation	Amino Acid Sequence
TI segment #7 (SEQ ID NO: 2)	LCFKRYELRLPAKRKRKRN
TI segment #60 (SEQ ID NO: 3)	LKIQKLQGKCSQPGMVGCSLTTWRTSMVLGRNI
TI segment #66 (SEQ ID NO: 4)	VKSPQKSYLFPSSMIGIGSLPSCWACWIQQ
TI segment #158 (SEQ ID NO: 5)	PSGPSWASWLRCWCWS
TI segment #162 (SEQ ID NO: 6)	SAKLSWTTFQILSWKPMFHFWY

TI segment #245 (SEQ ID NO: 7)	EFDIRRIRQMLIITK
TI segment #294 (SEQ ID NO: 8)	LQICAKYSSVTAWTPAAGRSCKMEGCRWWR
TI segment #367 (SEQ ID NO: 9)	FLISMPEKCVNTWIMKI

[00259] TI proteins are proteins comprising TI segments. TI protein is either a naturally occurring protein produced ubiquitously or an artificially constructed chimera comprising or consisting of, a complete or partial target protein, *e.g.*, LBD1, LBD2, ABD, fused with a selected TI segment having a defined amino acid composition. Both types of TI proteins have been shown to be immunogenic. In naturally produced TI proteins, the TI segment is on the carboxyterminal end, while in constructed chimera, it can be placed at either C-terminal extremity or N-terminal extremity or at both extremities or within the canonical protein.

[00260] In one or more embodiments, the antigen is a SARS-CoV-2 antigen. In one or more embodiments, the antigen is selected from LBD1, LBD2, ABD, Full Length Spike (FLS) protein and five most Exposed Spike domains (5ES).

[00261] B. Nucleic acid vaccines

[00262] The nucleic acid sequences disclosed herein can be used to prepare nucleic acid vaccines. In one or more embodiments, the nucleic acid vaccine is a DNA based vaccine. In one or more embodiments, the nucleic acid vaccine is an RNA based vaccine.

[00263] B. 1. Deoxyribonucleic acid (DNA)

[00264] In one or more embodiments, an immunogenic composition is a DNA vaccine. In one or more embodiments, the vaccine comprises at least one nucleic acid encoding one or more LBD1, LBD2, ABD, LSR, or ACE2. In one or more embodiments, at least one nucleic acid encoding one or more further comprises at least one nucleic acid encoding one or more TI segments. DNA vaccines are known in the art (see *e.g.*, Mol Immunol 47(7-8): 1507-1515; J. Immunol 162(7): 3915-3925; Vaccine 19(32): 4652-4660).

[00265] In one or more embodiments, a plasmid DNA vaccine is used to express at least one nucleic acid encoding an immunogen in a subject. For example, a nucleic acid molecule encoding one or more LBD1, LBD2, or ABD immunogen or one or more LBD1,

LBD2, or ABD immunogen coupled to one or more TI segments, can be administered to a subject to elicit an immune response to a SARS-CoV-2 spike protein. Similarly, a nucleic acid molecule encoding an LSR immunogen can be administered to a subject to elicit an immune response to a lipolysis stimulated receptor (LSR) protein. In one or more embodiments, the nucleic acid molecule is included on a plasmid vector for DNA immunization, such as the pVRC8400 vector (see *e.g.*, Barouch *et al.*, (2005) J. Virol, 79, 8828-8834).

[00266] In one or more embodiments, a disclosed immunogen is expressed by attenuated viral hosts or vectors or bacterial vectors. Recombinant vaccinia virus, adeno-associated virus (AAV), herpes virus, retrovirus, cytogmeglovirus or other viral vectors can be used to express the peptide or protein, thereby eliciting a cytotoxic T lymphocyte (CTL) response. Vaccinia vectors and methods useful in immunization protocols are disclosed, *e.g.*, in U.S. Pat. No. 4,722,848. BCG (Bacillus Calmette Guerin) provides another vector for expression of the peptides (see *e.g.*, Stover, Nature 351:456-460, 1991).

[00267] **B. 2. Ribonucleic acid (RNA)**

[00268] **mRNA Vaccines**

[00269] In one or more embodiments, the immunogenic composition is an mRNA vaccine. mRNA vaccines are known in the art *see e.g.*, US Patent Application Publication Nos. 2020/0282046, 2020/0085852, 2021/0220467, Nance, K.D. and Meier, J.L ACS Cent. Sci. 2021, 7, 5, 748–756. mRNA vaccines do not require viral or other forms of artificial replication to elicit a strong immune response, and therefore, have minimal toxicity. mRNA vaccines typically comprise an mRNA that comprises an open reading frame that encodes an immunogenic peptide or protein, formulated in a lipid nanoparticle in an amount sufficient to induce an immune response to the immunogenic peptide or protein in a subject.

[00270] As used herein, the term "open reading frame," abbreviated as "ORF," refers to a segment or region of an mRNA molecule that encodes a polypeptide. The ORF comprises a continuous stretch of non-overlapping, in-frame codons, beginning with the initiation codon and ending with a stop codon, and is translated by a ribosome.

[00271] In one or more embodiments, the ORF encodes one or more immunogenic peptides or proteins selected from the group consisting of: an LBD1, an LBD2, and an ABD. In one or more embodiments, the immunogenic peptide or protein comprises LBD1. In one or more embodiments, the immunogenic peptide or protein comprises LBD2. In one or more embodiments, the immunogenic peptide or protein comprises LBD1 and LBD2. In one or more embodiments, the immunogenic peptide or protein comprises LBD1, LBD2 and ABD. In one or more embodiments, the immunogenic peptide or protein is coupled to one or more Transcription Infidelity (TI) segments.

[00272] In one or more embodiments, the mRNA comprises at least one 5' terminal cap and at least one chemical modification, formulated within a lipid nanoparticle. In one or more embodiments m7GpppN, wherein N is the terminal 5' nucleotide of the nucleic acid carrying the 5'-cap, typically the 5'-end of an RNA. In one or more embodiments, a 5' terminal cap is 7mG(5')ppp(5')N1mpNp.

[00273] In one or more embodiments, at least one chemical modification is selected from pseudouridine, N1-methylpseudouridine, N1-ethylpseudouridine, 2-thiouridine, 4'-thiouridine, 5-methylcytosine, 5-methyluridine, 2-thio-1-methyl-1-deaza-pseudouridine, 2-thio-1-methyl-pseudouridine, 2-thio-5-aza-uridine, 2-thio-dihydropseudouridine, 2-thio-dihydrouridine, 2-thio-pseudouridine, 4-methoxy-2-thio-pseudouridine, 4-methoxy-pseudouridine, 4-thio-1-methyl-pseudouridine, 4-thio-pseudouridine, 5-aza-uridine, dihydropseudouridine, 5-methoxyuridine and 2'-O-methyl uridine. In one or more embodiments, the chemical modification is in the 5-position of the uracil. In one or more embodiments, the chemical modification is a N1-methylpseudouridine. In one or more embodiments, the chemical modification is a N1-ethylpseudouridine.

[00274] In one or more embodiments, a lipid nanoparticle comprises a cationic lipid, a PEG-modified lipid, a sterol and a non-cationic lipid. In one or more embodiments, a cationic lipid is an ionizable cationic lipid and the non-cationic lipid is a neutral lipid, and the sterol is a cholesterol. In one or more embodiments, a cationic lipid is selected from the group consisting of 2,2-dilinoleyl-4-dimethylaminoethyl-[1,3]-dioxolane (DLin-KC2-DMA), dilinoleyl-methyl-4-dimethylaminobutyrate (DLin-MC3-DMA), di((Z)-non-2-en-1-yl) 9-((4-(dimethylamino)butanoyl)oxy)heptadecanedioate (L319), (12Z,15Z)--N,N-dimethyl-2-nonylhenicosa-12,15-dien-1-amine (L608), and N,N-dimethyl-1-[(1S,2R)-2-octylcyclopropyl]heptadecan-8-amine (L530).

[00275] One or more embodiments of the present disclosure provide mRNA vaccines that comprise a polynucleotide encoding one or more antigens formulated in a carrier, *e.g.*, a lipid nanoparticle. mRNA vaccines, as disclosed herein may be used to induce a balanced immune response, comprising cellular and/or humoral immunity, without many of the risks associated with DNA vaccination.

[00276] IV. Preparation of Antibodies

[00277] The disclosure provides methods for making an antibody or antigen binding fragment that specifically binds to at least one LBD of a SARS-CoV-2 spike protein. Technology for producing antibodies is well known in the art (*see e.g.,* Coligan *et al.*, eds. (1994) Current Protocols in Immunology, John Wiley & Sons, Inc., New York, N.Y.).

[00278] In one or more embodiments, the method comprises immunizing a mammal with a polypeptide (or a nucleic acid that encodes a polypeptide) that comprises an LBD peptide, wherein the LBD peptide selected from the group consisting of LBD1 and LBD2. In one or more embodiments, the polypeptide comprises LBD1 and LBD2. Typically, immunizing the mammal with an LBD1 and/or LBD2 polypeptide comprises immunizing the mammal with a nucleic acid encoding an LBD1 polypeptide, or an LBD1 polypeptide comprising an amino acid sequence having at least 90% sequence identity to amino acid 25 to amino acid 85 of SEQ ID NO: 1, and/or a nucleic acid encoding an LBD2 polypeptide, or an LBD2 polypeptide comprising an amino acid sequence having at least 90% sequence identity to amino acid 607 to amino acid 691 of SEQ ID NO: 1. In one or more embodiments, the sequence identity of the LBD1 polypeptide is 91%, 92%, 93%, 94%, 95%, 96%, 97%, 98%, 99%, or 100% identical to amino acid 25 to amino acid 85 of SEQ ID NO: 1 and the sequence identity of the LBD2 polypeptide is 91%, 92%, 93%, 94%, 95%, 96%, 97%, 98%, 99%, or 100% identical to amino acid 607 to amino acid 691 of SEQ ID NO: 1. In one or more embodiments, the polypeptide is coupled to one or more Transcription Infidelity (TI) segments.

[00279] In one or more embodiments, immunizing the mammal with an LBD1 and/or LBD2 polypeptide comprises immunizing the mammal with a nucleic acid encoding a polypeptide comprising an amino acid sequence having at least 90% sequence identity to amino acid 25 to amino acid 691 of SEQ ID NO: 1. In one or more embodiments, the sequence identity is 91%, 92%, 93%, 94%, 95%, 96%, 97%, 98%, 99%, or 100%. Thus, in

one or more embodiments, polypeptide further comprises an ACE2 binding domain (ABD). In one or more embodiments, the polypeptide is coupled to one or more Transcription Infidelity (TI) segments.

[00280] As discussed below, in one or more embodiments the method is used to prepare polyclonal antibodies. The method comprises recovering antiserum from the immunized mammal and purifying polyclonal antibodies that specifically bind to at least one LBD of a SARS-CoV-2 spike protein.

[00281] In one or more embodiments, the method comprises recovering B-lymphocytes from the immunized mammal, fusing the recovered B-lymphocytes with a myeloma cell to produce a hybridoma cell, and selecting individual hybridoma cells that produce monoclonal antibodies that specifically bind to at least one LBD of a SARS-CoV-2 spike protein. In one or more embodiments, the antibody or antigen-binding fragment are humanized or human. Methods for preparing monoclonal antibodies, humanized and human antibodies are discussed in more detail below.

[00282] A. Polyclonal Antibodies

[00283] Polyclonal antibodies are well known in the art (see *e.g.*, Nielsen *et al.*, Single-Batch Production of Recombinant Human Polyclonal Antibodies, 2010, Mol. Biotechnol. 45: 257-266; Rasmussen *et al.*, Manufacture of recombinant polyclonal antibodies, 2007, Biotechnol Lett, 29: 845-852). Typically, polyclonal antibodies are prepared by immunizing a suitable subject (*e.g.*, rabbit, goat, mouse, or other mammal) with a polypeptide/protein of interest or a fragment thereof as an immunogen *e.g.,* an LBD1, LBD2, or ABD. Antibody titer in the immunized subject are monitored over time by standard techniques, such as *e.g.*, using an enzyme linked immunosorbent assay (ELISA). At an appropriate time after immunization, *e.g.*, when the antibody titers are highest, antibody-producing cells are obtained from the animal, *e.g.*, a mouse, and can be isolated and purified or used to prepare monoclonal antibodies *e.g.*, by methods known in the art *e.g.*, as disclosed above.

[00284] B. Monoclonal Antibodies

[00285] Monoclonal antibodies may be obtained, for example, using the hybridoma method first described by Kohler *et al.*, *Nature*, 1975, 256:495-497 (incorporated by

reference in its entirety), and/or by recombinant DNA methods (*see e.g.,* U.S. Patent No. 4,816,567, incorporated by reference in its entirety). Monoclonal antibodies may also be obtained, for example, using phage or yeast-based libraries. *See e.g.,* U.S. Patent Nos. 8,258,082 and 8,691,730, each of which is incorporated by reference in its entirety.

[00286] In the hybridoma method, a mouse or other appropriate host animal is immunized to elicit lymphocytes that produce or are capable of producing antibodies that will specifically bind to the protein used for immunization. Alternatively, lymphocytes may be immunized *in vitro*. Lymphocytes are then fused with myeloma cells using a suitable fusing agent, such as polyethylene glycol, to form a hybridoma cell. *See* Goding J.W., *Monoclonal Antibodies: Principles and Practice* 3rd ed. (1986) Academic Press, San Diego, CA, incorporated by reference in its entirety.

[00287] The hybridoma cells are seeded and grown in a suitable culture medium that contains one or more substances that inhibit the growth or survival of the unfused, parental myeloma cells. For example, if the parental myeloma cells lack the enzyme hypoxanthine guanine phosphoribosyl transferase (HGPRT or HPRT), the culture medium for the hybridomas typically will include hypoxanthine, aminopterin, and thymidine (HAT medium), which substances prevent the growth of HGPRT-deficient cells.

[00288] Useful myeloma cells are those that fuse efficiently, support stable high-level production of antibody by the selected antibody-producing cells, and are sensitive media conditions, such as the presence or absence of HAT medium. Among these, myeloma cell lines include murine myeloma cell lines, such as murine myeloma lines derived from MOP-21 and MC-11 mouse tumors (available from the Salk Institute Cell Distribution Center, San Diego, CA), and SP-2 or X63-Ag8-653 cells (available from the American Type Culture Collection, Rockville, MD). Human myeloma and mouse-human heteromyeloma cell lines also have been described for the production of human monoclonal antibodies. *See e.g.,* Kozbor, *J. Immunol.*, 1984, 133:3001, incorporated by reference in its entirety.

[00289] After the identification of hybridoma cells that produce antibodies of the desired specificity, affinity, and/or biological activity, selected clones may be subcloned by limiting dilution procedures and grown by standard methods. *See* Goding, *supra*. Suitable

culture media for this purpose include, for example, D-MEM or RPMI-1640 medium. In addition, the hybridoma cells may be grown *in vivo* as ascites tumors in an animal.

[00290] DNA encoding the monoclonal antibodies may be readily isolated and sequenced using conventional procedures (*e.g.*, by using oligonucleotide probes that are capable of binding specifically to genes encoding the heavy and light chains of the monoclonal antibodies). Thus, the hybridoma cells can serve as a useful source of DNA encoding antibodies with the desired properties. Once isolated, the DNA may be placed into expression vectors, which are then transfected into host cells such as bacteria (*e.g.*, *E. coli*), yeast (*e.g.*, *Saccharomyces* or *Pichia* sp.), COS cells, Chinese hamster ovary (CHO) cells, or myeloma cells that do not otherwise produce antibody, to produce the monoclonal antibodies.

[00291] Monoclonal antibodies can be prepared by any method known in the art. In one or more embodiments, monoclonal antibodies are prepared using mammalian cell display (see e.g., Beerli, et al. (2008) PNAS 105(38): 14336 –14341, which is incorporated herein by reference in its entirety). In one or more embodiments, monoclonal antibodies are prepared using selective PCR for antibody retrieval (SPAR) (*see e.g.*, Horns F, Quake SR (2020) Cloning antibodies from single cells in pooled sequence libraries by selective PCR. PLoS ONE 15(8): e0236477). In one or more embodiments, monoclonal antibodies are prepared from single human B cells by single cell RT-PCR and expression vector cloning (*see e.g.*, Tiller et al. (2008) Journal of Immunological Methods 329: 112-124) or other known methods. Thus, in one or more embodiments, monoclonal antibodies are produced by identifying B cells, plasma cells or plasmablast producing antibodies from any isotypes reactive with LBD1 or LBD2, then cloning the c-DNA encoding the antibody and producing it by transfection in appropriate mammalian cells.

[00292] Modifications can be made to monoclonal antibodies to increase the stability and half-life of the antibodies (*see e.g.*, Kang and Jung (2019) Experimental & Molecular Medicine 51:138; Dall'Acqua, et al. (2006) J. Biol. Chem. 281(33):23514-2; Mackness et al., (2019) MAbs. 11(7):1276-1288; Booth et al., (2018) Mabs.10(7):1098-1110). Accordingly, in one or more embodiments, monoclonal antibodies are subject to refinement steps to increase their stability.

[00293] C. Humanized Antibodies

[00294] Humanized antibodies may be generated by replacing most, or all, of the structural portions of a non-human monoclonal antibody with corresponding human antibody sequences. Consequently, a hybrid molecule is generated in which only the antigen-specific variable, or CDR, is composed of non-human sequence. Methods to obtain humanized antibodies include those described in, for example, Winter and Milstein, *Nature*, 1991, 349:293-299; Rader *et al.*, *Proc. Nat. Acad. Sci. U.S.A.*, 1998, 95:8910-8915; Steinberger *et al.*, *J. Biol. Chem.*, 2000, 275:36073-36078; Queen *et al.*, *Proc. Natl. Acad. Sci. U.S.A.*, 1989, 86:10029-10033; and U.S. Patent Nos. 5,585,089, 5,693,761, 5,693,762, and 6,180,370; each of which is incorporated by reference in its entirety.

[00295] D. Human Antibodies

[00296] Human antibodies can be generated by a variety of techniques known in the art, for example by using transgenic animals (*e.g.*, humanized mice). *See, e.g.,* Jakobovits *et al.*, *Proc. Natl. Acad. Sci. U.S.A.*, 1993, 90:2551; Jakobovits *et al.*, *Nature*, 1993, 362:255-258; Bruggermann *et al.*, *Year in Immuno.*, 1993, 7:33; and U.S. Patent Nos. 5,591,669, 5,589,369 and 5,545,807; each of which is incorporated by reference in its entirety. Human antibodies can also be derived from phage-display libraries (*see e.g.,* Hoogenboom *et al.*, *J. Mol. Biol.*, 1991, 227:381-388; Marks *et al.*, *J. Mol. Biol.*, 1991, 222:581-597; and U.S. Pat. Nos. 5,565,332 and 5,573,905; each of which is incorporated by reference in its entirety). Human antibodies may also be generated by *in vitro* activated B cells (*see e.g.,* U.S. Patent. Nos. 5,567,610 and 5,229,275, each of which is incorporated by reference in its entirety). Human antibodies may also be derived from yeast-based libraries (*see e.g.,* U.S. Patent No. 8,691,730, incorporated by reference in its entirety).

[00297] V. Cellular entry inhibitors

[00298] Inhibitors of cellular entry can be beneficial for treating a subject suffering from COVID-19. In one or more embodiments, the inhibitor of cellular entry is a siRNA that targets the LSR. In one or more embodiments, the siRNA molecules target either the α or β subunit of LSR. In one or more embodiments, the siRNA targets both the α and β subunits of the LSR. Target inhibition by siRNA is known in the art (*see e.g.,* Lagana et al. (2015) RNA Bioinformatics pp 393-412).

[00299] In one or more embodiments, inhibitors of cellular entry include proteins such as lactoferrin and lactoferrin derivatives (*see e.g.,* Fernandes and carter (2017) Front. Microbiol. Vol 8, Article 2; Strom and Svendsen (2000) J. Pept. Res. 56(5):265-74). Lactoferrin derivatives can be tested for their ability to inhibit the activity of LSR and/or ACE2 utilizing methods disclosed herein.

[00300] As noted above, the LSR is an endocytic receptor (Bihain et al. (1992) Biochemistry 31(19):4628-36) while the ACE2 is a fusion receptor. Acidification of early endosome is necessary for LSR mediated Clostridial iota toxin disruption of the actin network. Therefore, in one or more embodiments, endosome inhibitors are effective in late stage disease. In one or more embodiments, endosome inhibitors, e.g., chloroquine, are effective against the delta and omicron variants.

[00301] In one or more embodiments, an inhibitor of cellular entry is a synthetic chemical inhibitor of lipoprotein uptake, such as suramin and/or derivatives thereof (*see e.g.,* McCain et al., (2004) J. Biol. Chem. 279(15):14713-14725; Tsay et al., (2017) Organic & Medicinal Chem IJ Vol. 2, Issue 43).

[00302] In one or more embodiments, an inhibitor of cellular entry is an anti-LBD antibody, an anti-ABD antibody, an anti-S protein antibody, an anti-LSR antibody or combinations thereof.

[00303] VI. Pharmaceutical Compositions and Methods of Administration

[00304] The immunogenic compositions, cellular entry inhibitors, and antibodies provided herein can be formulated into pharmaceutical compositions using methods available in the art and those disclosed herein. Any of the immunogenic compositions, cellular entry inhibitors, or antibodies provided herein can be provided in the appropriate pharmaceutical composition and be administered by a suitable route of administration.

[00305] The methods provided herein encompass administering pharmaceutical compositions comprising at least one immunogenic composition, cellular entry inhibitor, or antibody provided herein and one or more compatible and pharmaceutically acceptable carriers. In this context, the term "pharmaceutically acceptable" means approved by a regulatory agency of the Federal or a state government or listed in the U.S. Pharmacopeia or other generally recognized pharmacopeia for use in animals, and more particularly in

humans. The term "carrier" includes a diluent, adjuvant (*e.g.*, Freund's adjuvant (complete and incomplete), excipient, or vehicle with which the therapeutic is administered. Such pharmaceutical carriers can be sterile liquids, such as water and oils, including those of petroleum, animal, vegetable or synthetic origin, such as peanut oil, soybean oil, mineral oil, sesame oil and the like. Water can be used as a carrier when the pharmaceutical composition is administered intravenously. Saline solutions and aqueous dextrose and glycerol solutions can also be employed as liquid carriers, particularly for injectable solutions. Examples of suitable pharmaceutical carriers are described in Martin, E.W., *Remington's Pharmaceutical Sciences*.

[00306] In clinical practice the immunogenic compositions, cellular entry inhibitors, or antibodies provided herein may be administered by any route known in the art. Exemplary routes of administration include, but are not limited to, the inhalation, intraarterial, intradermal, intramuscular, intraperitoneal, intravenous, nasal, parenteral, pulmonary, and subcutaneous routes. In one or more embodiments, a pharmaceutical composition provided herein is administered parenterally.

[00307] The compositions for parenteral administration can be emulsions or sterile solutions. Parenteral compositions may include, for example, propylene glycol, polyethylene glycol, vegetable oils, and injectable organic esters (*e.g.*, ethyl oleate). These compositions can also contain wetting, isotonizing, emulsifying, dispersing, and stabilizing agents. Sterilization can be carried out in several ways, for example using a bacteriological filter, by radiation or by heating. Parenteral compositions can also be prepared in the form of sterile solid compositions, which can be dissolved at the time of use in sterile water or any other injectable sterile medium.

[00308] In one or more embodiments, a composition provided herein is a pharmaceutical composition or a single unit dosage form. Pharmaceutical compositions and single unit dosage forms provided herein comprise a prophylactically or therapeutically effective amount of one or more prophylactic or therapeutic immunogenic composition, cellular entry inhibitor, antibodies, or combinations thereof.

[00309] The pharmaceutical composition may comprise one or more pharmaceutical excipients. Any suitable pharmaceutical excipient may be used, and one of ordinary skill in the art is capable of selecting suitable pharmaceutical excipients. Non-limiting examples of

suitable excipients include starch, glucose, lactose, sucrose, gelatin, malt, rice, flour, chalk, silica gel, sodium stearate, glycerol monostearate, talc, sodium chloride, dried skim milk, glycerol, propylene, glycol, water, ethanol and the like. Whether a particular excipient is suitable for incorporation into a pharmaceutical composition or dosage form depends on a variety of factors well known in the art including, but not limited to, the way in which the dosage form will be administered to a subject and the specific immunogenic composition, cellular entry inhibitor, or antibody in the dosage form. The composition or single unit dosage form, if desired, can also contain minor amounts of wetting or emulsifying agents, or pH buffering agents. Accordingly, the pharmaceutical excipients provided below are intended to be illustrative, and not limiting. Additional pharmaceutical excipients include, for example, those described in the *Handbook of Pharmaceutical Excipients*, Rowe *et al.* (Eds.) 6th Ed. (2009), incorporated by reference in its entirety.

[00310] In one or more embodiments, the pharmaceutical composition comprises an anti-foaming agent. Any suitable anti-foaming agent may be used. In some aspects, the anti-foaming agent is selected from an alcohol, an ether, an oil, a wax, a silicone, a surfactant, and combinations thereof. In some aspects, the anti-foaming agent is selected from a mineral oil, a vegetable oil, ethylene bis stearamide, a paraffin wax, an ester wax, a fatty alcohol wax, a long-chain fatty alcohol, a fatty acid soap, a fatty acid ester, a silicon glycol, a fluorosilicone, a polyethylene glycol-polypropylene glycol copolymer, polydimethylsiloxane-silicon dioxide, ether, octyl alcohol, capryl alcohol, sorbitan trioleate, ethyl alcohol, 2-ethyl-hexanol, dimethicone, oleyl alcohol, simethicone, and combinations thereof.

[00311] In one or more embodiments, the pharmaceutical composition comprises a co-solvent. Illustrative examples of co-solvents include ethanol, poly(ethylene) glycol, butylene glycol, dimethylacetamide, glycerin, and propylene glycol.

[00312] In one or more embodiments, the pharmaceutical composition comprises a buffer. Illustrative examples of buffers include acetate, borate, carbonate, lactate, malate, phosphate, citrate, hydroxide, diethanolamine, monoethanolamine, glycine, methionine, guar gum, and monosodium glutamate.

[00313] In one or more embodiments, the pharmaceutical composition comprises a carrier or filler. Illustrative examples of carriers or fillers include lactose, maltodextrin, mannitol, sorbitol, chitosan, stearic acid, xanthan gum, and guar gum.

[00314] In one or more embodiments, the pharmaceutical composition comprises a surfactant. Illustrative examples of surfactants include *d*-alpha tocopherol, benzalkonium chloride, benzethonium chloride, cetrimide, cetylpyridinium chloride, docusate sodium, glyceryl behenate, glyceryl monooleate, lauric acid, macrogol 15 hydroxystearate, myristyl alcohol, phospholipids, polyoxyethylene alkyl ethers, polyoxyethylene sorbitan fatty acid esters, polyoxyethylene stearates, polyoxylglycerides, sodium lauryl sulfate, sorbitan esters, and vitamin E polyethylene(glycol) succinate.

[00315] In one or more embodiments, the pharmaceutical composition comprises an anti-caking agent. Illustrative examples of anti-caking agents include calcium phosphate (tribasic), hydroxymethyl cellulose, hydroxypropyl cellulose, and magnesium oxide.

[00316] Other excipients that may be used with the pharmaceutical compositions include, for example, albumin, antioxidants, antibacterial agents, antifungal agents, bioabsorbable polymers, chelating agents, controlled release agents, diluents, dispersing agents, dissolution enhancers, emulsifying agents, gelling agents, ointment bases, penetration enhancers, preservatives, solubilizing agents, solvents, stabilizing agents, and sugars. Specific examples of each of these agents are described, for example, in the *Handbook of Pharmaceutical Excipients*, Rowe *et al.* (Eds.) 6th Ed. (2009), The Pharmaceutical Press, incorporated by reference in its entirety.

[00317] In one or more embodiments, the pharmaceutical composition comprises a solvent. In some aspects, the solvent is saline solution, such as a sterile isotonic saline solution or dextrose solution. In some aspects, the solvent is water for injection.

[00318] In one or more embodiments, the pharmaceutical compositions are in a particulate form, such as a microparticle or a nanoparticle. Microparticles and nanoparticles may be formed from any suitable material, such as a polymer or a lipid. In some aspects, the microparticles or nanoparticles are micelles, liposomes, or polymersomes.

[00319] Further provided herein are anhydrous pharmaceutical compositions and dosage forms comprising an antibody since, in one or more embodiments, water facilitates the degradation of some antibodies.

[00320] Anhydrous pharmaceutical compositions and dosage forms provided herein can be prepared using anhydrous or low moisture containing ingredients and low moisture or low humidity conditions. Pharmaceutical compositions and dosage forms that comprise lactose and at least one active ingredient that comprises a primary or secondary amine can be anhydrous if substantial contact with moisture and/or humidity during manufacturing, packaging, and/or storage is expected.

[00321] An anhydrous pharmaceutical composition can be prepared and stored such that its anhydrous nature is maintained. Accordingly, anhydrous compositions can be packaged using materials known to prevent exposure to water such that they can be included in suitable formulary kits. Examples of suitable packaging include, but are not limited to, hermetically sealed foils, plastics, unit dose containers (*e.g.*, vials), blister packs, and strip packs.

[00322] Lactose-free compositions provided herein can comprise excipients that are well known in the art and are listed, for example, in the U.S. Pharmocopia (USP) SP (XXI)/NF (XVI). In general, lactose-free compositions comprise an active ingredient, a binder/filler, and a lubricant in pharmaceutically compatible and pharmaceutically acceptable amounts. Exemplary lactose-free dosage forms comprise an active ingredient, microcrystalline cellulose, pre gelatinized starch, and magnesium stearate.

[00323] Also provided are pharmaceutical compositions and dosage forms that comprise one or more excipients that reduce the rate by which an immunogenic composition, cellular entry inhibitor, or antibody will decompose. Such excipients, which are referred to herein as "stabilizers," include, but are not limited to, antioxidants such as ascorbic acid, pH buffers, or salt buffers.

[00324] Parenteral Dosage Forms

[00325] In one or more embodiments, provided are parenteral dosage forms. Parenteral dosage forms can be administered to subjects by various routes including, but not limited to, subcutaneous, intravenous (including bolus injection), intramuscular, and intraarterial.

Because their administration typically bypasses subjects' natural defenses against contaminants, parenteral dosage forms are typically, sterile or capable of being sterilized prior to administration to a subject. Examples of parenteral dosage forms include, but are not limited to, solutions ready for injection, dry products ready to be dissolved or suspended in a pharmaceutically acceptable vehicle for injection, suspensions ready for injection, and emulsions.

[00326] Suitable vehicles that can be used to provide parenteral dosage forms are well known to those skilled in the art. Examples include, but are not limited to: Water for Injection USP; aqueous vehicles such as, but not limited to, Sodium Chloride Injection, Ringer's Injection, Dextrose Injection, Dextrose and Sodium Chloride Injection, and Lactated Ringer's Injection; water miscible vehicles such as, but not limited to, ethyl alcohol, polyethylene glycol, and polypropylene glycol; and non-aqueous vehicles such as, but not limited to, corn oil, cottonseed oil, peanut oil, sesame oil, ethyl oleate, isopropyl myristate, and benzyl benzoate.

[00327] Excipients that increase the solubility of one or more of the immunogenic composition, cellular entry inhibitor, or antibodies disclosed herein can also be incorporated into the parenteral dosage forms.

[00328] Dosage and Unit Dosage Forms

[00329] In human therapeutics, the doctor will determine the posology which he considers most appropriate according to a preventive or curative treatment and according to the age, weight, condition and other factors specific to the subject to be treated.

[00330] In one or more embodiments, a composition provided herein is a pharmaceutical composition or a single unit dosage form. Pharmaceutical compositions and single unit dosage forms provided herein comprise a prophylactically or therapeutically effective amount of one or more prophylactic or therapeutic immunogenic composition, cellular entry inhibitor, or antibody.

[00331] The amount of the immunogenic composition, cellular entry inhibitor, or antibody composition, which will be effective in the prevention or treatment of a disorder or one or more symptoms thereof will vary with the nature and severity of the disease or condition, and the route by which the composition is administered. The frequency and

dosage will also vary according to factors specific for each subject depending on the specific therapy (*e.g.*, therapeutic or prophylactic agents) administered, the severity of the disorder, disease, or condition, the route of administration, as well as age, body, weight, response, and the past medical history of the subject. Effective doses may be extrapolated from dose-response curves derived from *in vitro* or animal model test systems.

[00332] In one or more embodiments, exemplary doses of a composition include milligram or microgram amounts of the antibody per kilogram of subject or sample weight (*e.g.*, about 10 micrograms per kilogram to about 50 milligrams per kilogram, about 100 micrograms per kilogram to about 25 milligrams per kilogram, or about 100 microgram per kilogram to about 10 milligrams per kilogram). In one or more embodiments, the dosage of the antibody provided herein, based on weight of the antibody, administered to prevent, treat, manage, or ameliorate a disorder, or one or more symptoms thereof in a subject is 0.1 mg/kg, 1 mg/kg, 2 mg/kg, 3 mg/kg, 4 mg/kg, 5 mg/kg, 6 mg/kg, 10 mg/kg, or 15 mg/kg or more of a subject's body weight. In one or more embodiments, the dosage of the composition or a composition provided herein administered to prevent, treat, manage, or ameliorate a disorder, or one or more symptoms thereof in a subject is 0.1 mg to 200 mg, 0.1 mg to 100 mg, 0.1 mg to 50 mg, 0.1 mg to 25 mg, 0.1 mg to 20 mg, 0.1 mg to 15 mg, 0.1 mg to 10 mg, 0.1 mg to 7.5 mg, 0.1 mg to 5 mg, 0.1 to 2.5 mg, 0.25 mg to 20 mg, 0.25 to 15 mg, 0.25 to 12 mg, 0.25 to 10 mg, 0.25 mg to 7.5 mg, 0.25 mg to 5 mg, 0.25 mg to 2.5 mg, 0.5 mg to 20 mg, 0.5 to 15 mg, 0.5 to 12 mg, 0.5 to 10 mg, 0.5 mg to 7.5 mg, 0.5 mg to 5 mg, 0.5 mg to 2.5 mg, 1 mg to 20 mg, 1 mg to 15 mg, 1 mg to 12 mg, 1 mg to 10 mg, 1 mg to 7.5 mg, 1 mg to 5 mg, or 1 mg to 2.5 mg.

[00333] The dose can be administered according to a suitable schedule, for example, once, two times, three times, or for times weekly. It may be necessary to use dosages of the antibody outside the ranges disclosed herein in some cases, as will be apparent to those of ordinary skill in the art. Furthermore, it is noted that the clinician or treating physician will know how and when to interrupt, adjust, or terminate therapy in conjunction with subject response.

[00334] Different therapeutically effective amounts may be applicable for different diseases and conditions, as will be readily known by those of ordinary skill in the art. Similarly, amounts sufficient to prevent, manage, treat or ameliorate such disorders, but insufficient to cause, or sufficient to reduce, adverse effects associated with the

immunogenic compositions, cellular entry inhibitors, or antibodies provided herein are also encompassed by the herein described dosage amounts and dose frequency schedules. Further, when a subject is administered multiple dosages of a composition provided herein, not all of the dosages need be the same. For example, the dosage administered to the subject may be increased to improve the prophylactic or therapeutic effect of the composition or it may be decreased to reduce one or more side effects that a particular subject is experiencing.

[00335] In one or more embodiments, treatment or prevention is initiated with one or more loading doses of a composition provided herein followed by one or more maintenance doses, e.g., an initial vaccination followed by a booster.

[00336] In one or more embodiments, a dose of an immunogenic composition, cellular entry inhibitor, or antibody composition provided herein is administered to achieve a steady-state concentration of the therapeutic ingredient in blood or serum of the subject. The steady-state concentration can be determined by measurement according to techniques available to those of skill or can be based on the physical characteristics of the subject such as height, weight and age.

[00337] In one or more embodiments, administration of the same composition is repeated and the administrations is separated by at least 1 day, 2 days, 3 days, 5 days, 10 days, 15 days, 30 days, 45 days, 2 months, 75 days, 3 months, or 6 months. In one or more embodiments, administration of the same prophylactic or therapeutic agent is repeated and the administration is separated by at least 1 day, 2 days, 3 days, 5 days, 10 days, 15 days, 30 days, 45 days, 2 months, 75 days, 3 months, or 6 months.

[00338] VII. Assays

[00339] Disclosed herein are assays for examining and testing aspects of coronavirus, *e.g.,* SARS-CoV-2 biology. The disclosed assays include, but are not limited to, assays that examine or otherwise employ cellular entry and/or replication *in vitro*. Assays may lead to discovering useful mutant/variant strains, drug discovery, antibody testing, discovery of viral inhibitors, discovery, monitoring or practice of therapeutic treatments, etc. The methods utilize coronavirus protocols disclosed herein, including the "ACE2 protocol," and the "oleate/palmitate (O/P) protocol" both of which are discussed briefly below.

[00340] A. ACE2 protocol

[00341] The ACE2 protocol is a pre-treatment of live coronavirus, *e.g.*, SARS-CoV-2, or pseudovirus particles (PV) that leaves the virus "ACE2 competent" i.e., capable of cell entry and replication via binding of the ACE2 receptor (ACE2 pathway). The ACE2 protocol comprises not pre-incubating or otherwise treating the live coronavirus with any free fatty acid (FFA). In one or more embodiments, the "ACE2 protocol" comprises pre-treating live coronavirus with a saturated FFA, *e.g.*, palmitate.

[00342] B. O/P protocol

[00343] The oleate/palmitate "O/P protocol," "O+2P protocol," or "O+2P" is an assay that can be applied to either live coronaviruses, or to PV, which activates the LSR. LSR activation permits cellular entry of the virus upon S protein interaction and binding to the LSR. In the "O/P protocol," live coronavirus, *e.g.*, SARS-CoV-2, or PV are first treated with oleate to provide "ACE2 incompetent" virus. "ACE2 incompetent" SARS-CoV-2 are not capable of cell entry and replication via binding of the ACE2 receptor (ACE2 pathway). Treatment of live virus or pseudovirus with oleate comprises pre-incubating the live coronavirus with oleate, or adding oleate to a cell culture at the time of infection. Oleate exposure creates "ACE2 incompetent" virus. After infection of susceptible cells with ACE2 incompetent virus and incubation of the resulting cell culture for an appropriate length of time, e.g., 24 hours, infective media is removed and the cell culture is transiently (approximately 2.5 hours) exposed to palmitate. Palmitate activates LSR, thereby permitting cell entry and replication by the LSR pathway. Typically, a second transient incubation with palmitate is carried out to fully activate the LSR pathway.

[00344] Thus, in one or more embodiments, the cell culture is provided with more than one transient exposure to palmitate. In one or more embodiments, the cell culture is treated with palmitate three times. In one or more embodiments, the transient exposures are given at intervals of 24 hours.

[00345] C. Assays for cellular entry

[00346] In one or more embodiments, assays utilize pseudovirus particles. Pseudoviruses or equivalently, pseudoparticles, are known in the art *see e.g.,* Chen, M. and Zhang, X.E., (2021) Int. J. Biol. Sci 17(6): 1574-1580. Pseudoviruses offer the advantages

having surface proteins with high similarity to that of the native viral proteins and attenuated virulence that allows them to be safely handled. Pseudovirus assays can separate viral entry from other steps of the viral infection cycle (e.g., replication), allowing persons skilled in the art to analyze the viral entry step that is mediated by SARS-CoV-2 spike.

[00347] Accordingly, in one or more embodiments, the disclosure provides pseudovirus assays useful for characterizing the effect of free fatty acids, antibodies, *e.g.*, anti-LBD antibodies, putative inhibitors, etc., on cellular entry *in vitro*.

[00348] D. Assays for cellular entry and replication.

[00349] Disclosed herein are methods for assaying coronavirus cellular entry and/or replication *in vitro*. The methods utilize coronavirus, *e.g.,* SARS- CoV-2 that have been subjected to treatment using the ACE2 protocol, which are therefore ACE2 competent, and comparing the behavior of these coronaviruses to the behavior of viruses made ACE2 incompetent by treatment according to the oleate/palmitate (O/P) protocol.

[00350] Briefly, the assay method comprises incubating an initial titer of the ACE2 incompetent virus with host cells to provide a first cell culture, and an initial titer of ACE2 competent virus with host cells to provide a second host cell culture; wherein the host cells comprising the first cell culture and the second host cell culture express an ACE2 receptor and a lipolysis stimulated receptor (LSR); transiently exposing the first and second host cell cultures to a long-chain free fatty acid (FFA), and observing timing of viral production, wherein viral production is measured by the number of virus produced as compared to the initial titer of the ACE2 incompetent or ACE2 competent virus, and wherein an increase in the number of virus is indicative of viral entry and replication; wherein timing of the viral production is early or late; and wherein early timing of the viral production indicates entry via ACE2 receptor, and late timing of the viral production indicates entry via LSR.

[00351] Screening mutant libraries

[00352] In one or more embodiments, assays for coronavirus cellular entry and/or replication *in vitro* are used to examine the effects different mutations in the spike protein have on spike protein binding to LSR, ACE2, or both. For example, spike mutants can be screened for those that carry mutations rendering them ACE2 incompetent, or LSR

incompetent. For example, mutants that are ACE2 incompetent will exhibit similar replication patterns whether subjected to the ACE2 or LSR protocols.

[00353] Screening for inhibitors that block cell entry and replication

[00354] In one or more embodiments, assays for coronavirus cellular entry and/or replication *in vitro* is used to identify inhibitors cell entry and replication. Effective inhibitors of cellular entry and/or replication will be reflected in reduced viral production by that pathway. For example, inhibitors of spike binding to LSR will reduce viral production by the LSR pathway such that, *e.g.*, only ACE2 competent virus will be able to replicate and produce progeny virus.

[00355] Determining the receptor for cellular entry or replication of a coronavirus

[00356] Several variants of SARS-CoV-2 have emerged that are notable because of the potential for increased transmissibility, possible immune escape, or for other reasons. Understanding the receptor preference of such variants can *inter alia*; facilitate the development of vaccines or other treatments that can keep variants of concern in check. Therefore, in one or more embodiments, assays are provided for coronavirus cellular entry and/or replication *in vitro* to determine the receptor that is preferentially used for cellular entry by a particular SARS-CoV-2 variant.

[00357] In one or more embodiments, receptor preference is evaluated using competition assays. Competitive binding assays are known in the art (see *e.g.*, Goodman & Gilman's The Pharmacological Basis of Therapeutics. The McGraw Hill Companies Inc. 1996. pp. 29–37; Haylett DG (2003). "Direct Measurement of Drug Binding to Receptors" In Foreman JC, Johansen T (eds.). Textbook of Receptor Pharmacology (Second ed.). CRC L.L.C. pp. 153–180). Thus, in one or more embodiments, the binding of a spike protein whose receptor preference is unknown, is tested in the presence and absence of a ligand that is known to be capable of binding to either the ACE2 or LSR receptor. For example, an assay for cellular replication can be conducted in the presence and absence of a recombinant LBD or ABD polypeptide. Because recombinant LBD or ABD polypeptides effectively bind and compete for the LSR or ACE2 receptors, respectively, competition assays utilizing recombinant LBD or ABD polypeptide can be used to study the receptor binding preference of known and emerging SARS-CoV-2 variants. Appropriate and effective therapies can then be targeted for specific variants.

[00358] Evaluating the neutralizing capacity of patient antibodies directed against SARS-CoV-2

[00359] In one or more embodiments, assays for coronavirus cellular entry and/or replication *in vitro* is used to characterize the neutralizing capacity of antibodies directed against SARS-CoV-2. Neutralizing antibodies against SARS-CoV-2 variants can be tested using the disclosed assay for cellular entry and replication. In one or more embodiments, the method is used to measure the neutralizing capacity of antibodies produced by individuals after vaccination. Accordingly, such assays are useful for determining the most effective antigens for vaccines. Similarly, monoclonal antibodies individually or in the form of a "cocktail" of monoclonal antibodies, can be screened for their neutralizing activity against SARS-CoV-2 cellular entry and replication via either or both the ACE2 or LSR mediated pathways. Mixtures (cocktails) of antibodies can be refined to be effective against infection by different variants, *e.g.*, by the dominant variant in circulation at the time.

[00360] VIII. Therapeutic Applications

[00361] The disclosure provides new paradigms from which to view COVID-19 and other coronaviral infections, thus leading to innovative treatments and new therapeutic compositions.

[00362] A. Vaccination

[00363] In one or more embodiments, immunogenic compositions disclosed herein is used to vaccinate a subject against COVID-19. Vaccination typically comprises administering to a subject in need thereof with an immunogenic composition comprising at least one nucleic acid encoding at least one immunogen that comprises a lipolysis-stimulated receptor binding domain (LBD) of a SARS-CoV-2 spike protein, wherein the at least one nucleic acid encoding the immunogen is operably linked to an expression control sequence and wherein the LBD is selected from LBD1 and LBD2. In one or more embodiments, the immunogenic composition comprises at least one nucleic acid encoding at least one immunogen that comprises a lipolysis-stimulated receptor binding domain (LBD) of a SARS-CoV-2 spike protein or a fragment thereof, coupled to one or more TI segments. In one or more embodiments, the vaccine is provided to a subject in several sequential administrations of a same or different chimeric immunogen(s).

[00364] In one or more embodiments, the vaccination reduces the severity of COVID-19 disease. In one or more embodiments, reduces transmission of SARS-CoV-2. In one or more embodiments, the vaccination is used to stimulate an immune response and the antibodies elicited by the vaccination are recovered from the antiserum to prepare polyclonal or monoclonal antibodies. In one or more embodiments, the monoclonal antibodies are administered therapeutically to a subject suffering from COVID-19. In one or more embodiments, the monoclonal antibodies are administered with a second monoclonal antibody and/or a second therapeutic agent.

[00365] In one or more embodiments, the disclosure relates to a method of stimulating an immune response against the S protein of the SARS-CoV-2 in a subject, comprising administering to the subject at least one chimeric immunogen comprising the S protein, or a fragment thereof, coupled to one or more TI segments.

[00366] B. Monoclonal antibodies

[00367] In one or more embodiments, monoclonal antibodies disclosed herein are used to treat COVID-19. For therapeutic applications, monoclonal antibodies disclosed herein, which bind to and neutralize the SARS-CoV-2 in infected subjects, can be administered to a mammal, generally a human, in a pharmaceutically effective amount. For example, the antibody may be administered to a human intravenously as a bolus or by continuous infusion over a period of time, or by subcutaneous, or intramuscular routes.

[00368] Current therapeutic monoclonal antibodies are clinically effective, but only when provided to patients at the early stage of the disease. Monoclonal antibodies disclosed herein, which bind to SARS-CoV-2 LBD domains and neutralize cellular entry by way of LSR stand to improve the success of monoclonal therapies.

[00369] Accordingly, in one or more embodiments, administration of monoclonal antibodies disclosed herein with the effective amount of the pharmaceutical composition accelerate intestinal clearance of SARS-CoV-2. In one or more embodiments, administration an effective amount of monoclonal antibodies disclosed reduces transmission of SARS-CoV-2. In one or more embodiments, administration an effective amount of monoclonal antibodies disclosed alleviates one or more symptoms of long COVID-19 syndrome. In one or more embodiments, administration of an effective amount of monoclonal antibodies disclosed accelerates intestinal clearance of SARS-CoV-2,

reduces transmission, alleviates one or more symptoms of long COVID-19 syndrome, or brings about any combination thereof of the above results.

[00370] C. Fatty Acids

[00371] Disclosed herein is the finding that SARS-CoV-2 spike protein is capable of binding more than one cellular receptor through which it can gain cellular entry and replicate. The coordinated use of these cellular receptors for replication by SARS-CoV-2 is coordinated by fatty acids.

[00372] Unsaturated FFA irreversibly suppress SARS-CoV-2 capacity to bind ACE2 and inhibit subsequent replication by the ACE2 mediated pathway. The LSR, activated by FFA, endocytoses ACE2 competent and incompetent SARS-CoV-2 yielding immediate or delayed production of ACE2 competent progeny. Thus, the LSR may deliver SARS-CoV-2 into a replicative or a latent compartment and does not immediately deliver its cargo to the compartment where viral RNA is transferred to the cytoplasm.

[00373] Excessive dietary fat is the common factor associated with the four main comorbidities increasing COVID-19 severity i.e. obesity, diabetes, hypertension and cardiovascular diseases. Very high FFA concentrations are found in patients with severe COVID-19 (*see* Example 8, below). Accordingly, in one or more embodiments, therapeutic treatment of COVID-19 patients comprises reducing or temporarily suppressing the physiological supply of free fatty acids to the subject. In one or more embodiments, reducing or temporarily suppressing the physiological supply of free fatty acids to the subject comprises administering to the subject a composition suitable for treatment of diabetes or hyperlipidemia. In one or more embodiments, the composition is suitable for treatment of diabetes, and comprises administering comprises Metformin. In one or more embodiments the composition is suitable for treatment of hyperlipidemia and comprises administering Acipimox. In one or more embodiments reducing or temporarily suppressing the physiological supply of free fatty acids to the subject comprises administering to the subject a composition suitable for treatment of diabetes or hyperlipidemia, together with a second a therapeutic agent to treat the SARS-CoV-2 infection. In one or more embodiments, the therapeutic agent is selected from remdesivir, tocilizumab, sotrovimab, propofol-lipuro 1%, bamlanivimab, etesevimab, casirivimab,

imdevimab, baricitinib, COVID-19 convalescent plasma, regiocit replacement, freesenius kabi propoven, and combinations thereof.

[00374] IX. Kits

[00375] In one or more embodiments, an anti-LBD antibody and/or an anti-ABD antibody is provided in the form of a kit, i.e., a packaged combination of reagents in predetermined amounts with instructions for performing a procedure. In one or more embodiments, the procedure is a diagnostic assay. In one or more embodiments, the procedure is a therapeutic procedure.

[00376] In one or more embodiments, the kit further comprises solvents for the reconstitution of the antibody. In one or more embodiments, the antibody is provided in the form of a pharmaceutical composition.

[00377] In one or more embodiments, the disclosure provides a kit comprising an mRNA that comprises one or more open reading frames that encodes one or more of an LBD1, LBD2 or ABD polypeptides for use in the treatment or prevention of COVID-19. In one or more embodiments, the treatment or prevention of the disease comprises contacting the mRNA to the epidermis of a mammalian subject. In one or more embodiments, the mRNA is provided as a pharmaceutical composition.

EXAMPLES

[00378] Materials and Methods for Examples 1-10.

[00379] 1. Patients and serological assays

[00380] Patients generously donated human serum samples. Moderate Covid-19 patients signed informed consent authorizing the use of their samples for research purposes. The regulatory approvals for collecting and storing human samples for research purposes were obtained from France's Ministry of Health (AC2008-449 and CCTIRS 15.616 bis). In the case of severe Covid-19 patients, only oral non-opposition was requested (ClinicalTrials.gov Identifier NCT04405726). Free fatty acids (MAK044, Sigma), cholesterol (MAK043, Sigma), triglycerides (MAK266, Sigma), adiponectin (DRP300, R&D Systems), insulin (DINS00, R&D Systems), and leptin (DLP00, R&D Systems) were measured in serum according to manufacturer instructions.

[00381] 2. Reagents and biologicals

[00382] Oleic acid (O1008), palmitic acid (P0500), stearic acid (S4751), linoleic acid (L1376), octanoic acid (C2875) or heptanoic acid (75190) were purchased from Sigma, St-Quentin-Fallavier, France. ZEBA Spin Desalt Column were from ThermoFisher. Interferin (Ozyme – POL10100028), OptiMEM (ThermoFisher – 10149832), scramble (or control) (4390843) and LSR specific siRNA (4392421) were purchased from Life Technologies and antibodies reactive with LSR, ACE2 and GAPDH were from Invitrogen (MA5-36088), Novus – Biotechne (NBP1-8963) and Cell Signaling (5174), respectively. HRP recombinant ACE2 Binding, and wells coated with human ACE2 are part of in-vitro neutralization assay purchased from GenScript (L00847). Casirivimab and Imdevimab were generous gifts from Pr X (Samira). In other instances, Casirivimab, Imdevimab (Ronaprev – Regeneron Roche), Adalimumab (Humira – abbvie) and Ritonavir and Nirmatrelvir (Paxlovid – Pfizer) were purchased from a local pharmacy. Pseudo SARS-CoV-2 reporter kit (C1110G) were purchased from Montana Molecular.

[00383] Recombinant LBD1 and LBD2 proteins were produced as N-terminal-hexa-histidine-tagged proteins in BL21 *Escherichia coli* (*E. coli*) according to standard procedures with the modification that clones were engineered toward *E. coli* codon usage to increase their expression levels. The proteins were then purified from inclusion bodies by immobilized metal ion affinity chromatography (His Trap FF column, Cytiva, Vélizy, France). The recombinant proteins were eluted from the columns in a denaturing phosphate or Tris-buffered saline (PBS: 30 mM sodium phosphate, 150 mM NaCl, pH 7.4 or Tris: 30 mM Tris-HCl, 150 mM NaCl, pH 9) containing 500 mM imidazole, 8 M urea and 2 mM beta-mercapto-ethanol. Imidazole was removed using a Zeba Desalt Spin column (Thermo Fisher Scientific, Rockford, IL, USA) to enable their storage in a denaturing PBS (for SHB-2) or Tris (for SHB-1) containing 4 M urea. Protein concentrations were determined using a protein assay kit (Bio-Rad, Hercules, CA, USA). The final molecular weight of the recombinant purified proteins was verified by 12% SDS-PAGE (NuPAGE; Invitrogen, Saint Aubin, France) after Coomassie blue staining. Endotoxin concentrations were measured using the gel-clot Limulus Amebocyte Lysate (LAL) method and ENDOSAFE LAL reagents (Charles River Endotoxin Microbial Detection Europe, Ecully, France). Endotoxin concentrations were < 0.005 EU per microgram protein.

[00384] 3. Cell culture

[00385] Buffalo Green Monkey (BGM or equivalently, BGMK) cells, and 4T1 cells were grown in Dulbecco's modified Eagle's medium (DMEM) containing 4.5 g glucose (ThermoFisher – 11584496). CaCo-2 cells were grown in Dulbecco's modified Eagle's medium containing 4.5 g glucose (ThermoFisher – 11584496) or in Eagle's minimal essential medium (EMEM) (Dutscher – P04-08056). Both medium were supplemented with 10% (V/V) of Fetal Calf Serum (FCS) (Dutscher – S1810), 1% non-essential amino acids (ThermoFisher – 12084947), 1% glutamax 1X (ThermoFisher – 11574466) and 1% antibiotics (ThermoFisher – 11570486) at 37°C in a humid atmosphere with 5% CO_2.

[00386] 4. SARS-CoV-2 sources

[00387] The wild type (strain) was isolated from patients infected during the first wave of COVID 19 occurring is the east of France in the spring of 2020. The Delta variant was isolated from patients admitted to Strasbourg University Hospital in July 2021 or from patients admitted to Nancy University Hospital in 2022. The Omicron (BA.5) variant was isolated from pateints admitted to Nancy University Hospital in 2022.

[00388] SARS-CoV-2 ultra-deep sequencing was performed on an Illumina iSeq 100 system using RT-PCR assay (nucleic acid technique (NAT)) followed by Next Generation Sequencing (NGS) (DeepCheck® Whole Genome SARS-CoV-2 Genotyping V1, from Advanced Biological Laboratorires, ABL SA Group, Luxembourg). Genotyping was performed using the ABL DeepCheck®. Lineages and clades were interpreted using Pangolin and NextClade methods of lineage classification, before being submitted to the Global Initiative on Sharing Avian Influenza Data (GISAID) database.

[00389] 5. Cell Infection, FFA supplementation, quantification of viral particles, and culture media supplementation

[00390] Cells (from $4x10^4$ cells per well to $6x10^4$ cells per well) in 96-well plates the day before infection. Pilot studies established that the minimum time of BGM exposure to the SARS-CoV-2 yielding robust viral replication was 150 min. All infections were conducted using this time of exposure, and the culture of infected cells was systematically pursued for 96 hours. Incubating cells for 150 min with FFA did not cause cell floating or

cell toxicity translating in a detectable decrease in cell layer protein content determined by the Bradford method and/or the BCA method (ThermoFisher - 23227).

[00391] Unsaturated fatty acids were protected from light, without being frozen and without temperature variations from 4 to 37°C. FFA solubilized in isopropanol were added directly to the culture media containing FBS. The final isopropanol concentration did not exceed 2 % (v/v) and was most commonly 1 % (v/v). 2 % isopropanol had no cell toxicity and did not change SARS-CoV-2 replication when added without FFA. After incubation with FFA for 150 min, the media was removed and replaced with fresh media not supplemented with FFA.

[00392] In pre-incubation studies, FFA were incubated with the viruses or pseudoviruses. FFA not bound to viruses or pseudoviruses were removed by size exclusion chromatography using the ZEBA desalting column and the virus or pseudoviruses were eluted. With this procedure, it was verified that the fatty acid concentration in infective media was lower than 20 µM.

[00393] Imidazole was added to stabilize LBD1 and LBD2 but was removed using the ZEBA desalting column equilibrated with culture media to prevent imidazole-induced cell toxicity. Regarding recombinant LBDx, nuclear and spike proteins were added directly to the culture media before cell infection and again after each media replacement.

[00394] Casirivimab, Imdevimab, and Adalimumab were added to the viral suspension before cell infection.

[00395] Ritonavir and nirmatrelvir were solublilized in isopropanol, added to the culture media during the infection of the cells, and again after each media replacement.

[00396] The number of viral particles in the media and the cell layers was measured using calibrated qPCR. The number of particles in the media and the cell layer was concordant in all experiments. Accordingly, data is presented as the total viral production calculated as the sum of particles in the media and the cell layer.

[00397] qPCR Panther: RNA quantification was performed using an in-house RT-PCR assay targeting two virus sequences on the RNA-dependent RNA polymerase gene nCoV_IP2 and nCoV_IP4) running on the Fusion module of the Panther-Fusion system. (Etievant S., Bal A., Escuret V., Brengel-Pesce K., Bouscambert M., Cheynet V., et al.

Performance assessment of SARS-CoV-2 PCR assays developed by WHO referral laboratories. J Clin Med 2020;9:1871) (La phrase sur la PCR subgénomique et la référence de la méthode: A subgenomic RNA RT-qPCR was performed to explore the evidence of an active viral replication) (Wölfel, R., Corman, V.M., Guggemos, W. et al. Virological assessment of hospitalized patients with COVID-2019. Nature 581, 465–469 (2020)).

[00398] Experiments were conducted in 96 well plates, which at the time of infection contained 10^5 cells per well. The results are presented as the number of viral copies per well. Translation in multiple of infection unit can be readily calculated. In BGM cells without FFA, viral production reached a plateau with $2x10^6$ viruses in the infective media. When using the O+2P protocol the viral production plateaued with 10^7 viral copies per well. To ascertain the fatty acid inhibitory effect on the ACE2 mediated replication cells were infected with large excess of viruses but it was verified that the conclusions were valid when the infective titer were lower.

[00399] 6. RNA interference

[00400] Cells were plated either at $4x10^4$ cells by well in 96-well plates (SARS-CoV-2 transfections) or at $5x10^5$ cells by well in 6-well plates (Western blots). After 24 h of growth, 0.17 pmol (96-well plate) or 2.2 pmol (6-well plate) of LSR-siRNA or scramble-siRNA was mixed with 8 or 0.75 µL (in 6-well or 96-well plate respectively) of interferin in optiMEM medium (ThermoFisher – 10149832) and added to the growing cells. After 24 hours incubation with the siRNA mix, the medium was replaced with fresh medium and cells were grown 48 hours before starting experiments. In some instances, cells were grown 120 hours. LSR and ACE2 protein expression were assessed by western blot analysis.

[00401] 7. Preparation of cell extract and Western Blot analysis

[00402] BGM, Caco-2, 4T1 cells (and human adipose tissue where applicable) were washed in PBS 1X buffer (Sigma – P3813) and incubated for 10 minutes at 4°C in lysis buffer (RIPA buffer [Sigma – R0278] supplemented with protease inhibitors [Sigma – 05892791001]). After centrifugation for 20 minutes at 16000 x g, the concentration of proteins in the supernatant was measured by Pierce BCA Protein Assay (ThermoFisher – 10678484). 5 µg of total proteins were analyzed by 8 % SDS/PAGE (Invitrogen – NW00080BOX) gels and transferred to ethanol-activated PVDF membranes

(ThermoFisher – 88518). Membranes were blocked with 5% non-fat dry milk in tris-buffered saline (TBS) containing 0.1% Tween 20 for 2 hours at room temperature before an overnight incubation at 4°C with primary antibody. Primary antibodies bound to target were revealed using a secondary antibody coupled to horseradish peroxidase (Life Technologies – A16096) by enhanced chemiluminescence (GE Healthcare – RPN2106). Standardization was made using an anti-GAPDH antibody (immunodetection of GAPDH was used as an internal control). Protein levels were quantified using GeneTools software (Syngene).

[00403] 8. Pseudovirus assays (Virus-like particle assays)

[00404] BGM cells were seeded at $4x10^4$ cells per well in 96-well plates with black walls and clear bottom (Sarstedt – 94.6120.096) in DMEM supplemented with 10% FCS, 1% non-essential amino acids, 1% glutamax 1X and 1% antibiotics and incubated 24h at 5% CO_2 and 37°C. BGM cells were then once washed with warm phosphate-buffered saline (PBS) (Sigma – P3813) and put in 100 µL of fresh F12K medium (Dutscher – 702515) supplemented with 10% FCS. Next, pseudoviruses were treated for 2 h 30 min with 0 or 1 mM of FFA then passed through the ZEBA column to remove unbound FFA. Finally, 50 µL of pseudovirus transfection mix were added in each well, containing $13,2.10^8$ VG/mL of SARS-CoV-2 pseudovirus and 2 mM of sodium butyrate. The plate was then gently rocked 5 to 10 times to ensure uniform transduction before incubation at 37°C. Before the reading, the media was replaced with PBS $Ca^{2+}Mg^{2+}$ (Dutscher – P04-35500), and fluorescence was read in the Infinite 200 Pro reader by Tecan-Life Sciences (excitation = 490 nm, emission = 524 nm).

[00405] BGM cells were seeded at 10^5 cells per well in dark-walled 96-well plates with clear bottoms (Sarstedt, Marnay, France – 94.6120.096) in DMEM supplemented with 10% FCS, 1% non essential amino acids 100X, 1% glutamax 100X, and 1% antibiotics 100X and incubated 24 h at 5% CO2 and 37°C. BGM cells were then washed once with warm phosphate-buffered saline (PBS) (Sigma – P3813) followed by the addition of 100 µL of fresh F12K medium (Corning – 10-025-CV) containing 10% FCS. Pseudoparticles (or virus-like particles, VLP) were treated for 150 min at 37°C with 0 or 1 mM of FA and then passed through the ZEBA column to remove unbound FA. Pseudoparticles were added to cells following the manufacturer's instruction to measure viral entry.

[00406] 9. Monomeric spike competition assays, and trimeric spike competition assays

[00407] Pilot studies established that 80% inhibition of HRP-RBD binding to ACE2 was achieved after incubation of 100 µg/ml of recombinant full-length spike (FLS) protein with HRP-ABD diluted at 1:1000 after 10 min at 37°C, before incubation for additional 30 min at 37°C in wells coated with recombinant human ACE2. These conditions were used to test the effect of adding FFA in isopropanol with the spike protein. The results were expressed as the difference of maximal inhibition calculated as: OD value without FLS minus OD value with FLS at any given fatty acid concentrations. FFA in isopropanol were also directly added with HRP-ABD and tested for binding to ACE2 coated wells. Wells coated with human ACE2 were incubated with oleate 1 mM, the media was removed and the HRP-ABD binding capacity was determined.

[00408] 10. Bioinformatics and statistical analysis, LSR and ACE2 expression profiling, and structural analysis

[00409] The trimeric spike structure of SARS-CoV-2 in the closed conformation was obtained from the PDB database (6ZP0). The absent loops were predicted using Swissmodel server (Waterhouse, A., Bertoni, M., Bienert, S., Studer, G., Tauriello, G., Gumienny, R., Heer, F.T., de Beer, T.A.P., Rempfer, C., Bordoli, L., Lepore, R., Schwede, T. SWISS-MODEL: homology modelling of protein structures and complexes. Nucleic Acids Res. 46(W1), W296-W303 (2018)). The tetrameric extracellular LSR structure was obtained by using the Cluspro and RaptorX servers (Kozakov D, Hall DR, Xia B, Porter KA, Padhorny D, Yueh C, Beglov D, Vajda S. The ClusPro web server for protein-protein docking. *Nature Protocols.* 2017 Feb;12(2):255-278, Wang Z, Zhao F, Peng J, Xu J. Protein 8-class secondary structure prediction using conditional neural fields. Proteomics. 2011 Oct;11(19):3786-92). Briefly, the structure of the sequence corresponding to the alpha isoform of the LSR protein (NP_991403) was predicted using the RaptorX algorithm. The sequence corresponding to the extracellular part of the protein (1 to 170AA) folded as an IgV-like domain. The transmembrane domain folded as a helix and the c-terminal domain probably disordered is not shown. After energy minimization using the chimera software (UCSF Chimera--a visualization system for exploratory research and analysis. Pettersen EF, Goddard TD, Huang CC, Couch GS, Greenblatt DM, Meng EC, Ferrin TE. J Comput Chem. 2004 Oct;25(13):1605-12.), the tetrameric structure of LSR

was predicted using the Cluspro server with the Multimer Docking option. A model was selected where the 4 IgV-like domains interact with each other and transmembrane helices form a bundle. As the size of the tetrameric structure was important, only the extracellular part of the LSR (the 4 IgV-like domains) was used thereafter. After an energy minimization of this structure with chimera, the interaction of the spike closed conformation structure and the tetrameric LSR was predicted with the Cluspro server. The final model of interaction was selected by the cluspro score within the VdW+Elec (10 models) and by the orientation of the AA connected to the transmembrane segments. AA implicated in the interaction were identified using chimera.

[00410] RNA sequencing of PRJNA627122 (normal tongue tissues, n=6), PRJNA422174 (nasal epithelium control, n=8), PRJNA699591 (Calu3 control, n=12) and PRJNA698644 (Control, n=2) projects were downloaded from ncbi SRA ftp. STAR (STAR_2.4.2a) was used to align reads to the human reference genome (GRCh38.p13) and LSR, ACE2 and TMPRSS2 expression were estimated by counting number of reads per genes. TPM normalization (Transcripts Per Million) calculation was done using R (3.4.4).

[00411] All experiments reported here were performed at least twice, and each data point represents the mean of triplicate determinations, unless otherwise indicated. The F-tests followed by t-tests were used to compare differences between means of two populations after establishing normal distribution. Wilcoxon paired-and unpaired sample test was used to test for significance of differences between parameters that were not normally distributed. P-values are indicated by *$p < 0.05$, **$p < 0.01$, ***$p < 0.001$.

[00412] **<u>EXAMPLE 1</u>: Long-chain unsaturated FFA suppress SARS-CoV-2 spike binding to ACE2 and viral replication.**

[00413] To investigate the effect of fatty acids on the mechanisms of viral entry, RTqPCR was used to quantify the production of viral RNA copies in the media and the cell layers. Any loss of cells impacts these measurements of viral replication rates. Therefore, a cell model enabling SARS-CoV-2 replication while causing minimal damages to the cells layer (cell monolayers) was sought. Buffalo Green Monkey kidney (BGM) provided such model. Buffalo Green Monkey (BGM or equivalently BGMK) cells are kidney derived cells that efficiently replicate SARS-CoV-2.

[00414] BGM cells were infected with SARS-CoV-2 (wild-type Strain, 10^8 viruses per well). At day 4 post infection (DPI 4), 10^9 to 10^{10} viral RNA copies were produced in BGM cells. The viral RNA copy numbers were equivalent in the media and cell layers (FIG. 1A) and no detectable changes in the cell layer protein content were found (FIG. 1B). Plaques resulting from cell fusion were detected in BGM cells producing very high SARS-CoV-2 copy numbers (FIG. 1Z and FIG. 1C) but within this time frame SARS-CoV-2 infection did not reduce the cell protein content. Viral production in this cell line is suppressed by the monoclonal antibodies Casirivimab and Imdevimab alone or in combination (FIG. 1C). Both monoclonals target the spike protein RBD within the ACE2 binding domain (ABD). As shown in FIG. 1C, infection of BGM cells in the presence of Casirivimab, Imdevimab, or Casirivimab and Imdevimab (C & I) significantly reduces (by six logs reduction or by 99%) the number of virus produced as compared to the control (WT) without the antibodies. The monoclonal antibodies were most efficient (six logs reduction) at the lowest (10^4 particle per well). When combined, these monoclonal antibodies were most efficient (seven logs reduction) at the lowest infective dose (10^4 genome equivalent copies per well) (FIG. 1Z). Each antibody added independently remained highly efficient even at the highest infective dose (10^8 genome equivalent copies (gec) per well) (similar to FIG. 1A). Therefore, under usual cell culture conditions, the ACE2 pathway accounts for more than 99% of the SARS-CoV-2 viral production in BGM cells that egressed to the media without causing substantial cell loss even at a very high viral load. Thus, ACE2 is the functional SARS-CoV-2 receptor in this cell line.

[00415] To test the effect of unsaturated fatty acids on SARS-CoV-2 replication in BGM cells, increasing concentrations of oleic acid (OA) were added along with wild type (WT) SARS-CoV-2 to BGM cells during the infection phase (FIG. 1D and FIG. 1X). After 150 minutes (min), the infective media that contained very high number of SARS-CoV-2 (10^8 particles per well) was removed and replaced by culture media without any OA supplementation. The viral production measured at the fourth day post infection (DPI 4) decreased by 87% with 0.5 mM oleic acid and 99% with 1.0 mM oleic acid (FIG. 1D). The viral production decreased significantly with 0.2 mM OA and by at least 4 logs with 1 mM OA, respectively (FIG. 1X). However, between 0.2 and 0.5 mM, the OA inhibitory effect plateaued. SARS-CoV-2 pre-incubated with oleate/oleic acid (1 mM) followed by removal of unbound free fatty acids (FFA) before infection of BGM cells, also showed a 99% reduction in their replicative capacity (FIGS. 1E and 1V) compared to SARS-CoV-2 pre-

incubated without oleate/oleic acid. However, similar pretreatment of pre-incubating SARS-CoV-2 with 1 mM palmitic acid (PA), the most abundant saturated FA, followed by removing unbound FFA did not affect viral replication (FIG. 1V). Pre-incubations of the wild-type (WT), Delta, and Omicron (BA.5) variant with OA reduced the ACE2 mediated replication (FIG. 1W). These data confirmed that the inhibition of WT SARS-CoV-2 by OA occurred with both high (FIG. 1V) and low (FIG. 1W) infective titers.

[00416] Pseudovirus assays

[00417] Pseudoparticles (PP) (or equivalently, pseudoviruses (PV), or virus-like particles (VLP)) that express the wild-type SARS-CoV-2 S protein were used to study the effect of fatty acids (FA) on ACE2 mediated entry independent of viral replication. In these assays, incubation of pseudoparticles with BGM cells enables ACE2 fusion of PP with the cells and this leads to nuclear expression of DNA encoding a fluorescent protein reporter, thus indicating cell entry (FIG. 1F and FIG. 1Y).

[00418] Pseudoparticles pretreated were pre-incubated with 1 mM of the unsaturated fatty acids (FA), oleic acid (OA) or linoleic acid (LA) or with the saturated fatty acids, palmitic acid (PA) or Stearic Acid (SA) (other saturated fatty acids included, for example, octanoic acid and heptanoic acid). Unbound fatty acids were removed by size exclusion chromatography, and then incubated with 80% confluent BGMK cells. After 24 hours (h) incubation, the cells were washed and fluorescence intensity was measured. As shown in FIG. 1F (and FIG. 1Y), pseudoparticles pre-treated with OA or LA exhibited decreased cell fluorescence by comparison to pseudoparticles that were not pre-treated with fatty acids. In contrast, the same pseudoparticle pretreatment with the saturated fatty acids, palmitic acid (PA) or Stearic Acid (SA) did not inhibit PV entry (FIG. 1F and FIG. 1Y). Similar experiments were carried out with additional saturated and unsaturated fatty acids (FIG. 1I): oleate, linoleate, palmitate, stearate, octanoate, and heptanoate. The specific inhibitory effect of FFA on the PP entry was identical to that observed with recombinant proteins (FIG. 1P).

[00419] In these experiments only the PV, not the cells, were exposed to FFA. Thus, BGM cells were exposed to fatty acids bound to pseudoparticles. In 24 hours (h), it would have been expected that cell metabolism would lead to uptake of OA or LA thus restoring entry, yet this did not occur. Thus, the cells were unable to capture oleate or linoleate

bound to the PV and thereby restore the ACE2 binding. To test this observation further, pseudoviruses were pre-incubated with or without 1 mM oleate, and were then incubated with BGMK cells for 24 or 48 h. The fluorescence intensity was measured in triplicate. Even after incubating the PV with the BGMK cells, GFP expression remained undetectable (FIG. 1G).

[00420] Because serum and biological fluids contain a mixture of saturated and unsaturated fatty acids (FA), the possibility that saturated fatty acids could counteract the inhibitory effect of unsaturated FA was tested. FIG. 1H shows the fluorescence intensity of BGM cells following incubation with pseudoviruses that were pretreated prior to infection with no FFA followed by no FFA, with oleate followed by oleate, with oleate followed by palmitate, and twice with palmitate. After each incubation unbound FFA were removed. Notably, exposure of pseudoparticles to palmitate after oleate did not reverse the inhibitory effects of oleate (FIG. 1H).

[00421] Pseudoparticles failed to enter BGM cells when pre-incubated with OA then with palmitate or vice-versa, followed by the removal of unbound FA (FIG. 1K). Notably, oleate added after palmitate fully inhibited PV binding to ACE2. However, two consecutive incubations with PA did not inhibit PP entry (FIG. 1K).

[00422] The effect of sequential pre-incubations of the PV with and without oleate or palmitate were investigated further. Pseudoviruses were first incubated with either no FFA, oleate, or palmitate (1 mM). Pseudoviruses were then separated from the media by size exclusion chromatography, and each of the three fractions were again incubated without any FFA, with oleate (1 mM), or with palmitate (1 mM). Pseudoviruses were again separated from unbound FFA. The separated PV were added to BGMK cells to initiate infection. Cell fluorescence was measured after 24 h of incubation. The results are shown in FIG. 1J as the mean and standard deviation (SD) of three independent wells. The data shown in FIG. 1J confirms that oleate inhibited binding by the PV to ACE2.

[00423] Competition assays to evaluate the effect of fatty acids on ACE2 receptor binding

[00424] The effect of free fatty acids (FFA) on the capacity of the viral spike to bind the ACE2 receptor and the labeled spike-ACE2 binding domains (ABD) was tested. Similar experiments were carried out using Horse Radish Peroxidase (HRP) labeled RBD.

[00425] The effect of FFA on the S protein independently of its organization as a trimer, was tested in a competition assay using purified recombinant proteins: recombinant monomeric glycosylated wild type SARS-CoV-2 S protein (FIG. 1L), Horse Radish Peroxidase (HRP) labeled ACE2 binding domain (ABD), and the human ACE2. Recombinant spike was added to a media containing horseradish peroxidase (HRP) labeled ACE2 binding domain, and the mixture was added to plates coated with the human ACE2. Under these conditions, the recombinant spike inhibited 90% of the ABD binding. The data show the reduction of this inhibition caused by increasing concentration of the indicated FFA. In particular, long-chain unsaturated, but not saturated FFA suppressed the spike capacity to compete with the ABD for binding to the ACE2 receptor in a dose dependent manner (FIG. 1M). Maximal inhibition was achieved with 0.3 mM oleate or linoleate.

[00426] The inhibitory of effect of oleate on the spike binding to ACE2 was tested. Oleate did not inhibit the direct binding of HRP-ABD to the ACE2 (FIG. 1N), and pre-incubation of the ACE2 with oleate did not decrease its HRP-ABD binding capacity (FIG. 1O). Thus, the effect of oleate was not caused by the interaction of oleate with the ACE2 or ABD itself, as each of these retained their full binding capacity in the presence of oleate.

[00427] Further experiments to directly assess the effect of fatty acids on the S protein interaction with the human ACE2 were carried out. A competitive assay was carried out utilizing the three recombinant proteins: the trimeric wild type (WT)-Spike, Horse Radish Peroxidase (HRP) labeled RBD, and human ACE2 coated wells on a plate. OA and LA but not PA or SA suppressed the S protein capacity to compete the binding of HRP-RBD to the ACE2 (FIG. 1P). The OA and LA concentrations maximally inhibiting the S protein capacity to compete the RBD binding to the ACE2 was 0.3 mM. Further, OA (1 mM) did not affect the binding of HRP-RBD to the ACE2 (FIG. 1Q). However, as above, oleic acid did not inhibit the direct binding of HRP-RBD to the ACE2. Thus, it was verified that OA (1 mM) did not directly interfere with ACE2 nor affect the binding of HRP-RBD to ACE2 (for example, FIG. 1Q). Therefore, unsaturated fatty acids (with an angulated carbon chain, in this instance two unsaturated FA abundant in humans) but not saturated fatty acids (with a linear carbon chain) accessed the S protein hydrophobic pocket, causing a conformational change and preventing SARS-CoV-2 from interacting with ACE2, thereby reducing viral production.

[00428] Without being bound by theory it is believed that fatty acids with an angulated carbon chain such as unsaturated fatty acids, but not saturated FA with a linear carbon chain, enter/bind the S protein hydrophobic pocket (FIG. 1R and FIG. S). This, in turn, locks the S protein in closed conformation and thereby, suppresses SARS-CoV-2 S protein interaction with ACE2, dramatically reducing ACE2 mediated viral replication. Neither BGM cell metabolism nor saturated FA reversed this inhibition.

[00429] In this context, it is interesting to note that linoleate is known to bind tightly to SARS-CoV-2 spike protein in three composite binding pockets (*see e.g.*, Toelzer, C., *et al.* (2020) Science 370(6517):725-730). 3D modeling shows that not only linoleate (FIG. 1R), but also oleate (FIG. 1S) fully occupies this S-protein FFA binding pocket. The length of the palmitate carbon chain is insufficient to interact with the residues located at the bottom of the pocket, and the linear structure of stearate is not compatible with the angulation of the SARS-CoV-2 spike FFA binding pocket.

[00430] The results demonstrated and disclosed herein are consistent with the observation that angulated unsaturated, but not linear saturated FFA can access the S protein hydrophobic pocket (FIG. 1R and FIG. 1S). As demonstrated herein, in both simian and human cells, the consequence of S protein binding to unsaturated fatty acids such as oleate and linoleate is the dramatic reduction of ACE2 mediated viral replication.

[00431] Live virus assays

[00432] The effect of oleate on the replication of live viruses (Wuhan strain) was also examined. Replicative SARS-CoV-2 (Wuhan strain 10^8 copies per well) were applied to BGMK cells for 2 h 30 min without or with the indicated concentration of oleate. The cells were washed and incubated with fresh media for 96 hours. The media was removed, and the cell layer washed and recovered with trypsin. The amount of viral RNA in the media and cell layers was measured by quantitative PCR (qPCR). The results are the mean and SD of three independent wells (FIG. 1T). As can be seen in FIG. 1T, oleate (0.5 mM) reduced by 92 % (min 84% max 99 %; $p<0.04$) and 86 % (min 80 % max 94 % $p<0.004$) the number of viral particles released in the media and present in the cell layer, respectively. With 1 mM oleate, the number of viral RNA detectable in the media and the cell layer decreased by more than 99.9 % ($p<10^{-5}$).

[00433] To ascertain that this inhibition was caused by oleate interaction with the virus and not the cells, further experiments were carried out. Replicative SARS-CoV-2 was pre-incubated without or with 1 mM oleate or palmitate. Viruses were re-isolated by size exclusion chromatography and added to BGMK cells (10^8 copies per well) for 2 h 30 min. The infective media were removed and the cells were incubated for 96 hours. Viral production was measured as above. The data are the mean and SD of measurements performed in triplicate. Pre-incubation of the virus with oleate (1 mM) reduced viral replication by more than 99.9 % while pre-incubation with palmitate (0.4 mM) did not change the amount of viral RNA released in the media or detected in the cell layers (FIG. 1U). Oleate treated virus is referred to herein as ACE2 incompetent SARS-CoV-2.

[00434] These data confirmed that oleate, but not palmitate, changes the spike conformation and suppresses ACE2 binding. Furthermore, uptake of FFA bound to the virus by the cells does not reverse the loss of function imposed by oleate. Therefore, as shown in multiple experimental settings disclosed herein, long-chain unsaturated, but not saturated FFA, irreversibly suppresses ACE2 mediated SARS-CoV-2 entry and subsequent replication.

[00435] **EXAMPLE 2: FFA activate a second, alternate, SARS-CoV-2 receptor that enables cellular entry and replication of ACE2 incompetent SARS-CoV-2.**

[00436] The effect of oleate on SARS-CoV-2 binding to ACE2 was investigated further. Initial investigations utilized several transient exposures to oleate. BGMK cells were infected with SARS-CoV-2 (Wuhan strain at 10^8 copies per well) for 2 h 30 min in presence or absence of oleate. After this, all infective media were removed and replaced by the same media without viruses. For cells incubated with the virus only, the media and cell layer were recovered after 96 hours of culture. Cells incubated with virus and oleate were divided in three groups. The first group was maintained for 96 hour in growth media, the second group was incubated on day two for 2 h 30 min with oleate (1 mM), and after this incubation period, the media was removed and replaced by media without FFA. The third group was incubated for 2 h 30 min with oleate on day two and then again on day three. After 96 hours, media and cell layers were recovered and viral production measured by quantitative PCR (qPCR).

[00437] As can be seen in FIG. 2A (see also FIG. 2J), a single oleate incubation at the same time as the virus, reduced viral production by >99.9 % in both the media and the cell layers as compared to virus not exposed to oleate at the time of infection. Two short incubations with oleate every 24 h without adding new viruses did not consistently alter viral production. However, after three oleate cycles, the number of viral particles released in the media increased by 6.8 x 10^2 and that in the cell layers by 2.5 x 10^3 fold (FIG. 2A, see also FIG. 2J). The experiment was repeated and analysis of the combined data showed that after 3 cycles with oleate (1 mM) without new viruses, the increase viral production as detected in the media and cell layers was statistically significant: ($p < 0.007$ and $p < 0.02$) respectively.

[00438] The effect of palmitate on SARS-CoV-2 binding to ACE2 was also investigated. Specifically, BGMK cells were infected with SARS-CoV-2 (Wuhan strain 10^8 copies per well) in the absence or presence of palmitate (0.4 mM) for 2 h 30 min. After this, the infective media was replaced by media without viruses or FFA. The number of viral RNA in the media and cells layer were measured after 96 hours of incubation (FIG. 2B). Under these conditions, viral production increased 4.2-fold from 7.6 X 10^8 to 3.2 X 10^9 (4.2-fold, FIG. 2B). Compared to cells incubated without palmitate, addition of palmitate (0.4 mM) at the time of infection increased the number of virus released in the media by 236 % (min 93% max 352 % $p < 0.02$) and in the cell layer by 414 % (min 372 % max 427 % $p < 0.03$).

[00439] In contrast, pre-incubating the virus, but not the cells with palmitate did not affect viral replication (FIG. 2C). Because the increase was not observed when the virus was pre-incubated with palmitate and unbound palmitate removed, the palmitate enhancement of replication was due to its effect on the cells and not on the virus.

[00440] Physiologically, after each meal containing lipids, cells in the mouth and the digestive tract are transiently exposed to increased FFA levels. Without being bound by theory, it is believed that LSR is the primary route of oral infection and is also the receptor that causes the pulmonary destruction and most severe oral damage.

[00441] Therefore, the effect of adding fatty acids was tested by examining whether the palmitic acid stimulatory effect depended on the ACE2. Palmitate (0.4 mM) was added without new viruses briefly (150 min) every 24 h to cells infected with SARS-CoV-2 in the

presence of 1 mM oleate, i.e., under conditions suppressing the binding to the ACE2, i.e., ACE2 incompetent. Specifically, cells were transiently and sequentially incubated with palmitate (0.4 mM) without the addition of new viruses as described above. After 2 h 30 min the infective media was replaced and palmitate was added to the media either once: on day one, or twice: on day one and day two. After each incubation with palmitate (2 h 30 min), the media was removed and replaced by fresh media without FFA. The viral production was measured 96 hours post initial infection. The results are shown in (FIG. 2D, see also FIG. 2K).

[00442] A single exposure (150 min) to palmitate (0.4 mM) on the day following cell infection significantly increased viral production, by greater than 2 logs (FIG. 2D). After two palmitate incubations, viral production further increased by about two logs such that it was equivalent to that measured in cells infected without any FFA (FIG. 2D, see also FIG. 2K). In similar experiments, unsaturated LA and saturated SA (0.4 mM) also increased SARS-CoV-2 production when added transiently to cells infected in the presence of OA (FIG. 2L).

[00443] These data indicated that the SARS-CoV-2 were able to infect BGM cells despite their inability to interact with the ACE2. However, these infection conditions were insufficient to enable significant viral production without subsequent exposure to PA.

[00444] Increasing infective viral loads showed that SARS-CoV-2 production reached a plateau both in BGM cells incubated with the virus alone without any added fatty acids (FIG. 2E, solid line) and in BGM cells exposed to the virus in the presence of 1 mM oleate, then followed by two cyclic exposures to palmitate (0.4 mM) on day two and three (O+2P protocol) without adding new viruses (FIG. 2E dotted line). The number of virus released in the media in 48 h was 367 % (min 229% max 512% $p < 0.02$) higher than that released after 96 h of ACE2 mediated uptake and replication. Therefore, SARS-CoV-2 modified by unsaturated long-chain FFA do not replicate using the ACE2, but instead replicate through a mechanism that requires repeated transient exposures of infected cells to palmitate (two cycles 0.4 mM) and to a lower extent, oleate (three cycles with 1 mM, FIG. 2A, see also FIG. 2J).

[00445] FIG. 2E shows that both the ACE2 protocol (no added fatty acids) and the oleate followed by palmitate (O/P or O+2P) protocol show clear saturation kinetics

consistent with both pathways relying on a limited number of viral binding sites on the cell surface. The ACE2 protocol saturated after exposure to 2 million viruses for 2 h 30 min. Saturation of the O/P pathway required 10 million viruses and the same time of viral exposure. In both cases, production of SARS-CoV-2 viral RNA reached a plateau albeit with slightly different kinetics, indicative of two saturable cell entry mechanisms (FIG. 2E). Without viruses, the O+2P protocol did not alter BGM cell monolayers.

[00446] Media of cells infected with ACE2 incompetent virus that produced SARS-CoV-2 RNA through the Oleate/Palmitate protocol was collected. Fresh BGMK cells were exposed for 2 h 30 min to ¼ dilution of these media and incubated for 96 hours without addition of FFA. The total viral production was 4.74 x 10^9, which is within the range of the maximal production achieved by ACE2 mediated replication in the same period (FIG. 2F). Thus, viral RNA released in the media using the O+2P corresponded to authentic SARS-CoV-2 replicating through the ACE2 (FIG. 2F).

[00447] Different FFA

[00448] The effect of different FFA on the replication of ACE2 incompetent SARS-CoV-2 was investigated further. BGM cells were infected with ACE2 incompetent SARS-CoV-2 in presence or absence of oleate as above (Wuhan strain 10^8 copies per well, for 2 h 30 min). After this, cells incubated with oleate received either no further incubation with any free fatty acids or two transient incubations with the indicated FFA (2 h 30 min), 24 h apart followed by replacement with media without FFA. Viral production was measured 96 hours (h) post initial infection. All data points are the mean and standard deviation calculated using three wells. As shown in FIG. 2G, a striking increase in viral production was seen with palmitate and stearate (0.4 mM) (FIG. 2G). Oleate (0.4 mM) or linoleate (0.4 mM) also significantly increased the viral production of viruses unable to infect via the ACE2. Linoleate that inactivated the SARS-CoV-2 binding to the ACE2 was a more potent activator of the alternate SARS-CoV-2 replication mechanism than oleate. This dual effect of linoleate provided a first explanation to previous observations suggesting that linoleate had no direct impact on SARS-CoV-2 replication despite its capacity to lock the S protein in close conformation (Toelzer 2020, *supra*). Together, the results suggested that the wild type SARS-CoV-2 used a second receptor activated by both saturated and unsaturated FFA to enter BGM and replicate.

[00449] Without being bound by theory, these observations suggest that the SARS-CoV-2 has evolved mechanisms that rely on specific unsaturated fatty acids to suppress a critical viral function (prevent ACE2 binding), but also rely on fatty acids (mostly saturated long-chain fatty acids) to compensate this loss of function by activating a second receptor that enables entry and replication into ACE2 infective progeny.

[00450] The activity of the putative alternate receptor was tested in human colon (Caco-2 or Caco2) and murine mammary (mouse) (4T1) cell lines. The O+2P protocol (described above) yielded a viral production in Caco2 similar to that of BGM, but viruses were not produced in 4T1 (mouse) cells (FIG. 2H). Indeed, SARS-CoV-2 did not replicate in mouse 4T1 when using the either the "No FA" or the "O+2P" protocol. Similar to the result described above in BGM cells, oleate (1 mM) added with the virus at the time of infection of human Caco2 cells decreased viral production by more than 99 % (FIG. 2I). In the absence of fatty acids, BGM and Caco2, but not 4T1, efficiently replicated the SARS-CoV-2 (FIG. 2H). Therefore, in human and simian cells, fatty acids activated an ACE2 independent viral entry mechanism that can either synergize with the ACE2 to increase the viral production or compensate for the defective binding to the ACE2 caused by unsaturated FA. Furthermore, all long-chain FFA stimulated an alternate receptor with the capacity to either cooperate with the ACE2 to increase the viral production or compensate the defective binding to the ACE2 (FIG. 2G).

[00451] **EXAMPLE 3: The Lipolysis Stimulated Receptor (LSR) mediates ACE2-independent SARS-CoV-2 replication.**

[00452] Two plasma membrane proteins have been shown to bind or interact with fatty acids specifically: the cluster of differentiation 36 (CD36) (Abumrad, 1992) and the LSR (Bihain, 1992). The LSR is plasma membrane receptor that endocytoses lipoproteins containing Apo B or Apo E when free fatty acids (FFA) are present in the incubation media.

[00453] Western blots were carried out to study proteins reactive with specific anti-LSR IgG and anti-ACE2 IgG in BGM cells, CaCo2 cells, and 4T1 cells (FIG. 3A). Proteins reactive with specific anti-ACE2 IgG were present in BGM and CaCo2, but not in 4T1.

[00454] Western blots using BGM cell extracts revealed proteins reactive to anti-LSR and anti-ACE2 AB but not anti-CD36 (FIG. 3M). Both LSR and ACE2 expressed in

human Caco-2; murine LSR was expressed in 4T1. Silencing the LSR in BGM cells reduced LSR protein by 80% (Fig. 3N). This reduction was sufficient to suppress the cell protein loss caused by SARS-CoV-2 infections in the presence of OA and the two monoclonal AB targeting the RBD. LSR gene silencing also significantly inhibited the OA-induced infectivity of SARS-CoV-2 with the S protein in a conformation unable to react with the ACE2. LSR silencing did not change the ACE2-mediated SARS-CoV-2 replication (FIG. 3Q). Therefore, LSR accounted for both the FA-induced ACE2-independent infectivity of the SARS-CoV-2 and the antibody-enhanced cytolytic effects.

[00455] The effects of LSR specific siRNA ere also tested. LSR specific siRNA, but not scrambled siRNA (control siRNA) durably reduced the expression of proteins reactive with anti-LSR antibodies for at least six days without changing the protein reactivity with anti-ACE2 IgG or anti-GAPDH IgG antibodies (FIG. 3B). Furthermore, in BGM cells, LSR specific siRNA silencing reduced by 75% the increase in viral production induced by the O+2P protocol (FIG. 3C), but did not affect viral production in absence of fatty acids. This was consistent with the lack of effect of LSR silencing on the ACE2 protein expression.

[00456] Additionally, to confirm that the reduction in viral production induced by the O+2P protocol in BGM was due to LSR and not to CD36, western blots of lysate from BGM and Caco2 cells revealed proteins reactive with specific anti-LSR antibodies, but no protein reactive with anti-CD36 antibodies. Human adipose tissue protein extracts were used as positive control for anti-CD36 blots. As expected, BGM and Caco2 cells expressed the ACE2 (FIG. 3D).

[00457] Forty-eight hours after LSR silencing, BGM cells were infected with the Delta variant at MOI=1 using the O+2P protocol. After 96 hours of culture, viral RNA copy number was 1.6 $x10^8$ in cells transfected with control siRNA, and only $5x10^3$ in cells transfected with LSR specific siRNA (FIG. 3E).

[00458] To verify that the LSR enabled the replication of wild type (WT) SARS-CoV-2, the effect of LSR silencing was tested in BGM cells infected in the presence or absence of palmitic acid. Infection with PA was cytopathic in BGM cells transfected with control siRNA, but not in those transfected with LSR specific siRNA. In the absence of PA, BGM cell infection caused plaque formation but no destruction of the cell layer, irrespective of

control or LSR specific siRNA (for example, FIG. 3F). PA without virus had no detectable cytopathic effect.

[00459] Silencing of both receptors was also tested for the individual receptors alone or in combination. Accordingly, the expression of the LSR, the ACE2, and both receptors was silenced in BGM cells. After silencing, the BGM cells were infected with wild-type SARS-CoV-2 at an MOI=1000, in the presence or absence of palmitate. Cell loss at 3 day post infection (DPI 3) was quantified by measuring the amount of protein and DNA left after washing, LDH release in the media and verified by phase-contrast microscopy. LSR silencing, but not ACE2 silencing suppressed the SARS-CoV-2 cytopathic effect. LSR silencing did not affect the wild-type SARS-CoV-2 replication mediated by ACE2, but the ACE2 silencing did. Therefore, consistent with the results of other experiments disclosed herein, these experiments showed that the ACE2 mediated viral production produced between 10^9 and 10^{10} particles without causing cell loss. In contrast, a far lower viral production following LSR mediated entry. Cell layer protein and DNA content were reduced by more than 50%, LDH release in the media was increased, and cell layer integrity was impacted. A marker for cell lysis includes cell layer protein content, as the release of protease and nuclease upon cell lysis affects LDH, among other things including SARS-CoV-2.

[00460] Finally, expression of the LSR gene in human tissues that contribute to viral transmission, in particular, tissues of the respiratory organs was verified. An analysis of publicly available RNA-derived sequences from the human nasal epithelium (N=7, FIG. 3G) and tongue (N= 6, FIG. 3H) and lung (n=4, lung results not provided.) showed that in all three tissues, LSR mRNAs were more abundant than ACE2 mRNAs.

[00461] SARS-CoV-2 entry mediated by the fatty acid- activated LSR enables antibody-enhanced cytolysis.

[00462] To ascertain that the FA-activated mechanism enabling SARS-CoV-2 infectivity was indeed independent of the ACE2, tests were carried out to neutralize the SARS-CoV-2 binding to the ACE2 using specific monoclonal antibodies targeting the RBD. Infective media containing 10^7 viruses per well were incubated with the combination of casirivimab (C) and imdevimab (I) (15 +15 µg/ml), which degraded the cell monolayers when supplemented with OA and led to significant cell loss (FIG. 3I, top left panel).

Adalimumab (Ada), a monoclonal antibody targeting the tumor necrosis factor α (TNFα), did not cause cytopathic (cytolytic) effect in cells infected in the same condition (10^7 viruses and 1 mM OA) (FIG. 3I, top right panel). Furthermore, the cells were not visibly affected when OA or the combination of casirivimab and imdevimab (15 +15 µg/ml) was missing (FIG. 3I, bottom panels). Cell lysis was not observed under the test conditions in the absence of viruses. Specifically, the virus alone, the OA alone, the OA with C&I but without the virus did not induce any cytolytic effects (FIG. 3P).

[00463] Next, the effect of casirivimab (30 µg/ml) and imdevimab (30 µg/ml) was tested independently and in combination (15+15 µg/ml) using two infective doses. Well protein content after washing provided a quantitative estimate of cell loss. The well protein content decreased in wells having infected cells, supplemented with OA and the two monoclonal antibodies targeting the RBD added alone or in combination (FIG. 3J and FIG. 3K). Infections with 10^5 particles per well reduced the cell protein content by more than 60 %. Infections with 10^7 particles per well further reduced the cell protein compared to infections with 10^5 particles per well. The same cytolytic effects were observed with PA (0.4 mM) or OA (0.4 mM) added to media containing 10^7 viral copies and monoclonal antibodies targeting the RBD but not the anti-TNF AB (FIG. 3L). Therefore, fatty acid activated a mechanism of SARS-CoV-2 infectivity distinct from the ACE2 and demonstrating antibodies that reacted with the S-protein RBD to cause cytolysis.

[00464] LSR gene silencing suppressed the cell protein loss caused by SARS-CoV-2 infections in the presence of OA and the two monoclonal antibodies targeting the RBD (FIG. 3N). In addition, LSR gene silencing reduced the infectivity of SARS-CoV-2 with the S protein in a conformation unable to react with the ACE2 (FIG. 3O) but did not affect the SARS-CoV-2 replication in cells infected without fatty acid. Therefore, the LSR activated by fatty acid accounted for the ACE2-independent infectivity and the antibody-enhanced cytolytic effects of the SARS-CoV-2. LSR gene silencing did not affect SARS-CoV-2 replication in absence of fatty acid (i.e. ACE2-mediated). Therefore, repeated transient LSR activation by saturated and unsaturated FA enabled SARS_CoV-2 replication in BGM cells.

[00465] EXAMPLE 4: The human and simian LSR activated by FFA binds SARS-CoV-2 and facilitates rapid or delayed viral replication.

[00466] Lipolysis stimulated receptor (LSR) is a plasma membrane receptor that endocytoses lipoproteins only when FFA are present in the incubation media. LSR is found as monomeric α isoforms that possess a single transmembrane spanning domain and as multimeric complexes comprising LSRα eventually linked to β isoforms through disulfide bridges (see *e.g.*, Yen, *et al.*, JBC (1999) 274(19):13390-13398). LSRβ isoforms lack the transmembrane spanning domain. Suramin and lactoferrin inhibit LSR mediated lipoprotein uptake (*see e.g.,* Mann *et al.*, (1995) Biochemistry 34(33):10421-10431). Interestingly, Human lactoferrin (2 mg/ml) also inhibited production of the SARS-CoV-2 Wuhan strain ("wild-type") obtained through either the ACE2 or the O/P protocol by more than 99.9 % (data not shown).

[00467] Specific anti-LSR IgG, but not non-specific IgG, inhibited viral production obtained through the O/P protocol, but did not inhibit viral production resulting from the ACE2 mediated infection (data not shown). Furthermore, LSR specific siRNA, but not non-specific siRNA also specifically and significantly decreased viral production with the O/P protocol, but not the ACE2 protocol (*see* Example 3, FIG. 3C).

[00468] Ligand blotting using non-reduced LSR multimeric complexes showed that all four main FFA: oleate, linoleate, palmitate, and stearate, caused the binding of recombinant trimeric SARS-CoV-2 spike to LSR. This binding was inhibited by suramin, lactoferrin, and specific anti-LSR antibodies, but not by non-specific IgG.

[00469] The expression of both total and isoform specific LSR mRNA was measured using quantitative PCR (qPCR) in BGM cells sequentially incubated without or with oleate, linoleate, palmitate, and stearate. Oleate and linoleate increased total LSR expression, but primarily that of LSRα, and the difference between α and β was more pronounced with oleate than with linoleate. Palmitate and stearate increased the expression of both α and β, and became equivalently expressed. Western blotting confirmed that the differences seen at the mRNA levels translated at the protein levels. Therefore, the LSR is responsible for the O/P induced replication of SARS-CoV-2.

[00470] All four FFA: oleate, linoleate, palmitate, and stearate, enabled the binding of the spike to LSR and increased LSR expression, but only saturated FFA increased the expression of both LSR α and β equivalently. Previous studies have shown that the expression of LSR β is required for LSR to deliver its cargo to late endosomes. Oleate induces the conformational change enabling the spike binding to the LSR, but without leading to immediate replication, suggesting that LSR may store the virus into a non-replicative compartment.

[00471] SARS-CoV-2 was made ACE2 incompetent by incubation with oleate, followed by removal of unbound oleate. Cells were incubated with the ACE2 incompetent SARS-CoV-2 in the presence of or absence of oleate. After this, the cells were washed and passaged once. After trypsin and re-seeding, the cells were exposed twice to palmitate or no FFA. Cells exposed to the ACE2 incompetent virus in the presence of oleate produced significant amount of viruses when subsequently incubated with palmitate. This was not the case when cells were exposed only to ACE2 incompetent viruses without oleate. Therefore, without being bound by theory it is believed that the oleate-activated LSR delivers the virus into a non-replicative compartment unaffected by cell trypsin treatment. The virus in this compartment can be reactivated by subsequent incubation with palmitate.

[00472] LSR and ACE2 mediated replication was further examined by comparing SARS-CoV-2 replication in simian, human and mouse cell lines. Mouse LSR, although expressed in both cell lines at the mRNA and protein levels does not enable SARS-CoV-2 replication (see Example 3 and FIG. 3A), but human LSR expressed in the two cell lines does. Therefore, similar to the ACE2, LSR mediated uptake of SARS-CoV-2 is species specific.

[00473] **EXAMPLE 5: Distinctive SARS-CoV-2 spike binding domains mediate the uptake through the ACE2 or the LSR and variant spike mutations define their receptor preference.**

[00474] FIG. 4A shows a map of the SARS-CoV-2 spike annotated for its currently known functional domains as disclosed herein. A detailed description is provided in the figure description for FIG. 4C that shows a three-dimensional (3D or 3-D) model of the SARS-CoV-2 spike structure in closed and open conformation annotated for the ABD and the two segments constitutive of the LBD. The figure is based on *in silico*, three-

dimensional modeling of the published SARS-CoV-2 spike structure and the *in silico* predicted structure of the tetrameric LSR extracellular domain. The LSR extracellular domain is mainly constituted of a Type V Ig-like domain with two β sheets packing face to face (Potapov, 2004). The molecular weight of LSR complexes mediating lipoprotein endocytosis is 240 kDa. The molecular weight of its components ranges from 56 to 68 kDa.

[00475] As shown in FIG. 4A, a single linear segment of 56 amino acids (Y449 to Y505) constitutes the spike ACE2 binding motif (ABD) which is located within a larger receptor binding domain (RBD) (R319 to S541, see FIG. 4A) that defines its accessibility.

[00476] Three-dimensional (3D) modeling of the spike protein and LSR, predicted that the extracellular LSR Ig like domain binds two linearly distant, but structurally close, spike segments comprising 29 amino acids (AA) on the viral spike protein that potentially interact with LSR amino acids (FIG. 4A). Twenty-four of these amino acid interactions clustered in two linearly distant, but structurally close segments of the S protein. i.e., P25 to P85 (8 AA interactions, LBD1) and Q607 to S691 (16 AA interactions, LBD2), respectively (FIG. 4A and FIG. 4C). Five other possible sites of spike LSR amino acid interactions outside of these clusters are also shown on the map of FIG. 4A.

[00477] It was established that the recombinant S but not the nuclear (N) protein reduced the SARS-CoV-2 infectivity mediated by ACE2 and LSR. The LSR, upon activation by FA endocytoses lipoproteins in the liver. The LSR is a multimeric complex composed of isoforms linked in part through disulfide bridges. As above, computer modeling predicted that the tetrameric LSR extracellular domain interacted with 30 amino acids (AA) on the S protein (FIG. 4C) designated LSR binding domain (LBD). The twenty-four mentioned interactions clustered in two linearly distant segments of the S protein are brought to proximity by the trimeric S protein folding. Unlike the RBD, the changes in the S-protein structure between the closed and open conformation did not mask the two segments LBD1 and LBD2 (Fig. 4C).

[00478] Competitive binding assays were used to characterize the proteins that bind and interact with LSR and ACE2. First, competitive binding assays were carried out utilizing the full-length spike and the full length nucleocapsid protein. In these experiments, only the spike, but not the nucleocapsid significantly inhibited replication of live virus obtained

through either the ACE2 (FIG. 4B grey bars) or the LSR (FIG. 4B, black bars). More specifically, recombinant monomeric S protein, but not recombinant nucleocapsid protein inhibited viral replication by more than 99%. This was true both when BGM cells were infected without fatty acids, and when using the O+2P protocol (FIG. 4B). Therefore, SARS-CoV-2 interacts with LSR through the spike (S) protein, not the nucleocapsid protein.

[00479] Competitive binding assays were then used to test the predictions of the 3D modeling and characterize the regions of the spike protein that bind LSR and ACE2. To this end, the two putative recombinant LSR binding domains (rLBD1 and rLBD2) were produced and purified *from E. coli* (FIG. 4D). Recombinant ABD (rABD) was also prepared. Competition binding assays were carried out using the purified proteins.

[00480] Recombinant LBD1 and LBD2 inhibited production of wild-type virus obtained by infecting BGM cells using the O/P protocol, but the rABD did not (completion data for rABD not shown). As shown in FIG. 4E, when infection was carried out using the O+2P protocol, competition using either rLBD1 or rLBD2 lowered viral production from 10^9 to background levels (FIG. 4E, shaded bars). However, in cells incubated without fatty acids (ACE2 pathway, grey bars), neither rLBD1 nor rLBD2 detectably affected viral production (FIG. 4E). Thus, rLBDs had no effect on the ACE2 mediated replication that was inhibited by the rABD.

[00481] Competition experiments were also carried out with the Delta variant. Competition using either rLBD1 or rLBD2 lowered viral production of the Delta variant by 6 logs (FIG. 4F). It should be noted that the multiplicity of infection (MOI) of the wild-type SARS-CoV-2 was at one hundred while that of that of the Delta variant was hundred-fold higher in order to enable Delta variant replication through the ACE2 (*see* Example 6, FIG. 5B).

[00482] These results suggest that the binding of the SARS-CoV-2 to each receptor occurs through distinctive spike binding domains and results mainly from protein to protein interaction that may be facilitated by, but are not strictly dependent on carbohydrate components.

[00483] Without being bound by theory, it is believed that the structure of the spike protein (FIG. 4C) explains why LBD1 and LBD2 inhibit LSR mediated replication, but not

the ACE2 mediated replication. The structure of the spike protein (FIG. 4C) allows the spike to retain LSR binding capacity even when the S protein is locked in the closed conformation (FIG. 4C). This is consistent with bioinformatics modeling showing that LBD1 and LBD2 interactive sites on the S protein are not located in the RBD (FIG. 4C). Further, unlike the RBD, the LSR binding domain remained accessible even when the S protein was locked in the closed conformation (FIG. 4C) consistent with the results of viral replication experiments disclosed herein.

[00484] The LSR binding domain on the spike protein is distinct from the RBD.

[00485] A recombinant protein, designated LBDx (or rLBDx), was produced by joining the two S protein segments containing the amino acid predicted to contribute most to the interaction with the LSR. Also produced in recombinant form were the polypeptides corresponding to putative LBD1 and LBD2 (FIG. 4D). The predicted structure of the trimeric S protein interacting with the extracellular LSR while leaving accessible the RBD is shown in FIG. 4C.

[00486] The three polypeptides were purified to homogeneity and endotoxin free. LBDx at the concentration of 10 µg/ml suppressed the cytolytic effect that occurred in wells infected with the SARS-CoV-2 (10^7 particles) in the presence of OA (0.4 mM), and the combination of casirivimab (C) and imdevimab (I) (15+15 µg/ml) (FIG. 4G). The inhibitory effect of increasing LDBx concentration in cell protein loss is shown in FIG. 4H. Supplementing the media of infected BGM cells with OA and then twice with PA with increasing LBDx concentrations inhibited viral production with IC90 of 9.5 µg/ml (FIG. 4I). The LBDx with the amino acid sequence of the WT S protein suppressed the infectivity of not only the WT-SARS-CoV-2 but also the Delta and the Omicron variants when applying the O+2P protocol (FIG. 4I). The LBDx did not significantly reduce the replication of the three SARS-CoV-2 in BGM cells not supplemented with fatty acid (FIG. 4J). Each of the two S protein segments (LBD1 and LBD2) contributing to the LBD were verified to inhibit the SARS-CoV-2 infectivity through the LSR without affecting the ACE2-mediated replication. However, these recombinant protein segments (LBD1 and LBD2) were less stable in solution than the LBDx (Data not shown).

[00487] Therefore, the LSR activated by fatty acid bound a conformational domain of the S protein that based on *in silico* analysis formed a 90° angle with the RBD and remained accessible on the protein surface irrespective of its open or closed conformation.

[00488] **EXAMPLE 6: The Delta variant infects primarily through the LSR.**

[00489] The SARS-CoV-2 Delta variant has emerged as highly infectious and as the cause of severe disease. The Delta variant possesses two mutations, L452R and T478K, in the ACE2 binding motif that were assumed to translate into a gain of function. Delta variants from three infected patients were isolated and the S protein was sequenced. These sequences confirmed the presence of Delta variant-specific mutations in all three isolates. In addition to the mutations typically associated with the Delta variant, two additional mutations T95I and Q677H were identified in one of the isolates (Table 5).

[00490] **Table 5.** Sequences of SARS-CoV-2 Spike protein obtained from 3 patients compared to the Wuhan strain (YP_009724390) and the Delta variant (MZ359841).

Position	YP_009724390	Delta	Patient 1	Patient 2	Patient 3
19	T	R	R	R	R
95	**T**	**T**	**T**	**T**	**I**
142	G	D	D	D	D
156-157	EF	--	--	--	--
158	R	G	G	G	G
452	L	R	R	R	R
478	T	K	K	K	K
484	E	E	E	E	E
501	N	N	N	N	N
614	D	G	G	G	G
677	**Q**	**Q**	**Q**	**Q**	**H**
681	P	R	R	R	R
950	D	N	N	N	N

[00491] Viral entry and replication of the SARS-CoV-2 Delta variant was examined using the patient sera. BGMK cells were infected using a low number of viruses directly isolated from serum of patients infected with the Delta variant. Consistent with the results described below, the number of viruses released in the media was 550 fold greater when using the LSR (O/P protocol) compared to the ACE2 protocol (Data not shown).

[00492] Delta variant replication was further examined first by infecting BGM cells with delta variants isolated from three different patients using viral loads sufficient to saturate each receptor (both ACE2 and LSR). Cells were infected in the absence of FFA

(ACE2 protocol) or using the O+2P protocol. The number of Delta variants released in the media was on average 10^8 particles per well with the O+2P protocol and was at background levels after infection without FFA (FIG. 5A).

[00493] Replication of the delta variant was examined still further by comparing the viral production of cells initially infected at a low titer, and cells initially infected at a high titer. Specifically, replication of the delta variant was compared using O+2P protocol and the no FFA protocol with cells infected at either a low dose (10^4 particles per well) which corresponds to the median infective dose which is equal to the median of contaminated human sputum (10^4 particles per well) (Fajnzylber, 2020), or at a high dose (10^8 particles per well) (FIG. 5B). In each case, the virus was in contact with BGM cells for 150 min. Wild type SARS-CoV-2 were used as control.

[00494] As shown in FIG. 5B, at low initial dose, the delta variant did not replicate well in the absence of FFA, but did replicate efficiently using the O+2P protocol. At high initial dose and in the absence of FFA, the delta variant production increased above background, but remained four logs below that achieved with the O+2P.

[00495] Using a high initial dose (10^8 virus), the wild-type virus produced equally well in the absence of FFA and with the O+2P protocol. However, at the low initial dose (10^4 virus), viral production using the O+2P protocol produced significantly more viruses (FIG. 5B).

[00496] Similar experiments were carried out comparing viral production of wild-type SARS-CoV-2 with known SARS-CoV-2 variants of concern (VOC) beta and delta. FIG. 5C shows SARS-CoV-2 total copy numbers in media and cell layer of BGM infected with the indicated SARS-CoV-2 at two different infective doses (10^4 and 10^8 per well respectively) after incubation in the absence of FFA (Gray) or using the O+2P protocol (shaded).

[00497] In these experiments, both the Beta and Delta variants infected at an MOI=1 (10^4 virus) replicated far less efficiently through the ACE2 than through the FA-activated receptor (FIG. 5D and FIG. 5E). Furthermore, even when using MOI of ten thousand, ACE2 mediated replication of Beta and Delta variants remained significantly below that obtained through the FA-activated receptor (FIG. 5F).

[00498] To investigate these results regarding lower infectivity of the Delta variant through the ACE2, the Delta variants described above (Table 5), were tested further. Using MOI saturating each receptor, the number of Delta variants released in the media was on average 10^8 particles per well using the O+2P protocol and was six logs lower in BGM cells infected without FA. No differences in viral RNA production were associated with the two additional mutations in one of the isolates (Data not shown).

[00499] Finally, to confirm what was found in these experiments, that the ACE2-mediated replication of the Delta variant was less efficient than that of the WT SARS-CoV-2, HEK293T cells that did or did not overexpress the human ACE2 were used. As shown in FIG. 5G, in the absence of fatty acid supplementation, ACE2 overexpression increased the production of wild-type SARS-CoV-2 RNA copy numbers by three logs but did not change the Delta variant copy numbers (FIG. 5G). Accordingly, the data show that the FA-activated receptor is more efficient than the ACE2 for replicating the Delta variant. Further experiments show that of 8 isolates that were tested, 3 of 8 isolates do not efficiently replicate via ACE2. However, all 8 isolates efficiently replicate via LSR, as described above.

[00500] FA activates LSR enabling SARS-CoV-2 entry caused cell lysis irrespective of the virus lineage.

[00501] Casirivimab (C) and imdevimab (I) enhanced the fatty acid-induced cytolysis caused by the Delta but not by the Omicron (BA.5) variant consistent with these two monoclonals not reacting with the mutated Omicron RBD (FIG. 5H). The fatty acid-induced antibody-enhanced cytosis (FIAEC) induced by the Delta variant was suppressed by the recombinant LBD (FIG. 5I).

[00502] Without AB enhancement, PA (0.4 mM) supplementation of infective media containing 10^8 gec WT-SARS-CoV-2 led to a loss of cells within 24 h; this effect was suppressed by the LBDx (FIG. 5J). This explains why we used only viruses preincubated with PA in the experiment described in FIG. 1X, for example. PA supplementation did not affect the cell monolayer when the infective media contained 10^7 gec WT-SARS-CoV-2 (FIG. 5O, top row). The Delta and Omicron SARS-CoV-2 led to a significant loss of cells in the presence of PA but only when the infective titer was 10^8 gec (FIG. 5O, middle row). The LBDx suppressed the direct cell lysis caused by the two SARS-CoV-2 variants (FIG.

5O, bottom row). Following infection with 10^4 gec, the O + 2P protocol increased the number of viral RNA released into the media during the last 24 h of the infection, consistent with FIGS. 2J, 2K, and 2L. However, after three transient PA supplementations at DPI 1, 2, and 3, the cytopathic effect of SARS-CoV-2 reduced the viral production (FIG. 5K).

[00503] The 3C-like protease inhibitors nirmatrelvir and ritonavir decreased SARS-CoV-2 replication in a dose-dependent manner in BGM cells infected without FA or with the O+2P protocol (FIG. 5L and FIG. 5M). However, even at the highest dose, inhibition of viral replication failed to protect the cell layer from the SARS-CoV-2 FA-induced antibody-enhanced cytolysis (FIAEC) (FIG. 5N). Analysis of RNA-seq datasets from human samples showed that LSR expression exceeded the almost undetectable ACE2 expression in the lung, spleen, and liver, indicating that LSR expression was compatible with SARS-CoV-2 lung tropism. Analysis of RNA-seq datasets from human samples confirmed the LSR expression with very low ACE2 expression in the lung, spleen, and liver. In addition, the LSR mRNA levels exceeded those of ACE2 in the stomach and colon. However, the ACE2 mRNA levels exceeded those of LSR in the duodenum small intestine and heart (FIG. 5P).

[00504] **EXAMPLE 7: Plasma FFA concentrations in patients with severe COVID-19 exceed those that *in vitro* suppress SARS-CoV-2 binding to ACE2 and increase LSR mediated viral replication.**

[00505] To investigate whether FFA concentrations used in the *in vitro* experiments disclosed herein were within the range found in infected patients, the concentrations of lipids and three important regulatory hormones were measured in a small cohorts of patients with moderate or severe COVID-19. All severe patients were sedated and mechanically ventilated. As expected, severe patients were older and had significantly higher BMI. The increase in triglycerides, FFA, leptin and insulin observed in severe patients as compared to patients with mild COVID, or without COVID-19, is impressive and statically highly significant ($p < 10\text{-}5$ for FFA). However, plasma cholesterol and adiponectin were not different (Table 6). Interestingly, circulating plasma FFA levels in severe patients is on average at least three-fold higher than the maximum FFA concentration used in all *in vitro* experiments.

[00506] **Table 6.** Patient's characteristics

	Total (n=36)	Severe (n=20)	Non severe (n=16)	p-value
Age (years)	60 (27-78)	66 (28-78)	39 (27-73)	1.7E-3
Height (cm)	170 (145-187)	170 (145-187)	170 (163-184)	NS
Weight (kg)	79 (54-130)	90 (59-130)	61 (54-102)	4.3E-3
BMI ($kg.m^{-2}$)	28 (17-48)	30 (17-48)	21 (19-33)	1.9E-3
Metabolic parameters				
Cholesterol (g/L)	2.15 ± 0.59	2.08 ± 0.73	2.23 ± 0.34	NS
Triglycerides (mM)	1.25 ± 0.73	1.53± 0.74	0.91 ± 0.58	7.8E-3
Free Fatty Acids (mM)	1.28 ± 1.61	2.08 ± 1.80	0.28 ± 0.18	4.3E-5
PL activity (U/mL)	244 ± 85	196 ± 80	305 ± 42	1.1E-5
Leptin (ng/mL)	19.7 ±20.7	28.9 ± 23.3	9.4 ± 10.5	8.8E-4
Adiponectin (µg/mL)	7.9 ± 4.9	8.0 ± 5.5	7.7 ± 4.2	NS
Insulin (pM)	95 ± 91	123 ± 103	59 ± 60	0.02

Continuous values are expressed as median (range), metabolic parameters as mean +/- SD.
For 5 non severe patients, age, height, weight and BMI data were unavailable. Statistics were done without these patients for those parameters.

[00507] As expected, the age and body mass index of patients with severe disease were also significantly higher and may contribute to the differences in serum metabolites. Thus, serum FFA levels were on average tenfold higher in patients with severe COVID-19 compared to convalescents, twofold above the maximum FFA concentration needed to suppress the binding to the ACE2 and fivefold higher than those activating LSR mediated viral replication that caused cytopathic effects.

[00508] This suggests that in patients with severe COVID-19, ACE2 mediated viral replication is not functional while that occurring through LSR is.

[00509] **EXAMPLE 8: Discussion**

[00510] As demonstrated above in the experimental Examples, The SARS-CoV-2 uses two independent receptors, ACE2 and LSR, to enter cells and replicate. The ACE2 receptor enables the replication of the SARS-CoV-2 without causing substantial cytopathic effects. On the other hand, the LSR receptor enables a viral replication that causes cell loss *see e.g.*, Example 3. The wild-type SARS-CoV-2 and Alpha variant uses both the ACE2 receptor and the LSR receptor to enter cells and replicate. However, the Delta and, to a lesser extent, the Beta variant are far more infective through the LSR than the ACE2, *see e.g.,* Example 6. Without being bound by theory, it is believed that fatty acids differentially regulate the ACE2 and the LSR pathways as schematized in FIG. 6.

[00511] The ACE2 receptor was readily identified as the primary SARS-CoV-2 receptor because it is also the receptor of the SARS-CoV that caused the 2002 and 2003 outbreaks (Wan, 2020). As disclosed herein, unsaturated free fatty acids (FFA) disable the S protein capacity to bind the ACE2 receptor, *see e.g.*, Example 1. The S protein possesses a hydrophobic pocket in the vicinity of the ACE 2 binding domain (ABD) that binds fatty acids. However, the hydrophobic binding pocket only accommodates unsaturated fatty acids because of their angulated carbon chain *see e.g.,* Toezler et al. (2020) *supra* and FIG. 1R and FIG. 1S. Without being bound by theory, it is believed that inhibition of S protein binding to ACE2 effected by oleic acid (and other unsaturated fatty acids of an appropriate carbon chain length as disclosed herein) results from binding of the oleic acid to the hydrophobic pocket, which locks the S protein in a closed conformation, which shields the RBD and thus prevents binding of the S protein to the ACE2 receptor. Consistent with this theory, saturated FFA which have a linear carbon chain do not inhibit ACE2 mediated viral replication *see e.g.*, FIG. 1U, FIG. 2C. However, both saturated and unsaturated fatty acid activate the lipolysis stimulated receptor (LSR), which provides the SARS-CoV-2 with an alternative entry mechanism functional even when the S protein is locked in the closed conformation *see e.g.*, FIG. 2G.

[00512] Identification of LSR as a SARS-CoV-2 receptor, as disclosed herein, was demonstrated by at least three independent lines of evidence. First, LSR silencing suppressed FA-induced replication of the Delta variant, which does not replicate efficiently using the ACE2, see e.g., Example 3. Second, LSR silencing, but not ACE2 silencing, suppressed the cytopathic effect caused by wild-type SARS-CoV-2 cell infection, again see e.g., Example 3. Third, the production of both wild-type and Delta variant SARS-CoV-2 were reduced when the SARS-CoV-2 binding to the LSR was competed for by recombinant LBD1 and LBD2, *see e.g.*, Example 5, FIG. 4E, FIG. 4F. The production of wild-type SARS-CoV-2 using the O+2P protocol became almost undetectable when the SARS-CoV-2 was forced to compete for binding to the LSR using rLBD1 and rLBD2 (FIG. 4E). However, these competitions did not affect the ACE2 mediated replication (FIG. 4E). Thus, SARS-CoV-2 that are unable to bind ACE2 due to oleate inhibition (ACE2 incompetent) ceased to infect BGM cells when its capacity to bind the LSR was also suppressed.

[00513] The dramatic reduction of SARS-CoV-2 production seen in these experiments is explained by the synergy of two inhibitory mechanisms. In the first mechanism, oleic acid (OA) suppresses SARS-CoV-2 interaction with the ACE2, and in the second mechanism, the recombinant LBD1 and LBD2 compete with the S protein for LSR interaction.

[00514] Similarly, at an expected human infective dose of 10^4 particles per well, which corresponds to the median infective dose, and which is equal to the median of contaminated human sputum, the Delta variant failed to replicate using the ACE2, but replicated efficiently when the LSR was activated by fatty acids *see e.g.*, FIG. 5B.

[00515] Silencing experiments (FIG. 3C, FIG. 3E) provide results that are consistent with the competition experiments described herein. Silencing of LSR protein expression by an estimated 90% reduced the Delta variant production from fifty million to less than ten thousand particles (FIG. 3E). The LSR is therefore critical for the infectivity of the Delta variant.

[00516] The O+2P protocol was developed to disable the binding to the ACE2 and to activate the alternate receptor. However, it should not be concluded that all viral replication using the O+2P protocol applied to the WT SARS-CoV-2 results only from LSR activity. Indeed, SARS-CoV-2 unable to bind the ACE2, but entering cells through the LSR replicate into ACE2 competent infective SARS-CoV-2 *see e.g.*, FIG. 2F. The O+2P protocol was also established to minimize the effect of cell toxicity on viral production. Indeed, using this protocol less than 15% reduction in cell layer protein content was observed even when the viral production exceeded $5x10^9$ particles per well.

[00517] Both the LSR and the ACE2 mRNA are expressed in tissues where the first virus-host contact occurs, *see e.g.*, FIGS. 3L, 3M, 3N. The ACE2 is expressed more in the nasal epithelium where no fatty acids are produced than it is in the tongue. The LSR is expressed more in the tongue where the ACE2 expression is low. Salivary lipase increases free fatty acid levels in the mouth within minutes of consuming lipids. The Delta variant is clinically more infectious than the Alpha variant and replaced the Alpha variant as the dominant circulating strain in less than 6 months in the USA. Paradoxically this occurred in spite of its reduced capacity to bind the ACE2 in cultured cells. Therefore, the transmission of the virus, and that of the Delta variant, occurring through contaminated

food may represent an cause of infection that has not been sufficiently addressed in current preventive measures.

[00518] Linoleate both suppresses SARS-CoV-2 interaction with the ACE2 and stimulates the LSR, *see e.g.*, FIG. 2G. This dual effect offers an explanation for previous data showing linoleate to reduce SARS-CoV-2 replication but only when associated with Remdesivir (Toelzer, 2020). Palmitate increases fourfold SARS-CoV-2 production, because this saturated FFA activates the LSR without inhibiting the ACE2. High levels of FFA are commonly found in serum from obese patients and cause insulin resistance and cardiac toxicity. High circulating viral loads are associated with the progression of the infection toward severe COVID-19. Therefore, without being bound by theory, it is believed that high levels of saturated FFA associated with metabolic disorders contributes to a higher viral production hence to increased risk of severe disease.

[00519] Serum FFA levels are elevated in patients with moderate COVID-19 and reached very high levels in severe conditions. Therefore, without being bound by theory, it is believed that the progression of the disease toward severity, LSR contribution to the production of viruses becomes predominant. At the same time, that of the ACE2 regresses due to its inhibition by abundant unsaturated serum FFA. This explains why therapeutic monoclonals targeting exclusively the ABD are clinically effective only when provided early in the course of the infection. *In vitro* data suggest that these monoclonals may not be clinically beneficial even when provided at the early stage in patients infected with the Delta variant. Similar predictions for the effectiveness of therapeutic monoclonals targeting exclusively the ABD would apply to any SARS-CoV-2 variant that relies heavily on the LSR for replication and viral production.

[00520] Conserved accessible FFA binding pockets are present in the three human coronaviruses that infect the digestive tract (SARS-CoV, MERS-CoV, and OC43). An accessible FFA pocket is missing in the three human coronaviruses causing only aerial symptoms (HKU1, 229E, and NL63). Coronaviruses are not protected by a capsid but are enveloped by a phospholipid bilayer. Filling of the spike FFA binding pocket may afford resistance to upper gastrointestinal tract fluids. Fecal-Oral SARS-CoV-2 transmission occurs in ferrets but not in mice or golden hamsters. Ferret diet contains four times more lipids than that of mice and hamsters. Even if the fecal-oral cycle is incomplete in human, oral contamination complementing aerial dispersion of the SARS-CoV-2 is likely.

[00521] Several mutations in Omicron BA.1 and BA.2 impact the structure of fatty acid binding pocket without directly changing the amino acids with a hydrophobic lateral chain. Further, the R408S in Omicron BA.2 prevents stabilization the bound fatty acid carboxylic group. Finally, the Omicron P25 deletion in LBD1 and H655Y in LBD2 may impact LSR mediated replication.

[00522] The Delta variant is clinically more infectious than the Alpha variant, and in the United States, it replaced the Alpha variant as the dominant SARS-CoV-2 strain in less than six months (Bolze, 2021). However, paradoxically, in BGM cells or hACE2 transfected HEK293T cells, Delta variant replicated less efficiently than the wild-type SARS-CoV-2 through the ACE2, see e.g., FIG. 5G. These results support the hypothesis that a second receptor disclosed herein to be LSR, contributes to the natural SARS-CoV-2 replicative cycle.

[00523] Trimeric S-protein 3-D structure

[00524] The ACE 2 binding domains (ABDs) form the apex of the trimeric S protein. The LBDs are distant from one another and on the upper flanks of the trimer. The competing recombinant LBDs tested herein were not glycosylated, suggesting that the S protein interactions with LSR rely on amino acids and not complex carbohydrates.

[00525] SARS-CoV-2 replication data, and *in-silico* modeling indicate that the LSR binding domain remains accessible even when the trimeric S protein is in the closed conformation, *see e.g.*, FIG. 4C. Further, it is possible to suppress SARS-CoV-2 binding to the LSR without affecting the ACE2 mediated replication. The three ACE2 binding domains undergo conformational changes that create a dynamic in the apex of the S protein. The LSR binding domains are distant from one another on the upper flanks of the trimer, and their accessibility is not affected by the S protein conformational changes. Therefore, the data disclosed herein predict that antibodies targeting the ACE2 binding domain are ineffective when the LSR mediates viral replication.

[00526] The first segment of the S protein contributing to the LBD is located in the N terminal domain (NTD) that is the target of naturally produced neutralizing antibodies. NTD neutralizing antibodies improved the condition of 50% of infected Syrian hamsters, and increasing the dose of antibodies did not increase the percentage of responders. Therefore, in some embodiments, it may be clinically beneficial to produce antibodies

targeting the two spike segments that constitute the LBD and the second one is not in the NTD.

[00527] LSR gene and isoforms

[00528] The LSR gene, located on chromosome 19q 13.12, comprises ten exons and alternative splicing produced at least six and possibly nine transcripts encoding LSR subunits (Yen, 1999). The LSR α transcript contains all ten exons. It translates into an NH_2 terminal (N-terminal) extracellular domain annotated with a type V Ig-like motif that possesses five cysteines, a single transmembrane spanning domain, several intracellular sites of potential phosphorylation, and a cysteine-rich motif. Regrettably, the structure of the LSR is not available.

[00529] LSR activated by fatty acid enabled SARS-CoV-2 cell entry causing rapid cytolysis

[00530] The LSR activated by fatty acid enabled SARS-CoV-2 cell entry can cause rapid cytolysis. Fatty acid activated a mechanism that enabled SARS-CoV-2 infectivity even when the conformation of the S protein prevented any interaction with the ACE2. RNA interference that selectively decreased the LSR protein expression reduced the FA-induced ACE2-independent SARS-CoV-2 infectivity and the fatty acid-induced antibody-enhanced cytosis (FIAEC). The LBD on the S protein was structurally distinct from the RBD. Recombinant LBDx reduced FA-induced infectivity and suppressed the FA-induced cytolysis even when it was enhanced by antibodies reacting with the RBD. Further, the LBDx suppressed LSR-mediated infectivity of the WT, the Delta and the Omicron (BA.5) variant of the SARS-CoV-2.

[00531] It was known that linoleic acid (LA) filling of a well-defined fatty acid binding pocket in proximity to the S protein RBD induced a conformational shift that masked the ACE2 binding motif. Here, it was established that the two most abundant unsaturated FA, but not saturated FA, induced a conformational change of the S protein that suppressed the ACE2-mediated replication of not only the WT-SARS-CoV-2 but also the Delta and the Omicron variants. Therefore, the SARS-CoV-2 found in biological fluids and thus potentially with the fatty acid binding pocket filled could be considered non-infectious based on assays relying on the ACE2 while still being able to infect via the LSR. Competitions using recombinant LBDx established that the LSR is critical for the

infectivity of the SARS-CoV-2 that have lost their capacity to bind the ACE2. However, the virions produced when the LSR initiated the infection replicated through the ACE2. Therefore, which fraction of the progeny obtained with the O+2P protocol resulted from cell entry via the LSR or the ACE2 remains to be determined.

[00532] The LSR-mediated entry of the SARS-CoV-2 enabled cytolysis and the FIAEC which did occur when the ACE2-mediated viral entry. The FIAEC occurred rapidly with infective media, containing 10^5 to 10^7 copies of the WT or Delta variant, and were supplemented with monoclonal antibodies reactive with the RBD but not with irrelevant antibodies. The LBDx suppressed the FIAEC caused by the WT and Delta variants. The Omicron (BA.5) did not cause the FIAEC most probably because Casirivimab and Imdevimab do not react with the mutated Omicron RBD. Without enhancing antibodies, cytolysis was detectable within 24 hours of supplementing PA to media containing 10^8 WT or Omicron SARS-CoV-2. The Delta variant for currently unknown reasons caused only the FIAEC. The antibody enhanced cytolysis and the fatty acid induced cytolysis were inhibited by the LBDx with the amino acid sequence of the WT and this irrespective of the lineage of the SARS-CoV-2. LSR expression is abundant in the lung, which could explain the cytolysis resulting from LSR mediated SARs-CoV-2.

[00533] Contrary to the ACE2, the LSR-mediated viral entry did not yield abundant replication in cells that were not subsequently exposed to FA. Therefore, the LSR may first deliver the SARS-CoV-2 into a non-replicative cell compartment. Access of the viral RNA to the replicative compartment required subsequent reactivation and possibly reloading of the LSR. Fatty acids are required for the LSR to endocytose lipoproteins and the co-expression of both α and β LSR isoforms that are produced by alternative splicing of the LSR RNA is needed for the LSR-mediated proteolysis of ApoB (Yen, 1999). Further investigations on the routing in endocytic vesicles of the LSR and its ligands, i.e., Lipoproteins, Clostridial toxins, and now SARS-CoV-2, are needed to better understand the LSR physiological role. The LSR proteins are abundantly concentrated in hepatic endocytic vesicles. Indeed, LSR's primary physiological role was initially proposed to protect hepatocytes from fatty acid overload during the postprandial phase by storing triglyceride-rich lipoproteins in endocytic vesicles. The LSR-mediated delivery of the SARS-CoV-2 into a slowly replicative compartment could contribute to the persistence of the virus in human tissues even after the disappearance of the clinical symptoms.

[00534] LSR expressed in BGM cells required fatty acid supplementation to enable SARS-CoV-2 cell entry. The fatty acid concentrations neutralizing the binding to the ACE2 and activating the LSR were within the physiological range. Serum fatty acid concentrations increase in patients with COVID-19. Heparin used to prevent thrombosis in COVID-19 patients increases fatty acid levels in human plasma. Plasma fatty acid are elevated in obese and diabetic patients who are at higher risk for severe COVID-19. This indicates the clinically relevancy of measuring fatty acid concentrations in SARS-CoV-2 infected patients to evaluate the risk of progression toward severity.

[00535] FA binding to the LSR expressed in the liver modifies the structure of the tetrameric complexes necessary for the binding of lipoproteins. Both unsaturated and saturated fatty acid activate the LSR's ability to bind lipoprotein independently of membrane phospholipids. The fatty acid-activation of the LSR exposes the binding site that, if unoccupied, can be masked upon removal of fatty acids. Once Apo B is bound to the receptor, the FA-LSR activation is no longer reversible. However, while the LSR endocytoses *Clostridial Perfingens* Iota toxins without fatty acid supplementation, OA enhances the LSR-mediated cytopathic effect of this toxin in cancer cells. PA is covalently attached to the cysteine-rich motif of the LSR intracellular domain. Thus, the fatty acid-induced LSR binding of the SARS-CoV-2 may be dependent on non-covalent or covalent interactions with fatty acid.

[00536] The nirmatrelvir and ritonavir dose-dependently inhibited viral replication irrespective of the ACE2 or the LSR initiating the infection, but they did not attenuate the SARS-CoV-2 FIAEC. It is hypothesized that the endocytosis of a large number of particles caused multiple virus-host membrane fusion sites and the leakage of the endocytic vesicle content into the cytoplasm. The arrest of replication by distressed cells and the release of cellular proteases and nucleases in the incubation media likely contributed to the decrease of viral RNA concomitant with cytolysis. Lysosomal membrane permeabilization, if it occurs in lung alveoli, would explain the drop in upper airway viral loads concurrent with the COVID-19 hypoxia.

[00537] Antibodies targeting the SARS-CoV-2 S protein NH_2 terminal domain enhanced the ACE2-mediated infectivity without causing cytolysis. The data showed that antibodies that neutralize the ACE2-mediated replication enhanced LSR-dependent cytolysis. Antibody enhancement of viral diseases has been documented for the Dengue

Virus and is required for the induction of feline infectious peritonitis by the Feline Corona viruses. However, the data did not advocate against COVID-19 immunizations that have clinically proven their beneficial effects in preventing severe COVID-19. Further, the data identified the mechanisms of SARS-CoV-2 cell entry and cytopathic consequences. Therefore, the effects of polyclonal AB produced in response to natural infections or vaccines may be investigated. The identification of the LBD may assist in developing future vaccines possibly more resistant to the emergence of variants.

[00538] The SARS-CoV-2 S protein binding to the LSR could disrupt its functions currently known as twofold. First, the LSR expressed in the liver contributes to lipoprotein clearance. Second, the LSR gene encodes Angulin 1 that forms the tight tri-cellular junctions that maintain epithelial barrier integrity. Human SARS-CoV-2 infections delay the clearance of intravenous lipid emulsions and cause hypertriglyceridemia suggesting interference with LSR's role in lipoprotein clearance. Homozygous missense mutation Glu235Gly in the human LSR gene is associated with liver dysfunction and neurological disorders. The LSR gene transcript is found in the blood brain barrier (BBB) and its deletion causes BBB leakage in mice. Targeted disruption of the LSR gene expression in mouse astrocytes caused olfactory deficits and memory loss. The possibility that viral S protein interacts with the LSR and disrupts epithelial barriers, causing neurological, digestive, and vascular symptoms, requires further investigations.

[00539] The BGM model was selected after finding that it enabled an abundant ACE2-mediated viral production causing only moderate cytopathic effects hence minimizing interferences due to the release in the media of cellular enzymes. In VeroE6, CD44 interferes with LSR-mediated endocytosis of *Clostridium Perfingens* Iota Toxin, which is not the case in most other cell lines. In BGM cells and irrespective of the entry mechanism, the Omicron (BA.5) replicated less rapidly than the WT-SARS-CoV-2 or the Delta variant, consistent with its less frequent progression to severe COVID-19 despite the higher affinity for the ACE2. However, validation of this hypothesis requires testing multiple Omicron isolates.

[00540] The finding that SARS-CoV-2 entry via the LSR had cytopathic consequences far more important than those caused by the ACE2 mediated replication was consistent with clinical observations. This indicates that the delay between the initial infection and the development of severe pulmonary lesions is imposed by the viral threshold required for the

LSR mediated cell lysis. This viral threshold can be lowered if available antibodies exclusively neutralize the RBD. Viral replication inhibitors are effective in preventing the virus to reach the cytolytic threshold hence reduce the progression toward severe COVID 19. The Paxlovid that combined two viral replications inhibitors is clinically highly effective at preventing severe COVID-19 but without clinical benefit when pulmonary lesions are established. A significant percentage of non-vaccinated patients infected mostly with the Delta variant and of vaccinated patients infected mostly with the Omicron variant that were treated with Paxlovid developed severe COVID-19. The results indicate that LBD, such as intravenous LBD, if found safe in preclinical studies, would be therapeutically useful in COVID-19 patients with clinical or biological signs indicating the start of respiratory failure.

[00541] SARS-CoV-2 entry via PA-activated LSR causes BGM cell lysis.

[00542] In agreement with FIG. 2K, the O+2P protocol increased the number of viral RNA released in the media during the last 24 h of the culture following infection with 10^4 gec. However, a third PA supplementation at DPI 3 lowered the viral RNA copy numbers (FIG. 8A). Infections with SARS-CoV-2 (10^8 gec) and PA (0.4mM) destroyed the cell monolayer (FIG. 8B). Cell lysis did not occur without PA and was suppressed by LBDx. Control tests were carried out for the absence of the cytolytic effect of PA (0.4 mM) alone and with SARS-CoV-2 at a lower infective dose (10^7 gec). PA-induced cytolysis reduced the cell protein content by more than 70%. Dishes were surveyed to find islets of surviving cells shown in FIG. 8B (middle panel). Induction of cell lysis by PA occurred at threshold that was narrowed to 8 X 10^7 gec/well (FIG. 8C). No cell lysis was detected after infections without FA or with OA (0.4 mM) even when the infective titer was 10^8 gec (FIG. 8D). LBDx or LSR gene silencing suppressed the cell protein loss caused by SARS-CoV-2 infection (10^8 gec) with PA (0.4 mM) (FIG. 8D and FIG. 8E). Delta and Omicron SARS-CoV-2 caused massive cell lysis at the same infective threshold (10^8 gec) but again only when infective media was supplemented with PA (0.4 mM). LBDx suppressed the PA-induced cytolytic effect of the two variants of concern (FIG. 8F). None of the five monoclonal antibodies targeting the RBD protected the cell monolayers from PA-induced SARS-CoV-2 cytolysis (FIG. 8G). Nirmatrelvir and ritonavir that inhibited SARS-CoV-2 replication when applying the No-FA or the O+2P protocol (FIG. 8H) did not attenuate PA-induced cell lysis (FIG. 8I). Therefore, in BGM cells, above the same infective

threshold, the three SARS-CoV-2 lineages became highly cytolytic upon entry via PA-activated LSR.

[00543] LSR mediated SARS-CoV-2 replication and cytolysis in human pulmonary cells lacking ACE2.

[00544] At the protein level, human A549 cells expressed the LSR but no detectable ACE2. SARS-CoV-2 infection with media containing OA (0.4 mM) or PA (0.4 mM) followed by repeated transient exposure to the same FA induced SARS-CoV-2 replication. No SARS-CoV-2 replication was detected without FA consistent with the lack of functional ACE2 in this cell line. In A549 cells, FA-induced SARS-CoV-2 replication was inhibited by competing LBDx. SARS-CoV-2 entry via PA and OA activated LSR was cytolytic in A549 cells, but this required three infections with FA and viruses (10^8 gec). We verified that two prior incubations with PA or OA followed by a single exposure to infective media (10^8 gec) did not cause A549 cell lysis (Data not shown). CD44 protects mammary cancer cells from LSR mediated cytopathic effect caused by Clostridium perfringens binary iota toxin. CD44 was expressed in A549 but not in BGM cells.

[00545] LSR mediated FA- induced cytolytic effect of virus free recombinant spike protein.

[00546] Besides contributing to lipoprotein clearance, the LSR mediates cytopathic effect of Clostridial binary toxins. Thus, it was investigated whether the virus free full length S protein was directly cytotoxic upon binding to FA activated LSR. It was first verified by gel filtration chromatography that recombinant virus free S protein preparations contained mainly trimer and dimers without detectable trace of cleavage into S1. PA but not OA added to BGM cell with the spike protein caused massive cytolysis that was fully suppressed by LBDx.

[00547] Next, the cytolytic effect of the S1 segment was tested under the same conditions. A single exposure of A459 cells to the Full length S protein in the presence of FA was not sufficient to cause cell lysis.

[00548] Effect of LBDx on SARS-CoV-2 lethality in K18hACE2 mice.

[00549] LSR background

[00550] Lipoprotein receptor

[00551] The first identified LSR function is endocytosis of lipoproteins containing Apo B or ApoE. LSR physiological contribution to liver lipoprotein clearance was established and independently confirmed in mice. FA directly, and reversibly modify LSR conformation unmasking the lipoprotein binding site. Thus far there are no structural analysis characterized LSR FA-binding pocket nor LSR conformational changes enabling apolipoprotein binding. LSR designation stemmed from the hypothesis that endocytosis of triglyceride-rich lipoprotein (TGRL) under the control of FA generated by extracellular lipases, protects hepatocytes from FA overload. In human patients, SARS-CoV-2 infections delay the clearance of intravenous lipid emulsions without changes in lipolytic enzyme activity, consistent with the viral S protein interfering with LSR mediated lipoprotein clearance.

[00552] LSR mediated endocytosis of SARS-CoV-2 may proceed through caveolae or clathrin dependent or independent mechanism and with or without lipid raft involvement. The *LSR* gene produces by alternative splicing at least three functionally critical and possibly six isoforms. Transfection of the longest α isoform that contains a transmembrane spanning domain is sufficient for FA-induced binding and uptake of lipoproteins with a greater affinity for TGRL compared to LDL. However, co-transfection of α and β isoforms is required for lipoprotein proteolytic cleavage. The β isoform lack a transmembrane spanning domain. Competition between VLDL and LDL with the SARS-CoV-2 for binding to FA-activated LSR can occur but in tissues with fenestrated capillary endothelium (for example, the liver or hepatic tissue or liver tissue). However, HDL containing Apo E bind LSR and are present in interstitial fluids. The possibility that lipoproteins protects from SARS-CoV-2 cytopathic effect and that Apo E2 that has a lower affinity for LSR compared to Apo E3 is less protective is currently under investigation. However, TGRL may release FA, upregulate LSR expression and thereby potentially aggravate the cytopathic consequences.

[00553] The LSR gene encodes angulin 1.

[00554] The *LSR* gene encodes angulin 1, forming the tight tri-cellular junctions that maintain epithelial barrier integrity. Homozygous missense mutation Glu235Gly in the human *LSR* gene is associated with liver dysfunction and neurological disorders. Targeted

disruption of the *LSR* gene expression in mouse astrocytes caused olfactory deficits and memory loss. The *LSR* gene transcript is found in the blood-brain barrier (BBB), and BBB leakages in $LSR^{-/-}$ mice explain their embryonic lethality.

[00555] Other LSR ligands.

[00556] LSR endocytoses several clostridial binary toxins. FA-activation of LSR is not required for endocytosis of clostridial toxins. However, OA enhances LSR-mediated and CD44 interferes with C perfringens iota toxin cytopathic effects on cancer cells.

[00557] **Conclusion**

[00558] The complete SARS-CoV-2 S protein is the immunogen currently used for nucleic acid, vectored, or protein subunit vaccines. Monoclonal antibodies targeting all segments of the S protein have been isolated from patients after natural infection. Therefore, vaccine and infection-induced antibodies are likely reactive with both the ACE2 and the LSR binding domains. However, while the current vaccines are effective to protect against severe disease and hospitalization, breakthrough infections occur, and vaccinated individuals can still transmit virus. Therefore, improvements in vaccines and other therapy are still desirable and needed.

[00559] Fortunately, the present disclosure reveals the existence of a second SARS-CoV-2 receptor, LSR, which also actively participates in SARS-CoV-2 replication and viral production. Therefore, it is now possible to focus vaccine-induced immunological responses to this important receptor target, thereby improving the effectiveness of vaccines and other therapies for SARS-CoV-2 and COVID-19. Three segments of the spike protein: ABD, LBD1, and LBD2, together represent less than 36% of the full-length S protein, but comprise the two receptor binding domains, ACE2, and the LSR. As demonstrated herein, viral replication is suppressed by disabling the binding to the ACE2 and competing or otherwise blocking the binding of LBD1 and/or LBD2 to the LSR receptor. Therapies directed toward these mechanisms facilitate the fight against SARS-CoV-2 and COVID-19 and are within the scope and spirit of this disclosure.

[00560] **EXAMPLE 9: TI-assisted immunization against SARS-CoV-2**

[00561] SARS-CoV-2 coronavirus, the causative agent of COVID-19, was reported by Chinese authorities in December 2019 and WHO declared the pandemic on March 11,

2020. Spike protein or S protein lies on the outer envelope of the virus and leads to the entry of the virus into the human cells through interactions with Angiotensin Converting Enzyme-2 (ACE2), and as disclosed herein, through interactions with Lipolysis Stimulated Receptor (LSR).

[00562] Transcription infidelity and ribosomal frameshifts have been described as contributors to viral protein diversity (see *e.g.*, Atkins, *et al.*, (2016) *supra*). Viral mRNA sequences were aligned to the reference genomic RNA to identify RNA-RNA bases Divergences (RRD) using bioinformatics procedures applying the stringent filters previously described (Brulliard, et, al., (2007) Proc Natl Acad Sci, 2007; 104: 7522-7527; Thouvenot, 2020, *supra*). In SARS-CoV-2, 891 gapped positions were identified. Interestingly, the number of single base gap events in HCoV-HKU1, a benign human coronavirus, was 687. In most eukaryotic cells, RNAs gapped at a given position rarely exceed 1% of total mRNA (Thouvenot, 2020, *supra*), but in SARS-CoV-2, frameshifted RNA represented as much as 15% of the total mRNA. Frameshifted RNA does not exceed 5% in HCoV-HKU1. In both SARS-CoV-2 and HCoV-HKU1, these TI gaps are distributed on the entire viral genome. The TI gaps also affect the S transcript, and strikingly, the S transcripts of SARS-CoV-2 contain far more TI events than that of HCov-HKU1 ($p = 3.6e-15$). In addition, *in silico* translation of gapped RNA revealed that predicted TI segments of SARS-CoV-2 TI proteins have higher isoelectric point, higher global charge and lower hydrophobicity than those from HCoV-HKU1. Hence, this higher gap density in the Spike protein transcripts likely leads to the translation to many Spike-TI proteins with carboxyterminal TI segments.

[00563] Natural Spike protein exhibits conformational plasticity that modulates the accessibility of the ACE2 binding motif (or RBD for Receptor Binding Domain) (Walls, *et al.*, (2019) Cell 176:1026-1039.e15; Cai, *et al.*, (2020) Science 369: 1586–1592). These structural rearrangements may hinder antibody interaction. Accordingly, a construct was produced centered on the RBD of S protein that contains five noncontiguous domains. All domains are derived from the canonical S protein and all five are exposed on the S (5ES) surface irrespective of the open or closed conformation of the trimer. Four TI chimera of that construct were generated by fusion of TI segments described below at 5ES carboxy-terminal end to produce 5ES-TI Chimera A and D.

[00564] Mice were first immunized once a day during eight days with 20 mcg of canonical 5ES and/or 5ES-TI chimera provided alone and in combination. All immunizations yielded, as soon as on Day 14, an increase in IgG reactive with 5ES. The 5ES IgG detected on Day 14 and Day 31 did not cross-react with the Full-Length S protein (FLS).

[00565] Mice were maintained in their normal environment without further immunization until Day 36. On that day, they received a single injection of the same immunogens, which resulted, after 7 days (Day 43), in a significant increase in 5ES-specific IgG. These IgG became cross-reactive with the FLS, especially when 5ES Chimera A and 5ES Chimera D were combined.

[00566] The ability of serum to block the interaction between S protein and ACE2 has been evaluated *in vitro* (SARS-CoV-2 Surrogate Virus Neutralizing Test kit, Genscript Biotech; Tan, *et al.*, (2020) Nat Biotechnol. 38: 1073–1078). The combination of 5ES-TI Chimera A and D was more effective in the induction of serum neutralizing activity (SNA) than 5ES Chimera individually administrated. In mice sensitized, then boosted with the canonical 5ES construct alone, the SNA was not significantly increased ($p= 0.78$), while an increase in 5ES and FLS specific IgG was observed on Day 43 ($p= 0.04$). Furthermore, it was verified that the boosts were well tolerated with none of the clinical signs typically observed in allergic/hyper immunized mice. Hence, mouse immunizations with TI Chimera of 5ES, but not with canonical 5ES construct induce SARS-CoV-2 neutralizing antibodies. Together, the data show that the presence, at the carboxy-terminal end of the immunogen, of a cationic segment translated from frameshifted RNA is required for the conversion of these 5ES IgG into neutralizing antibodies. The combination of the 5ES-TI Chimera A and D yielded the highest neutralizing effect.

[00567] The timeframe for the induction of the 5ES and FLS IgG reactivity and SNA was examined. Between Day 0 and Day 4 post-boost, the median growth of 5ES and FLS IgG reactivities were 69% and 86%. Between Day 4 and Day 7, the median growth rates were 63% and 179%, respectively. This reflected the progressive acquisition of cross-reactivity of 5ES-IgG with the trimeric FLS. A significant SNA increase was detectable as early as 4 days post-boost. The median SNA grew by 57% between Day 0 and Day 4, and by 77% between Day 4 and Day 7.

[00568] In order to investigate the opportunity to treat COVID-19 patients by developing passive serotherapy using TI-assisted immunization, the inventors tested these findings in cows. The cow was selected because coronaviruses represent an important cause of calves' mortality by severe diarrhea and because cow may provide an abundant source of potentially neutralizing antibodies.

[00569] A combination of the four 5ES-TI Chimera A, B, C and D was intraperitoneally injected to cows once a day during eight days at two different doses (0.1 mg or 0.025 mg each). The induction of IgG to the canonical 5ES construct was detectable in all cows on Day 14 (and as early as Day 9 for Cow 22). A similar induction was obtained when the combination of the same four proteins (0.2 mg each per injection) was injected three times at a 1-week interval.

[00570] Canonical 5ES (for SARS-CoV-2 coronavirus; SEQ ID NO: 10)

[00571] MKHHHHHHMVYYHKNNKSWMESEFRVYSSANNCTFEYVSQPFLMDLEGKQGNF KNGGKRISNCVADYSVLYNSASFSTFKCYGVSPTKLNDLCGGSTEIYQAGSTPCNGVEGFN CYFPLQSYGFQPTGGVCGPKKSTNLVKNKCVNFNFGGDKNTQEVFAQVKQIYKTPPIKDFG G

[00572] 5ES-TI Chimera A (for SARS-CoV-2 coronavirus; SEQ ID NO: 11)

[00573] MKHHHHHHMVYYHKNNKSWMESEFRVYSSANNCTFEYVSQPFLMDLEGKQGNF KNGGKRISNCVADYSVLYNSASFSTFKCYGVSPTKLNDLCGGSTEIYQAGSTPCNGVEGFN CYFPLQSYGFQPTGGVCGPKKSTNLVKNKCVNFNFGGDKNTQEVFAQVKQIYKTPPIKDFG GPSGPSWASWLRCWCWS

[00574] 5ES-TI Chimera B (for SARS-CoV-2 coronavirus; SEQ ID NO: 12)

[00575] MKHHHHHHMVYYHKNNKSWMESEFRVYSSANNCTFEYVSQPFLMDLEGKQGNF KNGGKRISNCVADYSVLYNSASFSTFKCYGVSPTKLNDLCGGSTEIYQAGSTPCNGVEGFN CYFPLQSYGFQPTGGVCGPKKSTNLVKNKCVNFNFGGDKNTQEVFAQVKQIYKTPPIKDFG GVKSPQKSYLFPSSMIGIGSLPSCWACWIQQ

[00576] 5ES-TI Chimera C (for SARS-CoV-2 coronavirus; SEQ ID NO: 13)

[00577] MKHHHHHHMVYYHKNNKSWMESEFRVYSSANNCTFEYVSQPFLMDLEGKQGNF
KNGGKRISNCVADYSVLYNSASFSTFKCYGVSPTKLNDLCGGSTEIYQAGSTPCNGVEGFN
CYFPLQSYGFQPTGGVCGPKKSTNLVKNKCVNFNFGGDKNTQEVFAQVKQIYKTPPIKDFG
GLKIQKLQGKCSQPGMVGCSLTTWRTSMVLGRNI

[00578] 5ES-TI Chimera D (for SARS-CoV-2 coronavirus; SEQ ID NO: 14)

[00579] MKHHHHHHMVYYHKNNKSWMESEFRVYSSANNCTFEYVSQPFLMDLEGKQGNF
KNGGKRISNCVADYSVLYNSASFSTFKCYGVSPTKLNDLCGGSTEIYQAGSTPCNGVEGFN
CYFPLQSYGFQPTGGVCGPKKSTNLVKNKCVNFNFGGDKNTQEVFAQVKQIYKTPPIKDFG
GSAKLSWTTFQILSWKPMFHFWY

[00580] TI segments coupled to canonical proteins to generate Chimera:

[00581] TI segment #7 (SEQ ID NO: 2) LCFKRYELRLPAKRKRKRN

[00582] TI segment #60 (SEQ ID NO: 3) LKIQKLQGKCSQPGMVGCSLTTWRTSMVLGRNI

[00583] TI segment #66 (SEQ ID NO: 4) VKSPQKSYLFPSSMIGIGSLPSCWACWIQQ

[00584] TI segment #158 (SEQ ID NO: 5) PSGPSWASWLRCWCWS

[00585] TI segment #162 (SEQ ID NO: 6) SAKLSWTTFQILSWKPMFHFWY

[00586] TI segment #245 (SEQ ID NO: 7) EFDIRRIRQMLIITK

[00587] TI segment #294 (SEQ ID NO: 8) LQICAKYSSVTAWTPAAGRSCKMEGCRWWR

[00588] TI segment #367 (SEQ ID NO: 9) FLISMPEKCVNTWIMKI

[00589] **EXAMPLE 10: Selection of TI segments to be coupled to obtain Chimera for TI-assisted immunization**

[00590] Without being bound by theory, it is believed that TI proteins are immunogenic because they react specifically through their TI segment with Natural Immunoglobulins (NIg) that constitute the B cell Receptor (BCR) of naive B lymphocytes. Hence, exploring the repertoire of natural Ig of the organism in which a TI-assisted immunization is planned means to identify the TI segment(s) to be coupled to the immunization target.

[00591] Immobilized NIg on B cells also exist as circulating molecules in sera of different mammalian species. A large panel of segments resulting from TI has been constituted by the inventors through previous work (disclosed for instance in WO2008/009751). The sera of 4 different species (mouse, human, dog, cow) was tested, the reactivity of NIg with a representative panel of TI peptides (as enumerated in the below section entitled "Sequences") versus a canonical control peptide, i.e., a peptide encoded by RNA without frameshift. For this experiment, streptavidin plates were coated with biotinylated TI peptides (0.5 to 1 μM per well) and incubated with diluted sera for 30 min at 37°C. After washing, TIP-specific IgG were detected by alkaline-phosphatase-labeled anti-human, dog, cow or mouse IgG and development was performed with p-nitrophenyl phosphate (pNPP). The reactivities of NIg from the 4 mammalian species to TI peptides were significantly higher than those to the canonical peptide. The presence of detectable IgG against TI peptides in sera give an image of the nature of the NIg immobilized on B cells. Consequently, TI peptides leading to high level of TIAB should be of better chance to constitute good anchors for B cell receptors of naive B cells and would like to maximize the TI-assisted immunization process.

[00592] TI peptides used as probes for NIg detection:

[00593] TI peptide #1 (SEQ ID NO: 15) WRRWAAPWFWSSLQLGGLVFRGPGPRARSR

[00594] TI peptide #7 (SEQ ID NO: 16) LCFKRYELRLPAKRKRKRN

[00595] TI peptide #25 (SEQ ID NO: 18) RFPARAPWRCRAPRSTCCIPATIRWPRAST

[00596] TI peptide #38 (SEQ ID NO: 19) HLKCKLKKFDRWDPIKRGQ

[00597] TI peptide #39 (SEQ ID NO: 20) LLCCFSAFPSFLLKDGRRFSSPGWWSC

[00598] TI peptide #44 (SEQ ID NO: 21) WSIWLSREQRIGLAVPWRRRWRAWGPILMP

[00599] TI peptide #60 (SEQ ID NO: 22) LKIQKLQGKCSQPGMVGCSLTTWRTSMVLGRNI

[00600] TI peptide #66 (SEQ ID NO: 23) VKSPQKSYLFPSSMIGIGSLPSCWACWIQQ

[00601] TI peptide #76 (SEQ ID NO: 24) MLWMVQKAWLEARKYWILVHQSKFLLVLRLWAES

[00602] TI peptide #87 (SEQ ID NO: 25) LQICGKCSSVTAWTLAAGRSCKMEGCRWWK

[00603] TI peptide #90 (SEQ ID NO: 26) WRKRKRNWPRKQGRRLLTIWLLGKMNELGS

[00604] TI peptide #95 (SEQ ID NO: 27) LCAPRRSLLSVIGQKNLRNSTAK

[00605] TI peptide #92 (SEQ ID NO: 28) LTAPRAWRARTASPWTAATVASGRRKTRLT

[00606] TI peptide #131 (SEQ ID NO: 29) IPKDRLQHQQKLQWLMPYMKYQ

[00607] TI peptide #134 (SEQ ID NO: 30) MRSTLSGRDFHPCRWLMKSLAF

[00608] TI peptide #158 (SEQ ID NO: 31) PSGPSWASWLRCWCWS

[00609] TI peptide #162 (SEQ ID NO: 32) SAKLSWTTFQILSWKPMFHFWY

[00610] TI peptide #210 (SEQ ID NO: 33) LGLGRNGIRNHRNPETLQLKFVVIGK

[00611] TI peptide #221 (SEQ ID NO: 34) TLIPRGTRKHCIWVLS

[00612] TI peptide #234 (SEQ ID NO: 35) KIQKLQGKCSQPGMV

[00613] TI peptide #289 (SEQ ID NO: 36) QRKPRRRPRERALSCTRTLQIRKPHPVANL

[00614] TI peptide #290 (SEQ ID NO: 37) RCFKRCALRLPAKRRRKRN

[00615] TI peptide #291 (SEQ ID NO: 38) TWPRTSCGCERNCRRRCSRERKPKAPCSHS

[00616] TI peptide #292 (SEQ ID NO: 39) WRKKKRNWLRRQGRRLLTTWPPERMSEHAS

[00617] TI peptide #293 (SEQ ID NO: 40) HLKCKLKKSGR

[00618] TI peptide #294 (SEQ ID NO: 41) LQICAKYSSVTAWTPAAGRSCKMEGCRWWR

[00619] TI peptide #295 (SEQ ID NO: 42) MLWMALKAWLEARKYWIQGHQSKFLLVLRPWAES

[00620] TI peptide #296 (SEQ ID NO: 43) FAKLSWTTYQILSWRPMSLY

[00621] Canonical peptide (SEQ ID NO: 44) ALLQKVRAEIASKEKEEEE

[00622] One or more features from any embodiments described herein or in the figures may be combined with one or more features of any other embodiments described herein or in the figures without departing from the scope of the disclosure.

[00623] All publications, patents and patent applications cited in this specification are herein incorporated by reference as if each individual publication or patent application were specifically and individually indicated to be incorporated by reference. Although the foregoing disclosure has been described in some detail by way of illustration and example for purposes of clarity of understanding, it will be readily apparent to those of ordinary skill in the art in light of the teachings of this disclosure that certain changes and modifications may be made thereto without departing from the spirit or scope of the appended claims.

WHAT IS CLAIMED IS:

1. An immunogenic composition for inhibiting SARS-CoV-2 replication comprising:
at least one nucleic acid encoding at least one immunogen that comprises a lipolysis-stimulated receptor binding domain (LBD) of a SARS-CoV-2 spike protein, wherein the at least one nucleic acid encoding the immunogen is operably linked to an expression control sequence and wherein the LBD is selected from LBD1 and LBD2.

2. The immunogenic composition of claim 1, wherein the LBD is LBD1.

3. The immunogenic composition of claim 1 or 2, wherein the nucleic acid that encodes the LBD1 encodes a polypeptide that comprises an amino acid sequence having at least 90% sequence identity to amino acid 25 to amino acid 85 of SEQ ID NO: 1.

4. The immunogenic composition of claim 1, wherein the LBD is LBD2.

5. The immunogenic composition of claim 1 or claim 4, wherein the nucleic acid that encodes the LBD2 encodes a polypeptide that comprises an amino acid sequence having at least 90% sequence identity to amino acid 607 to amino acid 691 of SEQ ID NO: 1.

6. The immunogenic composition of any one of claims 1 to 5, wherein the at least one nucleic acid that encodes at least one immunogen, encodes a polypeptide that comprises LBD1 and LBD2.

7. The immunogenic composition of any one of claims 1 to 6, wherein the composition further comprises a nucleic acid that encodes at least one immunogen that comprises an ACE2 binding domain (ABD) operably linked to an expression control sequence.

8. The immunogenic composition of claim 7, wherein the LBD1, LBD2, and ABD are encoded by the same nucleic acid.

9. The immunogenic composition of claim 8, wherein the nucleic acid encoding the LBD1, LBD2, and ABD encodes a polypeptide that comprises an amino acid sequence having at least 90% sequence identity to amino acid 25 to amino acid 691 of SEQ ID NO: 1.

10. The immunogenic composition of claim 7, wherein the LBD1, LBD2, and ABD are encoded by different nucleic acids.

11. The immunogenic composition of any one of claims 1 to 10, wherein one or more immunogens is coupled to one or more Transcription Infidelity (TI) segments.

12. The immunogenic composition of any one of claims 1 to 11, wherein the immunogenic composition further comprises at least one adjuvant.

13. A method for immunizing a subject against COVID-19 disease resulting from a SARS-CoV-2 infection, the method comprising: administering to a subject with the immunogenic composition of any one of claims 1 to 12.

14. The method of claim 13, wherein the method reduces the severity of COVID-19 disease.

15. The method of claim 13 or claim 14, wherein the method reduces transmission of SARS-CoV-2.

16. A method of making an antibody or antigen binding fragment that specifically binds to at least one LBD of a SARS-CoV-2 spike protein, the method comprising: immunizing a mammal with a polypeptide that comprises an LBD peptide, wherein the LBD peptide selected from the group consisting of LBD1 and LBD2.

17. The method of claim 16, wherein the polypeptide comprises LBD1 and LBD2.

18. The method of claim 16 or claim 17, wherein the LBD1 comprises an amino acid sequence having at least 90% sequence identity to amino acid 25 to amino acid 85 of SEQ ID NO: 1 and LBD2 comprises an amino acid sequence having at least 90% sequence identity to amino acid 607 to amino acid 691 of SEQ ID NO: 1.

19. The method of any one of claims 16 to 18 wherein the polypeptide comprises an amino acid sequence having at least 90% sequence identity to amino acid 25 to amino acid 691 of SEQ ID NO: 1.

20. The method of any one of claims 16 to 19 wherein the polypeptide further comprises an ACE2 binding domain (ABD).

21. The method of any one of claims 16 to 20 wherein the polypeptide is coupled to one or more Transcription Infidelity (TI) segments.

22. The method of any one of claims 16 to 21, further comprising: recovering antiserum from the immunized mammal and purifying polyclonal antibodies that specifically bind to at least one LBD of a SARS-CoV-2 spike protein.

23. The method of any one of claims 16 to 21, further comprising:
recovering B-lymphocytes from the immunized mammal,
fusing the recovered B-lymphocytes with a myeloma cell to produce a hybridoma cell; and
selecting individual hybridoma cells that produce monoclonal antibodies that specifically bind to at least one LBD of a SARS-CoV-2 spike protein.

24. An antibody or antigen-binding fragment which is a product of the method of any one of claims 16 to 23.

25. The antibody or antigen-binding fragment of claim 24, wherein the antibodies or antigen-binding fragment are humanized or human.

26. A nucleic acid encoding the antibody or antigen-binding fragment of claim 24 or claim 25.

27. A pharmaceutical composition comprising the antibody or antigen binding fragment of claim 24 or claim 25.

28. The pharmaceutical composition of claim 27, further comprising a second therapeutic agent.

29. The pharmaceutical composition of claim 28, wherein the second therapeutic agent is a second antibody, or an antigen-binding fragment thereof, that binds a SARS-CoV-2 spike protein.

30. A method for treating or preventing COVID-19, the method comprising: administering a pharmaceutically effective amount of an antibody or antigen-binding fragment of claim 24 or claim 25 or the pharmaceutical composition of any one of claims 27 to 29 to a subject in need thereof.

31. The method of claim 30, wherein administering the pharmaceutically effective amount of the antibody or antigen binding fragment of claim 24 or claim 25 or the pharmaceutical composition of any one of claims 27 to 29, results in one or more of:
an acceleration in intestinal clearance of SARS-CoV-2,
a reduction of transmission of SARS-CoV-2,
an alleviation of one or more symptoms of long COVID-19 syndrome, or
a combination thereof in the subject.

32. A method for assaying SARS-CoV-2 cellular entry *in vitro*, the method comprising:
(1) pre-incubating a first subpopulation of SARS-CoV-2 pseudovirus (PV) with a long-chain unsaturated free fatty acid (uFFA), thereby providing ACE2 incompetent PV, and either pre-incubating a second subpopulation of SARS-CoV-2 PV with a long-chain saturated free fatty acid (sFFA) or not pre-incubating SARS-CoV-2 PV, thereby providing ACE2 competent PV;
(2) incubating the ACE2 incompetent and ACE2 competent PV with host cells, to provide a first and a second host cell culture;
wherein the first host cell culture comprises ACE2 incompetent SARS-CoV-2, and

the second host cell culture comprises ACE2 competent SARS-CoV-2; wherein the host cells comprising the first cell culture and the second host cell culture express an ACE2 receptor and a lipolysis stimulated receptor (LSR);
(3) transiently exposing the host cell cultures to a long-chain unsaturated fatty acid, or a long-chain saturated fatty acid; and
(4) observing the PV in the host cell cultures over time, to determine timing of PV entry into the host cells; wherein timing of the PV entry is early or late; and wherein early entry indicates entry via ACE2 receptor, and late entry indicates entry via LSR.

33. The method of claim 32, wherein the transient exposure of the host cell cultures to a long-chain free fatty acid (FFA), is carried out 3 times without adding new PV.

34. The method of claim 32 or claim 33, wherein the SARS-CoV-2 PV comprises:
(a) a nucleic acid that encodes a green fluorescent protein (GFP) operably-linked to an expression control sequence, wherein the GFP is expressed upon entry into a host cell; and
(b) a nucleic acid that encodes a SARS-CoV-2 spike protein, wherein the spike protein comprises one or more of an LBD1, LBD2, or ABD.

35. The method of claim 34, wherein observing the PV over time comprises: observing the level of fluorescence in the host cell cultures over time, wherein the level of fluorescence increases with the number of PV that are able to enter the host cells; and wherein early fluorescence indicates entry via ACE2 receptor, and late fluorescence indicates entry via LSR.

36. The method of claim 35, further comprising:
selecting PV that show late fluorescence indicative of entry via LSR, thereby providing LSR specific pseudoviruses.

37. Use of the method of claim 36 to evaluate the effectiveness of a test antibody directed against LBD1, LBD2, ABD or combinations thereof for

neutralizing entry via LSR, wherein the method comprises incubating the test antibody with the PV and host cells in step (2); and
observing the effect on late fluorescence as compared late fluorescence in the absence of the antibody.

38. A method for assaying coronavirus cellular entry or replication *in vitro*, the method comprising:
(1) pre-incubating a first subpopulation of live coronavirus with a long-chain unsaturated free fatty acid (uFFA), thereby providing a population of ACE2 incompetent virus; and
either pre-incubating a second subpopulation of live coronavirus with a long-chain saturated free fatty acid (sFFA) or not pre-incubating the second subpopulation of live coronavirus with any FFA, thereby providing ACE2 competent virus;
(2) incubating an initial titer of the ACE2 incompetent and ACE2 competent virus with host cells, to provide a first and a second host cell culture;
wherein the first host cell culture comprises the ACE2 incompetent virus, and the second host cell culture comprises the ACE2 competent virus; and
wherein the host cells comprising the first cell culture and the second host cell culture express an ACE2 receptor and a lipolysis stimulated receptor (LSR);
(3) transiently exposing the first and second host cell cultures to a long-chain free fatty acid (FFA), and
(4) observing timing of viral production, wherein viral production is measured by the number of virus produced as compared to the initial titer of the ACE2 incompetent or ACE2 competent virus, and wherein an increase in the number of virus is indicative of viral entry and replication;
wherein timing of the viral production is early or late; and
wherein early timing of the viral production indicates entry via ACE2 receptor, and late timing of the viral production indicates entry via LSR.

39. The method of claim 38, wherein the live coronavirus comprises:
a nucleic acid that encodes a coronavirus spike protein, and wherein the spike protein comprises one or more of an LBD1, LBD2, or ABD.

40. The method of claim 38 or claim 39, wherein the transient exposure of the first and second host cell cultures to a long-chain free fatty acid (FFA), is carried out 3 times without adding new virus.

41. The method of any one of claims 38 to 40, wherein the coronavirus is selected from the group consisting of SARS-CoV-2, SARS-CoV, MERS-CoV, OC43, a bovine coronavirus, a feline coronavirus, and a porcine coronavirus.

42. The method of claim 41, wherein the coronavirus is SARS-CoV-2.

43. The method of claim 38, wherein the long-chain uFFA is selected from oleate and linoleate.

44. The method of claim 43, wherein the long-chain uFFA is oleate.

45. The method of any one of claims 38 to 44, wherein the long-chain FFA of step 3 is selected from the group consisting of a long-chain unsaturated fatty acid, and a long-chain saturated fatty acid.

46. The method of claim 45, wherein the long-chain FFA of step 3 is a long-chain saturated fatty acid.

47. The method of claim 46, wherein the long-chain saturated fatty acid is selected from palmitate and stearate.

48. The method of claim 47, wherein the long-chain saturated fatty acid is palmitate.

49. The method of any one of claims 38 to 48, wherein the method is used to screen mutant libraries for ACE2 and/or LSR incompetent viral variants.

50. The method of claim 49, wherein the live coronavirus is SARS-CoV-2.

51. The method of claims 49 or 50, wherein the ACE2 and LSR incompetent viral variants are sequenced, and the resulting sequences are used to create viruses that are immunogenic, but non-replicative.

52. The method of claims 38 to 48, further comprising in step (2) adding a putative inhibitor of entry via either or both LSR and ACE2, to screen for inhibitors that block cell entry and replication by LSR, ACE2, or LSR and ACE2.

53. The method of claim 52, wherein the putative inhibitor is a small molecule inhibitor.

54. The method of claim 52, wherein the putative inhibitor is an antibody.

55. The method of claim 54, wherein the antibody is directed against one or more of LBD1, LBD2, or ABD.

56. The method of claim 52, wherein the putative inhibitor is a lactoferrin derivative.

57. The method of claim 56, further comprising selecting a lactoferrin derivative having improved ACE2 and LSR neutralizing activity.

58. Use of an inhibitor according to any one of claims 52 to 57, to treat a subject experiencing severe COVID-19.

59. The method of any one of claims 38 to 48 further comprising in step (2) adding an inhibitor of cellular entry via either LSR or ACE2, to determine the receptor for cellular entry or replication of a coronavirus.

60. The method of claim 59, wherein the coronavirus is a coronavirus variant.

61. The method of claim 59 or 60, wherein the inhibitor of cellular entry is a recombinant LBD1 or LBD2.

62. The method of claim 61, wherein the recombinant LBD1 or LBD2 blocks late entry, and the receptor for cellular entry is LSR.

63. The method of claim 59 or 60, wherein the inhibitor of cellular entry is a recombinant ABD.

64. The method of claim 63, wherein the recombinant ABD blocks early entry, and the receptor for cellular entry is ACE2.

65. The method of claim 59 or 60, wherein the inhibitor of cellular entry is a recombinant trimeric spike polypeptide.

66. The method of claim 65, wherein the recombinant trimeric spike polypeptide comprises one or more mutations relative to a wild type trimeric spike polypeptide.

67. The method of any one of claims 59 to 66, wherein the method is used to characterize coronavirus variants.

68. The method of any one of claims 59 to 67, wherein the coronavirus is SARS-CoV-2.

69. The method of claim 68, wherein the SARS-CoV-2 is a SARS-CoV-2 variant selected from the group consisting of an alpha, beta, gamma, delta, epsilon, omicron, or other variant.

70. The method of claim 68, wherein the SARS-CoV-2 is a SARS-CoV-2 variant having a gain of function mutation.

71. The method of claim 70, wherein the gain of function mutation is selected from substitution mutation D80A of SEQ ID NO: 1 and the receptor for cellular entry is LSR.

72. The method of claim 68, wherein the SARS-CoV-2 is a SARS-CoV-2 variant has a loss of function mutation.

73. The method of claim 72, wherein the loss of function mutation is H655Y of SEQ ID NO:1 and the receptor for cellular entry is ACE2.

74. The method of claim 72, wherein the loss of function mutation is selected from substitution mutations L452R and T478K of SEQ ID NO: 1 and the receptor for cellular entry is LSR.

75. A method for evaluating the neutralizing capacity of patient antibodies directed against SARS-CoV-2, the method comprising:
removing free fatty acids from the patient serum prior to testing, and
evaluating the level of immune protection against COVID-19 disease.

76. The method of claim 75, wherein the method is used to evaluate the effectiveness of a vaccine.

77. The method of claim 75 or claim 76, wherein the evaluating includes evaluating multiple measurements that are taken over time.

78. The method of claim 75, wherein the neutralizing capacity after removal of free fatty acids is compared to the neutralizing capacity before removal of free fatty acids.

79. The method of claim 78, wherein a difference in is observed in the neutralizing capacity after removal of free fatty acids compared to the neutralizing capacity before removal of free fatty acids, wherein the neutralizing capacity after removal of free fatty acids is greater than the neutralizing capacity before removal of free fatty acids.

80. The method of claim 79, further comprising administering to the patient an inhibitor of lipolysis stimulated receptor (LSR).

81. The method of claim 80, wherein the LSR inhibitor is an LSR specific antibody or an siRNA molecule that targets LSR.

82. An siRNA molecule that targets a lipolysis stimulated receptor (LSR).

83. A pharmaceutical composition comprising one or more siRNA molecule of claim 82, and a pharmaceutically acceptable carrier.

84. The pharmaceutical composition of claim 83, wherein the siRNA molecule targets LSRβ.

85. The pharmaceutical composition of claim 83 or 84, wherein the pharmaceutical composition comprises at least two different siRNA molecules that target the LSR,
wherein a first siRNA targets LSRα and a second siRNA targets LSRβ.

86. The pharmaceutical composition of any one of claims 83 to 85, further comprising at least one other therapeutic agent.

87. The pharmaceutical composition of claim 86, wherein the at least one therapeutic other agent is selected from suramin and lactoferrin.

88. A method of treating a subject suffering from a SARS-CoV-2 infection, the method comprising: administering to the subject a pharmaceutically effective amount of the pharmaceutical composition of any one of claims 83 to 87.

89. The method of claim 88, wherein treating the subject with the effective amount of the pharmaceutical composition results in one or more of:
an acceleration in intestinal clearance of SARS-CoV-2,
a reduction of transmission of SARS CoV-2,
an alleviation of one or more symptoms of long COVID-19 syndrome, or
a combination thereof.

90. A method of treating a subject suffering from a SARS-CoV-2 infection, the method comprising: reducing or temporarily suppressing the physiological supply of free fatty acids to the subject.

91. The method of claim 90, wherein the method comprises:
administering to the subject a composition suitable for treatment of diabetes or hyperlipidemia.

92. The method of claim 91, wherein the composition is suitable for treatment of diabetes.

93. The method of claim 92, wherein the composition comprises Metformin.

94. The method of claim 91, wherein the composition is suitable for treatment of hyperlipidemia.

95. The method of claim 94, wherein the composition comprises Acipimox.

96. The method of any one of claims 90 to 95, further comprising administering a therapeutic agent to treat the SARS-CoV-2 infection.

97. The method of claim 96, wherein the therapeutic agent is selected from remdesivir, ritonavir, nirmatrelvir, tocilizumab, sotrovimab, propofol-lipuro 1%, bamlanivimab, etesevimab, casirivimab, imdevimab, adalimumab, baricitinib, COVID-19 convalescent plasma, regiocit replacement, freesenius kabi propoven, and combinations thereof.

98. A polypeptide, comprising: a lipolysis-stimulated receptor binding domain (LBD) of a SARS-CoV-2 spike protein.

99. The polypeptide of claim 98, wherein the LBD is LBD1.

100. The polypeptide of claim 98 or 99, comprising an amino acid sequence having at least 90% sequence identity to amino acid 25 to amino acid 85 of SEQ ID NO: 1.

101. The polypeptide of claim 98, wherein the LBD is LBD2.

102. The polypeptide of claim 98, comprising an amino acid sequence having at least 90% sequence identity to amino acid 607 to amino acid 691 of SEQ ID NO: 1.

103. The polypeptide of any one of claims 98 to 102, comprising LBD1 and LBD2.

104. The polypeptide of any one of claims 98 to 103, comprising an ACE2 binding domain (ABD).

105. The polypeptide of any one of claims 98 to 104, comprising an amino acid sequence having at least 90% sequence identity to amino acid 25 to amino acid 691 of SEQ ID NO: 1.

106. The polypeptide of any one of claims 98 to 105, coupled to one or more Transcription Infidelity (TI) segment.

107. The polypeptide of claim 106, wherein the coupling is terminal.

108. The polypeptide of claim 106 or 107, wherein the polypeptide is A, an antigen part, and the TI segment is P, having the structure A-P, P-A, or A1-P-A2, where A1 and A2 are two parts of A.

109. A method for immunizing a subject against COVID-19 disease resulting from a SARS-CoV-2 infection, the method comprising: administering to a subject with the polypeptide of any one of claims 98 to 108.

110. The method of claim 109, wherein the method reduces the severity of COVID-19 disease.

111. The method of claim 109 or 110, wherein the method reduces transmission of SARS-CoV-2.

112. An immunogenic composition for inhibiting SARS-CoV-2 replication comprising the polypeptide of any one of claims 98 to 108.

113. The immunogenic composition of claim 112, further comprising at least one adjuvant.

114. A method for immunizing a subject against COVID-19 disease resulting from a SARS-CoV-2 infection, the method comprising: administering to a subject with the immunogenic composition of any one of claims 112 to 113.

115. The method of claim 114, wherein the method reduces the severity of COVID-19 disease.

116. The method of claim 114 or 115, wherein the method reduces transmission of SARS-CoV-2.

5

FIGURES

FIG. 1A

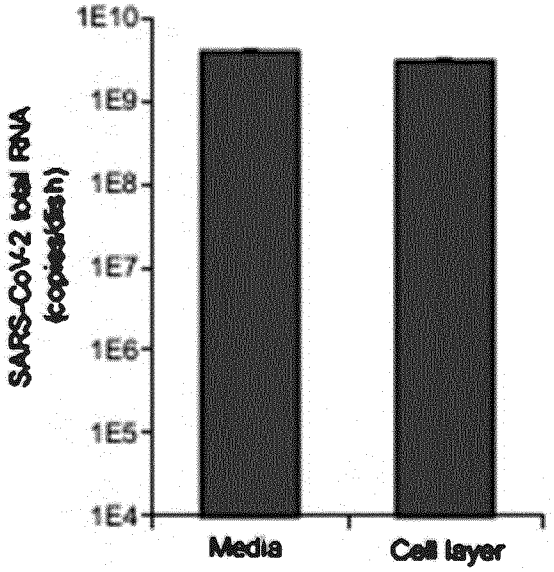

FIG. 1B

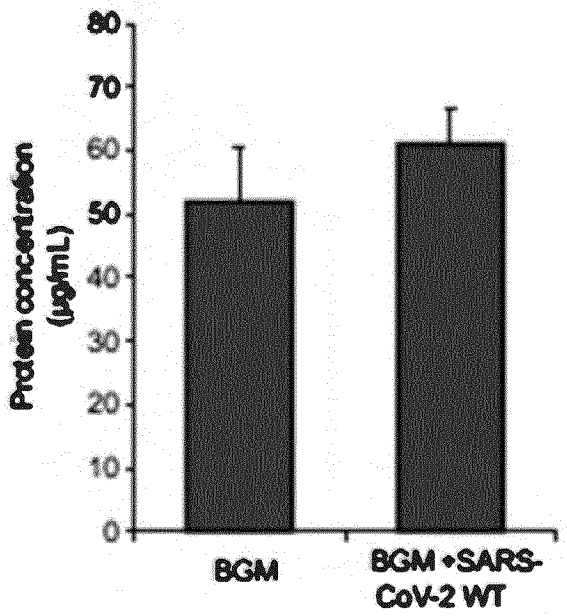

FIG. 1C

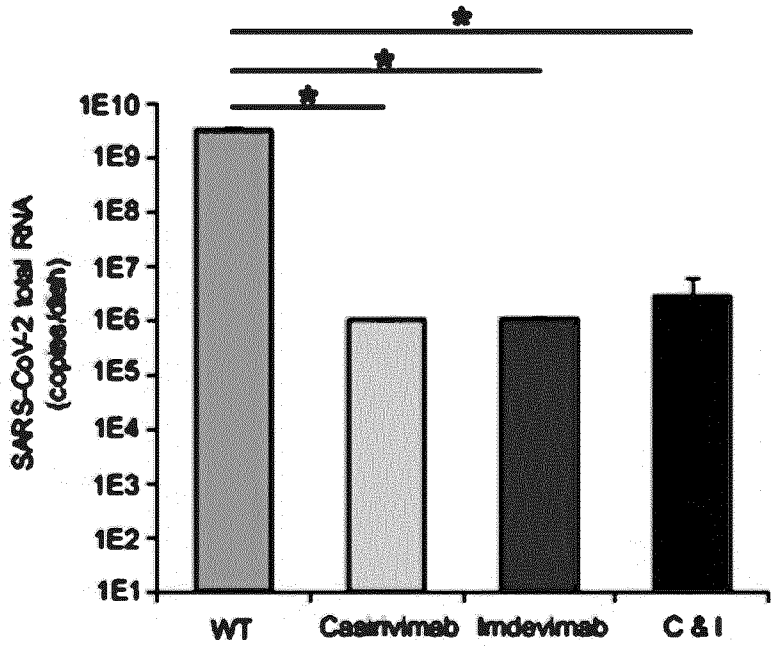
*
*
*
1E10
1E9
1E8
1E7
1E6
1E5
1E4
1E3
1E2
1E1
SARS-CoV-2 total RNA (copies/dish)
WT
Casirivimab
Imdevimab
C & I

FIG. 1D

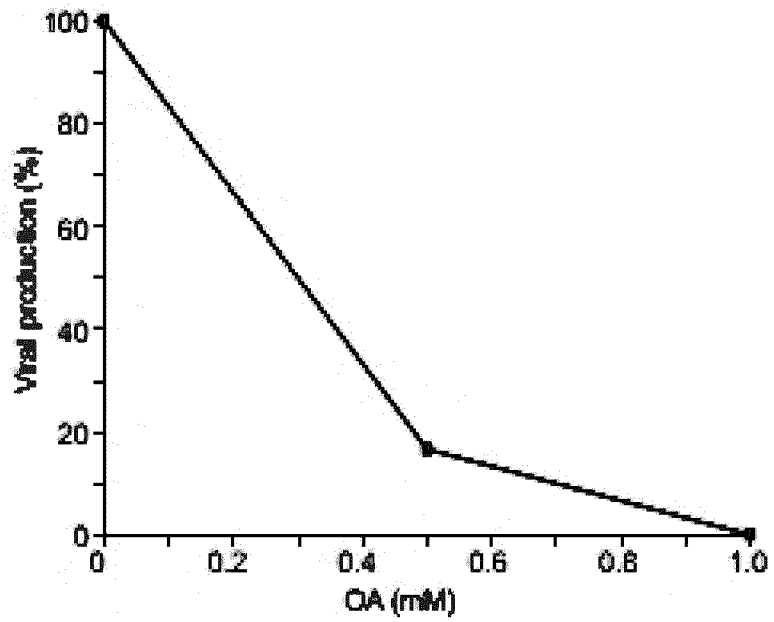
100
80
60
40
20
0
Viral production (%)
0
0.2
0.4
0.6
0.8
1.0
CA (mM)

FIG. 1E

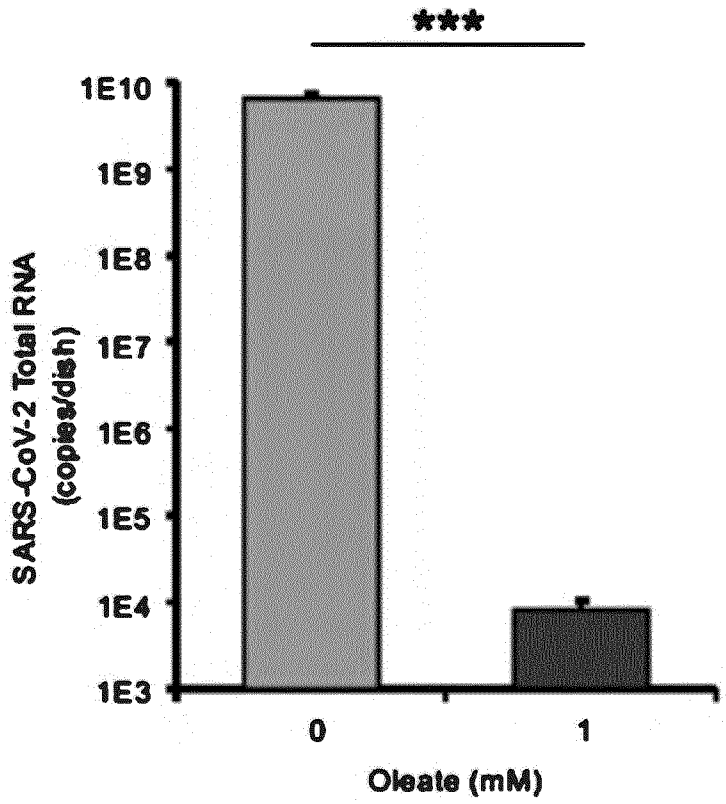
***
1E10
1E9
1E8
1E7
1E6
1E5
1E4
1E3
SARS-CoV-2 Total RNA (copies/dish)
0
1
Oleate (mM)

FIG. 1F

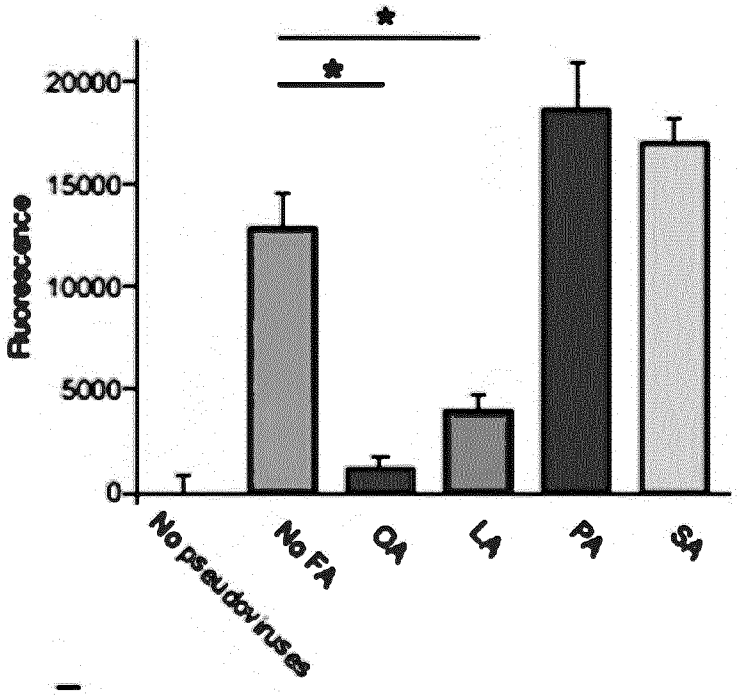
*
*
20000
15000
10000
5000
0
Fluorescence
No pseudoviruses
No FA
OA
LA
PA
SA

FIG. 1G

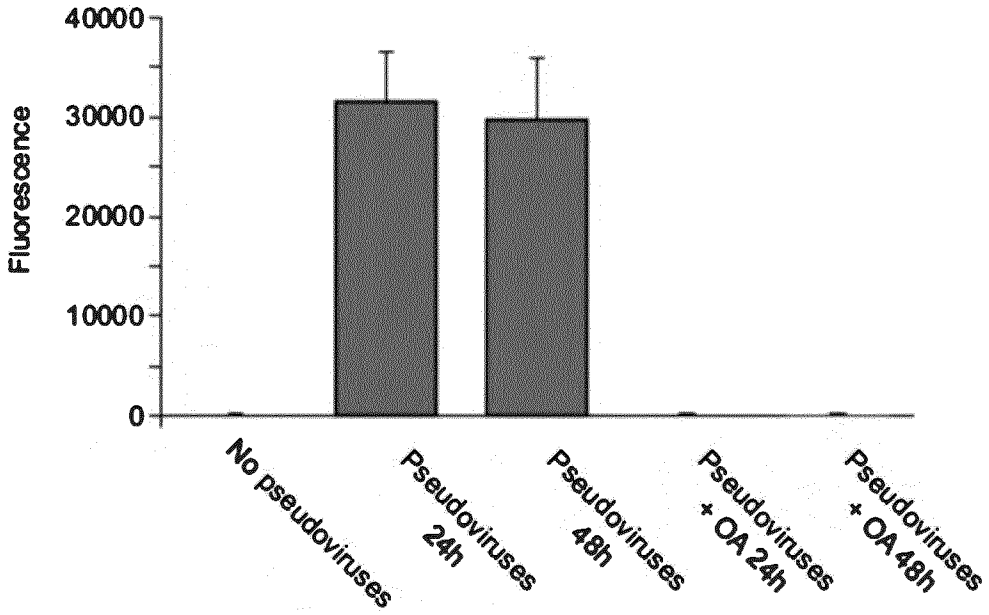
40000
30000
20000
10000
0
Fluorescence
No pseudoviruses
Pseudoviruses 24h
Pseudoviruses 48h
Pseudoviruses + OA 24h
Pseudoviruses + OA 48h

FIG. 1H

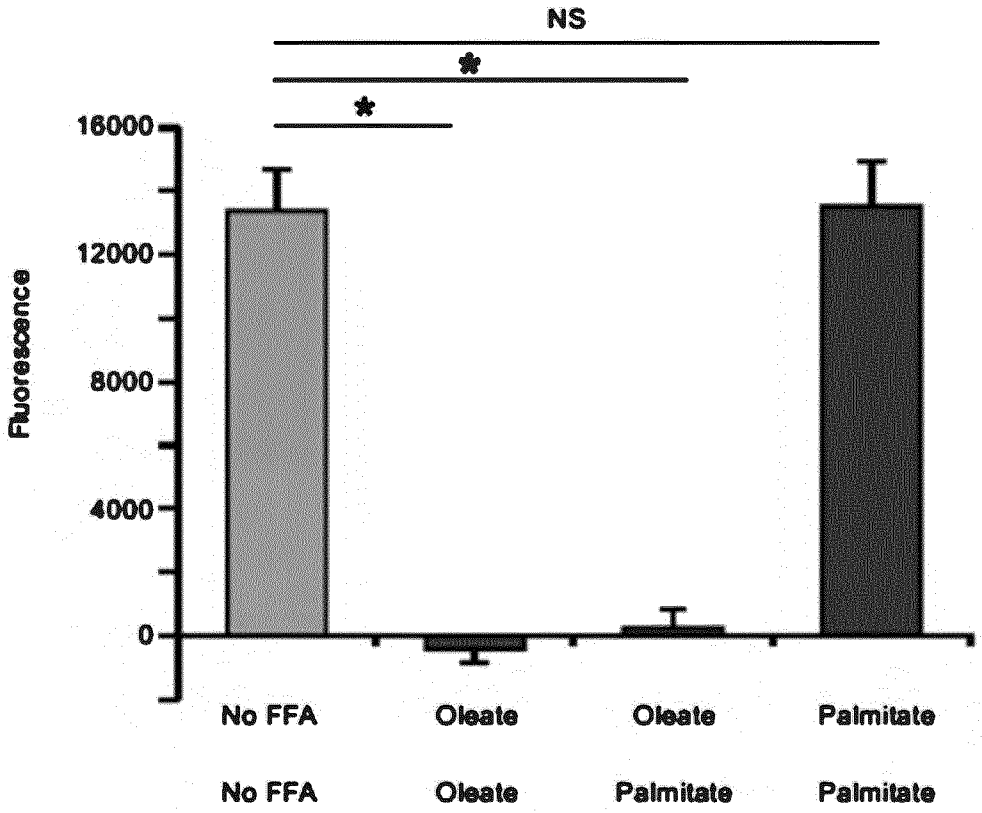
NS
*
*
16000
12000
8000
4000
0
Fluorescence
No FFA
Oleate
Oleate
Palmitate
No FFA
Oleate
Palmitate
Palmitate

FIG. 1I

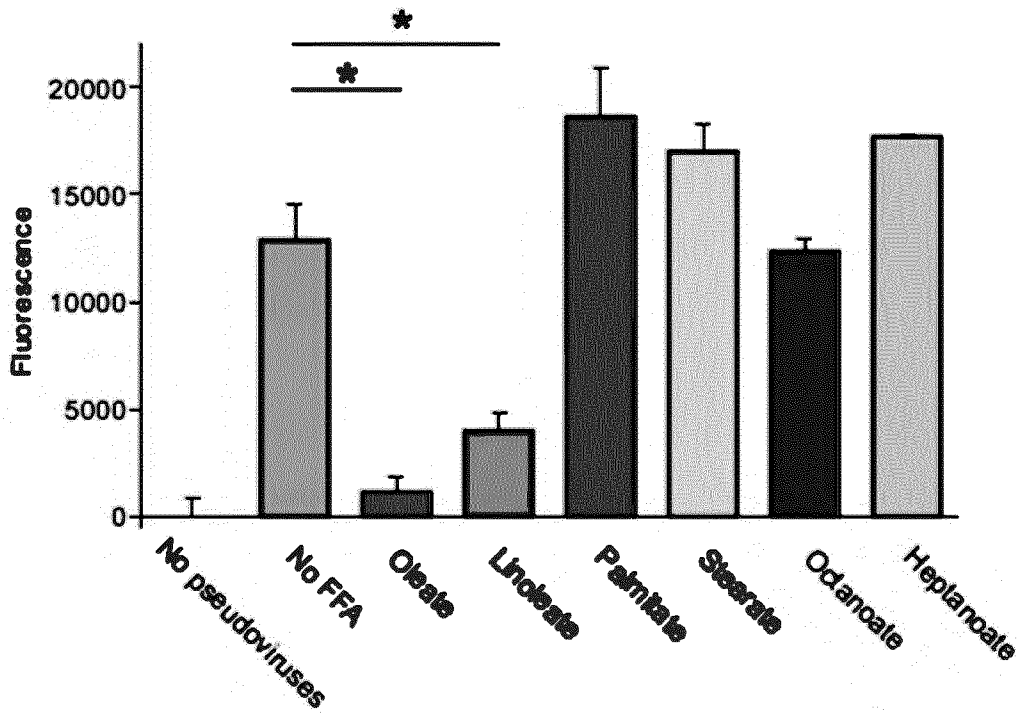
*
*
20000
15000
10000
5000
0
Fluorescence
No pseudoviruses
No FFA
Oleate
Linoleate
Palmitate
Stearate
Octanoate
Heptanoate

FIG. 1J

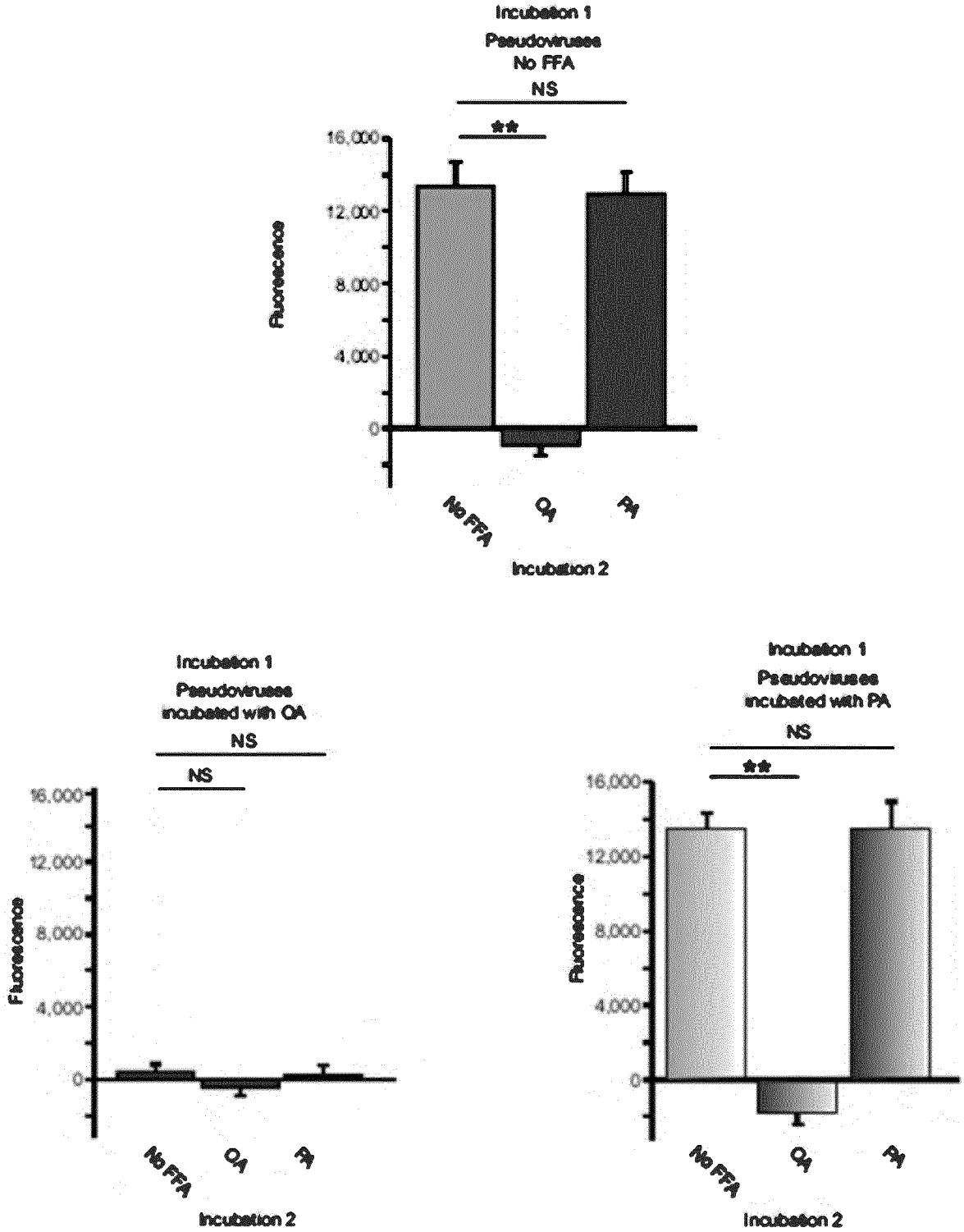
Incubation 1
Pseudoviruses
No FFA
NS
**
16,000
12,000
8,000
4,000
0
Fluorescence
No FFA
OA
PA
Incubation 2
Incubation 1
Pseudoviruses
incubated with OA
NS
NS
16,000
12,000
8,000
4,000
0
Fluorescence
No FFA
OA
PA
Incubation 2
Incubation 1
Pseudoviruses
incubated with PA
NS
**
16,000
12,000
8,000
4,000
0
Fluorescence
No FFA
OA
PA
Incubation 2

FIG. 1K

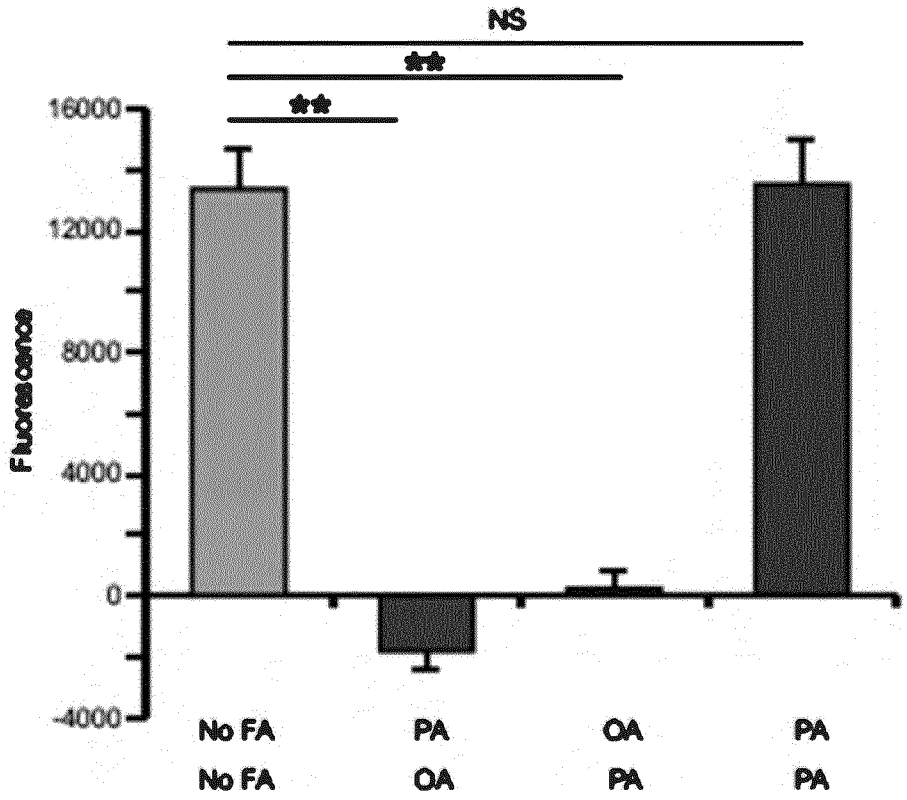
NS
**
**
16000
12000
8000
4000
0
-4000
Fluorescence
No FA
No FA
PA
OA
OA
PA
PA
PA

FIG. 1L

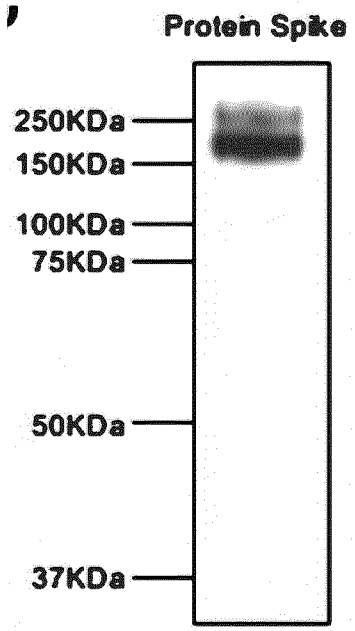
Protein Spike
250KDa
150KDa
100KDa
75KDa
50KDa
37KDa

FIG. 1M

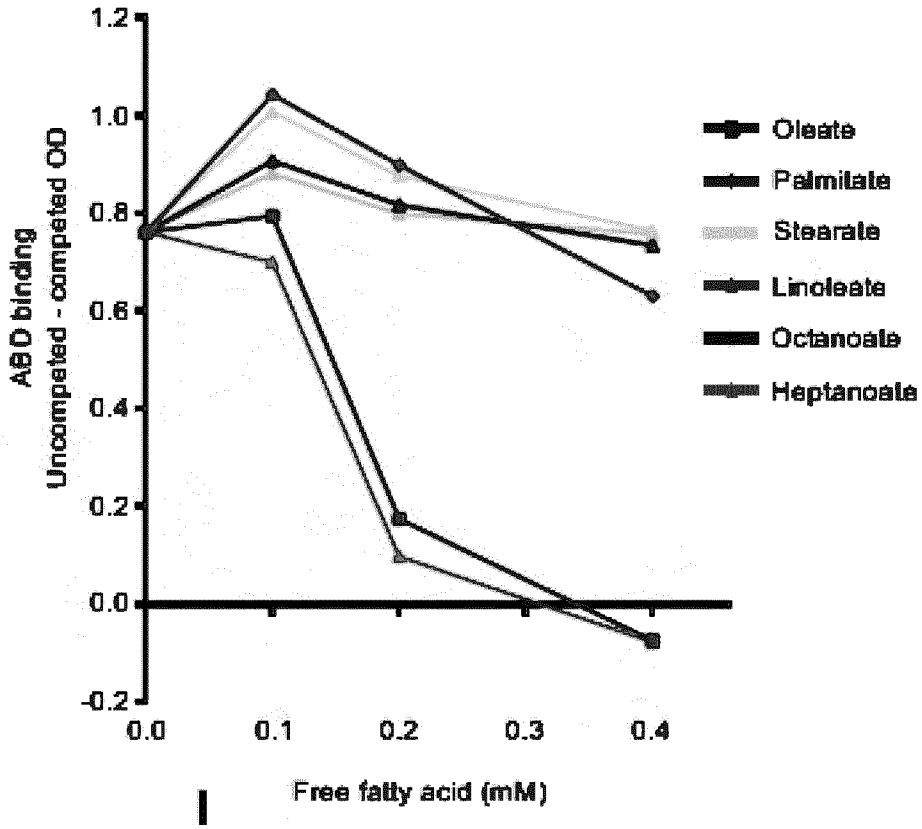
ABD binding
Uncompeted - competed OD
1.2
1.0
0.8
0.6
0.4
0.2
0.0
-0.2
0.0
0.1
0.2
0.3
0.4
Free fatty acid (mM)
Oleate
Palmitate
Stearate
Linoleate
Octanoate
Heptanoate

FIG. 1N

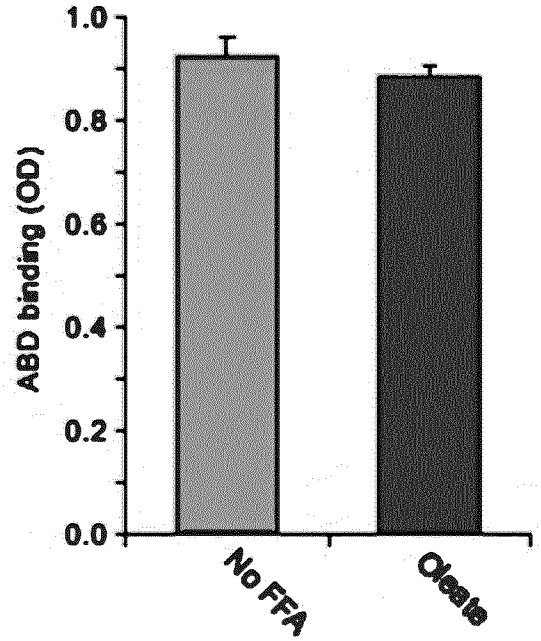
ABD binding (OD)
1.0
0.8
0.6
0.4
0.2
0.0
No FFA
Oleate

FIG. 1O

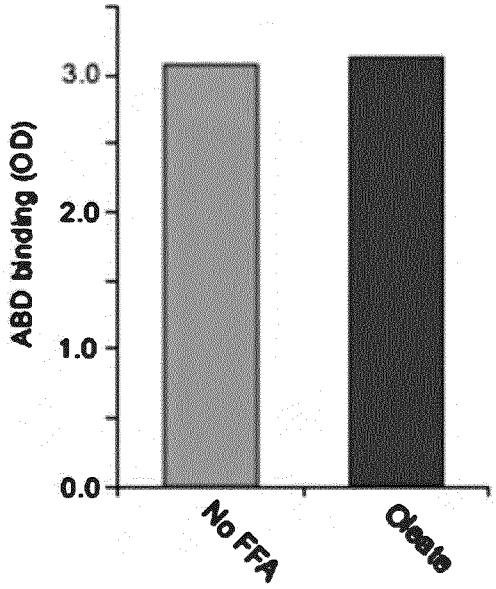
ABD binding (OD)
3.0
2.0
1.0
0.0
No FFA
Oleate

FIG. 1P

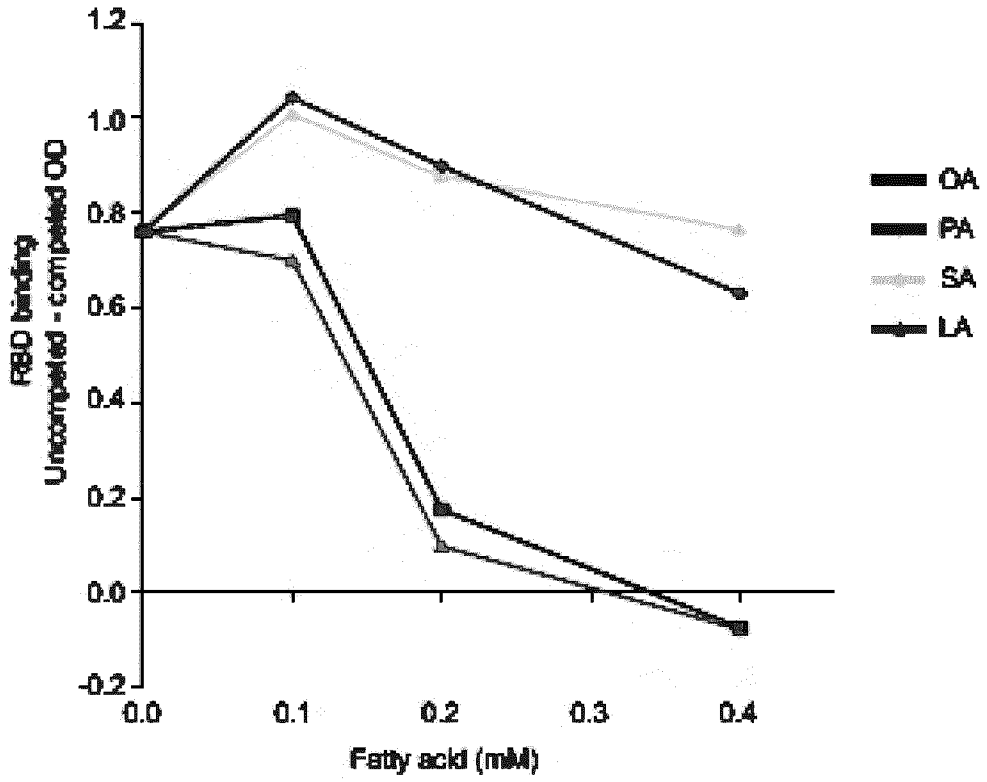
RBD binding
Uncomplexed - complexed OD
1.2
1.0
0.8
0.6
0.4
0.2
0.0
-0.2
0.0
0.1
0.2
0.3
0.4
Fatty acid (mM)
OA
PA
SA
LA

FIG. 1Q

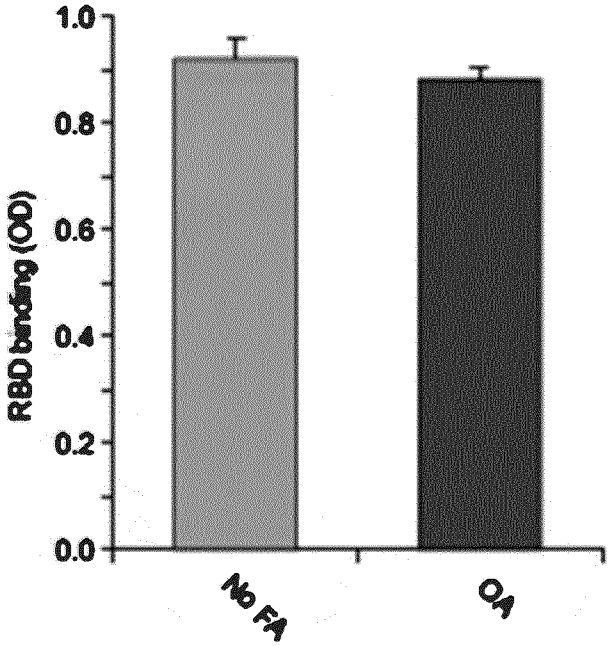

FIG. 1R

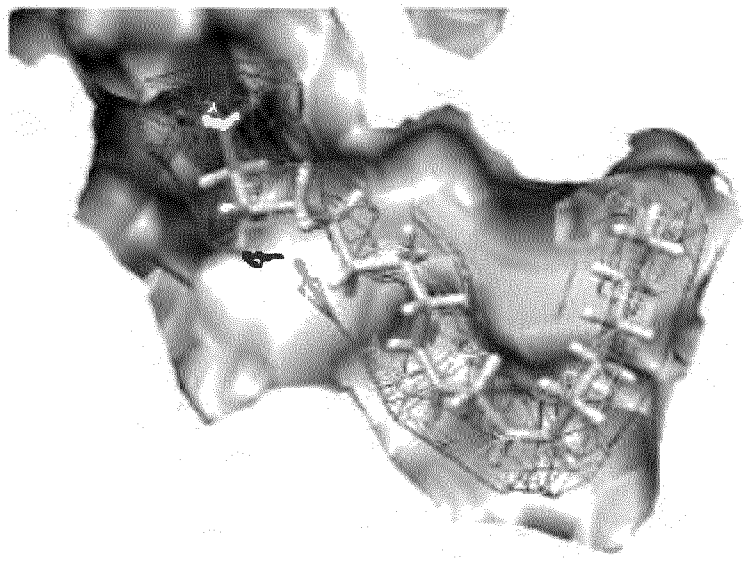

LA (Recalculated from Toelzer et al., 2020)

FIG. 1S

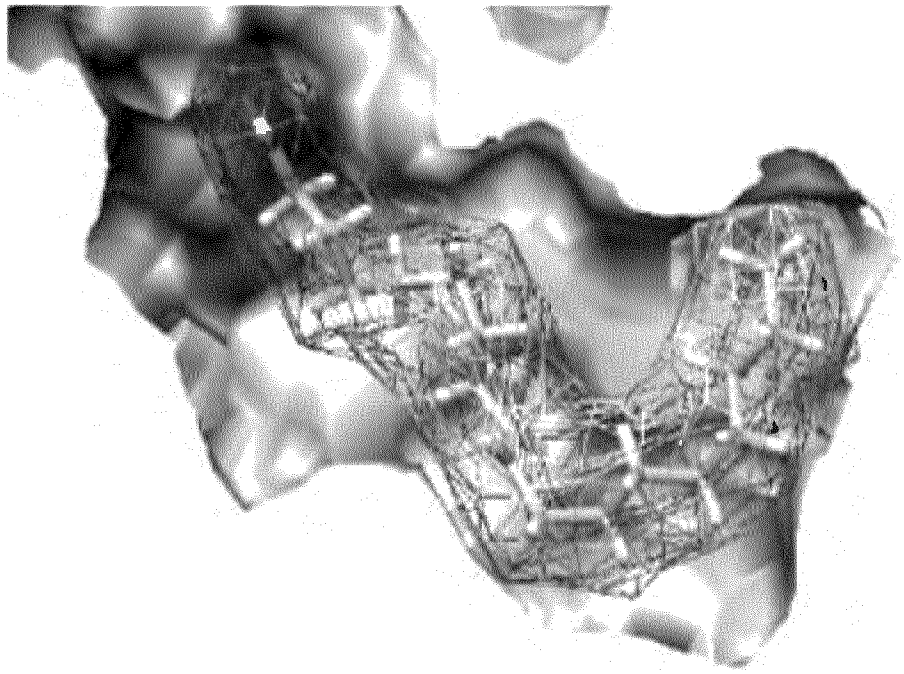
Oleate

FIG. 1T

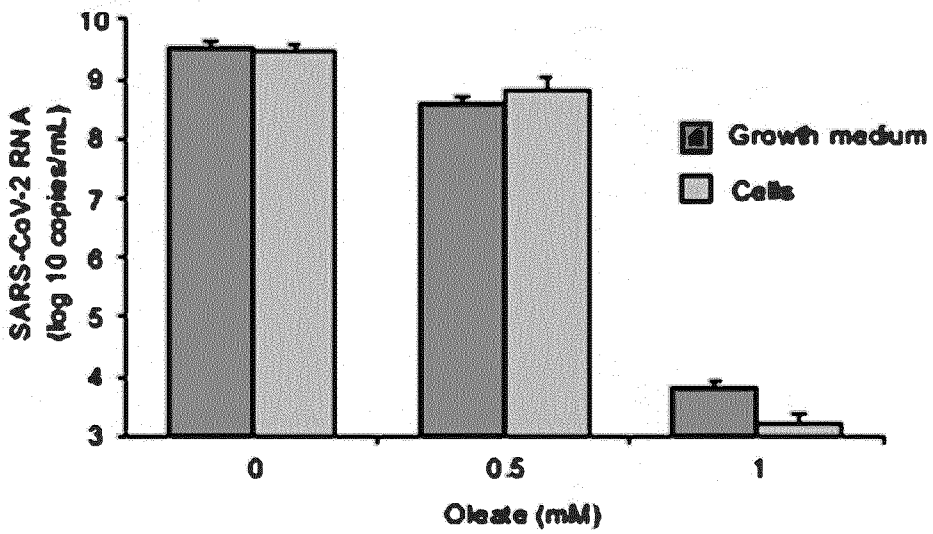
SARS-CoV-2 RNA
(log 10 copies/mL)
10
9
8
7
6
5
4
3
0
0.5
1
Oleate (mM)
Growth medium
Cells

FIG. 1U

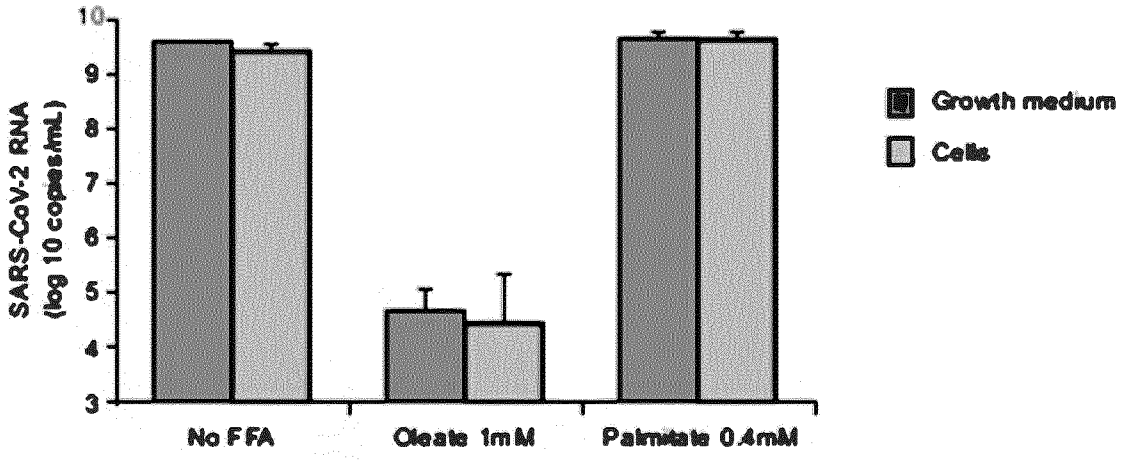
SARS-CoV-2 RNA
(log 10 copies/mL)
10
9
8
7
6
5
4
3
No FFA
Oleate 1mM
Palmitate 0.4mM
Growth medium
Cells

FIG. 1V

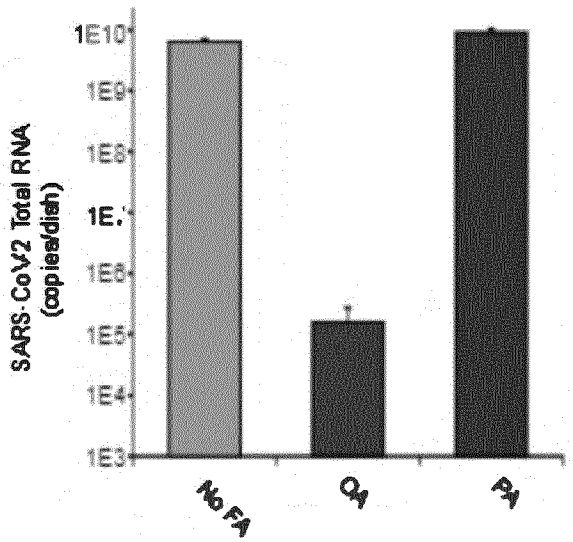
SARS-CoV2 Total RNA
(copies/dish)
1E10
1E9
1E8
1E7
1E6
1E5
1E4
1E3
No FA
Oy
Py

FIG. 1W

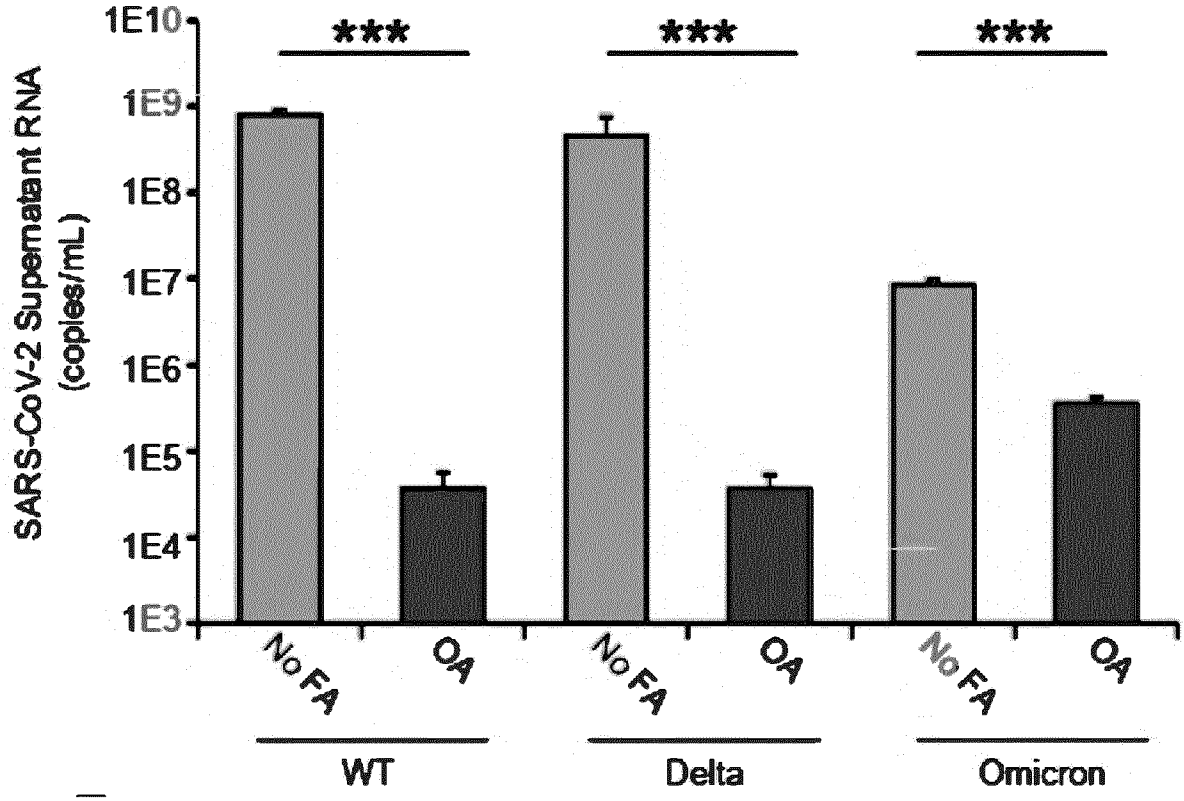
SARS-CoV-2 Supernatant RNA (copies/mL)
1E10
1E9
1E8
1E7
1E6
1E5
1E4
1E3
***
***
***
No FA
OA
No FA
OA
No FA
OA
WT
Delta
Omicron

FIG. 1X

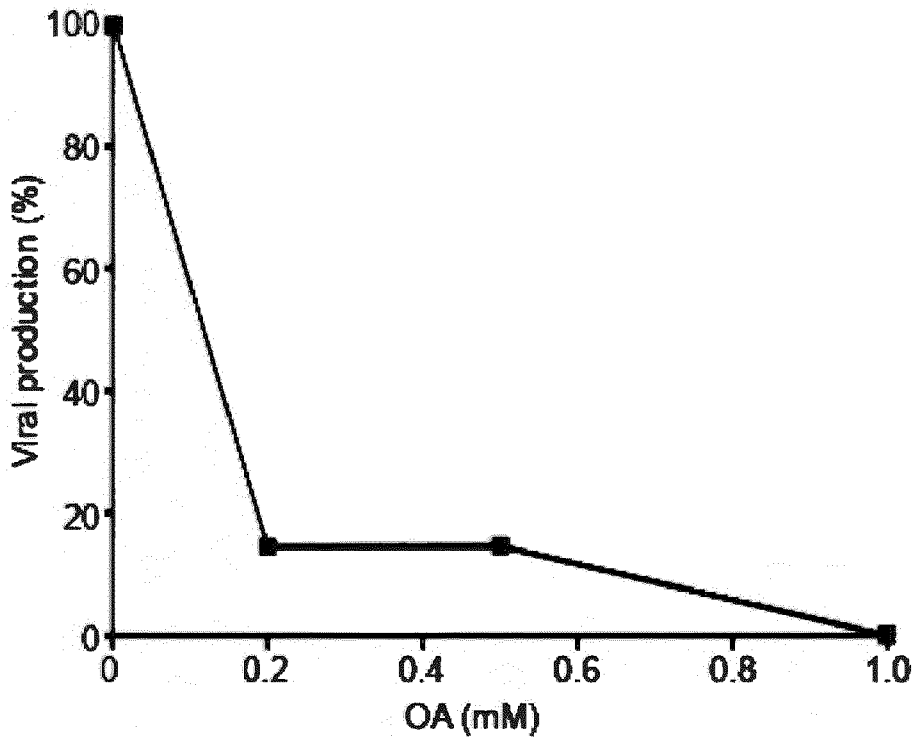
Viral production (%)
100
80
60
40
20
0
0
0.2
0.4
0.6
0.8
1.0
OA (mM)

FIG. 1Y

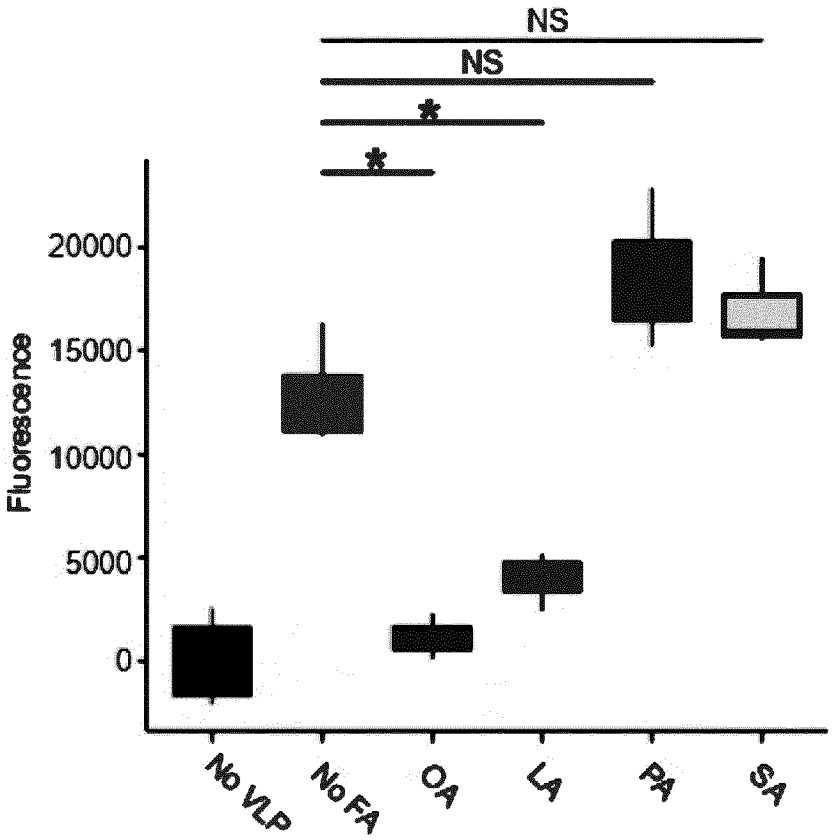
NS
NS
*
*
Fluorescence
20000
15000
10000
5000
0
No VLP
No FA
OA
LA
PA
SA

FIG. 1Z

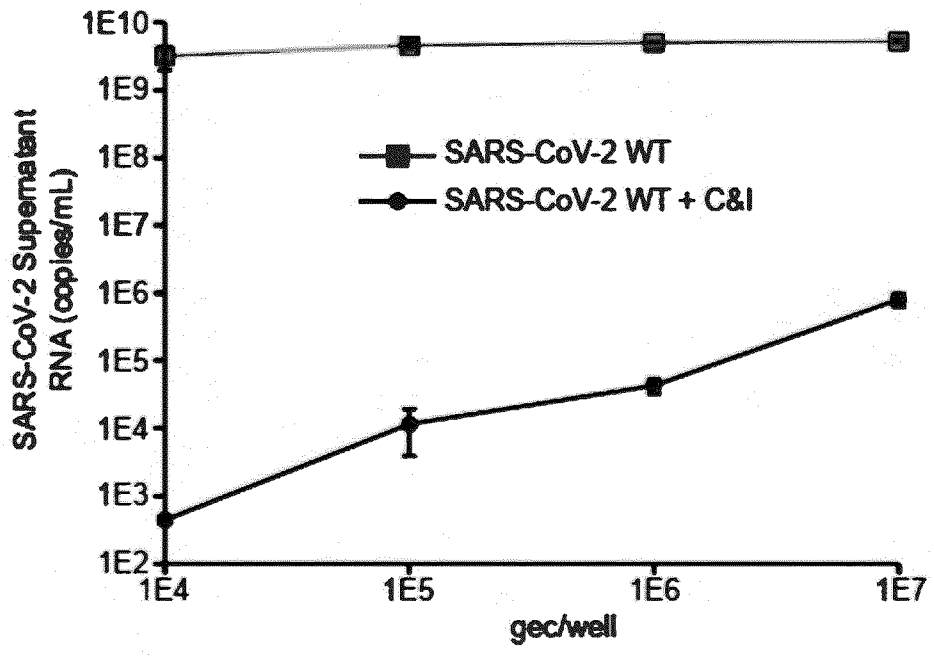
SARS-CoV-2 Supernatant RNA (copies/mL)
1E10
1E9
1E8
1E7
1E6
1E5
1E4
1E3
1E2
SARS-CoV-2 WT
SARS-CoV-2 WT + C&I
1E4
1E5
1E6
1E7
gec/well

FIG. 2A

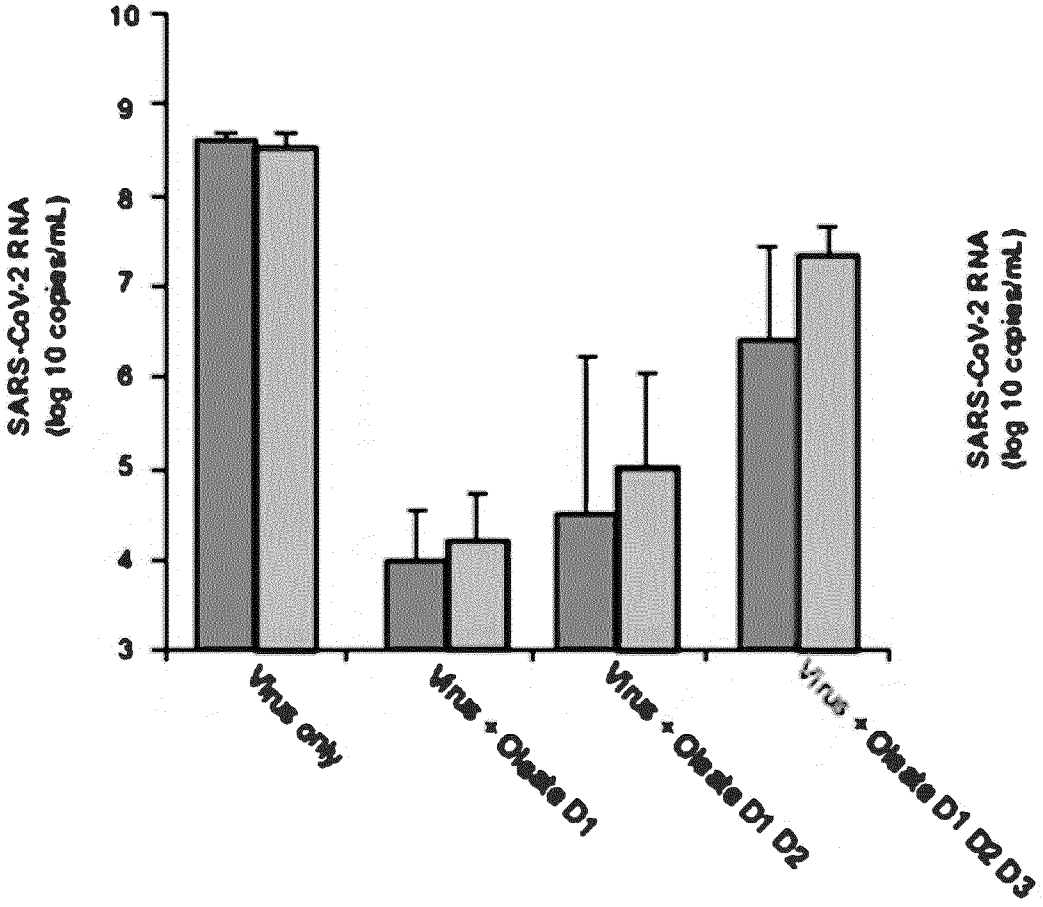
SARS-CoV-2 RNA
(log 10 copies/mL)
10
9
8
7
6
5
4
3
Virus only
Virus + Oleacle D1
Virus + Oleacle D1 D2
Virus + Oleacle D1 D2 D3
SARS-CoV-2 RNA
(log 10 copies/mL)

FIG. 2B

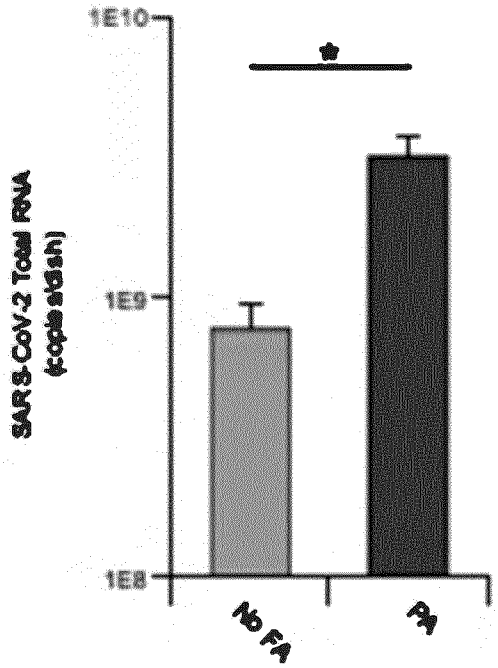
SARS-CoV-2 Total RNA
(copies/ml)
1E10
1E9
1E8
*
No FA
FA

FIG. 2C

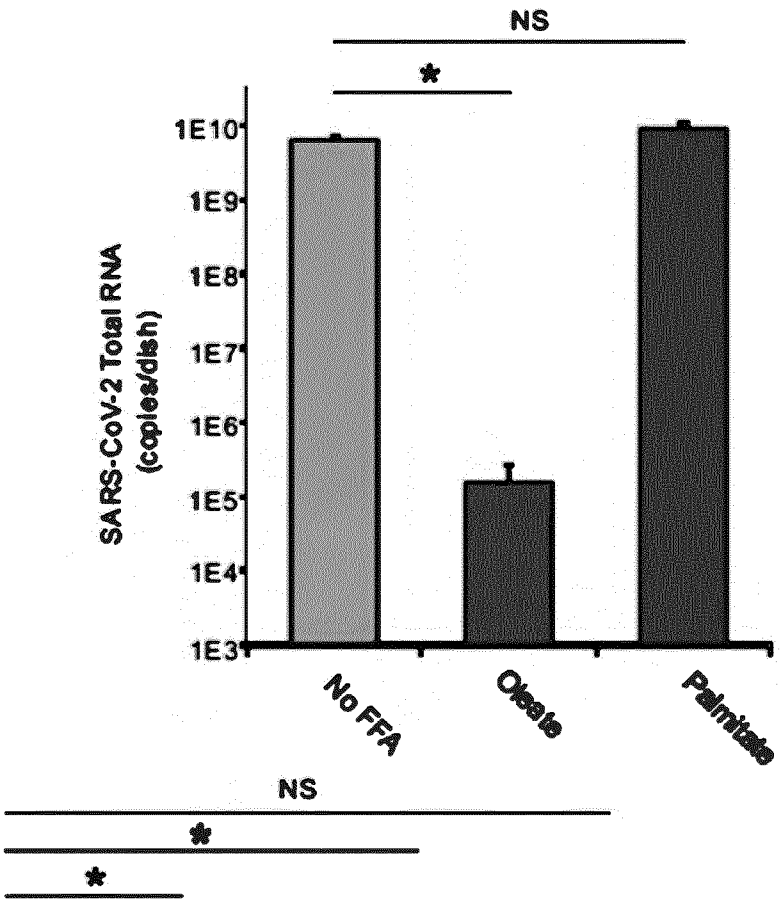
NS
*
1E10
1E9
1E8
1E7
1E6
1E5
1E4
1E3
SARS-CoV-2 Total RNA (copies/dish)
No FFA
Oleate
Palmitate
NS
*
*

FIG. 2D

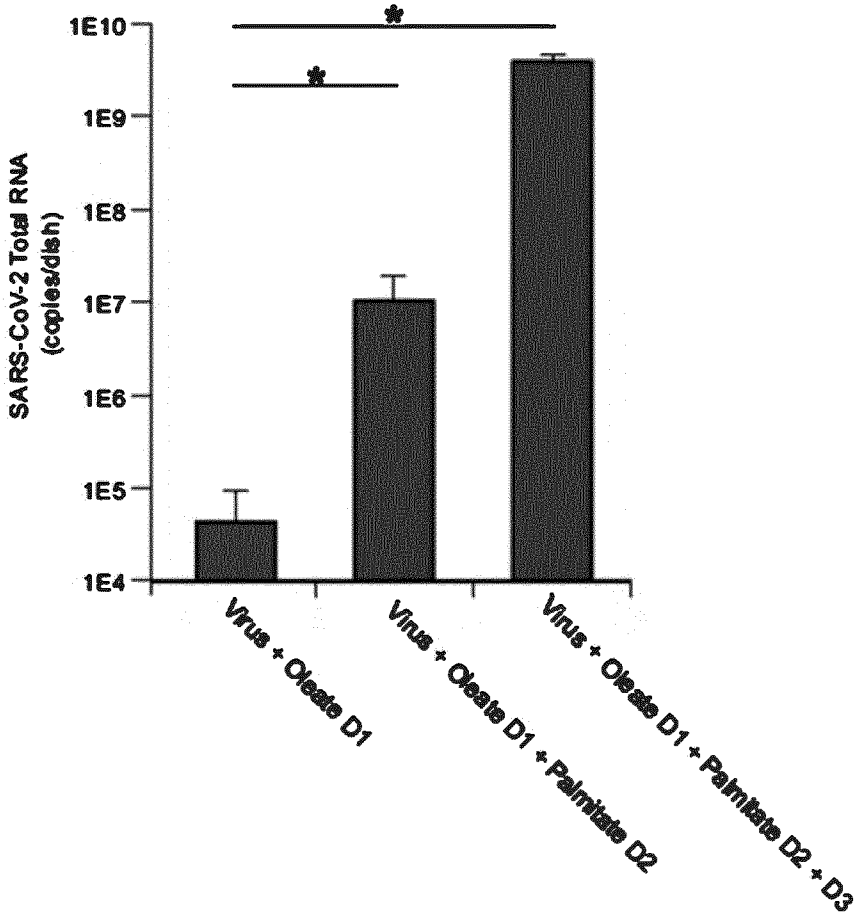
*
*
1E10
1E9
1E8
1E7
1E6
1E5
1E4
SARS-CoV-2 Total RNA (copies/dish)
Virus + Oleate D1
Virus + Oleate D1 + Palmitate D2
Virus + Oleate D1 + Palmitate D2 + D3

FIG. 2E

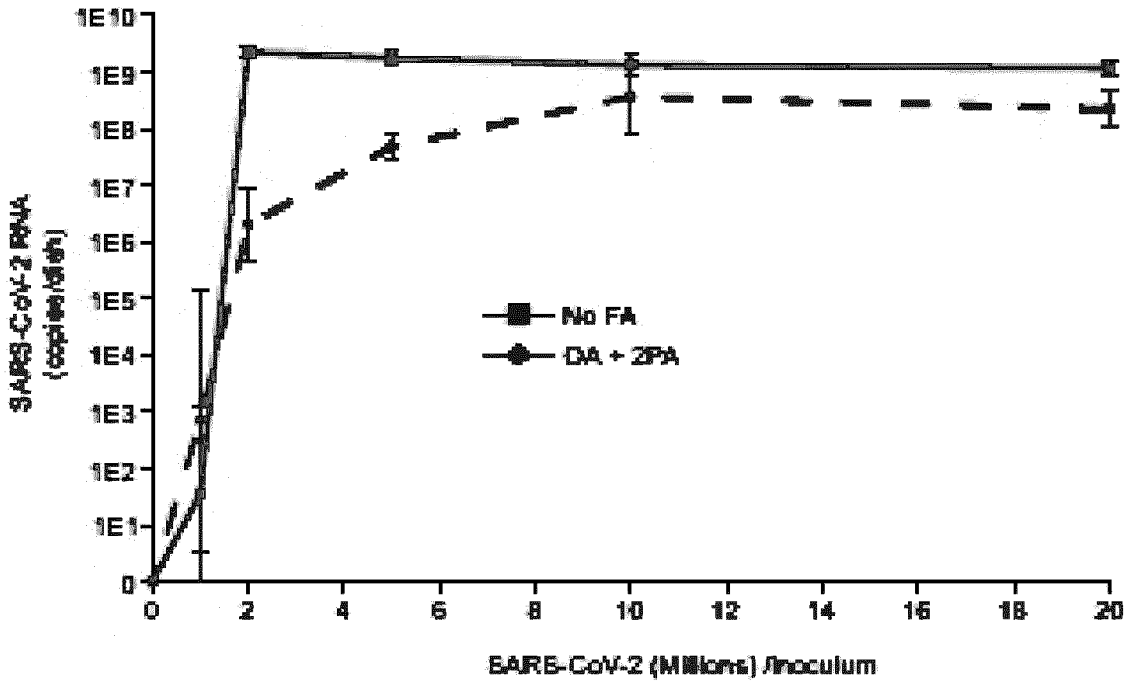
1E10
1E9
1E8
1E7
1E6
1E5
1E4
1E3
1E2
1E1
0
SARS-CoV-2 RNA (copies/dish)
No FA
OA + 2PA
0
2
4
6
8
10
12
14
16
18
20
SARS-CoV-2 (Millions) Inoculum

FIG. 2F

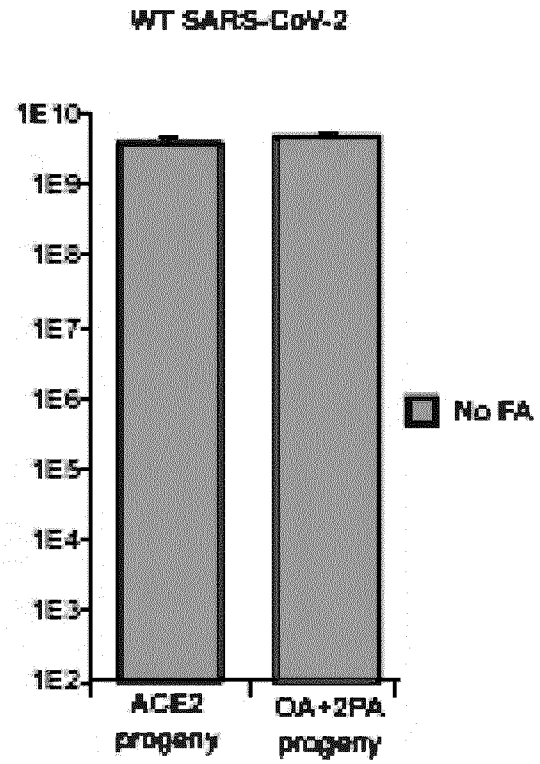
WT SARS-CoV-2
1E10
1E9
1E8
1E7
1E6
1E5
1E4
1E3
1E2
No FA
ACE2 progeny
OA+2PA progeny

FIG. 2G

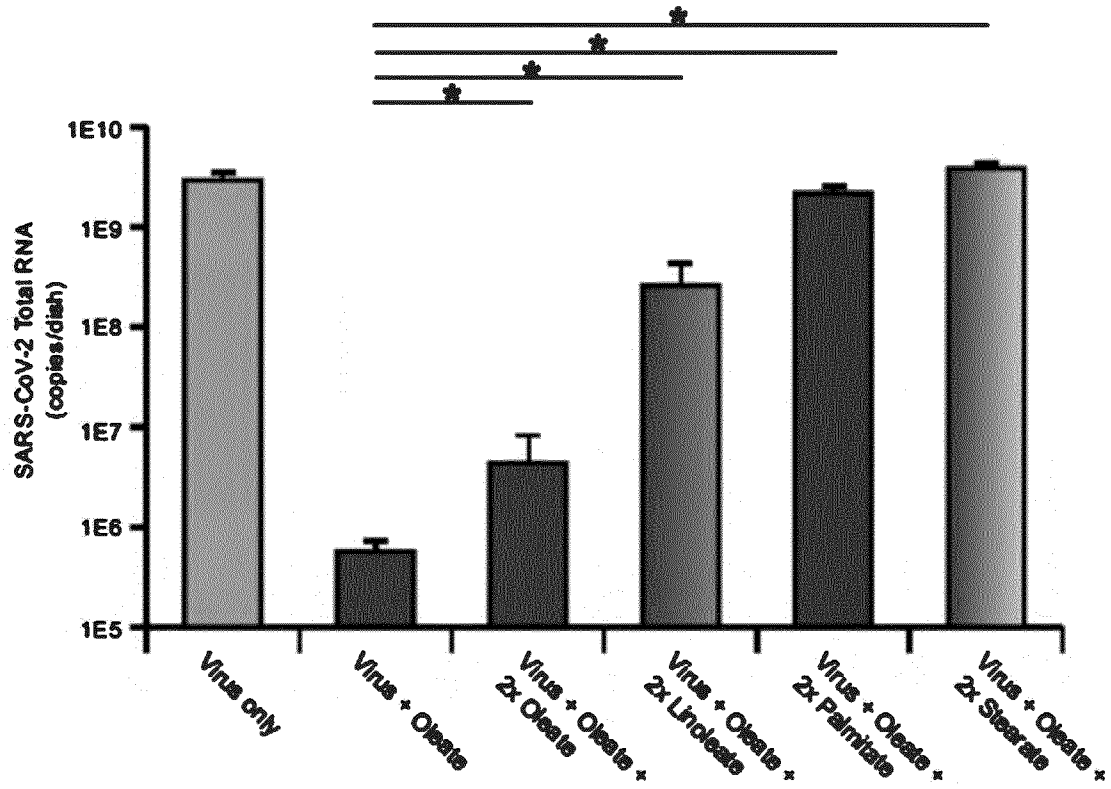
SARS-CoV-2 Total RNA (copies/dish)
1E10
1E9
1E8
1E7
1E6
1E5
Virus only
Virus + Oleate
Virus + Oleate + 2x Oleate
Virus + Oleate + 2x Linoleate
Virus + Oleate + 2x Palmitate
Virus + Oleate + 2x Stearate

FIG. 2H

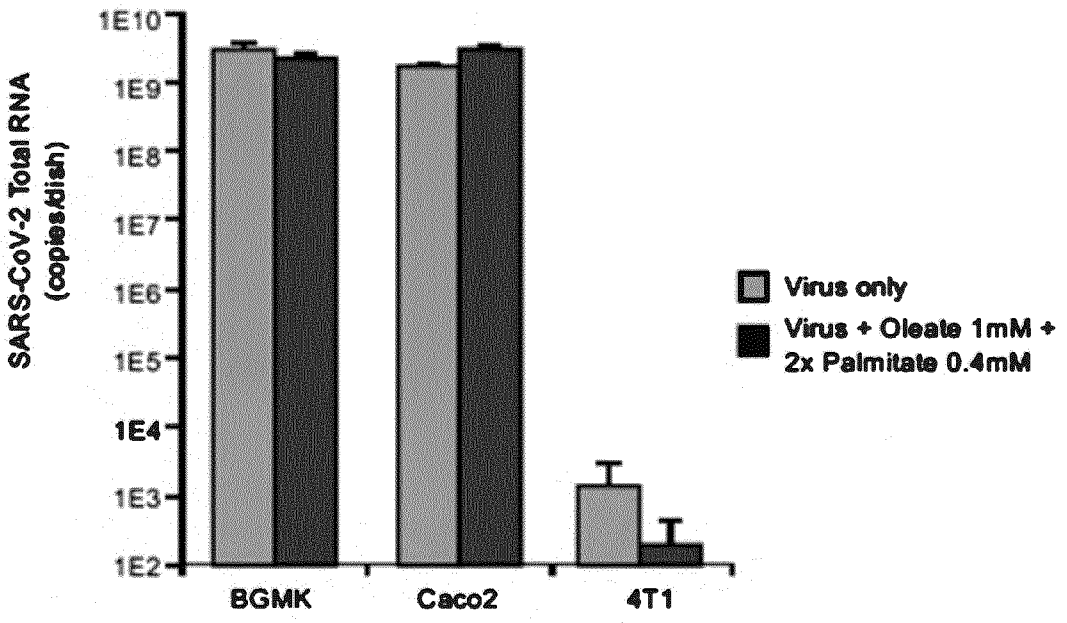
SARS-CoV-2 Total RNA (copies/dish)
1E10
1E9
1E8
1E7
1E6
1E5
1E4
1E3
1E2
BGMK
Caco2
4T1
Virus only
Virus + Oleate 1mM + 2x Palmitate 0.4mM

FIG. 2I

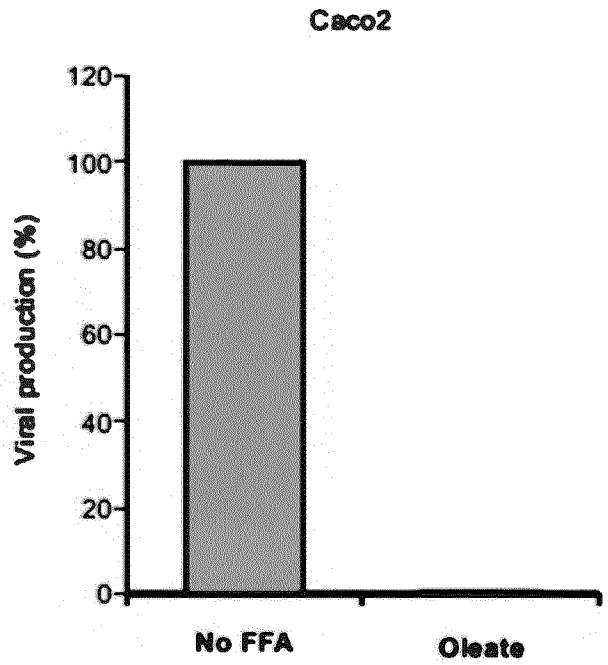
Caco2
Viral production (%)
120
100
80
60
40
20
0
No FFA
Oleate

FIG. 2J

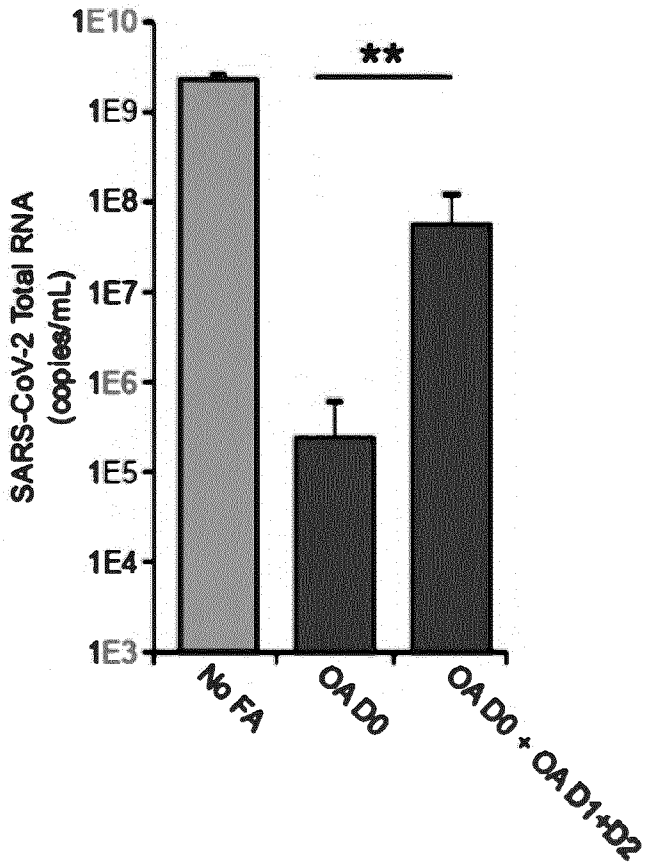
SARS-CoV-2 Total RNA (copies/mL)
1E10
1E9
1E8
1E7
1E6
1E5
1E4
1E3
**
No FA
OA D0
OA D0 + OA D1+D2

FIG. 2K

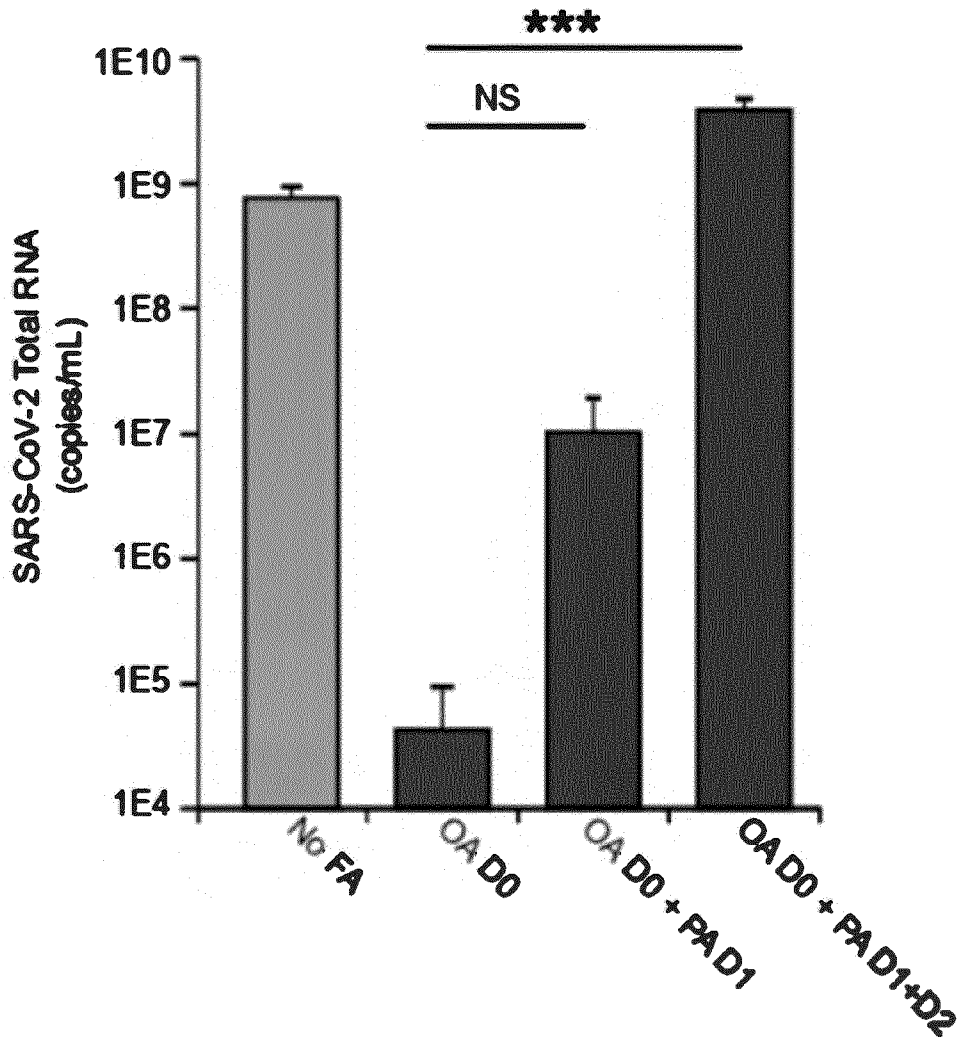
***
NS
1E10
1E9
1E8
1E7
1E6
1E5
1E4
SARS-CoV-2 Total RNA (copies/mL)
No FA
OA D0
OA D0 + PA D1
OA D0 + PA D1+D2

FIG. 2L

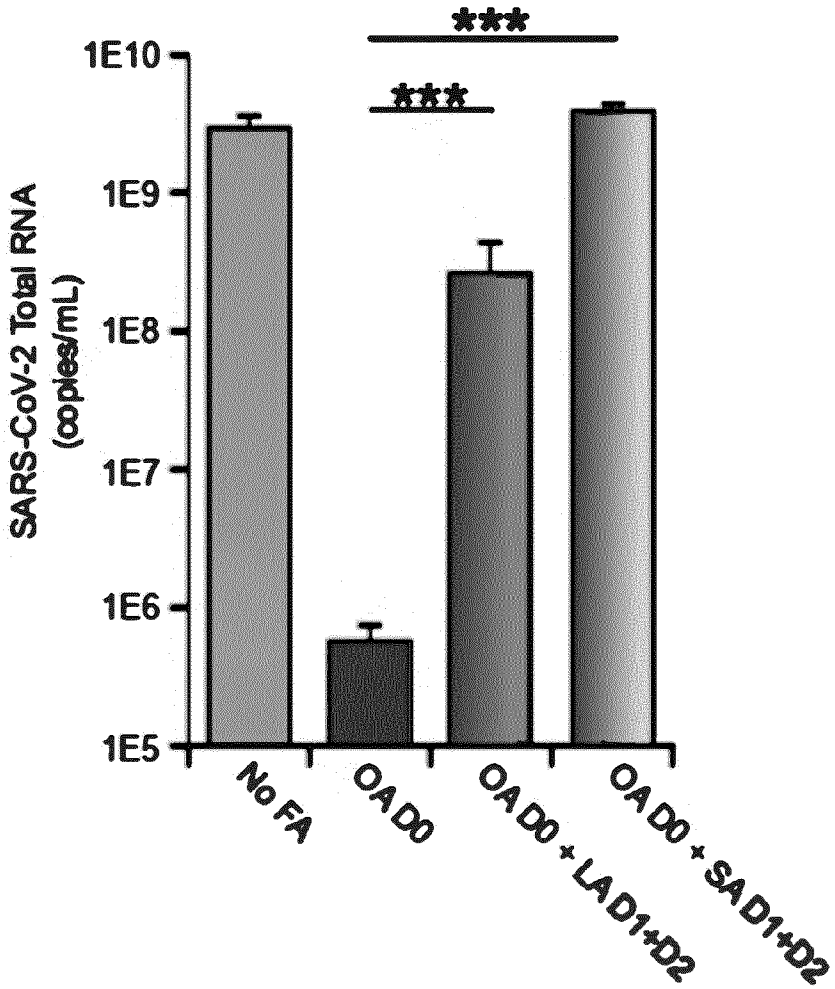
***
***
1E10
1E9
1E8
1E7
1E6
1E5
SARS-CoV-2 Total RNA (copies/mL)
No FA
OA D0
OA D0 + LA D1+D2
OA D0 + SA D1+D2

FIG. 3A

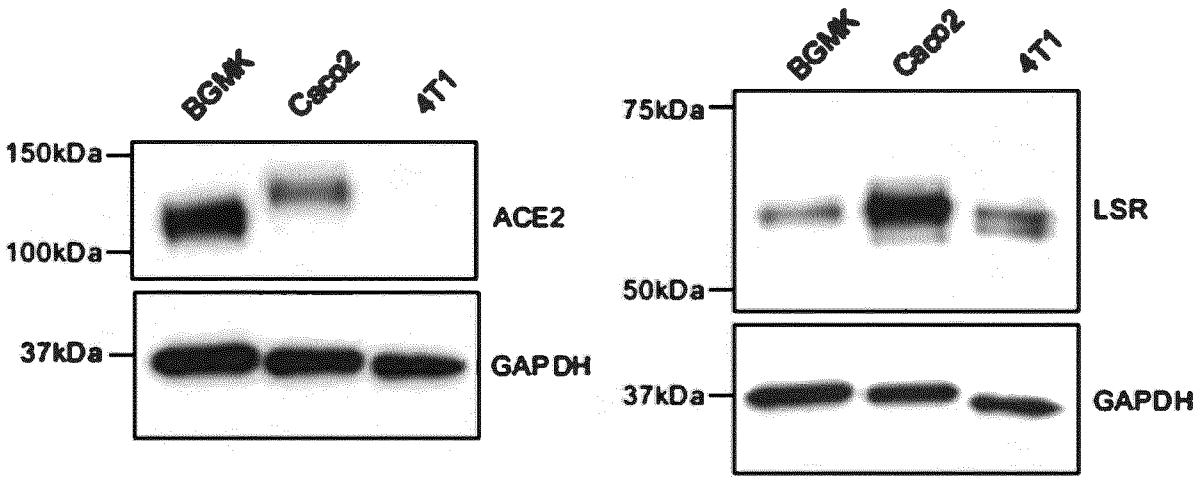
BGMK
Caco2
4T1
150kDa
100kDa
ACE2
37kDa
GAPDH
BGMK
Caco2
4T1
75kDa
LSR
50kDa
37kDa
GAPDH

FIG. 3B

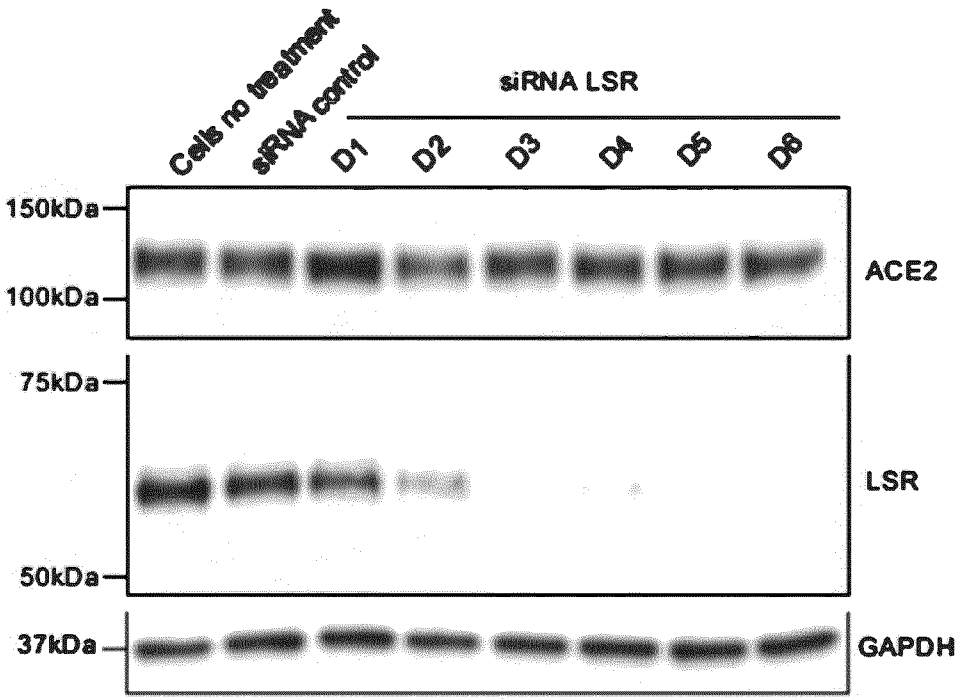
Cells no treatment
siRNA control
siRNA LSR
D1
D2
D3
D4
D5
D6
150kDa
100kDa
ACE2
75kDa
LSR
50kDa
37kDa
GAPDH

FIG. 3C

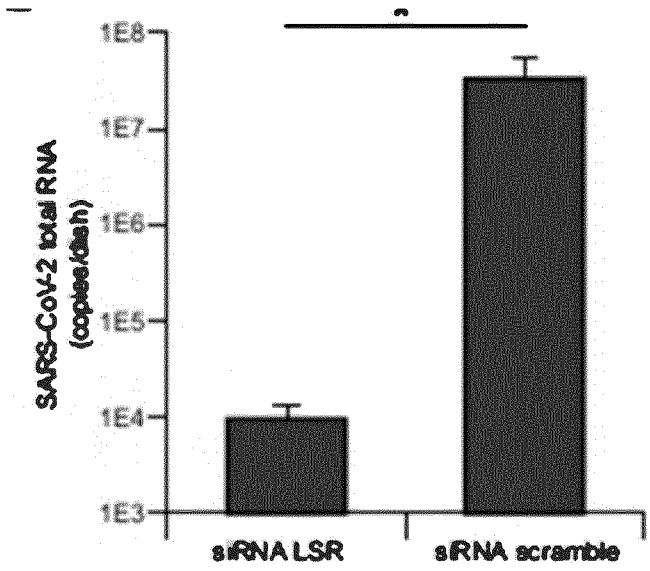
1E8
1E7
1E6
1E5
1E4
1E3
SARS-CoV-2 total RNA (copies/data h)
siRNA LSR
siRNA scramble

FIG. 3D

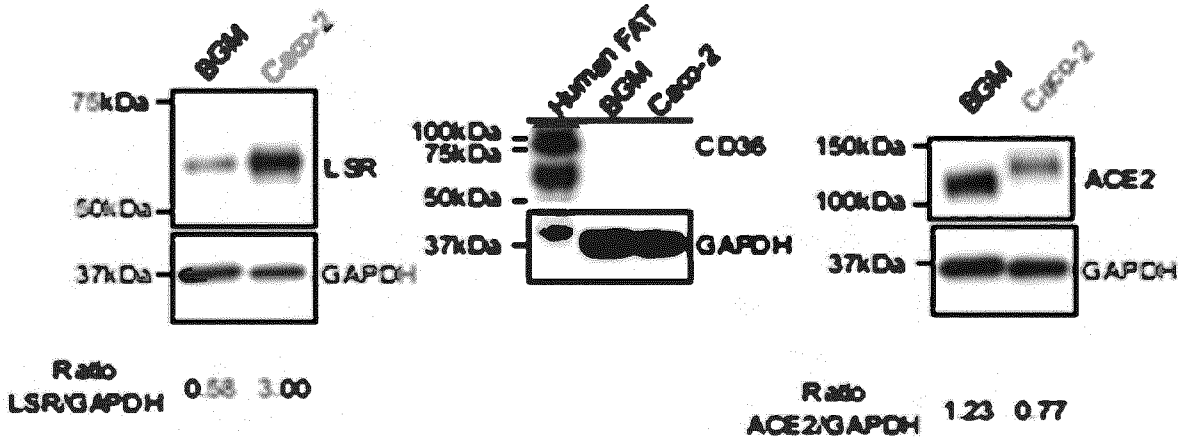
BCRM
Caco-2
75kDa
50kDa
37kDa
LSR
GAPDH
Ratio LSR/GAPDH 0.58 3.00
Human FAT
BCRM
Caco-2
100kDa
75kDa
50kDa
37kDa
CD36
GAPDH
BCRM
Caco-2
150kDa
100kDa
37kDa
ACE2
GAPDH
Ratio ACE2/GAPDH 1.23 0.77

FIG. 3E

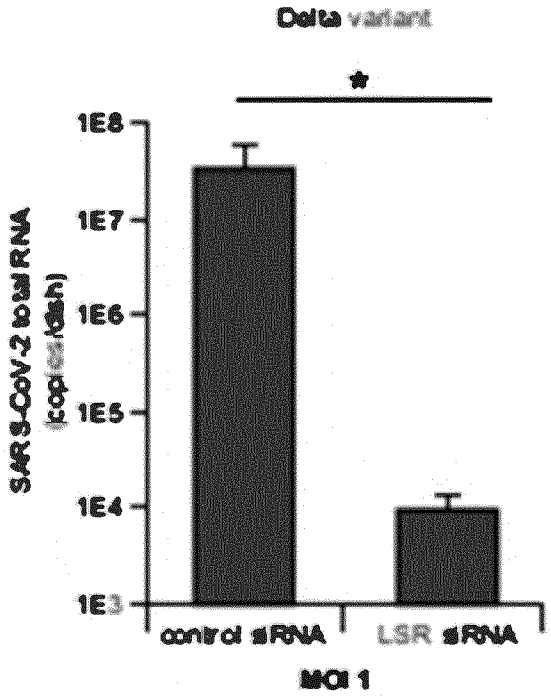
Delta variant
*
1E8
1E7
1E6
1E5
1E4
1E3
control siRNA
LSR siRNA
MOI 1

FIG. 3F

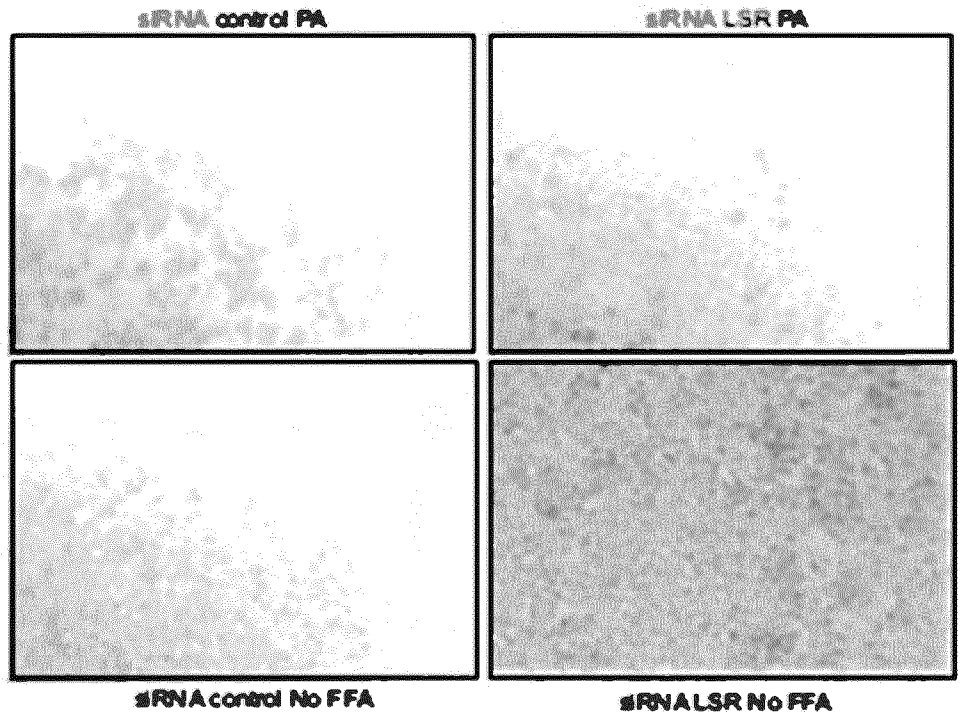
siRNA control PA
siRNA LSR PA
siRNA control No FFA
siRNA LSR No FFA

FIG. 3G

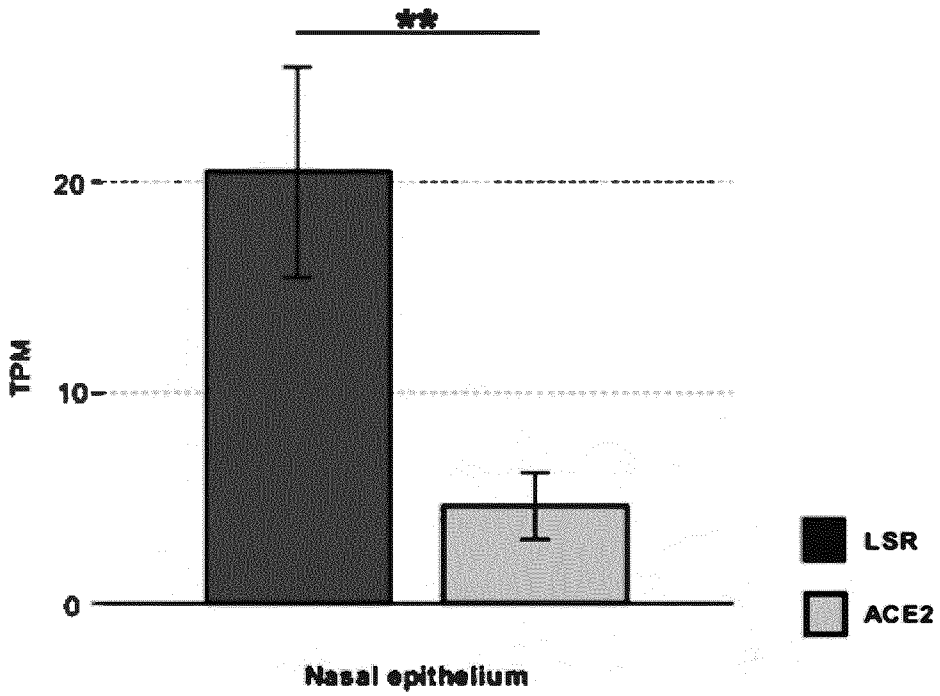
**
20
10
0
TPM
LSR
ACE2
Nasal epithelium

FIG. 3H

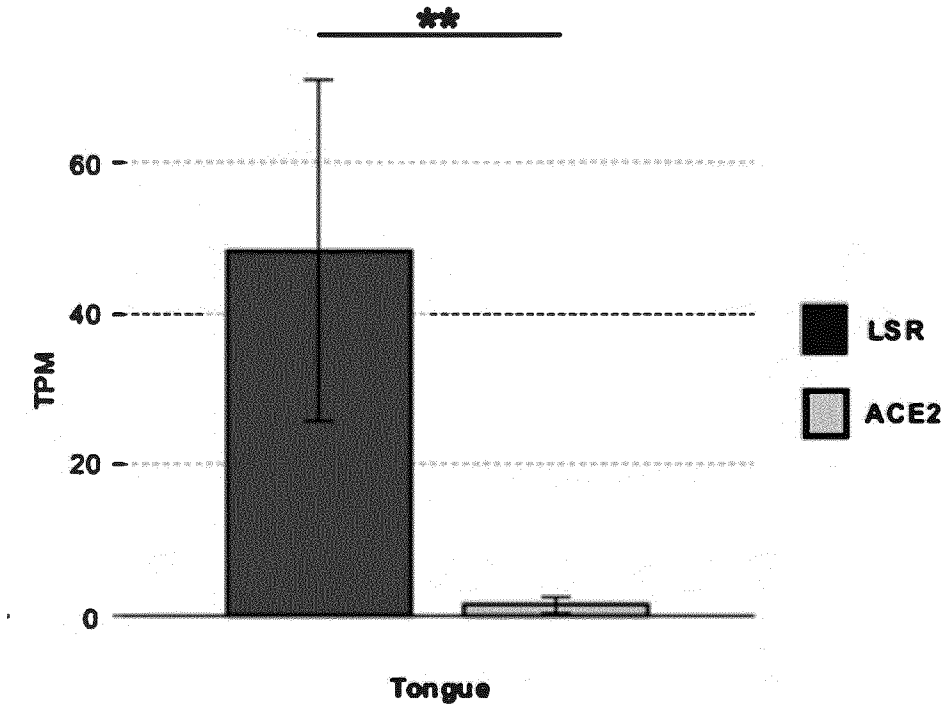
**
60
40
20
0
TPM
LSR
ACE2
Tongue

FIG. 3I

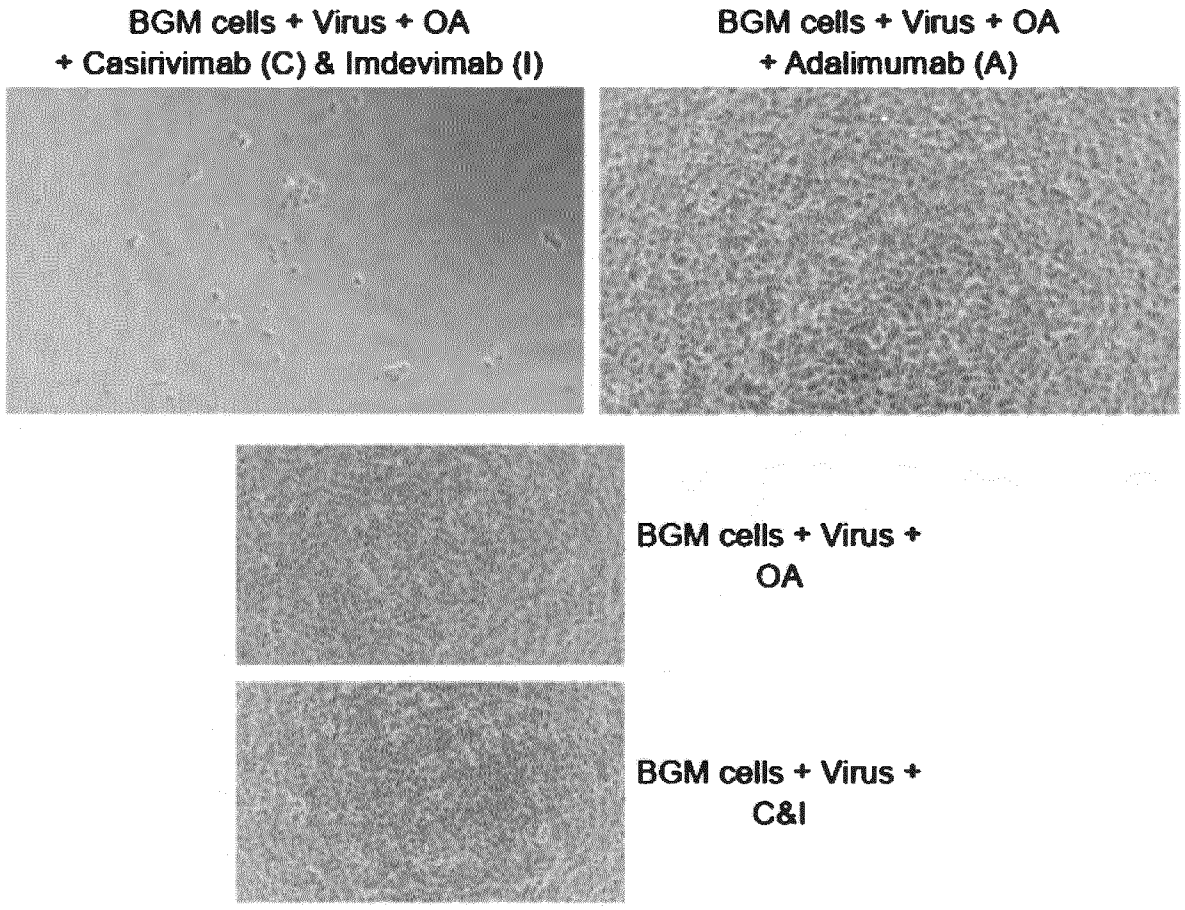
BGM cells + Virus + OA
+ Casirivimab (C) & Imdevimab (I)
BGM cells + Virus + OA
+ Adalimumab (A)
BGM cells + Virus +
OA
BGM cells + Virus +
C&I

FIG. 3J

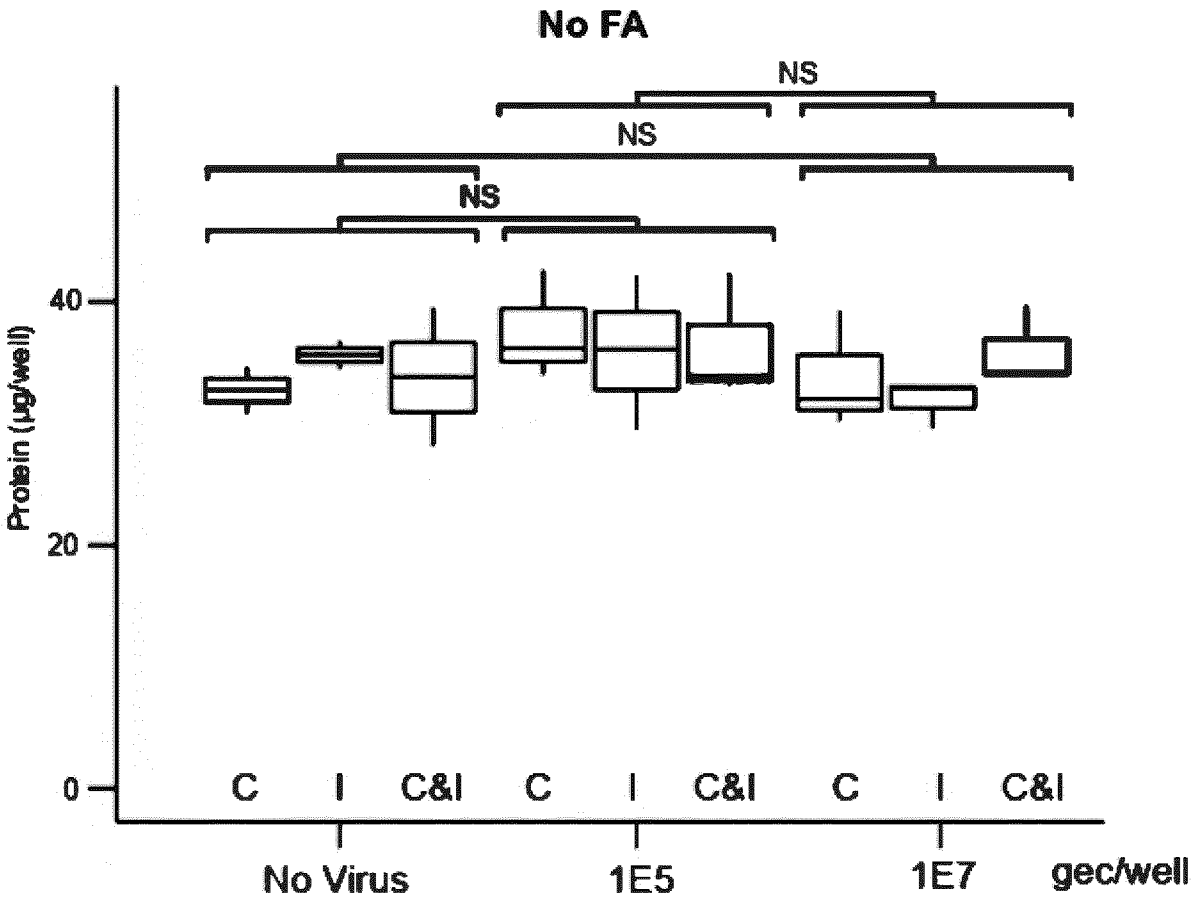
No FA
NS
NS
NS
Protein (µg/well)
40
20
0
C
I
C&I
C
I
C&I
C
I
C&I
No Virus
1E5
1E7
gec/well

FIG. 3K

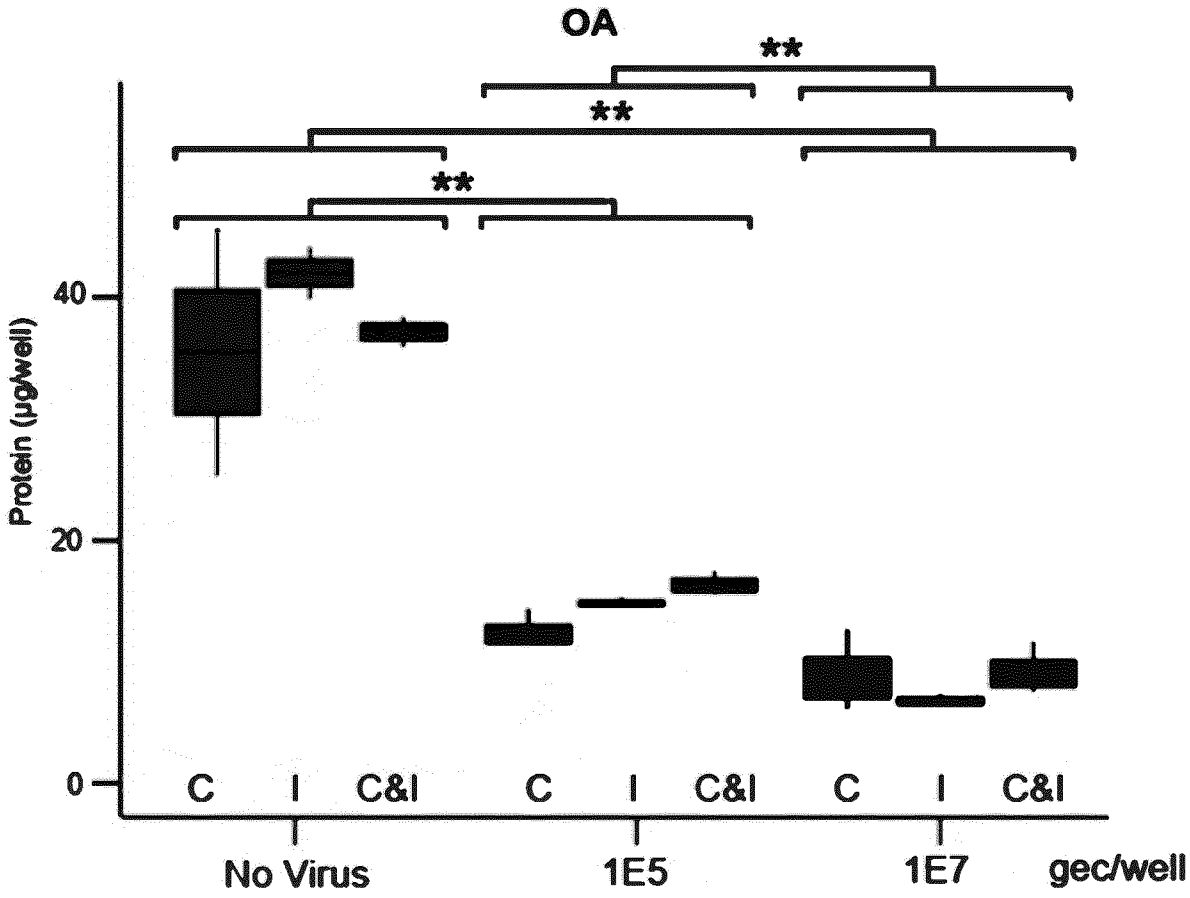
OA
**
**
**
Protein (µg/well)
40
20
0
C
I
C&I
C
I
C&I
C
I
C&I
No Virus
1E5
1E7
gec/well

FIG. 3L

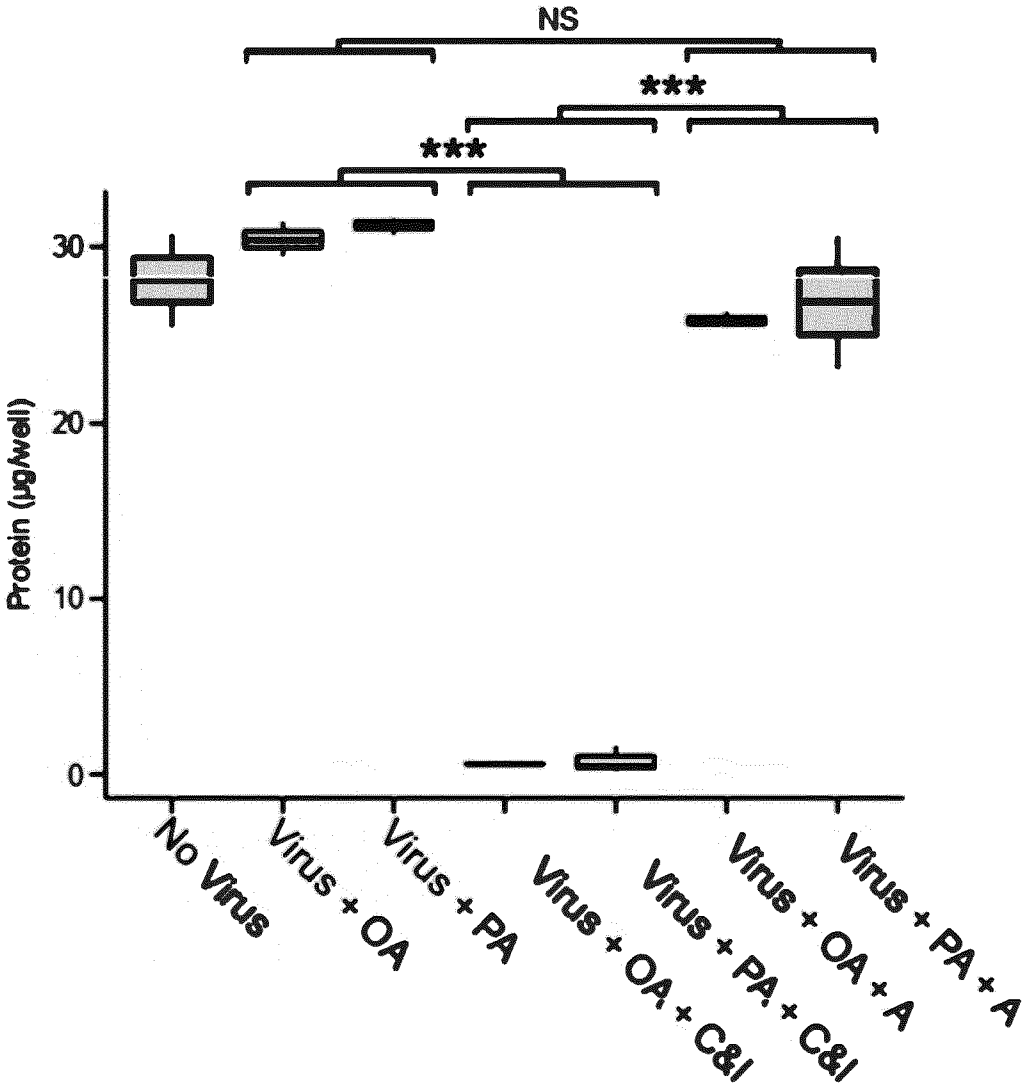
NS
***
***
30
20
10
0
Protein (µg/well)
No Virus
Virus + OA
Virus + PA
Virus + OA + C&I
Virus + PA + C&I
Virus + OA + A
Virus + PA + A

FIG. 3M

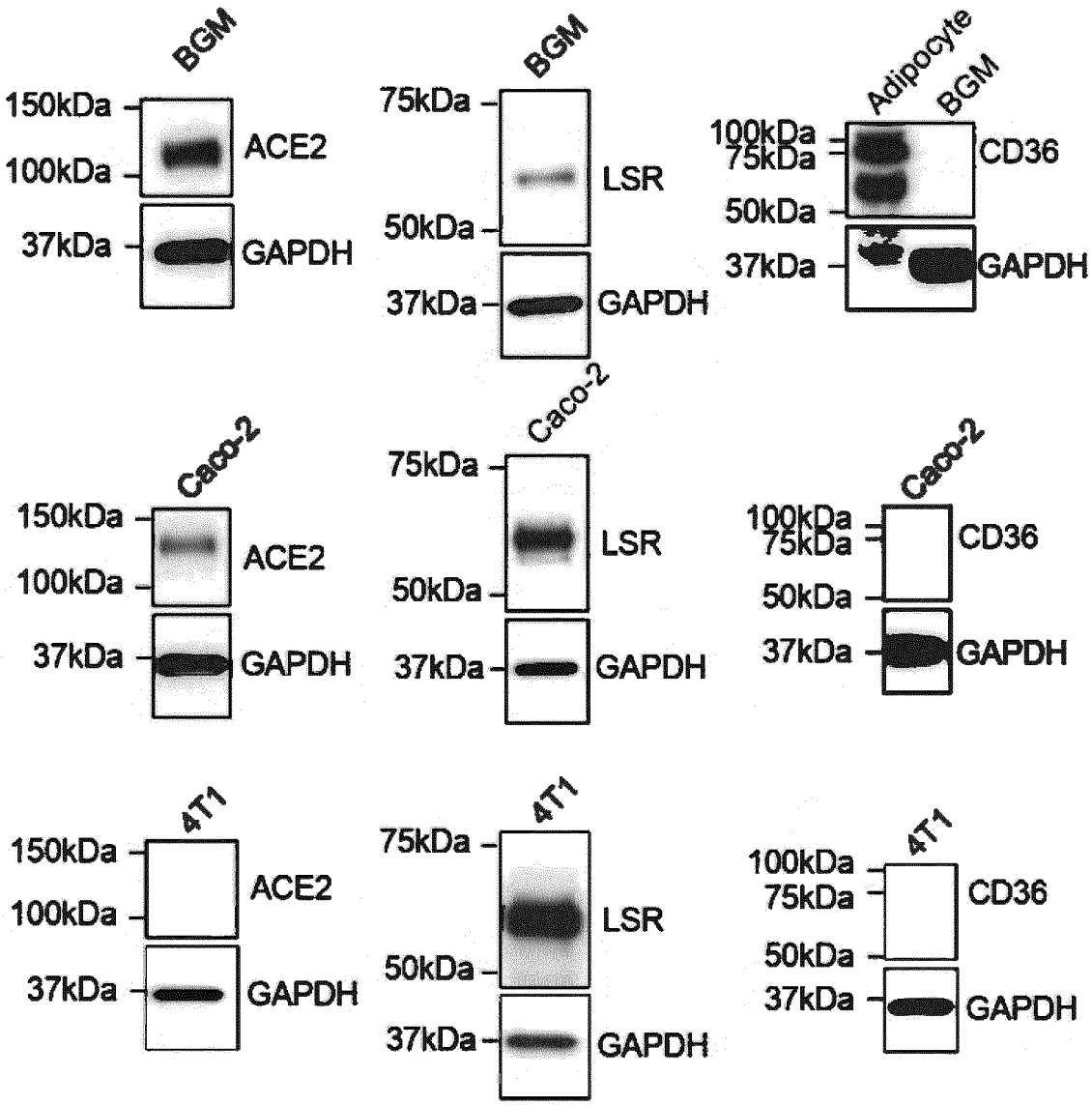
BGM
150kDa
100kDa
ACE2
37kDa
GAPDH
BGM
75kDa
LSR
50kDa
37kDa
GAPDH
Adipocyte
BGM
100kDa
75kDa
CD36
50kDa
37kDa
GAPDH
Caco-2
150kDa
100kDa
ACE2
37kDa
GAPDH
Caco-2
75kDa
LSR
50kDa
37kDa
GAPDH
Caco-2
100kDa
75kDa
CD36
50kDa
37kDa
GAPDH
4T1
150kDa
100kDa
ACE2
37kDa
GAPDH
4T1
75kDa
LSR
50kDa
37kDa
GAPDH
4T1
100kDa
75kDa
CD36
50kDa
37kDa
GAPDH

FIG. 3N

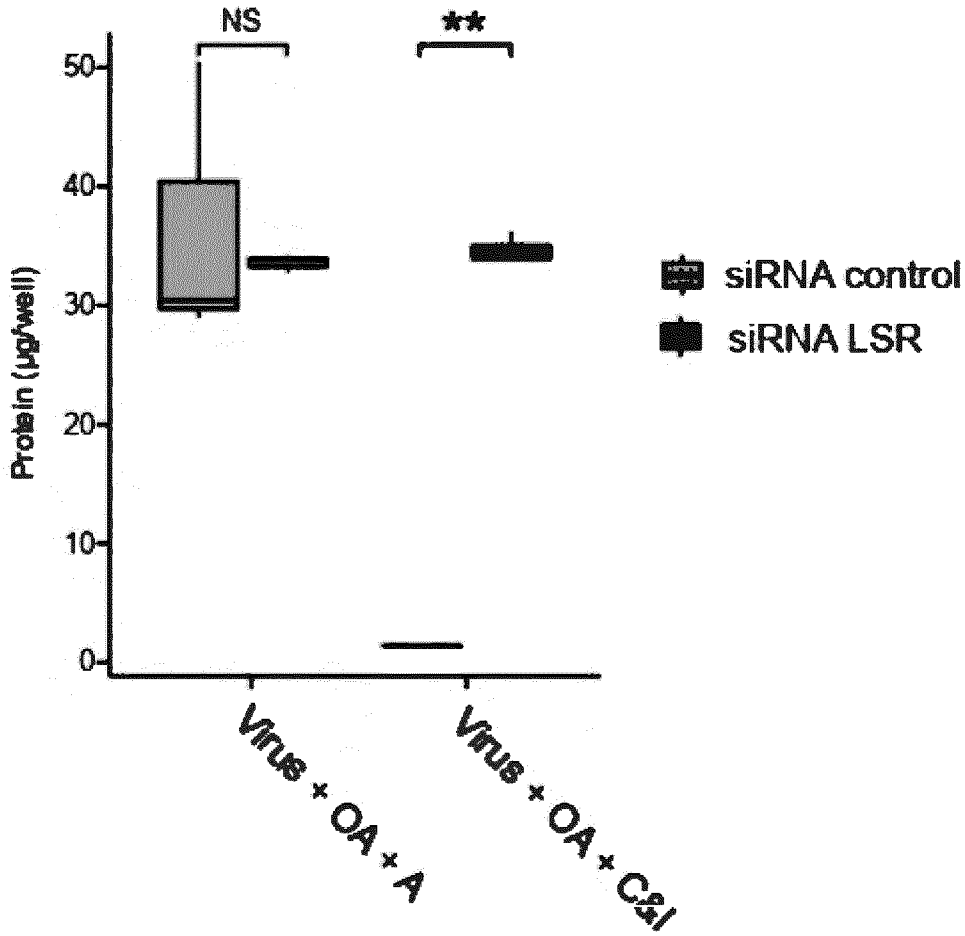
NS
**
50
40
30
20
10
0
Protein (µg/well)
siRNA control
siRNA LSR
Virus + OA + A
Virus + OA + C&I

FIG. 3O

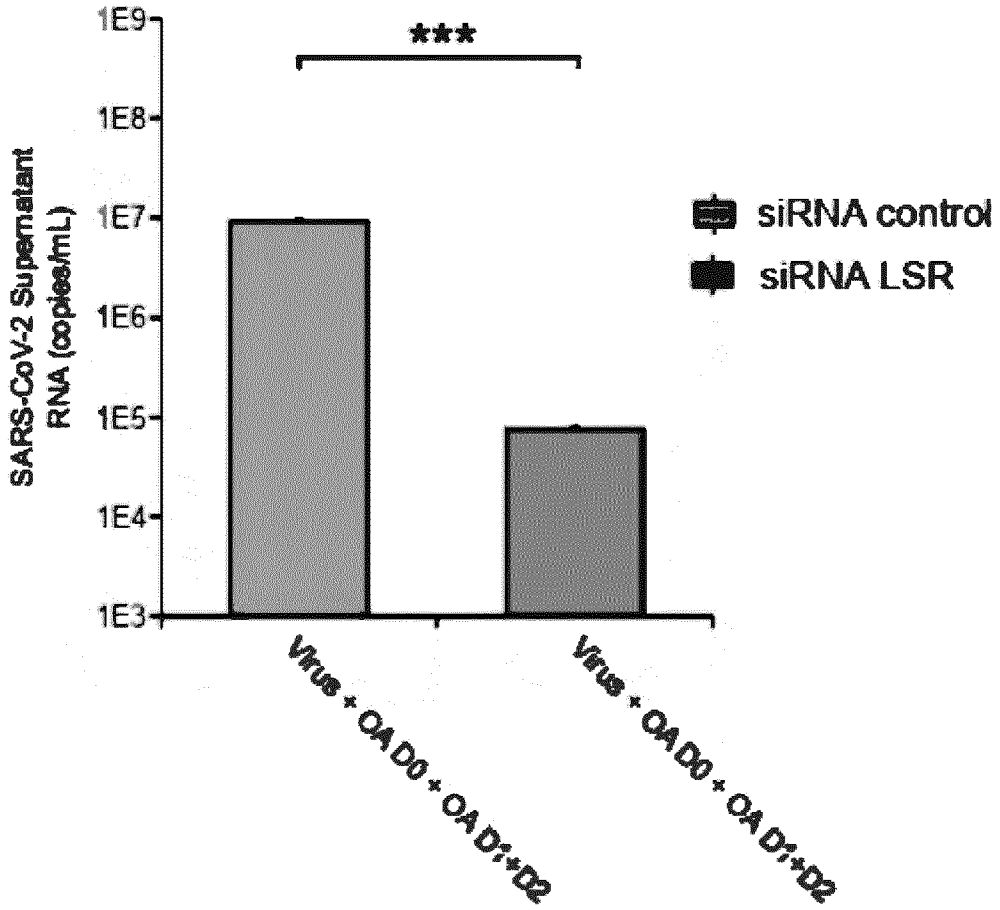
***
1E9
1E8
1E7
1E6
1E5
1E4
1E3
SARS-CoV-2 Supernatant RNA (copies/mL)
siRNA control
siRNA LSR
Virus + OA D0 + OA D1+D2
Virus + OA D0 + OA D1+D2

FIG. 3P

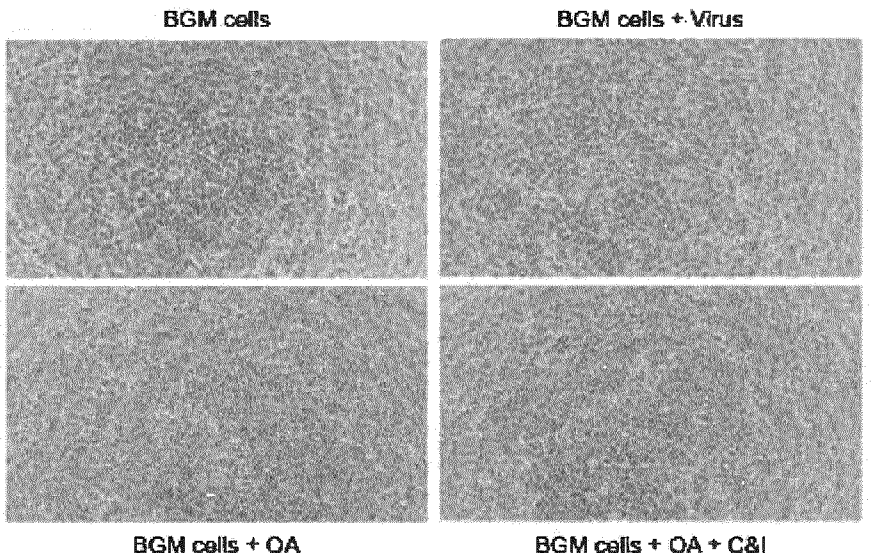
BGM cells
BGM cells + Virus
BGM cells + OA
BGM cells + OA + C&I

FIG. 3Q

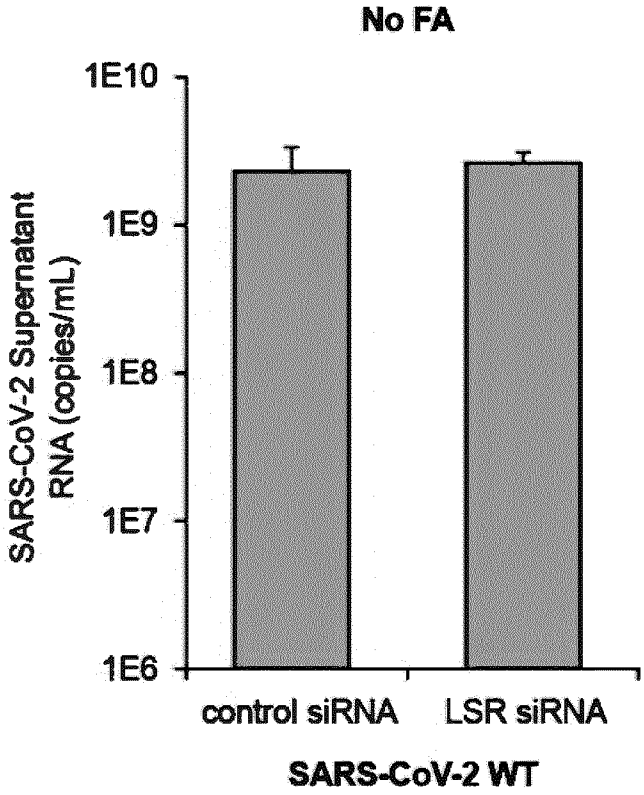
No FA
1E10
1E9
1E8
1E7
1E6
SARS-CoV-2 Supernatant RNA (copies/mL)
control siRNA
LSR siRNA
SARS-CoV-2 WT

FIG. 4A

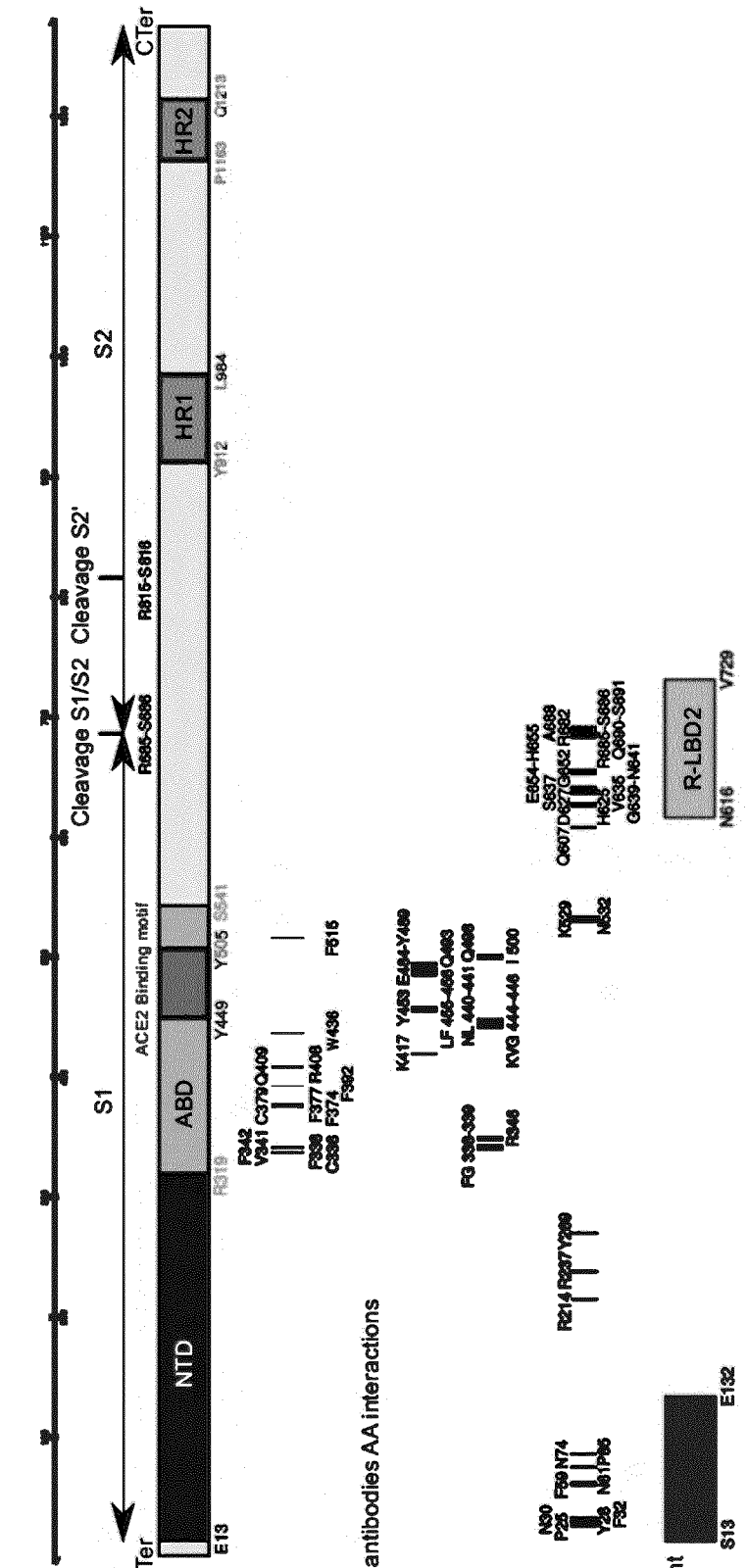
A
Spike (WT)
NTer
CTer
S1
S2
Cleavage S1/S2
Cleavage S2'
ACE2 Binding motif
NTD
ABD
HR1
HR2
R319
Y449
Y505
S541
R685-S686
R815-S816
Y912
L984
P1163
Q1213
E13
S13
E132
R-LBD2
N616
V729
AA linoleate interactions
Monoclonal antibodies AA interactions
Casirivimab
Imdevimab
AA LSR interactions
Recombinant proteins

FIG. 4B

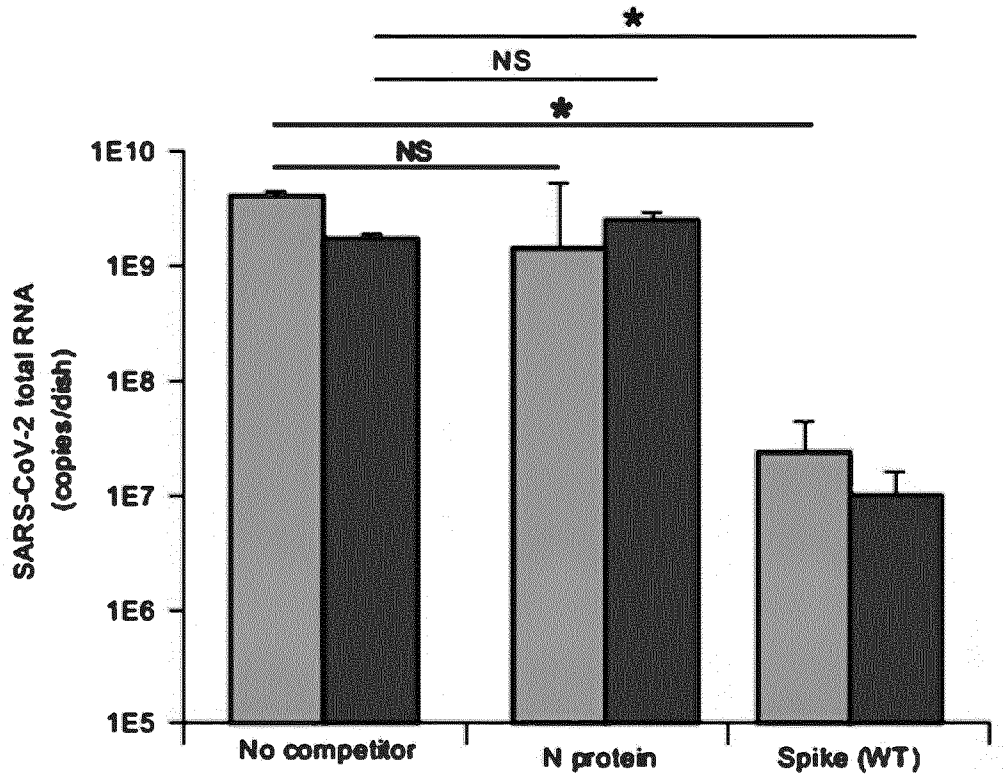
*
NS
*
NS
1E10
1E9
1E8
1E7
1E6
1E5
SARS-CoV-2 total RNA (copies/dish)
No competitor
N protein
Spike (WT)

FIG. 4C

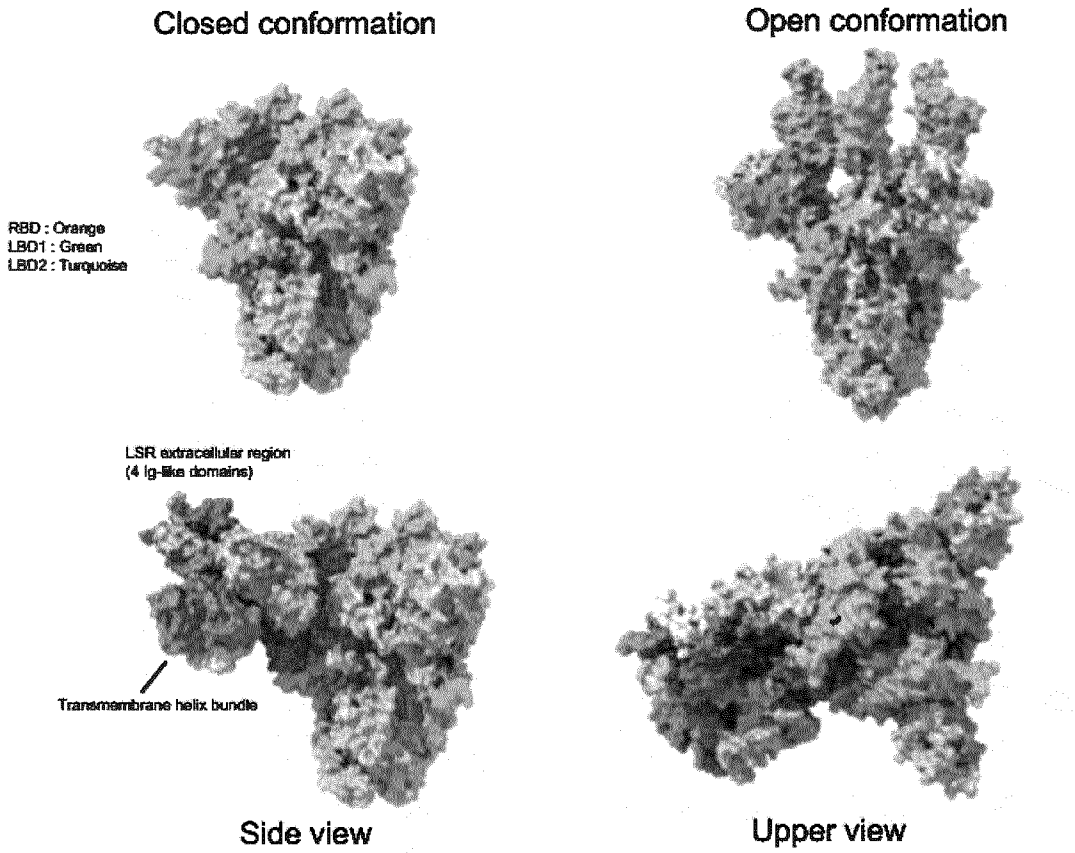
Closed conformation
Open conformation
RBD : Orange
LBD1 : Green
LBD2 : Turquoise
LSR extracellular region
(4 Ig-like domains)
Transmembrane helix bundle
Side view
Upper view

FIG. 4D

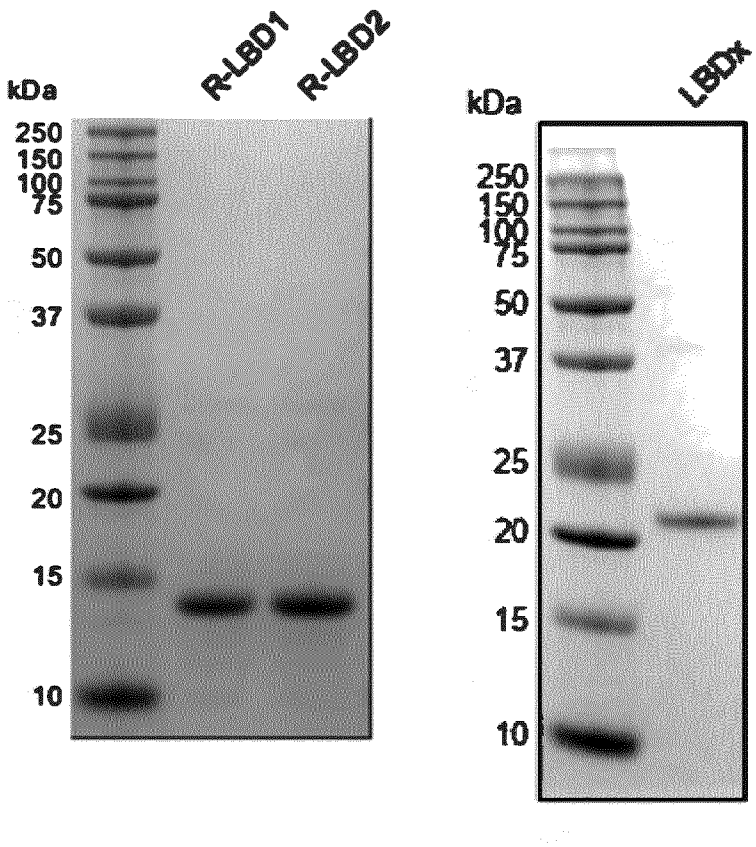
kDa
R-LBD1
R-LBD2
250
150
100
75
50
37
25
20
15
10
kDa
LBDx
250
150
100
75
50
37
25
20
15
10

FIG. 4E

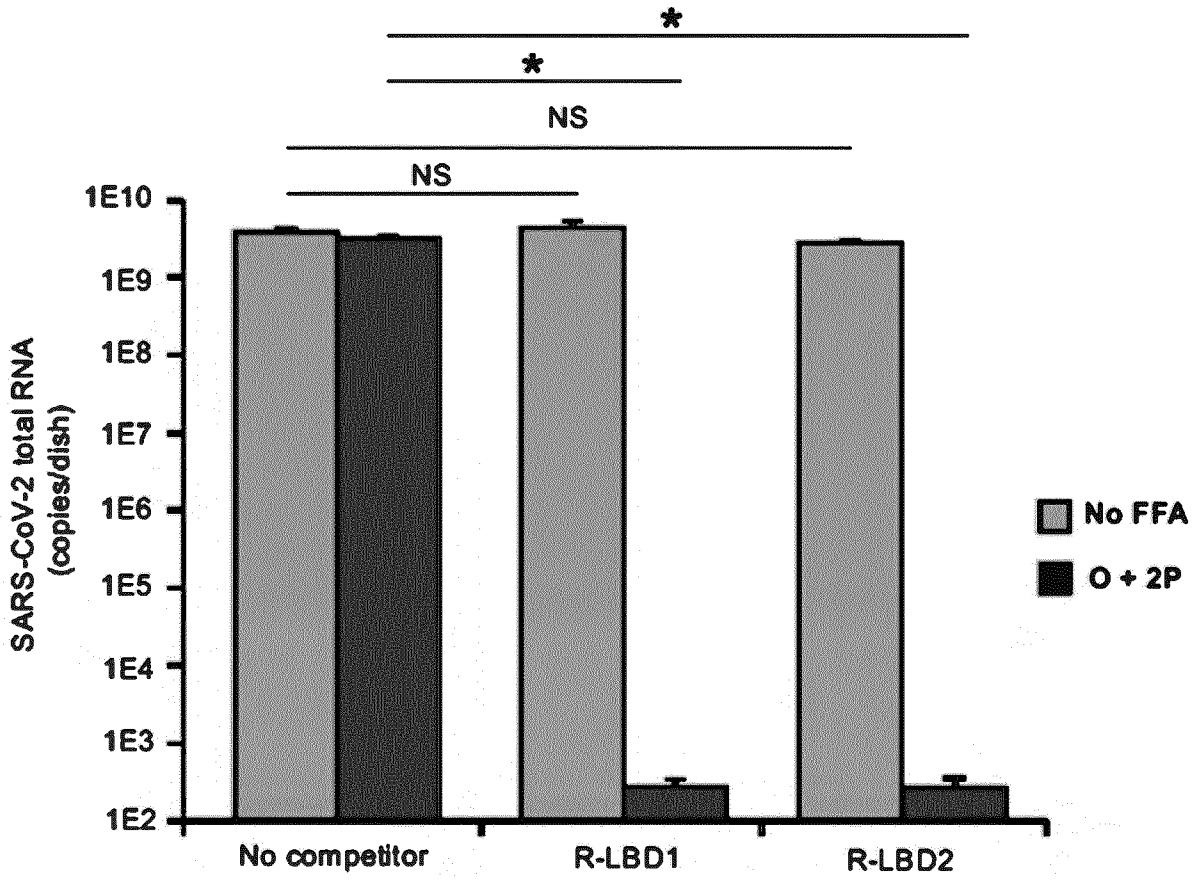
*
*
NS
NS
SARS-CoV-2 total RNA (copies/dish)
1E10
1E9
1E8
1E7
1E6
1E5
1E4
1E3
1E2
No competitor
R-LBD1
R-LBD2
No FFA
O + 2P

FIG. 4F

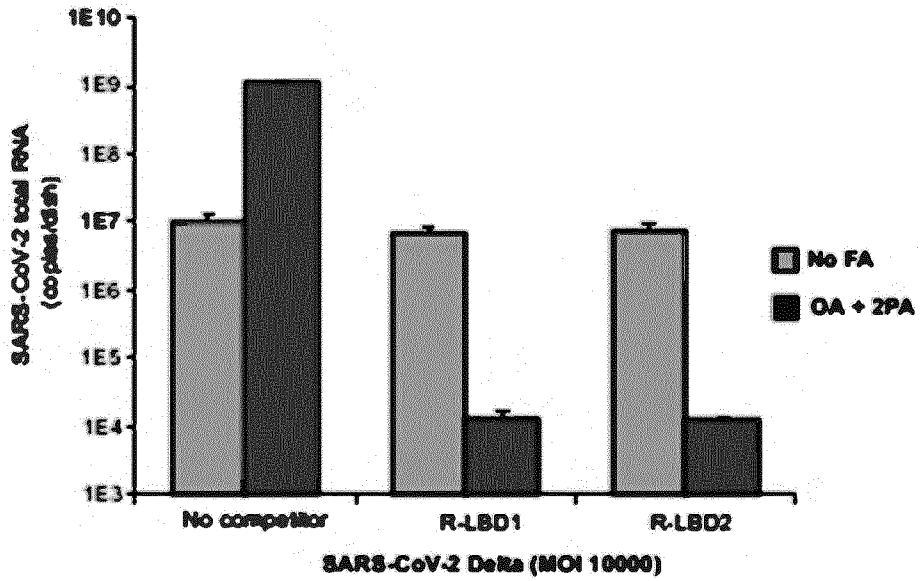
SARS-CoV-2 total RNA (copies/dish)
1E10
1E9
1E8
1E7
1E6
1E5
1E4
1E3
No competitor
R-LBD1
R-LBD2
SARS-CoV-2 Delta (MOI 10000)
No FA
OA + 2PA

FIG. 4G

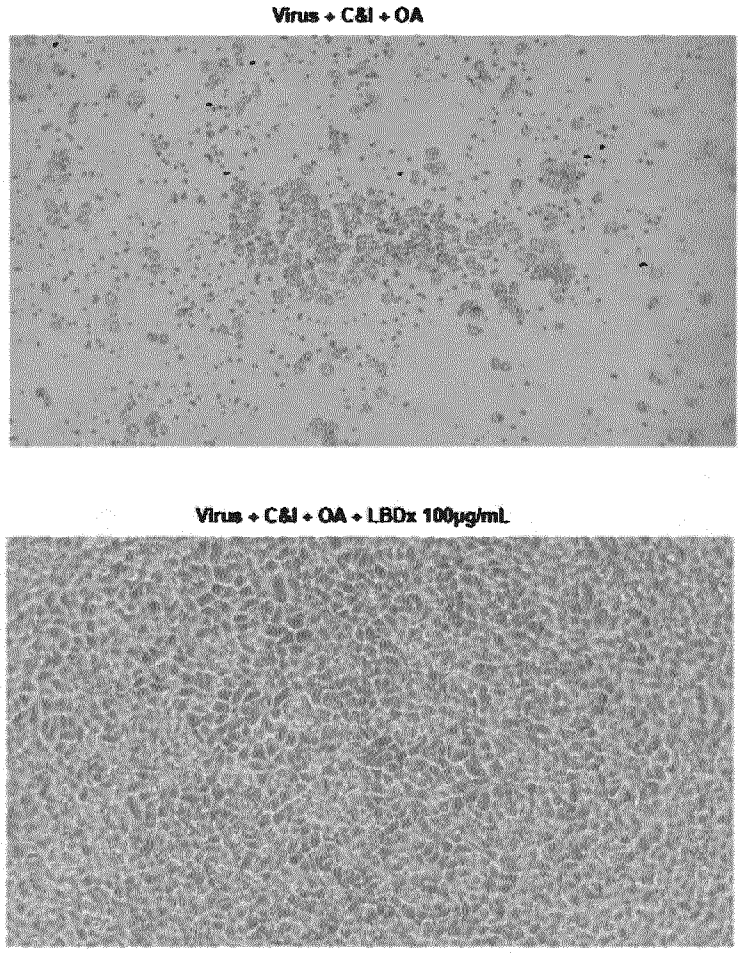

FIG. 4H

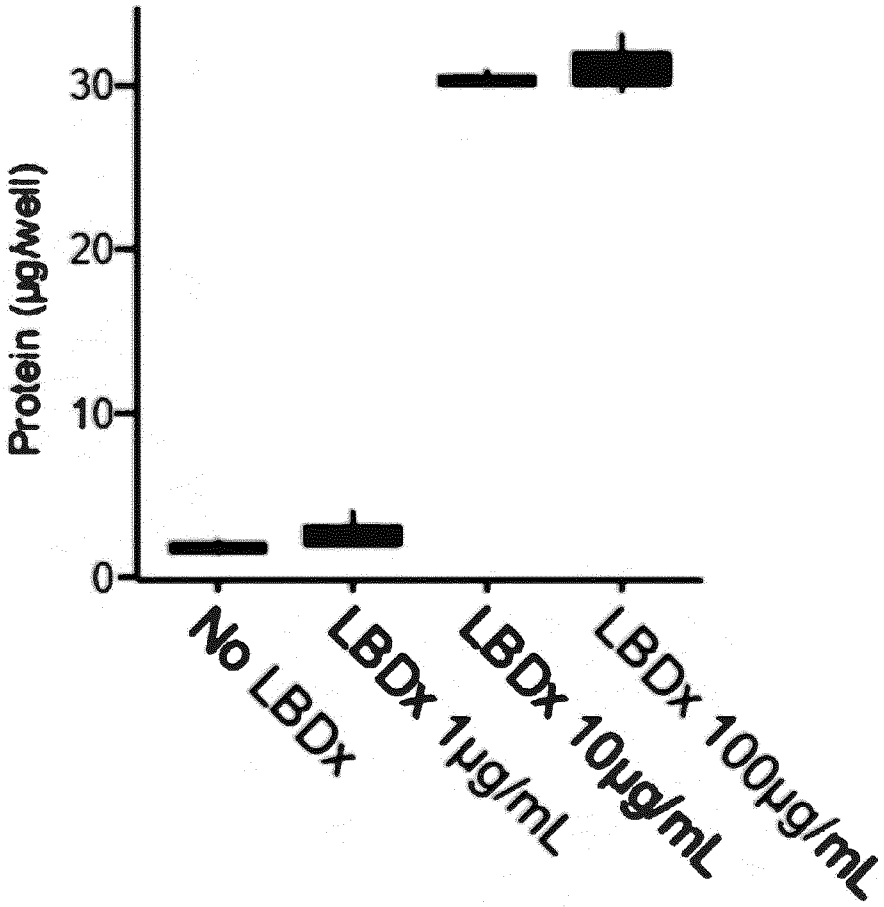
Protein (µg/well)
30
20
10
0
No LBDx
LBDx 1µg/mL
LBDx 10µg/mL
LBDx 100µg/mL

FIG. 4I

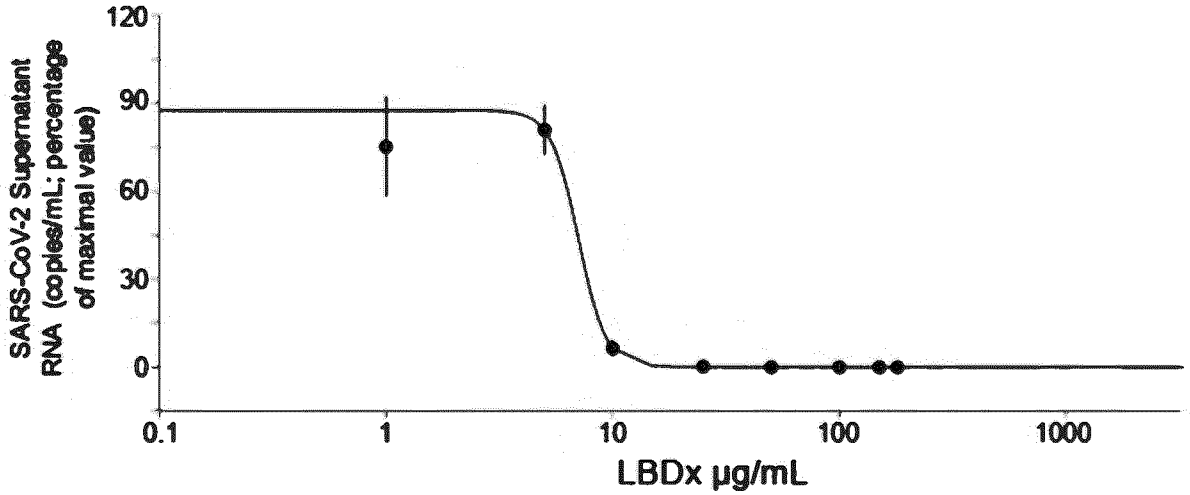
SARS-CoV-2 Supernatant RNA (copies/mL; percentage of maximal value)
120
90
60
30
0
0.1
1
10
100
1000
LBDx µg/mL

FIG. 4J

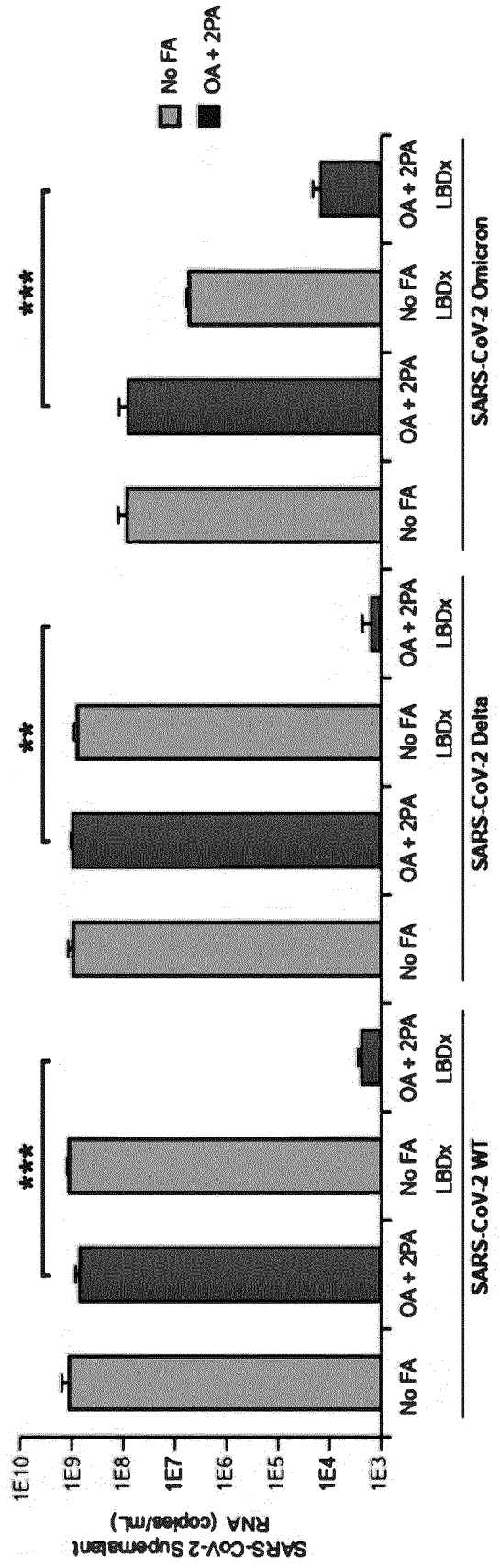
No FA
OA + 2PA
SARS-CoV-2 Supernatant RNA (copies/mL)
1E10
1E9
1E8
1E7
1E6
1E5
1E4
1E3
***
**
***
No FA
OA + 2PA
No FA
OA + 2PA
LBDx
LBDx
SARS-CoV-2 WT
SARS-CoV-2 Delta
SARS-CoV-2 Omicron

FIG. 5A

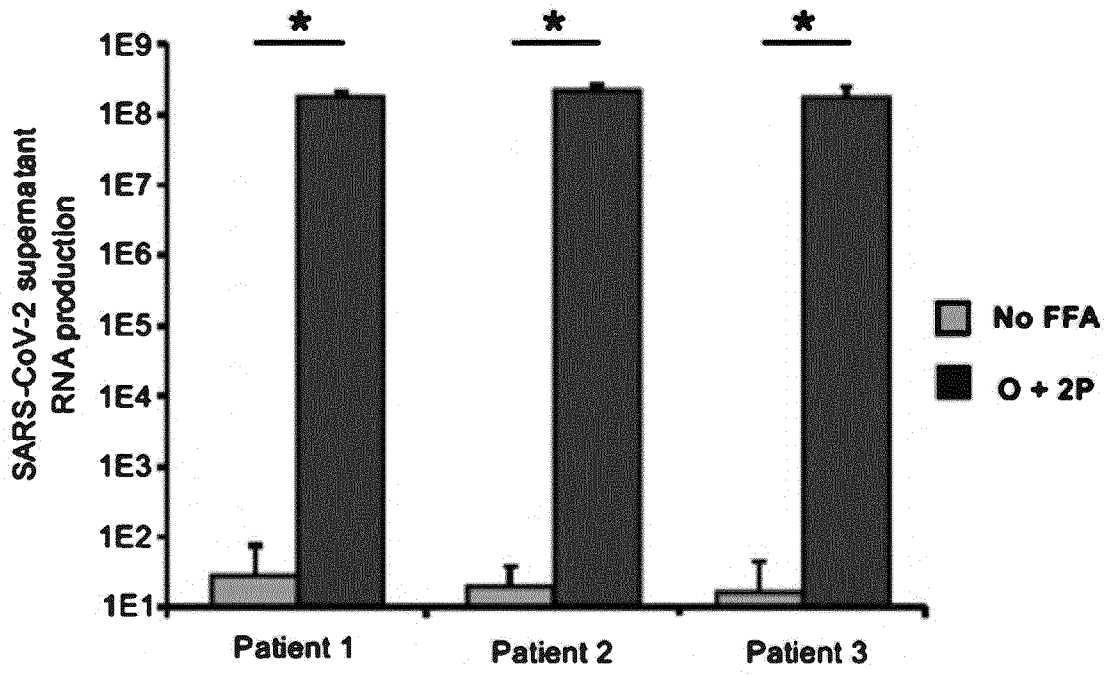
SARS-CoV-2 supernatant RNA production
1E9
1E8
1E7
1E6
1E5
1E4
1E3
1E2
1E1
*
*
*
Patient 1
Patient 2
Patient 3
No FFA
O + 2P

FIG. 5B

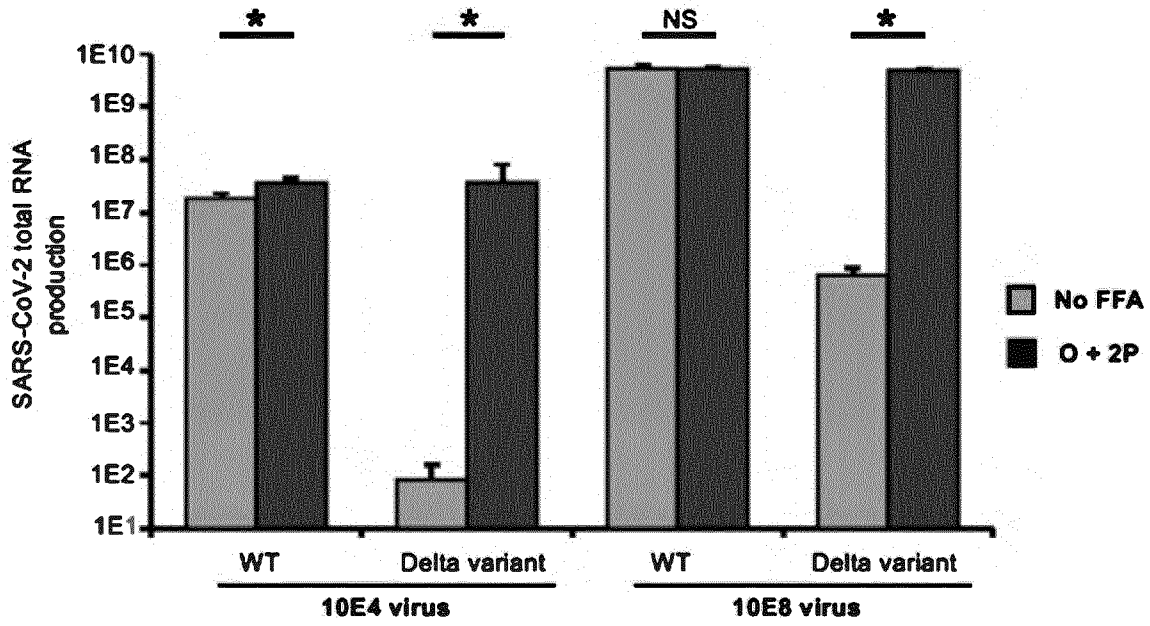
SARS-CoV-2 total RNA production
1E10
1E9
1E8
1E7
1E6
1E5
1E4
1E3
1E2
1E1
*
*
NS
*
WT
Delta variant
WT
Delta variant
10E4 virus
10E8 virus
No FFA
O + 2P

FIG. 5C

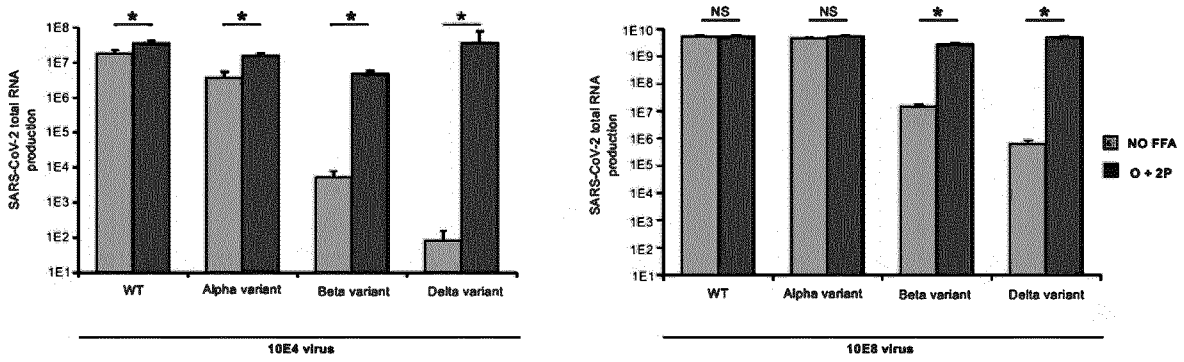
SARS-CoV-2 total RNA production
1E8
1E7
1E6
1E5
1E4
1E3
1E2
1E1
*
*
*
*
WT
Alpha variant
Beta variant
Delta variant
10E4 virus
SARS-CoV-2 total RNA production
1E10
1E9
1E8
1E7
1E6
1E5
1E4
1E3
1E2
1E1
NS
NS
*
*
WT
Alpha variant
Beta variant
Delta variant
10E6 virus
NO FFA
O + 2P

FIG. 5D

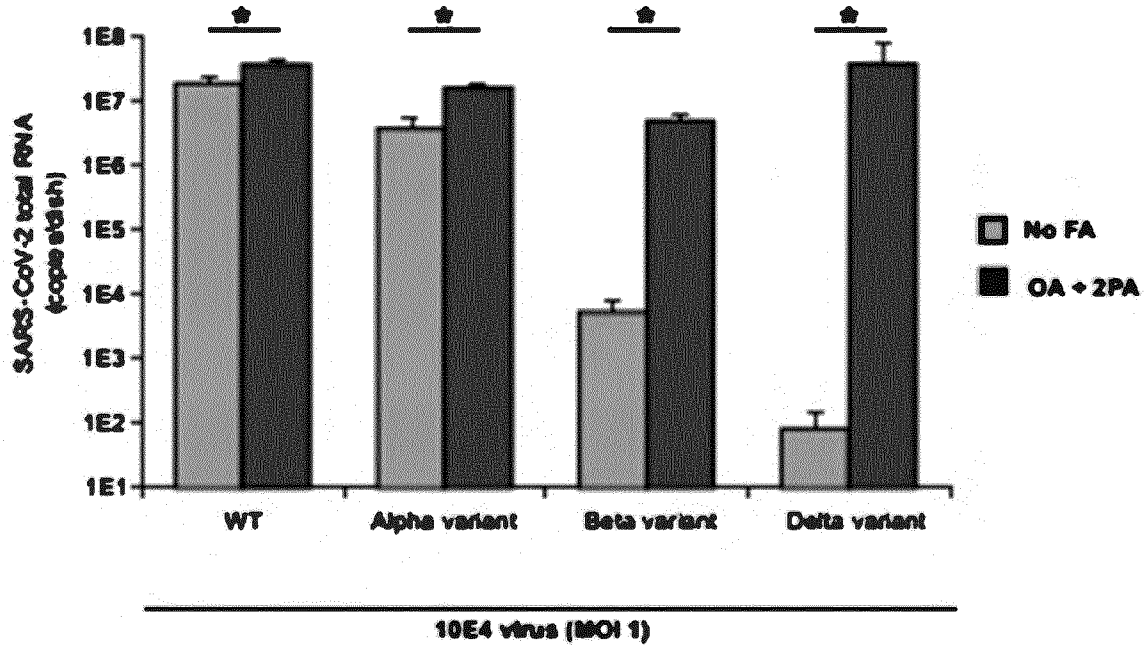
SARS-CoV-2 total RNA (copies eq/ml)
1E8
1E7
1E6
1E5
1E4
1E3
1E2
1E1
*
*
*
*
WT
Alpha variant
Beta variant
Delta variant
10E4 virus (MOI 1)
No FA
OA + 2PA

FIG. 5E

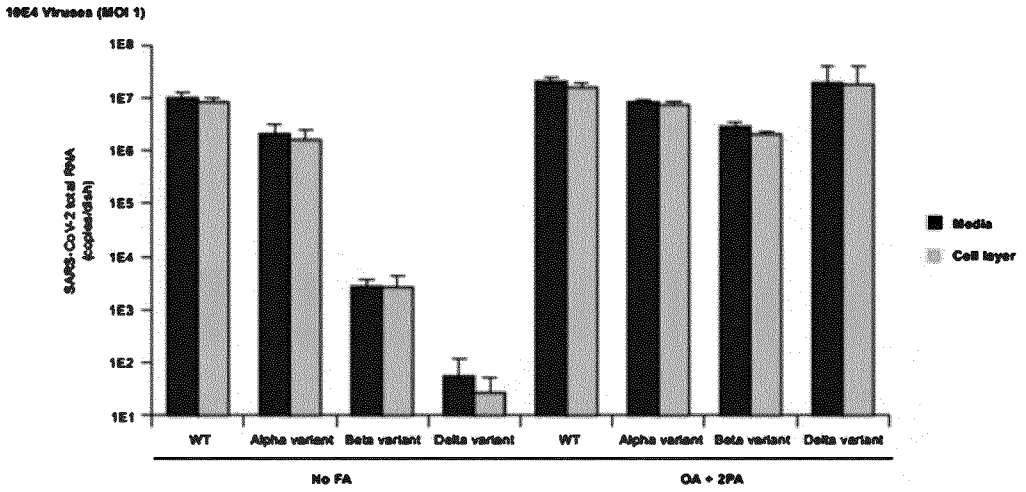
10E4 Viruses (MOI 1)
SARS-CoV-2 total RNA (copies/dish)
1E8
1E7
1E6
1E5
1E4
1E3
1E2
1E1
WT
Alpha variant
Beta variant
Delta variant
WT
Alpha variant
Beta variant
Delta variant
No FA
OA + 2PA
Media
Cell layer

FIG. 5F

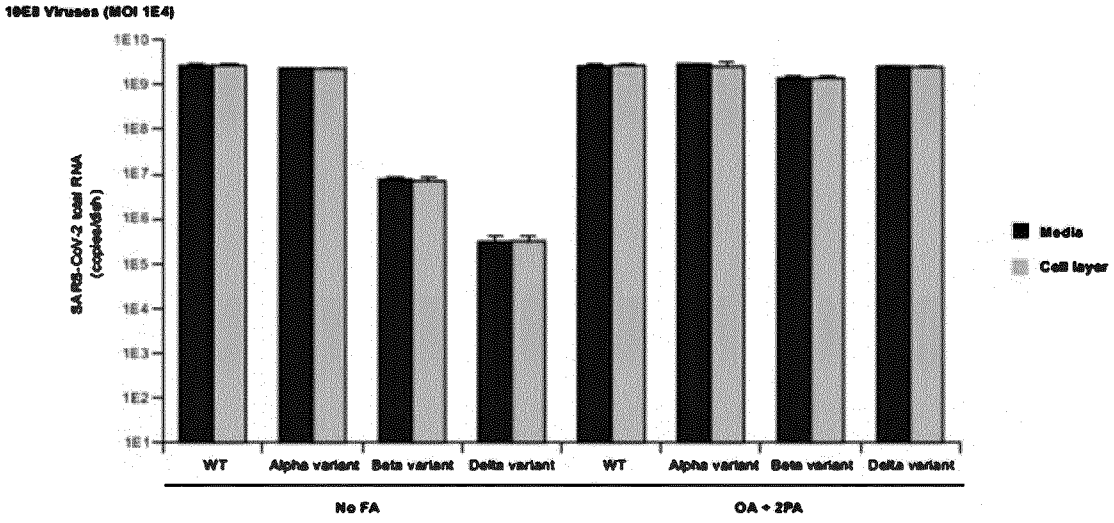
10E8 Viruses (MOI 1E4)
SARS-CoV-2 total RNA (copies/dish)
1E10
1E9
1E8
1E7
1E6
1E5
1E4
1E3
1E2
1E1
WT
Alpha variant
Beta variant
Delta variant
WT
Alpha variant
Beta variant
Delta variant
No FA
OA + 2PA
Media
Cell layer

FIG. 5G

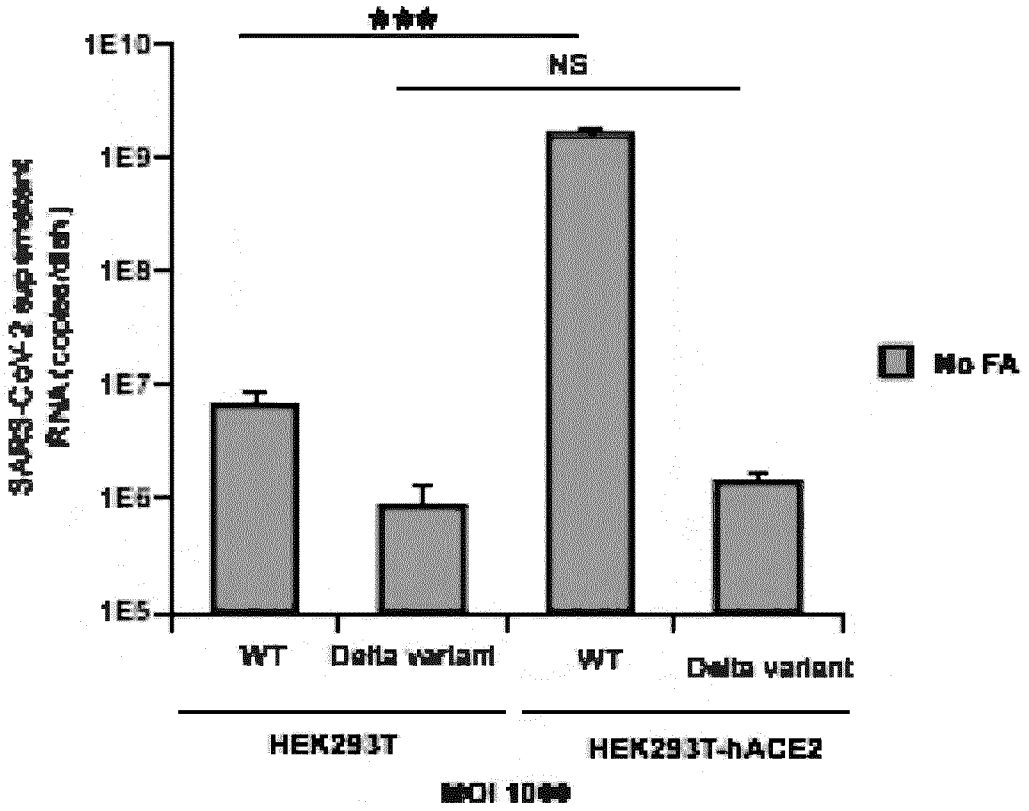
***
NS
1E10
1E9
1E8
1E7
1E6
1E5
SARS-CoV-2 supernatant RNA (copies/well)
No FA
WT
Delta variant
WT
Delta variant
HEK293T
HEK293T-hACE2
MOI 1000

FIG. 5H

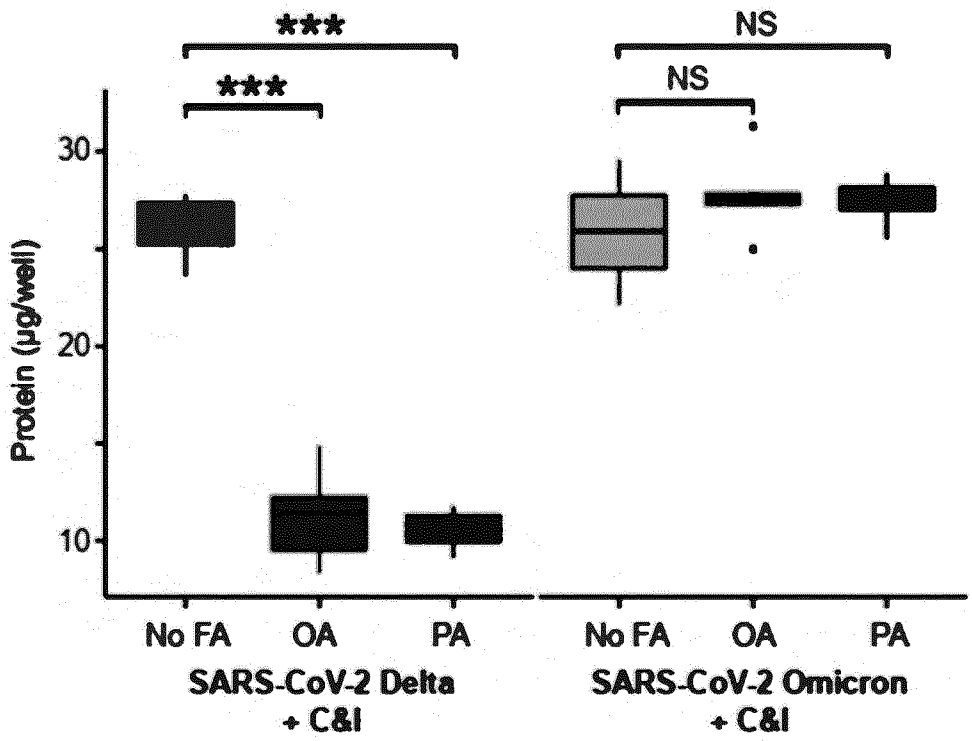
***
***
NS
NS
30
20
10
Protein (µg/well)
No FA
OA
PA
No FA
OA
PA
SARS-CoV-2 Delta + C&I
SARS-CoV-2 Omicron + C&I

FIG. 5I

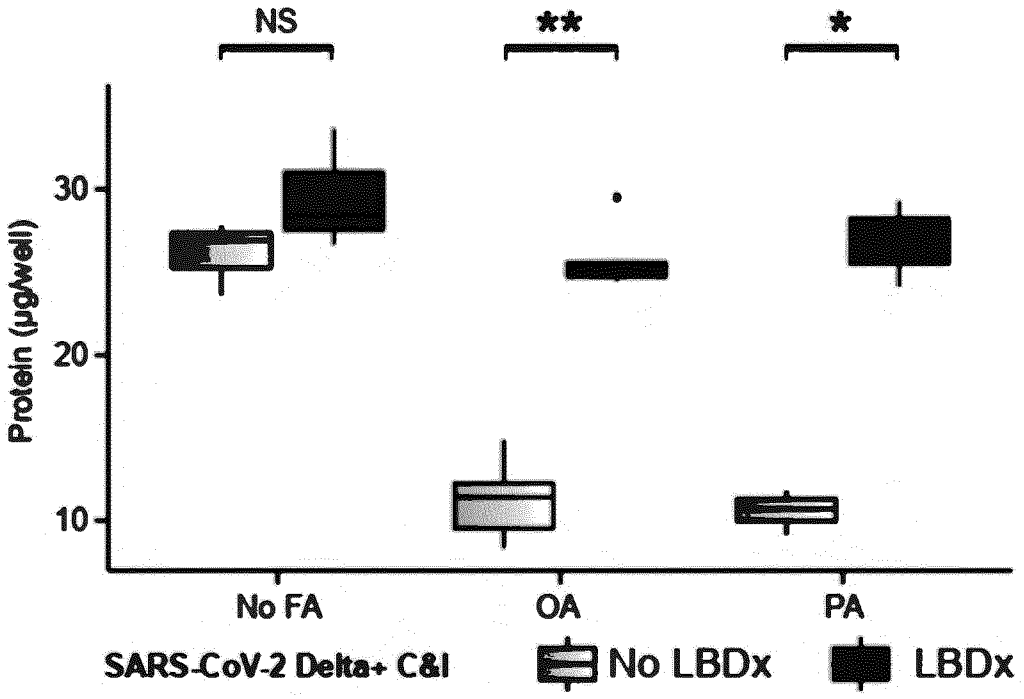
NS
**
*
Protein (µg/well)
30
20
10
No FA
OA
PA
SARS-CoV-2 Delta+ C&I
No LBDx
LBDx

FIG. 5J

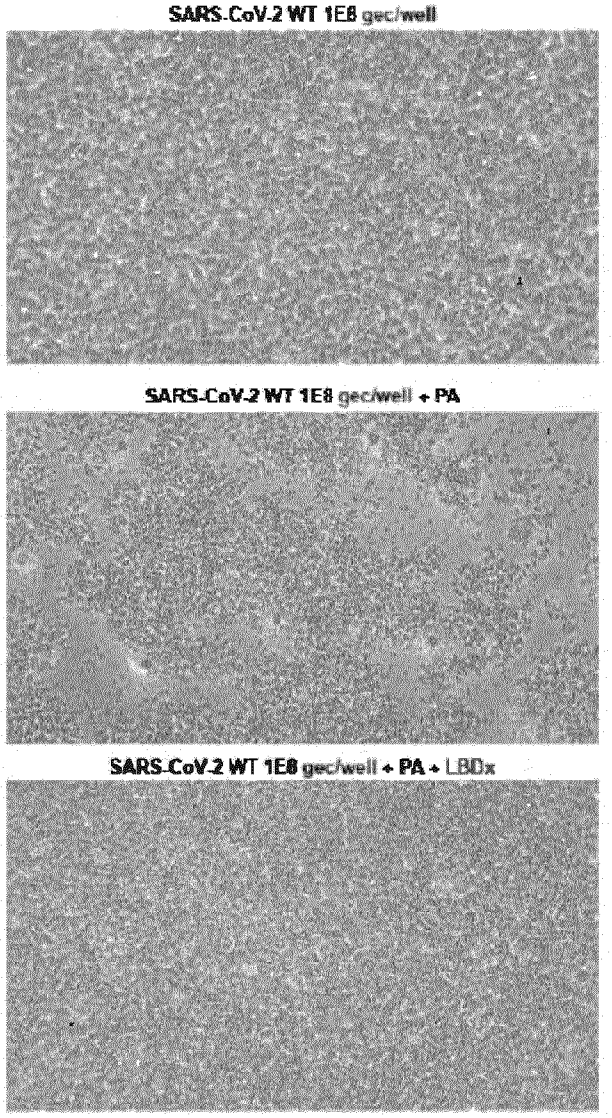
SARS-CoV-2 WT 1E8 gec/well
SARS-CoV-2 WT 1E8 gec/well + PA
SARS-CoV-2 WT 1E8 gec/well + PA + LBDx

FIG. 5K

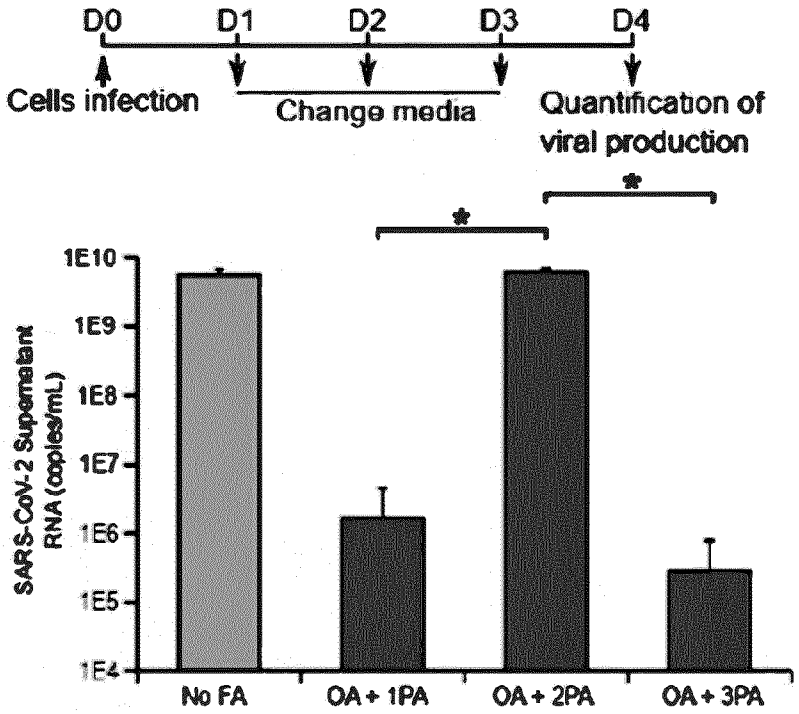
D0
D1
D2
D3
D4
Cells infection
Change media
Quantification of viral production
*
*
SARS-CoV-2 Supernatant RNA (copies/mL)
1E10
1E9
1E8
1E7
1E6
1E5
1E4
No FA
OA + 1PA
OA + 2PA
OA + 3PA

FIG. 5L

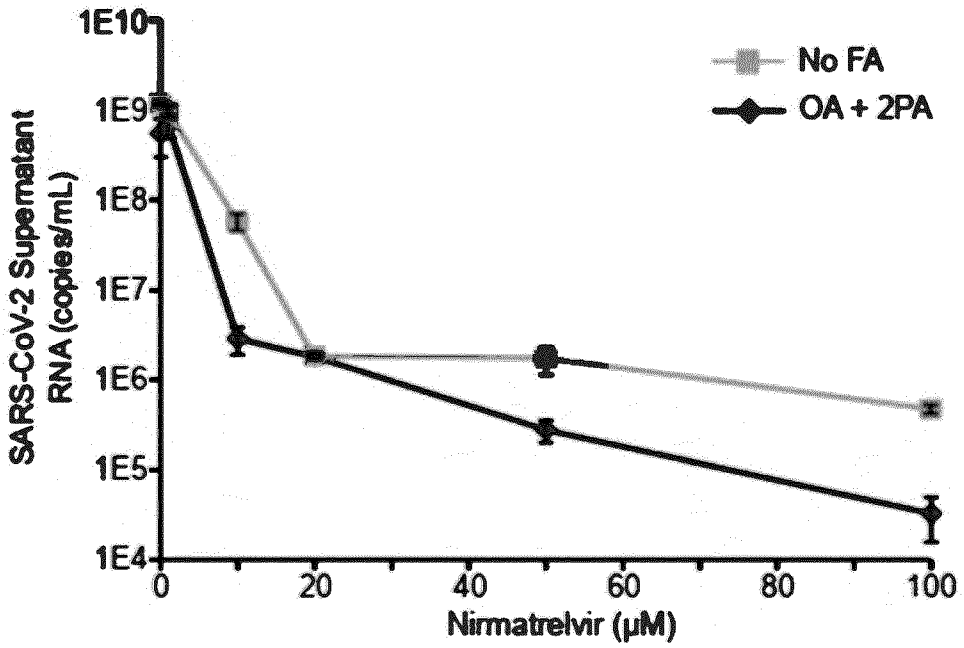
No FA
OA + 2PA
SARS-CoV-2 Supernatant RNA (copies/mL)
1E10
1E9
1E8
1E7
1E6
1E5
1E4
0
20
40
60
80
100
Nirmatrelvir (μM)

FIG. 5M

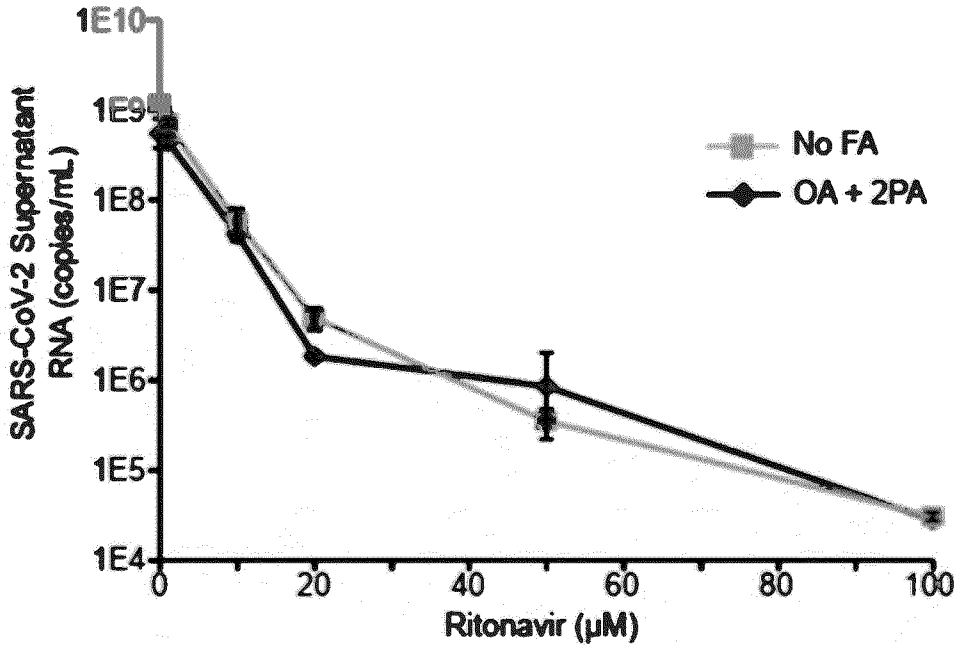
1E10
1E9
1E8
1E7
1E6
1E5
1E4
SARS-CoV-2 Supernatant RNA (copies/mL)
0
20
40
60
80
100
Ritonavir (μM)
No FA
OA + 2PA

FIG. 5N

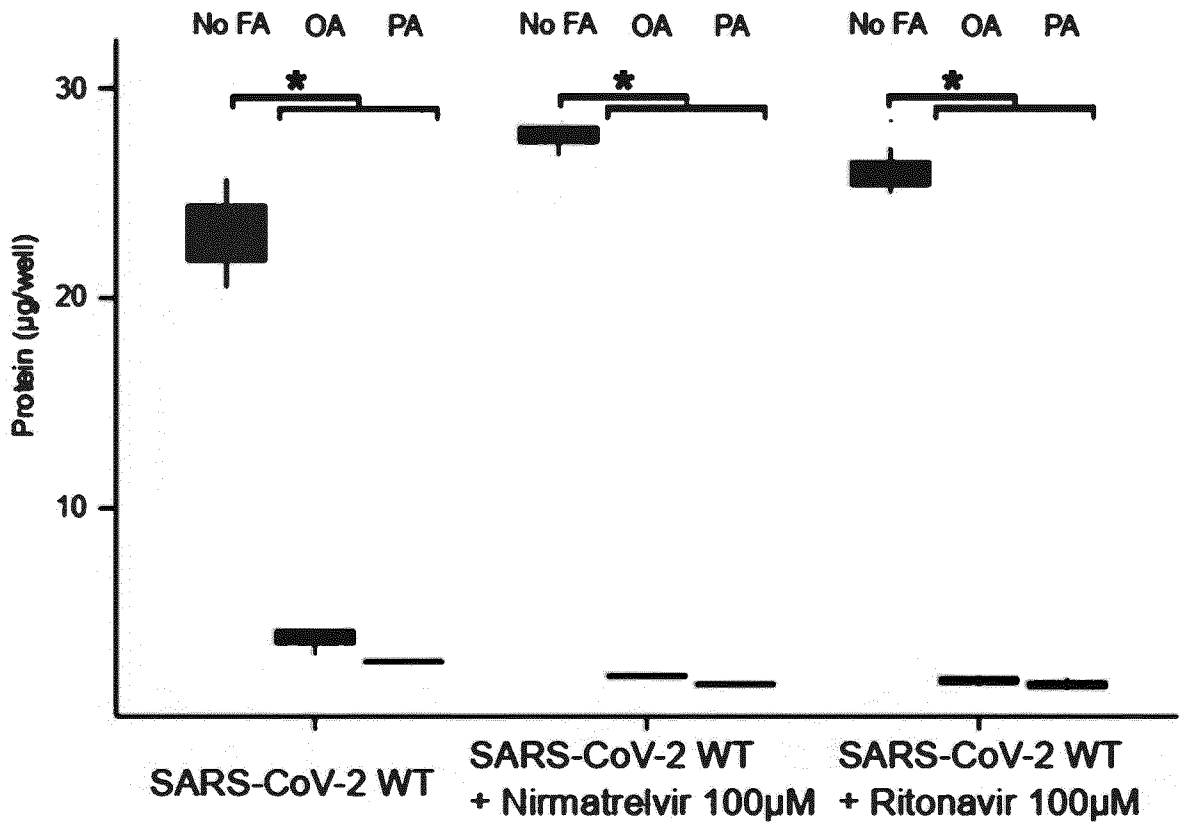
No FA
OA
PA
No FA
OA
PA
No FA
OA
PA
30
20
10
Protein (µg/well)
*
*
*
SARS-CoV-2 WT
SARS-CoV-2 WT
+ Nirmatrelvir 100µM
SARS-CoV-2 WT
+ Ritonavir 100µM

FIG. 5O

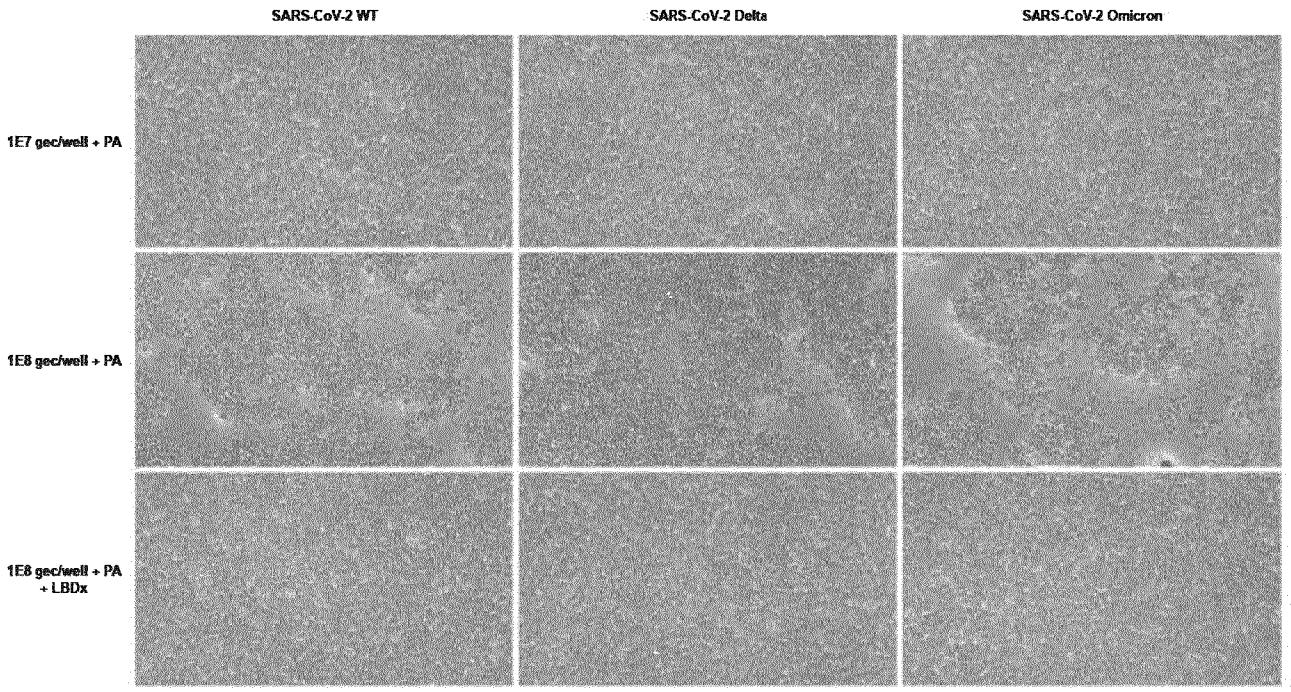
SARS-CoV-2 WT
SARS-CoV-2 Delta
SARS-CoV-2 Omicron
1E7 gec/well + PA
1E8 gec/well + PA
1E8 gec/well + PA
+ LBDx

FIG. 5P

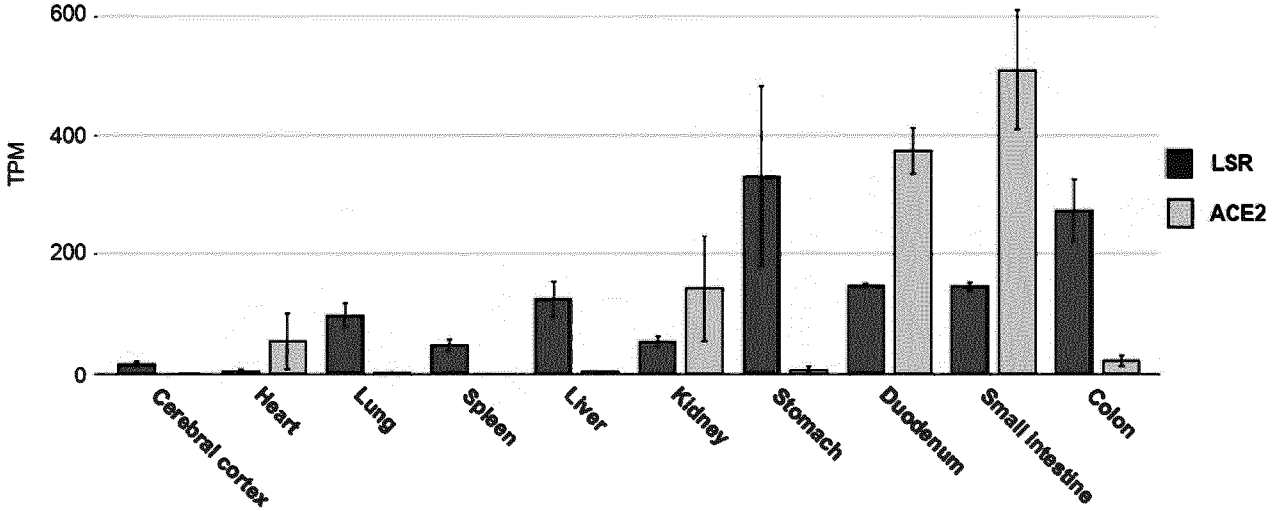
600
400
200
0
TPM
LSR
ACE2
Cerebral cortex
Heart
Lung
Spleen
Liver
Kidney
Stomach
Duodenum
Small intestine
Colon

FIG. 6

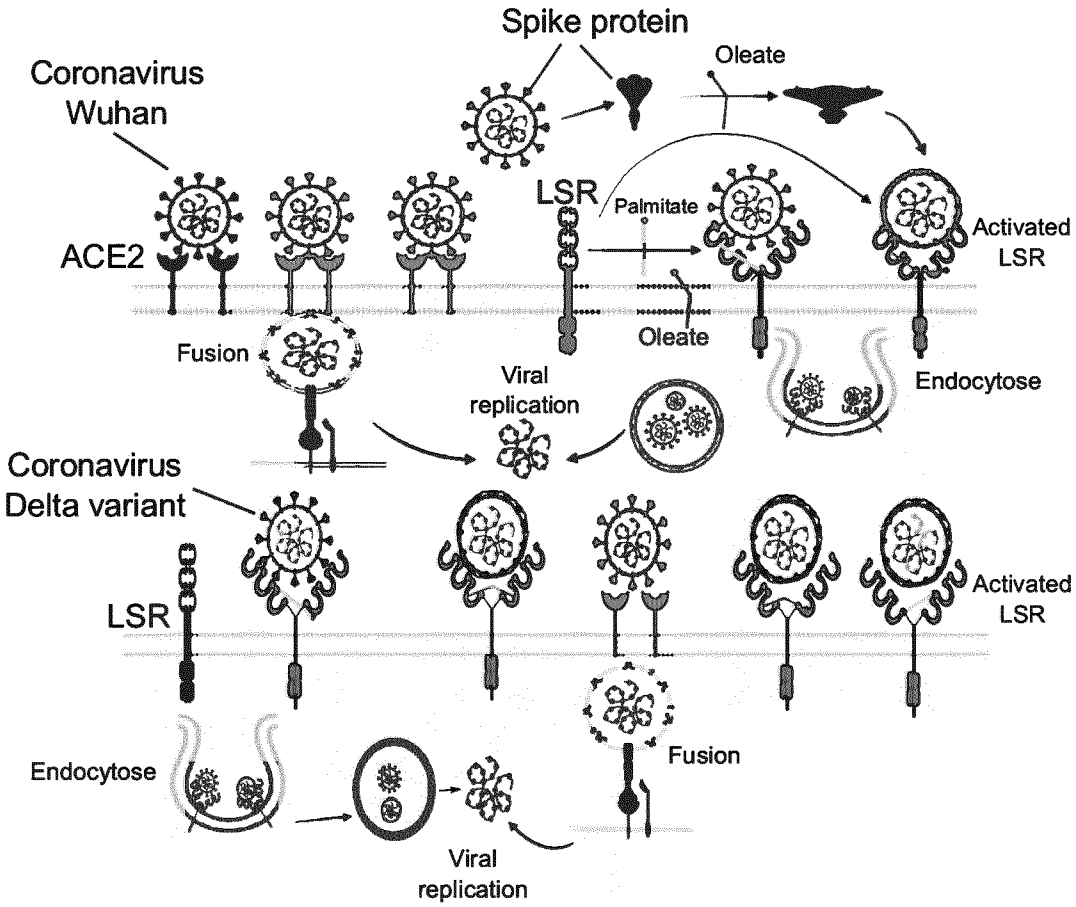
Spike protein
Oleate
Coronavirus
Wuhan
LSR
Palmitate
ACE2
Activated
LSR
Fusion
Oleate
Viral
replication
Endocytose
Coronavirus
Delta variant
LSR
Activated
LSR
Fusion
Endocytose
Viral
replication

FIG. 7

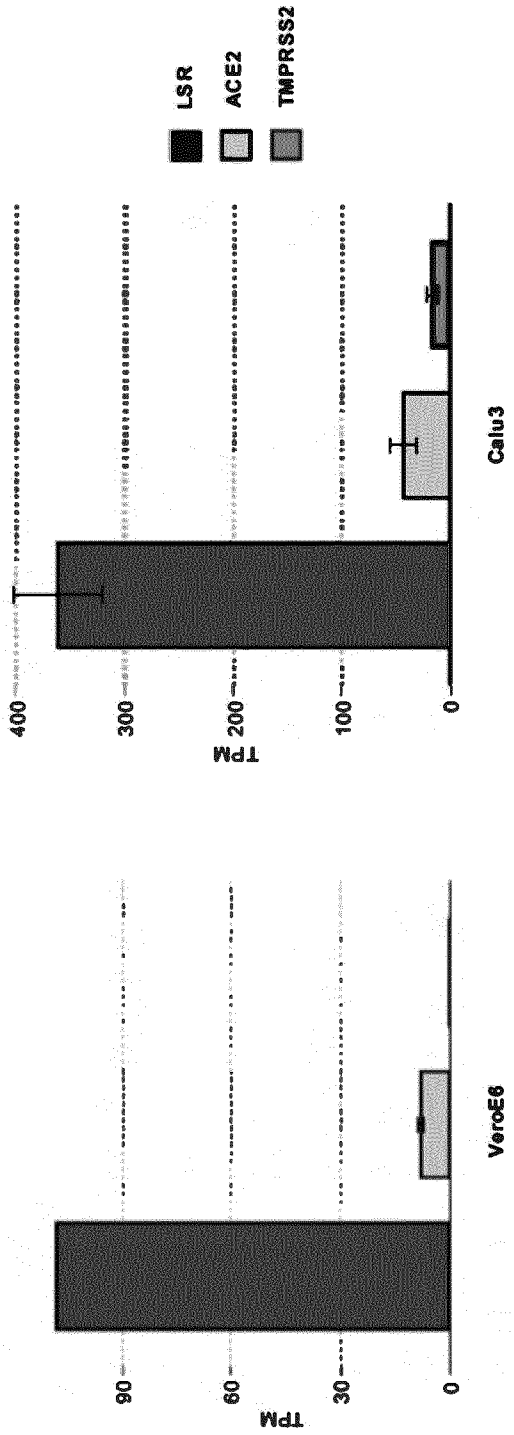
LSR
ACE2
TMPRSS2
Calu3
TPM
400
300
200
100
0
VeroE6
TPM
90
60
30
0

FIG. 8A

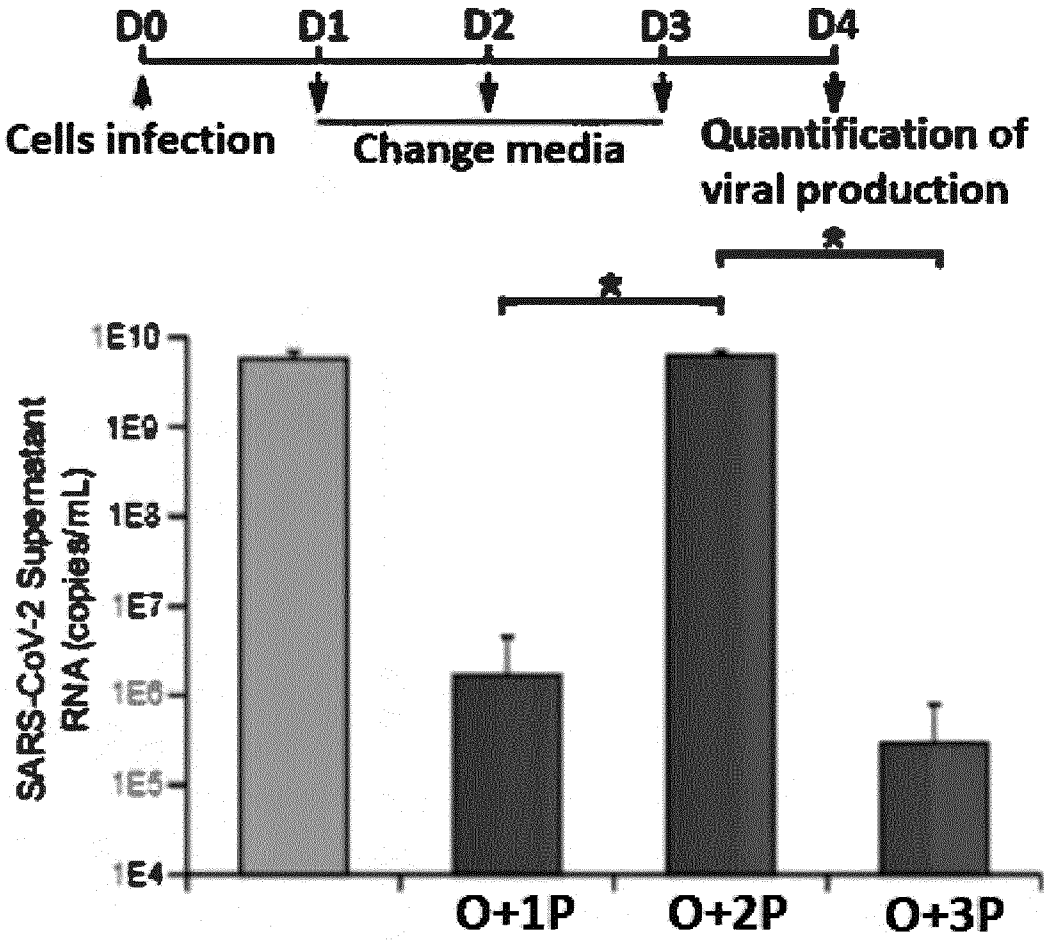
D0
D1
D2
D3
D4
Cells infection
Change media
Quantification of viral production
*
*
SARS-CoV-2 Supernatant RNA (copies/mL)
1E10
1E9
1E8
1E7
1E6
1E5
1E4
O+1P
O+2P
O+3P

FIG. 8B

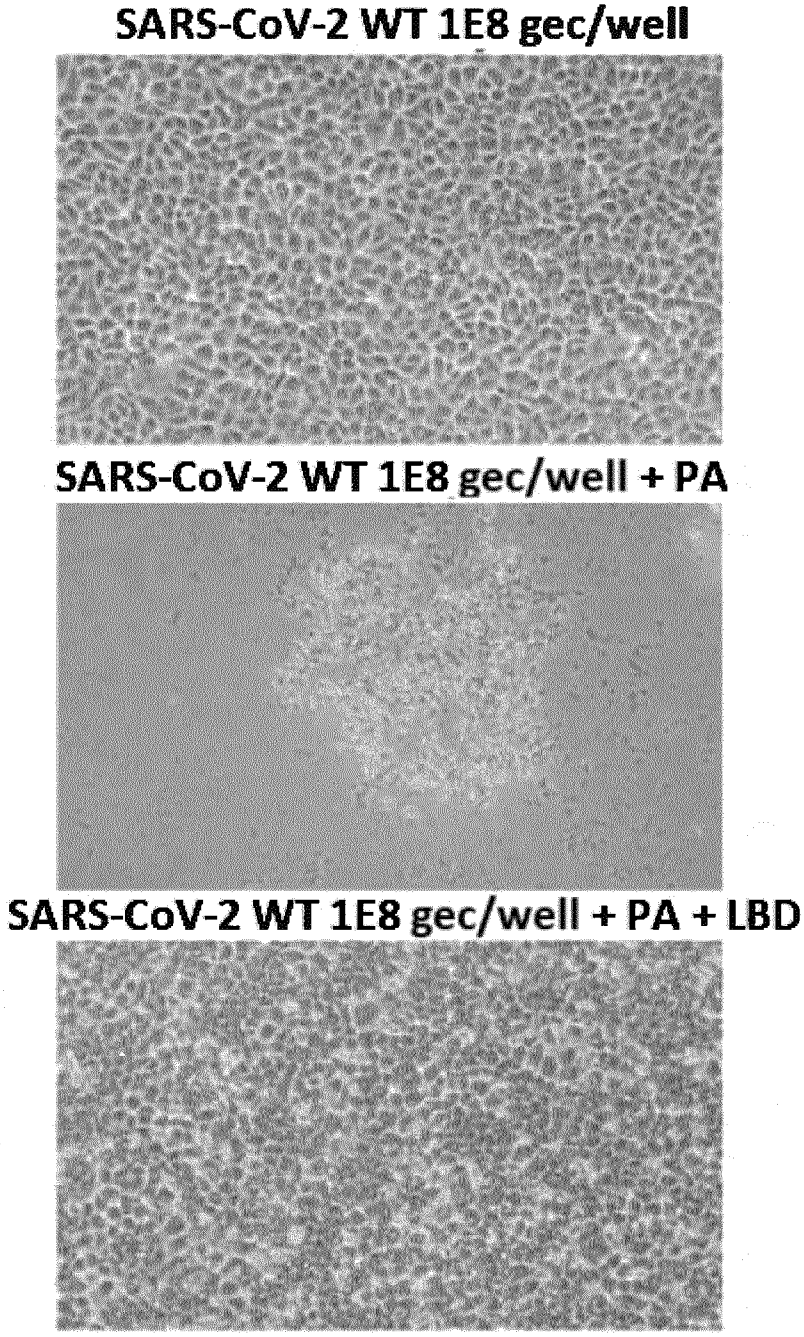
SARS-CoV-2 WT 1E8 gec/well
SARS-CoV-2 WT 1E8 gec/well + PA
SARS-CoV-2 WT 1E8 gec/well + PA + LBD

FIG. 8C

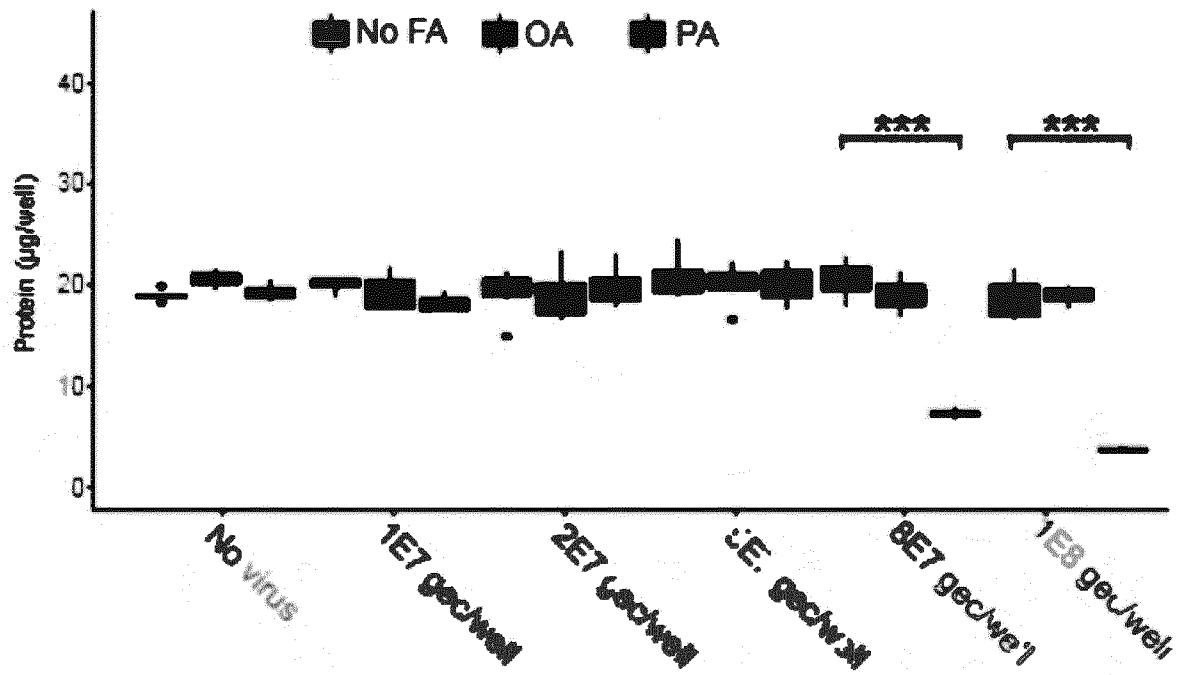
No FA
OA
PA
Protein (µg/well)
40
30
20
10
0
***
***
No virus
1E7 gec/well
2E7 gec/well
5E7 gec/well
8E7 gec/well
1E8 gec/well

FIG. 8D

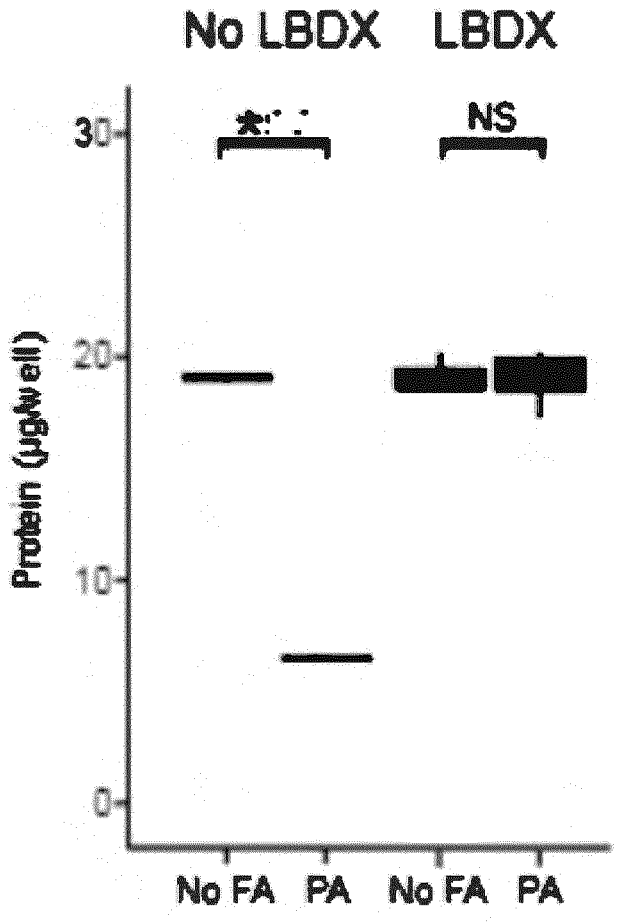
No LBDX
LBDX
*
NS
Protein (µg/well)
30
20
10
0
No FA
PA
No FA
PA

FIG. 8E

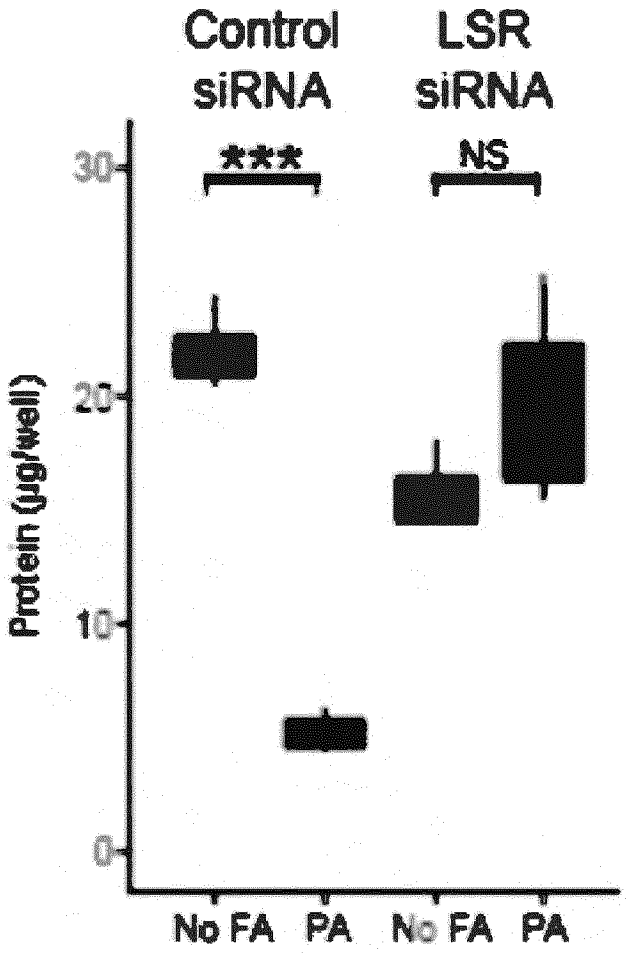
Control siRNA
LSR siRNA
***
NS
Protein (µg/well)
30
20
10
0
No FA
PA
No FA
PA

FIG. 8F

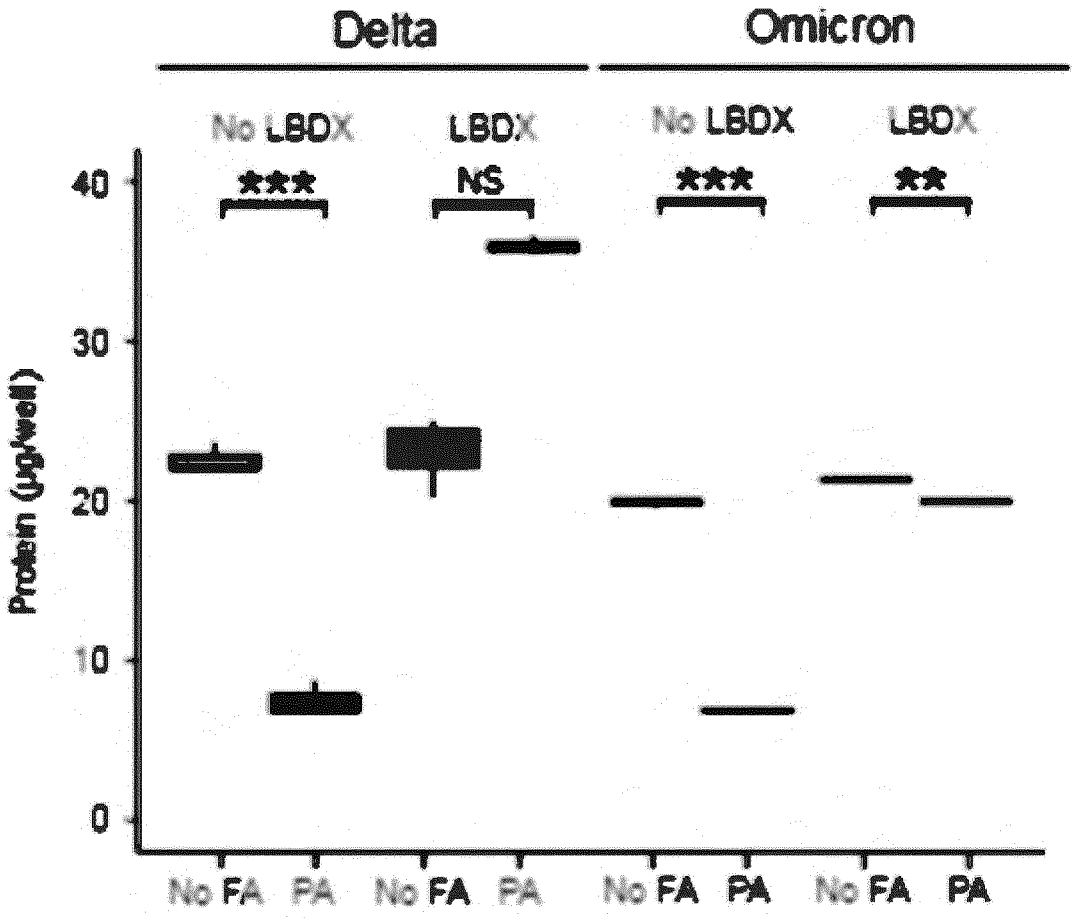
Delta
Omicron
No LBDX
LBDX
No LBDX
LBDX
***
NS
***
**
Protein (µg/well)
40
30
20
10
0
No FA
PA
No FA
PA
No FA
PA
No FA
PA

FIG. 8G

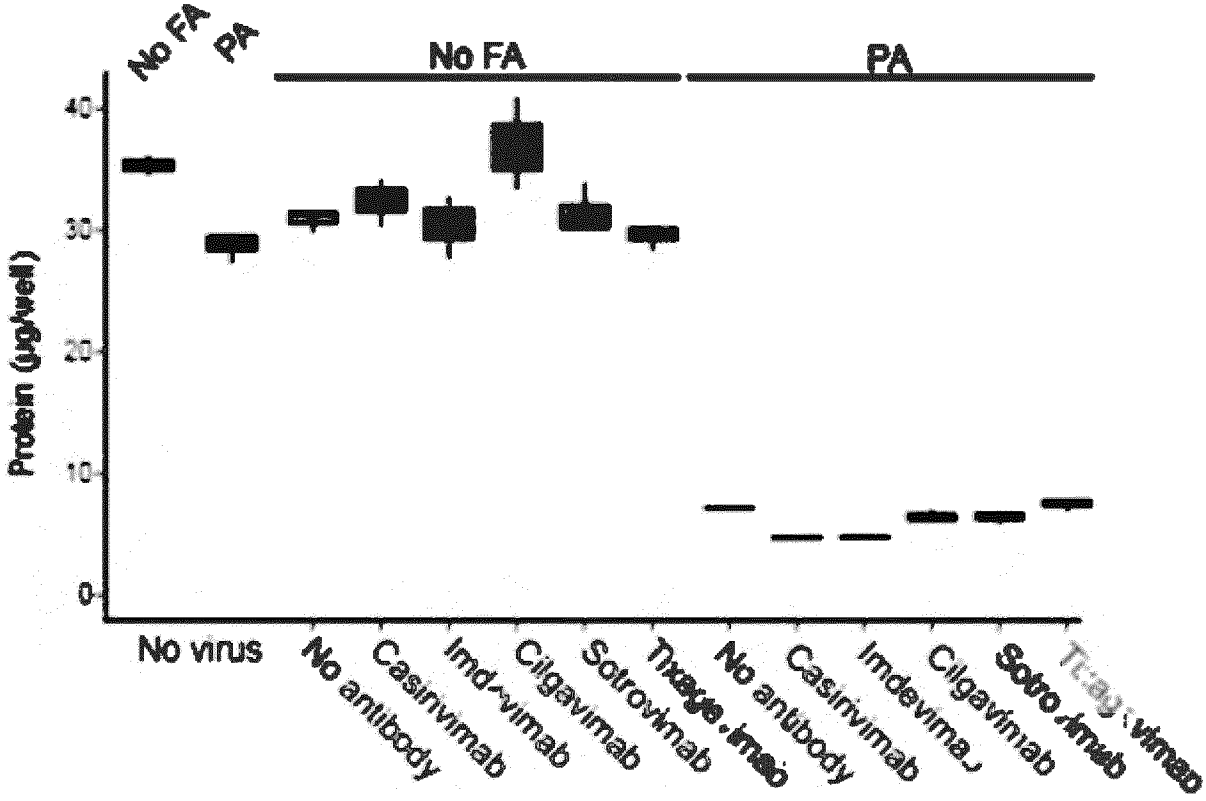
No FA
PA
No FA
PA
Protein (µg/well)
40
30
20
10
0
No virus
No antibody
Casirivimab
Imdevimab
Cilgavimab
Sotrovimab
No antibody
Casirivimab
Imdevimab
Cilgavimab

FIG. 8H

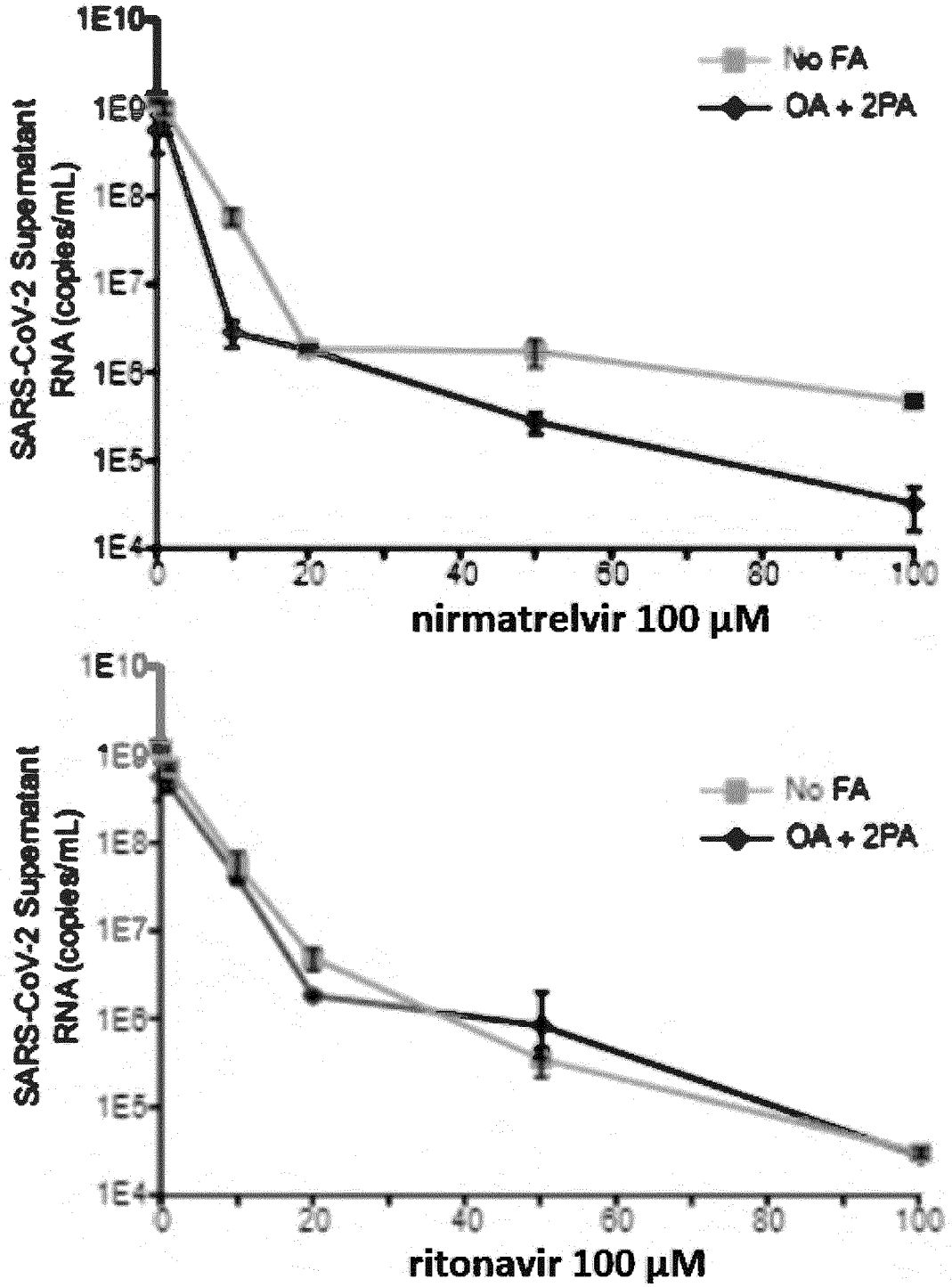
SARS-CoV-2 Supernatant RNA (copies/mL)
1E10
1E9
1E8
1E7
1E6
1E5
1E4
0
20
40
60
80
100
No FA
OA + 2PA
nirmatrelvir 100 µM
SARS-CoV-2 Supernatant RNA (copies/mL)
1E10
1E9
1E8
1E7
1E6
1E5
1E4
0
20
40
60
80
100
No FA
OA + 2PA
ritonavir 100 µM

FIG. 8I

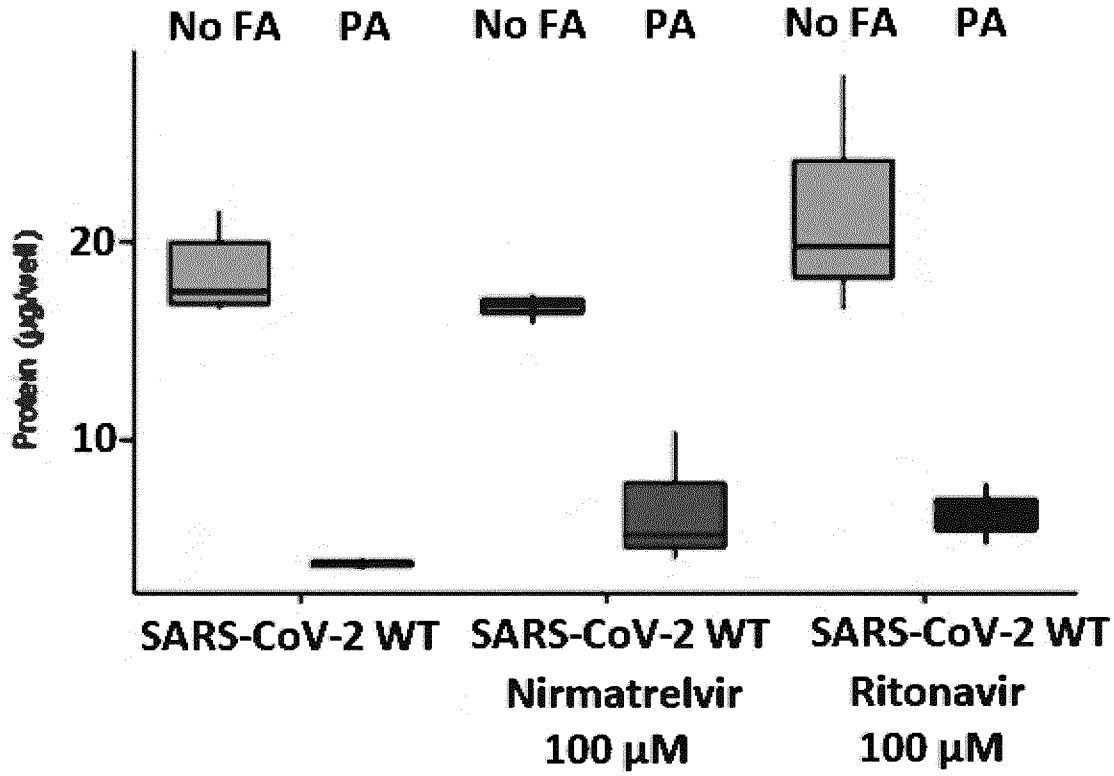
No FA
PA
No FA
PA
No FA
PA
Protein (µg/well)
20
10
SARS-CoV-2 WT
SARS-CoV-2 WT
Nirmatrelvir
100 µM
SARS-CoV-2 WT
Ritonavir
100 µM

FIG. 9

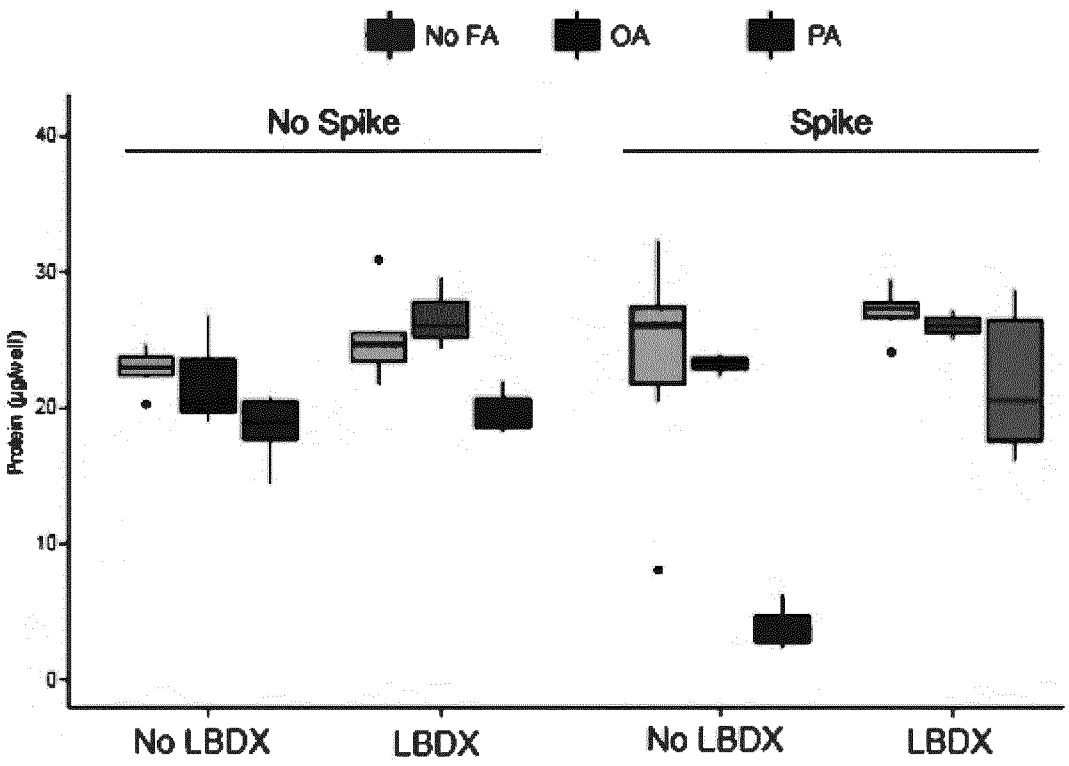
No FA
OA
PA
No Spike
Spike
Protein (µg/well)
40
30
20
10
0
No LBDX
LBDX
No LBDX
LBDX